
# Impacts of Coastal Eutrophication on Benthic Ecosystem Functions

Alejandra Maria Zazueta-Lopez

The University of Leeds

School of Geography

Submitted in accordance with the requirements for the degree of Doctor of Philosophy

April 2024

# Intellectual property

I confirm that the work submitted is my own and that appropriate credit has been given where reference has been made to the work of others.

# Acknowledgments

This work wouldn't be possible without the incredible support of my supervisors Clare Woulds and Christian März who helped to shape this research during a global pandemic and were key for developing my first fieldwork experience. Clare, I'm immensely grateful for all the support and patience through my PhD journey, could not have asked for a better guidance and inspiration in research.

I would also like to thank Michelle Devlin, Dave Sivyer, Ruth Parker, Silke Kroeger and Jhon Aldridge, from Cefas; Mike Best and Keith McGruer from the Environment Agency who provided access to the secondary data for the second chapter and valuable advice for fieldwork in the UK estuaries. Jonathan Carrivick for the advice during my early stages practising with GIS analysis.

Greg Cowie (University of Edinburgh), Tom Jilbert (University of Helsinki) and Clare Woulds for their support and experience learned during fieldwork in Finland and for providing the basis for the macroalgae derived carbon research in the Baltic Sea and southern UK estuaries. Steve Mowbay from the University of Edinburgh, for the assistance and wonderful help through the laboratory and further data analysis of CuO oxidation products results.

I'm grateful to the RanTrans project team from the Institute of Marine Science from the University of Portsmouth. Gordon Watson who had the disposition for collaborating and provided valuable advice during fieldwork and access to the facilities. Andrew VanDerSchatteOlivier thank you for your wonderful hospitality and help during fieldwork in Langstone Harbour. To Eric Harris-Scott who helped me slicing mud and taking sediment cores during my seasonal sampling fieldwork. Thank you for storing and sending over the samples to Leeds.

Thank you to the amazing team from the School of Geography laboratories, Rachel Graisor from whom I've learned analytical skills, thank you to David Ashley who was always available for providing the assistance on nutrients, organic carbon, and sediment demineralisation analyses, a great proportion of this thesis wouldn't be possible without his help. To Josh, Holly and Santi, that where great help and company during the lonely pandemic days in the labs.

To the National Environmental Isotopes Facility team for the support to this project for the analyses of stable isotopes and their patience for waiting for different batches of samples being sent. Thank you to CONACyTH Mexico for providing the funding for this research project.

To the amazing water@leeds team, who was my first contact in the University of Leeds and had the opportunity to work with. Thank you for the funding provided through the S.P.R.I.N.G. Award that allowed me to perform CuO oxidation products

analyses. Thank you to Gabriela Lopez-Gonzalez who has been of great support on a professional and personal level. To Sussanah Hopson, who is always a joy to be around and is a valuable part of my formation. I would like to thank the PGR community of the School of Geography that was an amazing company during these years. Thank you to my friends and family from home who were always present and supportive.

To my husband and best friend David Andrews who has been always by my side, for believing in me when I doubted and for encourage me to be better. Thank you for being my rock and my support during challenging times and lastly thank you to Judy bunny who has been a joy to be around in these last months.

# Abstract

Estuaries are among the most productive marine ecosystems and macroalgae is recognized to be the most abundant and productive among the benthic marine primary producers. When eutrophic conditions are present, one of the most evident responses of this condition is the proliferation of macroalgae blooms mainly caused by opportunistic macroalgae. Nonetheless, the impacts of macroalgae blooms on sediment biogeochemistry and organic carbon storage is not fully understood, especially on unvegetated coastal areas.

The present thesis evaluates historical records of macroalgae blooms in the UK estuaries and results from field measurements of sediment biogeochemistry are presented to assess the impacts of macroalgae blooms on benthic ecosystem services by comparing impacted sites and the influence of seasonality. Furthermore, an evaluation was made of the potential for macroalgae derived carbon identification within estuarine and coastal sediments.

This work presents the impacts of excessive macroalgae blooms on sediment biogeochemistry and analyses the historical data from southern UK estuaries subject to different impacts of eutrophication and macroalgae growth. Results from sediment and porewaters data indicate the enhanced capacity for organic carbon storage

within more impacted sites by eutrophication and macroalgae. Furthermore, results from sediment biogeochemistry on different seasons also suggest more accumulation of organic C during colder months, which is suspected to be due to less degradation happening. In addition, evidence of macroalgae derived carbon within sediment carbon stocks is provided. This research demonstrates the relevance of estuarine unvegetated sediments impacted with macroalgae blooms for organic carbon cycling and storage and provides basis for future exploration on macroalgae derived organic carbon in sediment carbon stocks.

# Table of Contents

# Table of Tables

# Table of Figures

Chapter 1.

# Introduction

## 1.1 Motivation

Coastal benthic ecosystems provide a variety of ecological services to human populations such as food production, climate regulation, nutrient cycling, and carbon storage (Galparsoro et al., 2014; Townsend et al., 2011). These services are mainly driven by biological activity including bioturbation and bioirrigation of the sediments, and thus depend on biodiversity. For this reason, it is important to maintain a healthy ecosystem in order to have access to benthic ecological services. Nonetheless, the accumulation of stressors such as eutrophication and climate change, threatens natural ecosystem functioning (Snickars et al., 2015).

Coastal eutrophication is the large biogeochemical and ecological responses, either direct or indirect, to anthropogenic fertilization of ecosystems at the land-sea interface (Cloern, 2001). Eutrophication symptoms, particularly macroalgae blooms, have a negative impact on important benthic ecosystem functions, potentially leading to undesirable alterations in faunal community composition, bioturbation, bio irrigation, oxygen levels, and carbon storage.

The contribution of macroalgae to carbon sequestration is an area of increasing interest due to its potentially important role mitigating climate change effects;

(Krause-Jensen & Duarte, 2016; Sondak & Chung, 2015), and the potential inclusion of macroalgae derived carbon to account as blue carbon stocks (Krause-Jensen et al., 2018a). Besides, the economic value of coastal blue carbon for the European shelf has been estimated as US$180 million (Luisetti et al., 2013), comprising only saltmarshes and seagrass beds, therefore the inclusion of macroalgae derived carbon could significantly increase this amount. Nonetheless, understanding of the factors that determine the size and dynamics of sediment carbon stocks is at a very early stage, and the contribution of macroalgal carbon to those stocks is almost completely unknown.

In UK coastal areas, the most pronounced impact of eutrophication is the occurrence of macroalgal blooms. The development and duration of a macroalgae bloom depends on several factors including high nutrient concentrations, light availability, salinity levels, sediment composition and wind and wave influence. The grade of influence of each of these factors will depend on site-specific characteristics. Nonetheless, high inputs of nutrients, mainly nitrogen and phosphorous, into coastal ecosystems remains a constant for macroalgae bloom development. However, the extent and occurrence of macroalgae blooms has not responded proportionally to reductions in nutrients inputs into coastal ecosystems (Ni Longphuirt et al., 2016a). Therefore, the controls on macroalgae bloom occurrence are still not well understood.

# 1.2 Background

## 1.2.1 Coastal eutrophication

Anthropogenic stressors such as agricultural runoff, atmospheric deposition and untreated wastewater inputs have loaded coastal marine ecosystems with an excess of nutrients leading to a state of eutrophication. The word eutrophication is formed by two greek words: “eu” = well and “trope” nourishment, this phenomenon was first studied in lakes in the 1960’s. In contrast, coastal marine eutrophication has been a relatively new topic of scientific interest, with increasing popularity by the 1980’s, two decades after lake freshwater eutrophication (Cloern, 2001). Coastal eutrophication was first associated with nitrogen and phosphorus inputs, which act as fertilizers by increasing primary productivity. In later years, Nixon (1995), defined coastal eutrophication as an increase in the rate of organic matter supply to an ecosystem. He classifies four trophic states in the marine environment defined as follows: Oligotrophic (< 100 gC $m^{-2}y^{-1}$), mesotrophic (100-300 gC $m^{-2}y^{-1}$), eutrophic (301-500 gC $m^{-2}y^{-1}$) and hypertrophic (>500 gC $m^{-2}y^{-1}$). This classification was made in relation to autochthonous organic carbon supply to a marine ecosystem given as gCm-2y-1. In most marine ecosystems the natural trophic state varies from oligotrophic to eutrophic. Some ecosystems do not show detrimental direct responses by increasing organic carbon (Jorgensen & Richardson 1997 Richardson, 1997). In more recent years, Cloern (2001), proposed a new definition to coastal eutrophication as the “large biogeochemical and ecological responses, either direct or indirect, to anthropogenic fertilization of ecosystems at the land-sea interface” (p. 4). This definition describes more accurately the use of the word eutrophication in scientific

literature, since is often used to refer to the effects rather than the amount of organic matter production.

Thus, human-induced eutrophication of coastal ecosystems is the result of nutrient inputs from different anthropogenic activities such as agriculture runoff and atmospheric deposition (Paerl, 1995), which accelerates primary production of organic matter. Phytoplankton growth rate is stimulated by the large amounts of nutrients available, creating an imbalance between algae production and consumption (Cloern, 2001). After that, the excess of organic matter is sedimented and processed, increasing oxygen demand which will lead to hypoxic events or in the worst case, anoxia (Levin et al., 2009). Eutrophication is a major threat to coastal ecosystems and has great ecological consequences. Shallow ecosystems such as estuaries, bays, enclosed seas, and fjords are more likely to suffer from coastal eutrophication (Diaz & Rosenberg, 2008) due to long water residence times. It is expected that eutrophication in estuarine and coastal waters will continue spreading and intensifying due to global change and increase in human population (Rabalais et al., 2009), with major consequences for benthic ecosystem functioning. Multiple coastal ecosystems around the globe have been identified as eutrophic, however only few of them have been subject of long-term study (Bonsdorff et al., 1997; Rabalais et al., 2014).

Research into the impacts of coastal eutrophication tend to be limited to describing changes in benthic community composition (Dimitriou et al., 2017; Hale et al., 2018;

Pearson et al., 1978; Trannum et al., 2018), and there is less information relating the eutrophication stressor with benthic functions.

#### 1.2.1.1 Global status of coastal eutrophication

Eutrophication has been a persistent problem in diverse coastal ecosystems around the world. Its recognition began in the 1980's and was a subject of concern in coastal areas from Europe, United States, Japan, India and the Caribbean (Nixon, 1995). Coastal eutrophication has been linked to population growth development and population growth since the beginning of its study (Valiela, 1992).

One of the best documented examples in the world of coastal eutrophication is the Baltic Sea. Nutrient trends in the central area of the Baltic for the period of 1970-1995 showed an increase in $NO_3^-$ and $PO^{4+}$ pools both in surface and deep (>100 m) water (Murray et al., 2019). This excess of nutrient availability led to a shift from slow-growing endemic species such as *Fucus* and *Furcerallia* to more rapid growing filamentous macroalgae (Bonsdorff et al., 2002). A more recent evaluation of multiple datasets from the period 2007–2011 confirmed that in the full extent of the open Baltic Sea is affected with eutrophication (Fleming-Lehtinen et al, 2015).

Chesapeake Bay is the largest estuary in the US and one of the most well-studied coastal areas in the world related to eutrophication. Consequences of eutrophication such as algae blooms and seasonal hypoxia has been well-documented in

Chesapeake Bay since 1930's (Zimmerman, 2000), however it was until the 1970's that the problematic became acknowledged by society and government (Harding et al., 2020). Multiple restoring and monitoring programs have been put in place in order to improve the status of the bay. As a result, nutrient reductions have been achieved, leading to a substantial reduction in hypoxia spread within Chesapeake Bay (Frankel et al., 2022).

Eutrophication has become a concern in other parts of the world such as Latin America, India, and China (Aranda-Cirerol et al., 2011; Sinha, Biswas, & Bhattacharyya, 2011; Wang et al., 2018). After the rapid economic development in China particularly near coastal areas, eutrophication became the primary pressure on coastal ecosystems (Wang et al., 2018). This contributed to the development of the largest macroalgae bloom in the world, which occurred in the period of 2008-2012 in the transregional area of the Yellow Sea (Liu et al., 2013). The massive macroalgae bloom also referred as "Green tide" was primarily caused by macroalgae from the genus *Ulva* and covered a maximum area of 84,109 $km^2$ in 2008 (Liu et al., 2013).

Other blooming species such as *Sargassum* is causing major problems in the Caribbean, expanding to the Gulf of Mexico to Western Africa coasts (Wang et al., 2018). This over production of macroalgae is ultimately transported to the beaches, producing what is known as "Golden tides". This phenomenon is causing major problems including preventing sea turtles from nesting (Maurer et al., 2022),

impacting tourism activities and even human health after the decomposition of the biomass (Robledo et al., 2021). In 2011 an unprecedent event took place in the Atlantic where tonnes of *Sargassum* was transported to the west African from Ghana to Sierra Leon and in the Caribbean side was reported from Trinidad to Dominican Republic and Mexican coasts (Smetacek & Zingone, 2013).

Green and golden tides events have been on the rise since the early 2000's and it is clear that a joint international effort should be achieved in order to control and prevent these blooms. While the examples of the Baltic Sea and Chesapeake Bay show recovery is possible when monitoring programs and prevention measures are put in place to prevent nutrients to reach coastal ecosystems, other countries are still in the early stages of recognition of this problematic.

One of the first references of coastal eutrophication in the UK estuaries in the literature was recorded in 1980's when Montgomery et al 1981 reported eutrophic conditions within Langstone Harbour, highlighting the problematic of persistent macroalgae mats and its effects on bird communities. Eutrophication is still a problem in Langstone Harbour and other estuaries in the UK, a more in depth evaluation on this regard will be discussed in Chapter 2.

### 1.2.1.2 Eutrophication Assessment

Measures to prevent, monitor and control eutrophication in coastal ecosystems have been implemented by most of the European Union parties under the Marine Strategy Framework Directive (2008). The recognition of coastal eutrophication as a threat to marine ecosystems is included in The Marine Strategy Framework Directive 2008/56/EC (COUNCIL, 17 June 2008) which aimed to achieve or maintain good environmental status in the marine environment by the year 2020.

After the Oslo convention in 1972 and the Paris convention in 1974 addressing land-based sources of marine pollution and the offshore industry, the “OSPAR (OS: Oslo and PAR: Paris) Commission” was created. The OSPAR Commission is *“The mechanism by which 15 Governments and the European Union cooperate to protect the marine environment of the North-East Atlantic”* (Ospar, 2015). In support of the legal framework, OSPAR commission includes the Eutrophication Strategy with the *objective to achieve and maintain a healthy marine environment where anthropogenic eutrophication does not occur* (Bonsdorff et al., 2002; OSPAR, 2017) and was developed for the Identification of Eutrophication for the North Sea and the Celtic Sea.

The evaluation of eutrophication status of the OSPAR maritime area is made based on changes in the assessment parameters stablished by the Common Procedure (COMP). Assessment parameters are divided into 4 categories, the first category is degree of nutrient enrichment (Causative) which includes nutrient inputs, winter

Dissolved Inorganic Nitrogen (DIN), Dissolved Inorganic Phosphorus (DIP) and winter N:P ratio. Category II evaluates direct effects including changes in chlorophyll α, phytoplankton indicator species and macrophytes. Finally, categories III and IV: Indirect effects/Other possible effects, comprises oxygen deficiency, changes/kills in zoobenthos and fish kills, organic carbon/matter and algal toxins. The final output of the COMP classifies the assessed areas as No Problem Areas (NPA), Potential Problem Areas (PPA) and Problem Areas (Problem Areas) by its deviation from reference parameters.

In addition to OSPAR COMP, different indexes have been developed trying to relate eutrophication parameters to a numerical scale. For instance, Vollenweider et al., (1998), proposed the Trophic Index (TRIX) to classify coastal areas from low productive to high productive on a scale from 0-10. This index is calculated using N, P, Chl α, and Dissolved Oxygen as indicators. It has been used in several coastal areas with different characteristics such as, the Adriatic Sea (Vollenweider et al., 1998). Thames and Medway estuaries (Devlin et al., 2011) and Mediterranean Sea (Dimitriou et al., 2017). This Index has the advantage of being applicable in different sites with distinct characteristics. However, the assessed parameters are causative, and it does not consider intermediate effects. Besides, it has been identified that its application is more suitable in estuaries and shallow ecosystems where total primary productivity is mainly from phytoplankton communities, excluding other primary producers such as seagrasses and macroalgae (Devlin et al., 2011).

### 1.2.2 Modelling macroalgae growth

Spatial analysis, theoretical analysis and numerical modelling are required to evaluate the responses of an estuary to nutrient enrichment (CEFAS, 2003). A variety of models have been developed for the prediction of macroalgae growth and species distribution, among them, box models seem to be a suitable tool used in most of them (Aldridge & Trimmer, 2009; Graiff et al., 2020; Ni Longphuirt et al., 2016) that allows theoretically simplifying the complex dynamics of estuaries.

Other approaches like Species Distribution Models, have been used for the study of future scenarios related to eutrophication mitigation measures in the Baltic Sea (Bergstrom et al., 2013). Although remote sensing has been successfully used to map seagrass meadows (Poursanidis et al., 2018) and macroalgae beds (CEFAS, 2003), it is not useful in sites with high turbidity (Downie et al., 2013). In a similar case in the UK, remote sensing in turbid estuaries (Medway and Swale) was unable to differentiate between macroalgae and diatom mats (CEFAS, 2003).

For the case of the Medway estuary where high turbidity is present, Aldridge & Trimmer (2009), successfully developed a model that considers site-specific hydrodynamic features (Tidal dynamics) and nutrient inputs to predict macroalgae growth predictions.

## 1.2.3 Effects of Coastal Eutrophication

### 1.2.3.1 Hypoxia

Although hypoxic areas in the ocean can be formed naturally, enhanced nutrient inputs to coastal ecosystems have created more low-oxygen and anoxic sites since human activities and population growth increased (Rabalais et al., 2014). Hypoxia in estuarine and coastal ecosystems is strongly driven by eutrophic conditions in the water column (Diaz & Rosenberg, 2008), and it is commonly found seasonally between late spring and early fall as a consequence of water stratification (Levin et al., 2009). Hypoxic conditions in marine environments can be found from 2.0 ml $l^{-1}$ declining to 0.0 ml $l^{-1}$ the absence of oxygen, which is considered anoxia (Diaz & Rosenberg, 1995). The largest affected zones by eutrophication-induced hypoxia can be found in the Gulf of Mexico (< 20,000 $km^2$), Baltic Sea (84,000 $km^2$) and the Black Sea ($\leq$ 20,000 $km^2$). Gren et al. (1997), estimated that nutrient inputs to the Baltic Sea were 1 096 000 tons of N and 36 200 tons of P annually. As an effect of the great nutrient amounts discharged, hypoxic events expanded through the ecosystem (Figure 1) and now is the largest case of eutrophication-induced dead zone, with important consequences for the benthos (Diaz & Rosenberg, 2008).

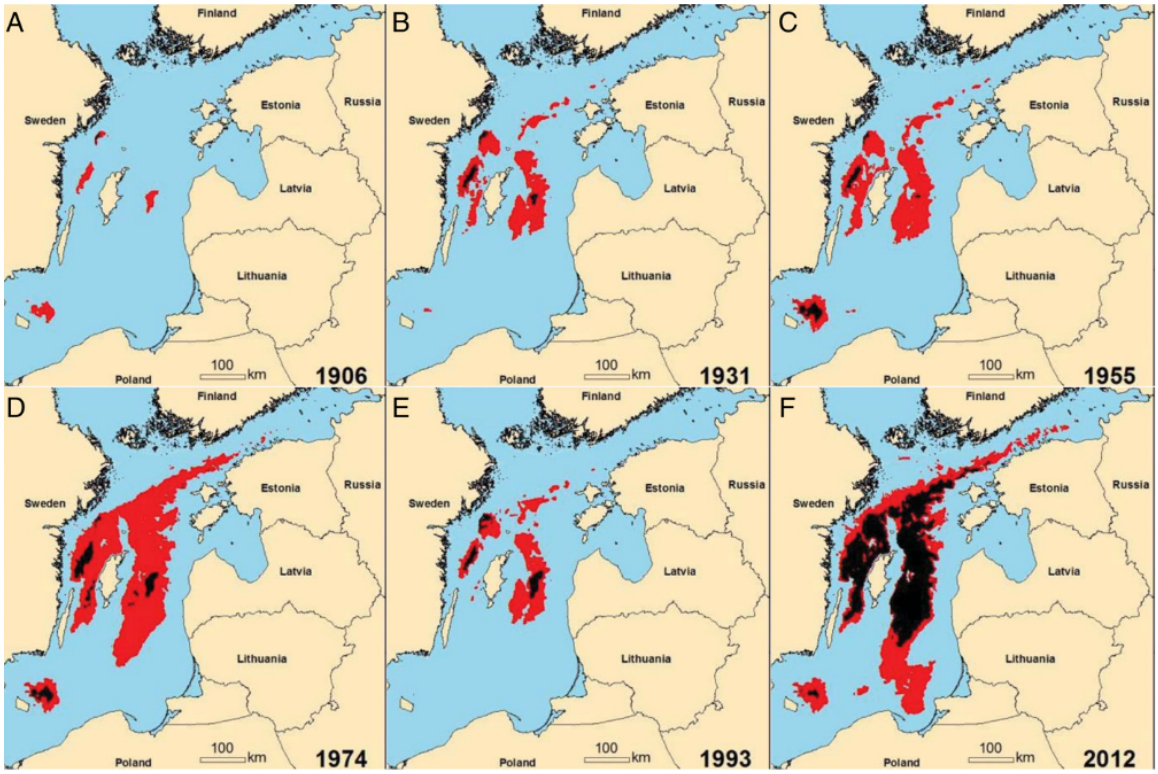


**Figure 1. Spatial distribution changes of hypoxia and anoxia over time (Means between January and December). Estimated bottom oxygen concentrations <2 mg·L$^{-1}$ shown in red and concentrations of 0 mg·L$^{-1}$ shown in black. (Carstensen et al., 2014).**

The impact on the benthic community will depend on the duration and severity of the low oxygen events; longer periods of hypoxia can lead to permanent low oxygen or anoxic sites in the water bodies (Levin et al., 2009). These changes have been well documented in Chesapeake Bay, the largest estuary in the United States, where seasonal hypoxia has been reported since 1900. However, its extent, duration and severity have increased in the 20$^{th}$ century due to land use changes and the extensive use of crop fertilizers (Levin et al., 2009). The increased frequency and extension of seasonal low oxygen conditions is a consequence of anthropogenic nutrient enrichment; this is supported by spatial distribution of these events. Some

changes reported for Chesapeake Bay were reduction of benthic species abundance and dominance of small short-lived species (Diaz & Rosenberg, 1995). Besides the seasonal events, at deeper sites in the bay were recorded “periodic hypoxic events”, which can last from days to weeks and have harmful effects on the benthos from changes in species composition to elimination of some taxa (Diaz & Rosenberg, 1995).

Oxygen depletion and eutrophication are strongly correlated phenomena, and it is often difficult to differentiate between their effects on coastal ecosystems (Gooday et al., 2009). Gray et al. (2002), suggest that most of the effects on benthic fauna are hypoxia-driven rather than eutrophication-driven, however, foraminifera species that are used as an indicator of hypoxia have also been found in the absence of bottom hypoxic conditions which relates with organic enrichment (as cited in Gooday et al., 2009). For this reason, is important to assess how nutrient enrichment affects benthic ecosystem functions besides eutrophication-induced hypoxia, which is a sign of severe eutrophic conditions.

### 1.2.3.2 Changes in Benthic Community Composition.

Benthic communities and sediments are particularly sensitive to eutrophication and hypoxia (Jorgensen & Richardson, 1997). The grade of disturbance of benthic communities in an ecosystem is generally indicated by their number of Species, Abundance and Biomass (SAB) (Rosenberg, 2001b). In conditions of high food availability for the benthos, SAB is higher, whereas in low food availability SAB tends

to be low (Rosenberg, 2001b). Based on research between 1964-1974 on a Swedish fjordic estuary, Pearson et al. 1978, described macrobenthic changes along a gradient of organic enrichment. In the study site, nutrient enrichment was the dominant stressor affecting benthic systems. They classified these changes in three successional stages: Peak of Opportunists, with abundance of few opportunistic species; Ecotone point, characterized by low abundance with high diversity and Transition zone, with fluctuant populations and a more stable community. This model, also known as P-R model, has been well exemplified by a general SAB diagram that represents in a graphic way the changes in community composition (Figure 2).

Since the model was published, it has been tested numerous times in different types of disturbance such as organic enrichment (Magni et al., 2009) and low oxygen zones (Hale et al., 2018). However, Gray et al. (2002) pointed out that almost all pollutants will show similar patterns of changes on benthic community structures. This statement could apply in different cases, although not all stressors have been tested.

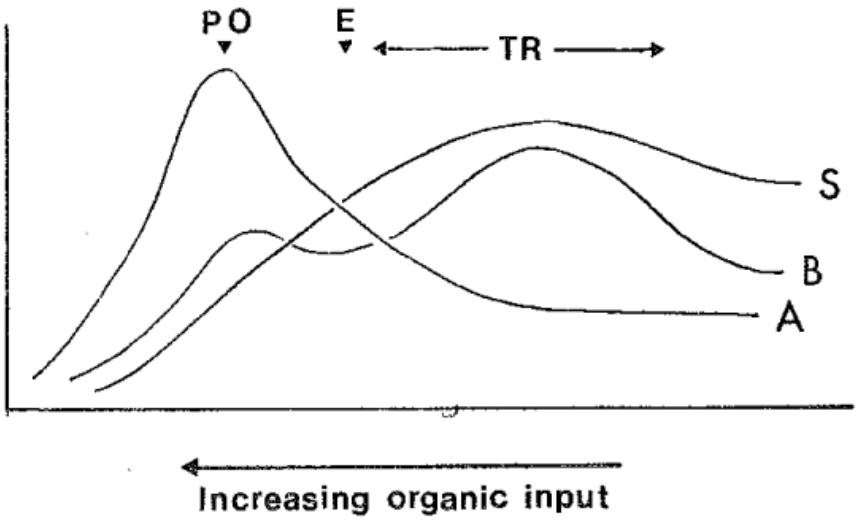


**Figure 2. Generalized SAB diagram of changes in community composition along a gradient of organic enrichment: S (Number of Species); A (Total abundance); B (Total biomass); PO (Peak of opportunists); E (Ecotone point); TR (Transition zone) (Pearson et al., 1978).**

Narragansett Bay, U.S. was studied by Hale et al. (2018), where historical data was evaluated to understand how species biodiversity and community composition changed through six decades of nutrient enrichment. They assessed community structure and changes in biogeochemical functioning of dissolved inorganic nitrogen and dissolved oxygen from seasonally hypoxic and normoxic areas of the bay, finding that the number of species (S) was less in the hypoxic areas (S= 17) than the normoxic ones (S= 30). Abundance did not show a significant difference between hypoxic (A= 653) and normoxic (A= 536) data, however big differences were found in abundances for hypoxia-sensitive (*Ostracoda*) and hypoxia-tolerant (*Spionidae*) species. Finally, in the case of biomass, this was significantly lower in the hypoxic (65.5 $mg/m^2$) than the normoxic areas (203.8 $mg/m^2$). Short-term changes were mainly conformed by small, opportunistic, short life cycle species like *Mediomastus*,

*Nucula*, and *Ampelisca*, whereas long-term composition changes included larger fauna. These results were closely similar to the descriptions made by the Pearson-Rosenberg model.

Nilsson & Rosenberg (1997), developed an alternative index to assess benthic successional stages with the use of sediment profile images called Benthic Habitat Quality (BHQ). This Index gives different values to benthic surface structures (A), benthic subsurface structures (B) and mean depth of apparent RPD (C) (Table 1); It is calculated with the following equation: $BHQ = \sum A + \sum B + C$. The Benthic Habitat Quality index is classified with scale values from 0 to 15, classified in the following way: Stage 0: BHQ <2; Stage 1: BHQ 2-4; Stage 2: BHQ 5-10; Stage 3: BHQ> 10.

**Table 1. Benthic Habitat Quality Index Values. Modified from: (Nilsson & Rosenberg, 1997).**

| Faunal and Sediment Structures | BHQ Values |
|---|---|
| **A: Surface structures** | |
| Faecal Pellets | 1 |
| Tubes < 2mm in diameter | 1 |
| Tubes > 2mm in diameter | 2 |
| Feeding pit or mound | 2 |
| **B: Subsurface structures** | |
| Infauna | 1 |
| Burrows #1-3 | 1 |
| Burrows # > 3 | 2 |
| Oxic void at < 5 cm depth | 1 |
| Oxic void at > cm depth | 2 |
| 0 cm | 0 |
| **C: Mean depth of apparent RPD** | |

| | |
|---|---|
| 0.1 – 1.0 cm | 1 |
| 1.1 – 2.0 cm | 2 |
| 2.1 – 3.5 cm | 3 |
| 3.6 – 5.0 cm | 4 |
| 5 cm | 5 |

Then in 2000, the same authors used sediment profile imaging to document SAB changes in response to hypoxia at the Swedish West Coast from sites at depths of: 75, 85 and 95 m. At the two deepest stations significant lower BHQ were reported, and correlations were demonstrated between SAB curves and BHQ index showing similar results to the Pearson-Rosenberg model (Figure 3). Benthic Habitat Quality index is a non-invasive method to evaluate benthic successional stages through gradients of disturbance with the advantage of being cost-effective (Nilsson & Rosenberg, 2000).

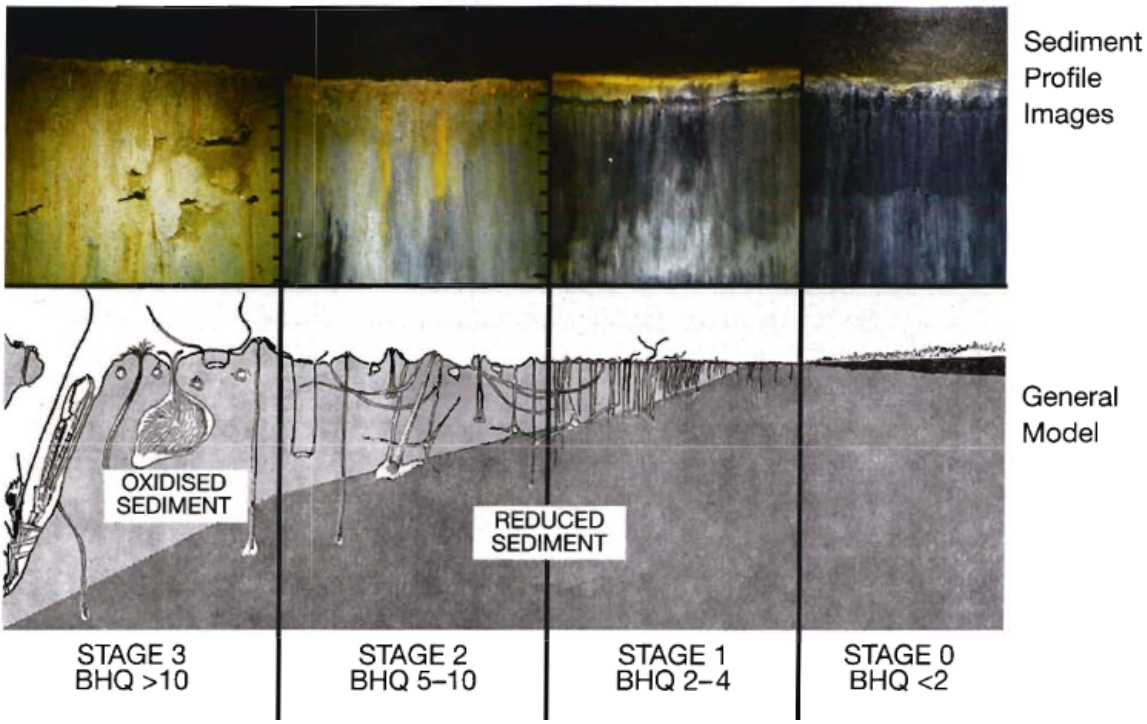


**Figure 3. Comparison between benthic infaunal successional stages along gradient of increasing environmental disturbance and benthic-habitat quality (BHQ) index with sediment profile images from (Nilsson & Rosenberg, 2000).**

### 1.2.3.3 Opportunistic macroalgae blooms

Macroalgae are marine macrophytes with a great diversity of species, including the four main groups Rhodophyta (Red), Phaeophyta (Brown), Chlorophyta (Green) and Cyanophyta (Blue). Macroalgae communities are naturally part of the marine ecosystems, species such as *Laminares* and *Fucales* are important for providing food source and shelter for many other higher organisms (Rinne et al 2020).

An algae bloom on the other hand, is the fast growing of a single photosynthetic species that is accumulated in a water body (Jorgensen & Richardson, 1997), the specie responsible for the bloom can be either micro or macro-organisms. Macroalgae blooms are a characteristic effect of anthropogenic eutrophic conditions on coastal marine ecosystems (Grall & Chauvaud, 2002).

Opportunistic macroalgae blooms are caused predominantly by green species such as *Enteromorpha spp*. and *Ulva spp*. The affinity of these species for nitrate ($NO_3^-$) and ammonium ($NH_4^+$) gives them an advantage compared with more slowly growing species (Pedersen & Borum, 1997). These species are responsible for seasonal blooms in all latitudes, from temperatate to warm coastal waters including coastal ecosystems in Sweden, United Kingdom, Mexico, and the United States to mention some (Liu et al., 2019; Ochoa-Izaguirre et al., 2002; Raffaelli et al., 1998; Rosenberg et al., 1990).

In an enriched environment, macroalgae blooms are light limited (Grall & Chauvaud, 2002) consequently are more likely to develop in spring or summer seasons (Raffaelli, 2000), due to higher temperatures and more sunlight exposure. However, other factors besides sunlight exposure have influence on the formation of a bloom.

### 1.2.3.4 Fish Farming and eutrophication

The impacts of fish farming on benthic communities are considered here as an additional source of information on the potential impacts of eutrophication, given that fish farming results in localized intense addition of organic carbon to the seafloor. The mass production of fish using cage-culture in marine coastal waters is likely to produce negative effects in their surroundings. Some of the most common environmental concerns related to marine fish culture includes eutrophication of local waters and impacts on benthic communities near cage sites (Watts & Conklin, 1998). This due to the great amounts of organic matter that is sedimented to the bottom, mainly derived from uneaten food and feces. The excess of organic matter creates a gradient of organic enrichment from the cages to their enclosing areas (Mayor et al., 2010).

Some of the impacts that can occur near fish farms due to over enrichment are increased algae biomass, changes in phytoplankton species composition, increased frequency of algae blooms, loss of bioturbation, fluctuations in dissolved oxygen and deoxygenation of the bottom sediments (Watts & Conklin, 1998). Although these effects are expected for an area with eutrophic conditions, eutrophication indicators

such as Chlo-a and increased total organic carbon are not commonly found in the water column near fish cages (Kalantzi & Karakassis, 2006). Which suggests that fish farming effects are not directly affecting the water column.

However, these consequences are present at the sediment water interface affecting benthic ecosystem. As demonstrated by Brown et al. (1987), who evaluated the effects of salmon farming on the benthos of the Scottish coast using biogeochemistry indicators. It was reported that dissolved oxygen increased, and carbon content decreased in the sediment with increasing the distance from the cages. They pointed out that benthic indicators of abundance, biomass and number of species were also increasing with distance. These results suggest that fish farming effects are dissipated with increasing the distance from the nutrients source and are not detectable at distances of ~200m (Mayor et al., 2010). This benthic composition pattern is generally observed for other gradients of enrichment (Pearson et al., 1978).

### 1.2.4 Factors controlling macroalgae blooms.

#### 1.2.4.1 Nutrient concentrations and ratios

The role of high nutrient concentrations as a predictor for macroalgae blooms is well established for most coastal systems. In major extent, primary productivity in marine ecosystems is either P or N limited. Redfield (1934), proposed an elemental ratio for inorganic nutrient requirement by marine phytoplankton of being ~16 N:1 P. This atomic ratio, also known as the Redfield ratio, is widely used in marine science

studying nutrient limitation (Lapointe et al., 1992; Quan & Falkowski, 2009). Generally, greater N:P ratios than the required from living plankton (16:1) indicate P limitation and lower ratios are for N limited systems (Downing, 1997).

Water nutrient ratios have been widely used in phytoplankton community studies, in both marine (Weston et al., 2008) and fresh water systems (Vrede et al., 2009), as a reference to assess changes in community composition. In contrast, little is known about the possible effects of N:P ratios on macrophytes. Bloom forming species like Enteromorpha and *Ulva* store nitrogen and phosphorus, and their growth rates depend on their internal nutrient concentrations (Björnsäter & Wheeler, 1990). Thus, nutrient ratios are more commonly used as a reference for nutritional uptake in tissue to evaluate macroalgae growth (Lapointe & Bedford, 2011; Wheeler & Bjornsater, 1992).

Most of these nutrient reduction measures have aimed to achieve reduction in single sources of nutrients either nitrogen or phosphorous (Greenwood, 2019) altering marine N:P ratios. The changing N:P ratio has been proved to alter phytoplankton abundance and community composition (Turner et al., 2003). However, little is known about changing N:P ratios affecting macroalgae bloom development. Research community concerns have highlighted potential consequences for phytoplankton changes in community composition and biodiversity (Burson et al., 2018; Paerl et al., 2014; Turner et al., 2003).

In early studies of nutrient limitation on marine ecosystems, it was assumed that N was the element that limited primary productivity (Boynton et al., 1982). This was thought because measurements taken by that time generally included only a portion of the entire N and P pools ($NO_2^-$, $NO_3^-$, $NH_4^+$ and $PO_4^{3-}$) (Downing, 1997), missing the dissolved and particulate fractions of nutrients present in organic matter. A data analysis of N:P ratios available from different marine environments carried by Downing (1997), concluded that in the open ocean N:P ratios are significantly high compared to very low ratios for estuaries and coastal ecosystems, indicating N limitation for coastal systems and P limitation in the case of the open ocean.

There are different scenarios for nutrient limitation on tropical and template marine systems. In tropical environments, known for having carbonate-rich sediments as seen in the Caribbean Sea, P might be the limiting element for macroalgae growth (Teichberg et al., 2010). This is explained by the adsorption of $PO_4^{3+}$ on sediment surfaces and consequently low rates of P remineralisation (Lapointe et al., 1992). Whereas in the case of temperate, silicate dominated systems, N generally plays the limiting role (Lapointe et al., 1992). However, there is evidence for hypereutrophic coastal sites where neither N nor P are the limiting elements for macroalgae growth. This can be seen in Jamaica Bay, USA (Wallace & Gobler, 2015), where excessive inputs of wastewater from treatment plants prevented N or P from limiting the growth of phytoplankton or macroalgae. It was rather stated that for this hypereutrophic

system, growth for primary producers including macroalgae are a function of nutrient loading, silicate concentrations, light exposure, and residence time.

### 1.2.4.2 Light exposure

Besides the well stablished role of nutrients, physical and environmental factors can enhance macroalgae growth as illustrated in Jamaica Bay. As a necessity for every photosynthetic organism, light is an essential physical factor to consider for macroalgae growth and becomes even more important at sediment level for benthic macrophytes (Taylor et al., 1995). *Ulva* blooms have a negative effect on seagrass ecosystems by blocking light exposure (Krause-Jensen et al., 2000) which consequently leads to the elimination of seagrass beds (McGlathery, 2001).

### 1.2.4.3 Salinity

Estuaries are transition environments where fresh and salty water meet, thus salinity gradients are found horizontally along river discharges and vertically. Previous research in laboratory, showed that low salinity concentrations decrease growth rates of *Enteromorpha Intestinalis* (especially under values of 15 psu) (Fong et al., 1996).

Salinity effects have been also tasted for Ulva species in a semi-enclosed elgrass bed ecosystem in Korea (Choi et al., 2010). In his laboratory experiment under non-limiting nutrient or light variability, showed that extreme salinity levels (Less 15 psu

and greater than 25 psu) decreased growth rates of the specie *Ulva pertusa*. Other studies have found that *Enteromorpha I.* cannot survive for long time under 0 psu conditions (Kamer et al., 2004). When tested simultaneously: Low salinity and nitrogen enrichment, the negative effect of salinity alone was ameliorated by the excessive N additions (Kamer & Fong, 2000). This can lead to algae proliferation in the winter when nitrogen and freshwater inputs are high, with even greater growth in the summer if nutrient inputs continue (Kamer et al., 2001).

Therefore, bloom forming species such as *Ulva* and *Enteromorpha* can tolerate a wide range of salinity levels (Choi et al., 2010; FitzGerald, 1978), and can proliferate even with moderate salinity fluctuations (Kamer & Fong, 2000) as the expected on field. Reductions in salinity are of lesser importance than the presence of high nutrient levels (CEFAS, 2003)) and macroalgae blooms are still expected if nutrient inputs are not reduced (Kamer et al., 2001).

### 1.2.4.4 Physical and morphological factors

For a Swedish shallow coastal site, Pihl et al. (1999) described how physical factors such as wave and wind exposure, constitute an important factor decreasing the effect of high nutrient concentrations. This effect has been studied within the UK coast, for the Medway estuary. The Medway is characterized for having high nutrient concentrations and a relatively small presence of opportunistic macroalgae compared with other less enriched sites (Aldridge & Trimmer, 2009). For this estuary it was found that besides nutrient concentrations, site-specific hydrodynamic factors

such as tide and wave exposure, bathymetry and turbidity play an important role limiting macroalgae growth. This was explained by the water mixing occurring with high wave exposure and consequently nutrient dissipation (Aldridge & Trimmer, 2009).

A main concern for bloom management, has been the reduction of nutrient inputs on coastal ecosystems from external anthropogenic sources. In the case of Argideen estuary in Ireland, despite the efforts from the government and agricultural industry of preventing N and P to reach coastal environments (Humphreys, 2008), high nutrient concentrations have remained (Ni Longphuirt et al., 2016), compared with two Irish estuarine systems (Argideen and Black water estuaries) with similar nutrient loadings but different hydrological regimens. While the Argideen has a shallower average depth with a greater intertidal area (70%), in the Black Water the intertidal area only covers a 37% of the estuary, residence water time being three times greater for the Black Water. Another notable difference is the freshwater input to the estuaries where annual averages are 106.6 $m^3/s$ and 2.5 $m^3/s$ for the Argideen and the Black Water respectively. Showing that river flow variability and water residence time influenced the source and number of nutrient inputs into both estuaries.

From these previous cases it seems clear that factors such as, tidal energy, wave movement, water residence times and hydrological regime play an important role decreasing the chances to develop a bloom even when nutrient concentrations are high enough. However as pointed out by (Bermejo et al., 2019), this cannot be

generalized for all macroalgae, not even between *Ulvae* sub species. He highlights the importance of the morphology of the macrophyte specie triggering the bloom, as wave energy and wind are more likely to affect floating than sediment-attached macroalgae. While tubular morphologies tend to be buried into the sediment, laminar *Ulva* is usually found free-floating or tangled in the tubular canopy.

### 1.2.1 Marine Sediment properties

Characteristics of marine sediments such as composition, grain size and organic C content are important determiners for nutrient availability and porewater exchange (CEFAS, 2003). Sandy sediments are liked with high rates of porewater exchange (Idestam-Almquist & Kautsky, 1995). It has been widely accepted that sediment nutrients can be an important source for macroalgae (Bermejo et al., 2019; Kamer et al., 2004; Kregting et al., 2008; Pedersen & Borum, 1997; Pihl et al., 1999) and can support future blooms on early growth season (Robertson & Savage, 2018; Trimmer et al., 2000) even if management measures have previously reduced nutrient concentrations in the water column (Bermejo et al., 2019). In the conceptual model proposed by Corzo et al. (2009), it is described how the mineralisation of the bloom detritus by highlighting the role of nutrient recycling in fueling macroalgal proliferation, thus sustaining the bloom (Figure 4).

Some studies have attempted to measure the amount of benthic remineralised nutrients utilised by macroalgae compared to water column. In a combined study

with laboratory and field measurements Sundback et al. (2003), estimated that benthic efflux of inorganic nutrients could supply up to 55% to 100% of the estimated nitrogen demand and 30 to 70% of the phosphorus need for the macroalgae growth. Furthermore, the amount and type of benthic infauna play a crucial role in determining the availability of pore water nutrients for macroalgae. It is suggested that this process can be the cause of the time lag between the decrease of nutrient supply and improvements in the macroalgae bloom conditions (Sundback et al., 2003).

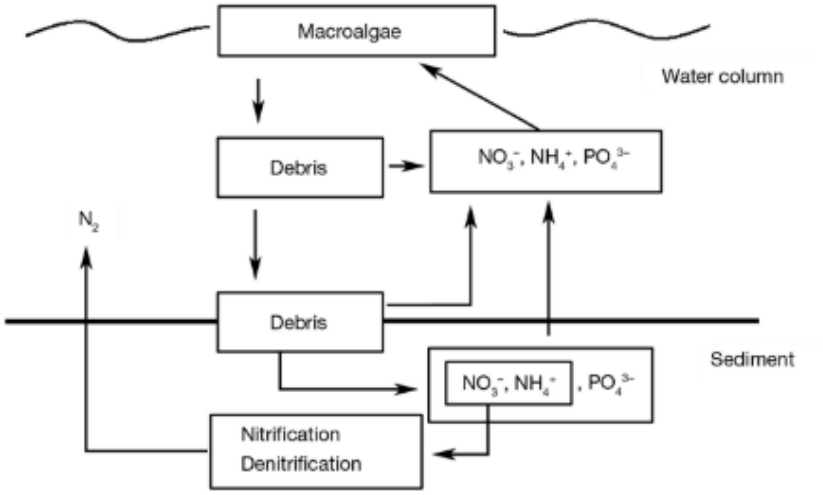


**Figure 4. A conceptual model illustrating nutrient dynamics during a macroalgal bloom, depicting interactions between macroalgae, the water column, and sediment. The macroalgae contribute organic debris to both the water column and sediment. This debris undergoes decomposition, releasing inorganic nutrients such as nitrate ($NO_3^-$), ammonium ($NH_4^+$), and phosphate ($PO_4^{3-}$) into both the water column and the sediment. In the sediment, nitrification and denitrification processes further influence the availability of nitrogen, with nitrogen gas ($N_2$) being released from the sediment. (Corzo et al., 2009).**

Measurements of the exact fraction of N and P released from the sediment and captured by the macroalgae to sustain growth are likely to variate depending on the physiological state of the macroalgae and hydrodynamic conditions (Corzo et al., 2009). However, this might not be the case for a great portion of shallow estuaries where the macroalgae bloom problem is recurrent.

## 1.2.2 Benthic Ecosystem Functions

### 1.2.2.1 Bioturbation and bioirrigation

To provide context for the understanding of the impacts of coastal eutrophication, the following section gives a background introduction to important benthic ecosystem functions. Bioturbation is an important process of benthic infauna and includes deposit feeding, reworking, constructions of burrows and tubes and irrigation of sediments (Rosenberg et al., 2001). Kristensen et al. (2012), proposed a definition of the term bioturbation in aquatic environments: “All transport processes carried out by animals that directly or indirectly affect sediment matrices. These processes include both particle reworking and burrow ventilation” (p.4). Bioturbation plays a crucial role oxygenating and mixing the sediments, controls biogeochemical processes and redox conditions at the bottom (Levin et al., 2009; Solan et al., 2004).

Bioturbation is a relevant process for the organic carbon cycle, most of the organic carbon is remineralised within the bioturbated upper sediment (Aller, 1994). This decomposition is enhanced by the $O^2$ penetration into the benthos. The transition

zone between well-oxygenated and poorly oxygenated sediments is known as Redox Potential Discontinuity (RPD). This layer is often characterised with a grey colour above the black anaerobic zone. The depth and specific chemical conditions of the RPD is dependent on faunal bioturbation, burrowing, and feeding voids (Rosenberg, 2001a). An excess of organic matter at the sediment surface will increase oxygen consumption and consequently reduce the depth of the RPD (Rosenberg, 2001a). Therefore, bioturbation is used as an indicator of environmental change (Murray et al., 2017).

As a consequence of sediment mixing, irrigation of deeper sediments takes place by benthic infauna. Animals need dissolved oxygen for respiration, and this is transported into deep sediments through the process of bioirrigation (Rosenberg, 2001a). Bioirrigation is the enhanced exchange between pore water and overlying water column as a result of active or passive burrow flushing as well as pumping to fluidize sediments to facilitate peristaltic burrowing (Gooday et al., 2009). This process influences nutrient dynamics in the sediments and porewater nutrient profiles (Renz & Forster, 2014). Lack of bioirrigation within sediment causes increased concentrations of ammonium, phosphate, silicate, and sulphide in the porewater (Volkenborn et al., 2007).

External disturbances in benthic ecosystems have been demonstrated to directly affect faunal activity. Different interactions have been tested between faunal activity and ecosystem changes to evaluate impacts on bioturbation. Some studies have

focused on assessing how hypoxia affects particle reworking; there is evidence of reductions in bioturbation by metazoans, meiofauna and macroinfauna (Levin et al., 2009). Other studies have analysed how bioturbation and bioirrigation of sediments by certain species can influence oxygen and solute fluxes (Mermillod-Blondin et al., 2004). However, eutrophication impacts on bioturbation and bioirrigation processes have received less attention and only few studies have analysed the impacts of organic enrichment on bioturbation activities (Murray et al., 2017; Dimitriou et al., 2017).

In their study, Murray et al. (2017) evaluated particle reworking by *H. diversicolor* with changing levels of environmental conditions including algae derived organic matter. Powdered *U. intestinalis* was used to enrich the sediment surface. Bioturbation was measured using fluorescent Sediment Profile Images and fluorescent dyed particles (Luminophores <250μm), consequently luminophore depths were measured showing that the mean mixed lum depth of sediment mixing was affected by algal enrichment, increasing the length of particle reworking at 1g of enrichment, however for 2 g and 3 g burrowing depth were less compared to the control at 1g of enrichment. They identified a significant algal enrichment effect on particle reworking activity.

In a mesocosm experiment conducted in the eastern Mediterranean (Dimitriou et al., 2017), evaluated the response of ecosystem functioning along a eutrophication gradient. In this experiment they measured bioturbation potential (BPc), an index

created by Solan et al. (2004), which relates community abundance and biomass with information about life traits of specific taxa. BPc describes modes of sediment reworking and mobility of benthic infauna.

However, they did not measure bioturbation rates directly. At the end of the experiment, they found that an increase in organic matter in the sediment caused changes in macrofaunal community structure by promoting an increase in abundance of deposit-feeding species, consequently enhancing bioturbation of the sediments. This increase in bioturbation and high organic matter consumption prevented development of hypoxia, buffering detrimental effects of eutrophication. Nonetheless, only this study was found linking the stressor of eutrophication and bioturbation and none in the case of bioirrigation. This highlights the need for experiments relating the pressure of eutrophication with these two important ecosystem functions.

### 1.2.2.2 Organic carbon cycling

Inputs of organic matter into marine sediments can be either from terrestrial or marine origin (Burdige, 2007). Whereas marine organic matter is produced within the system (Autochthonous) mainly by primary producers, terrestrial originated organic matter (Allochthonous) is produced out of the system (Pinckney et al., 2001). Burial of organic matter into marine sediments removes $CO_2$ and provides atmospheric oxygen, being an important process in long-term climate regulation (Diesing et al., 2017).

In order for organic carbon to be stored on a long-time scale organic matter must sink through the water column and escape degradation (Hedges & Keil, 1995) 99.5% of the total organic matter input in the ocean is remineralized (respired) and only a 0.05% is buried in marine sediments (Burdige, 2007). A number of variables have been identified as important in governing the efficiency with which organic carbon is preserved in sediments. These include sedimentation rate, oxygen availability, interaction with particle surfaces, and the activity of benthic faunal communities. However, these factors involved in organic matter burial have complex interactions, and the overall controls on organic matter burial are not yet well understood (Burdige, 2007; LaRowe et al., 2020).

Sediment chemistry plays an important role in the way that organic matter is processed as redox reactions govern the seafloor biogeochemistry (Lønborg & Søndergaard, 2009). Benthic bioturbation, irrigation and structures building, are important mechanisms by which benthic fauna can oxygenate deeper sediments (Rosenberg, 2001a). In the absence of oxygen, nitrate, redox-active metals: $Mn^{2+}$ and $Fe^{2+}$, and eventually $SO_4^-$ act as electron acceptors to oxidize organic matter (Hedges & Keil, 1995).

The highly productive nature of coastal systems and their location near continental margins, makes organic matter preservation patterns more complex due to sediment deposition and resuspension events plus horizontal particle transport (Middelburg, 2018). Coastal sediments, can also be subject of changing redox conditions referred

to as redox oscillations, altering between oxic and anoxic conditions as a consequence of macrobenthic bioturbation and bioirrigation processes (Burdige, 2007). Benthic macrofaunal activity can affect the amount of organic matter buried in sediments because its presence enhances remineralisation (Burdige, 2007) which is typically related to less organic matter preservation (Hedges & Keil, 1995).

The combination of different stressors into marine ecosystems such as global warming, acidification and eutrophication will impact the way carbon is processed in sediments (LaRowe et al., 2020). Eutrophication signs such as nutrient enrichment, macroalgae blooms and hypoxia have an effect in the way organic matter is processed. The presence of macroalgae modify the organic matter decomposition within the sediments since the oxygen availability is reduced with depth, decreasing the portion of organic matter that can be aerobically mineralized (Corzo et al., 2009).

### 1.2.2.3 Carbon stocks

In order to better understand how biogeochemical processes influence carbon cycling and how the functioning will be affected in the future due to anthropogenic pressures, it is required to quantify the stock of organic carbon stored within marine sediments (Diesing et al., 2017). Recent studies have measured carbon stocks in vegetated sediments known for their large storage capacity (Duarte et al., 2013), Mangrove (Garcias-Bonet et al., 2019), salt marshes (Geoghegan et al., 2018) and elgrass ecosystems (Kindeberg et al., 2018). However, less much information is known about carbon stocks in coastal unvegetated sediments, which difficult comparisons between vegetated and unvegetated carbon stocks (Kindeberg et al., 2018).

Using existing data of particulate organic carbon stocks, Diesing et al. (2017), proposed a quantitative spatial model to predict values for carbon stocks in the Northwest continental shelf. The model considers the following variables: mud content, annual average water column bottom temperature, eastings, distance to shoreline, gravel content and peak wave velocity, being mud content the most relevant one. Finding an important association between the amount of organic matter stored and coarse-grained sediments.

Riekenberg et al. (2018), studied the potential storage of unvegetated microphytobenthic dominated sediments and how nutrient enrichment affects the amount of organic carbon buried in short-term using labile $^{13}C$. At 30 days of their

experiment, the amount of organic C buried into the sediments accounted for 58 and 54% for ambient and low treatments respectively; contrastingly, for moderate and elevated treatments, increased nutrient loading reduced organic C retention considerably. They concluded that the combination of increased nutrient inputs and bare photic sediment, might resulted in considerable release of previously captured carbon leading to a substantial reduction of carbon storage potential.

### 1.2.3 Blue carbon and macroalgae

In 2009 a revolutionary report published jointly by United Nations Environment Program (UNEP), Food and Agriculture Organization of the United Nations (FAO) and The United Nations Educational, Scientific and Cultural Organization (UNESCO); This report recognises the importance of the oceans in the global C cycle, defining blue carbon for the first time as all the carbon captured by marine organisms (Nelleman, 2009). Coastal vegetated ecosystems such as seagrasses, mangroves and saltmarshes are known for being carbon sinks and and therefore blue carbon ecosystems (Mcleod et al., 2011; Lovelock & Duarte, 2019). It's been estimated that these vegetated coastal ecosystems that cover <2% of the ocean surface, account for almost 50% of all carbon burial in the ocean (Duarte, 2005).

Although salt marshes, mangrove and seagrasses are recognized for having a considerable high organic C burial rate (4.8-87.35, 22.5-24.935 and 48-1125 TgC $yr^{-1}$ respectively), its worldwide area extension of is small compared to 3 400 000 101

$km^2$ for macroalgae (Duarte et al., 2013). Recently, multiple studies have evaluated the possibility to include macroalgae as part of blue carbon stocks (Hill et al., 2015; Hardison 2010; Krause-Jensen et al., 2018; Raven et al., 2018; Duarte et al., 2013).

Most macroalgae species grow either attached to rocks or free floating (Luning, 1990), whereas marine angiosperms have roots that are directly in contact with the sediment. Therefore, has been hypothesised that macroalgae can contribute to carbon sequestration by transportation to the depositional areas rather than contributing directly within the production site (Hill et al., 2015; Trevathan-Tackett et al., 2015; Krause-Jensen & Duarte, 2016) (Figure 5). Brown macroalgae has been the primary focus on these new studies on macroalgae derived carbon, the thickness and chemical structure of these species such as Fucales and Laminariales, makes them more resistant to degradation and their buoyancy capacity makes them more likely to be transported to depositional sites (Krause-Jensen, 2018), compared to green macroalgae that lack polysaccharide components, making them more easily degradable (Hill et al., 2015).

A priority into blue carbon research is the provenance of the organic C (Krause Jensen 2018, Graves, 2021), in other words the origin of the organic C. In order to identify whether macroalgae derived C is being stored and ultimately preserved, evidence of its presence in organic C stocks is required. Recently, eDNA studies have found the presence of macroalgae derived carbon in mangrove (Ortega 2019) and deep sea sediments (Ortega 2020).

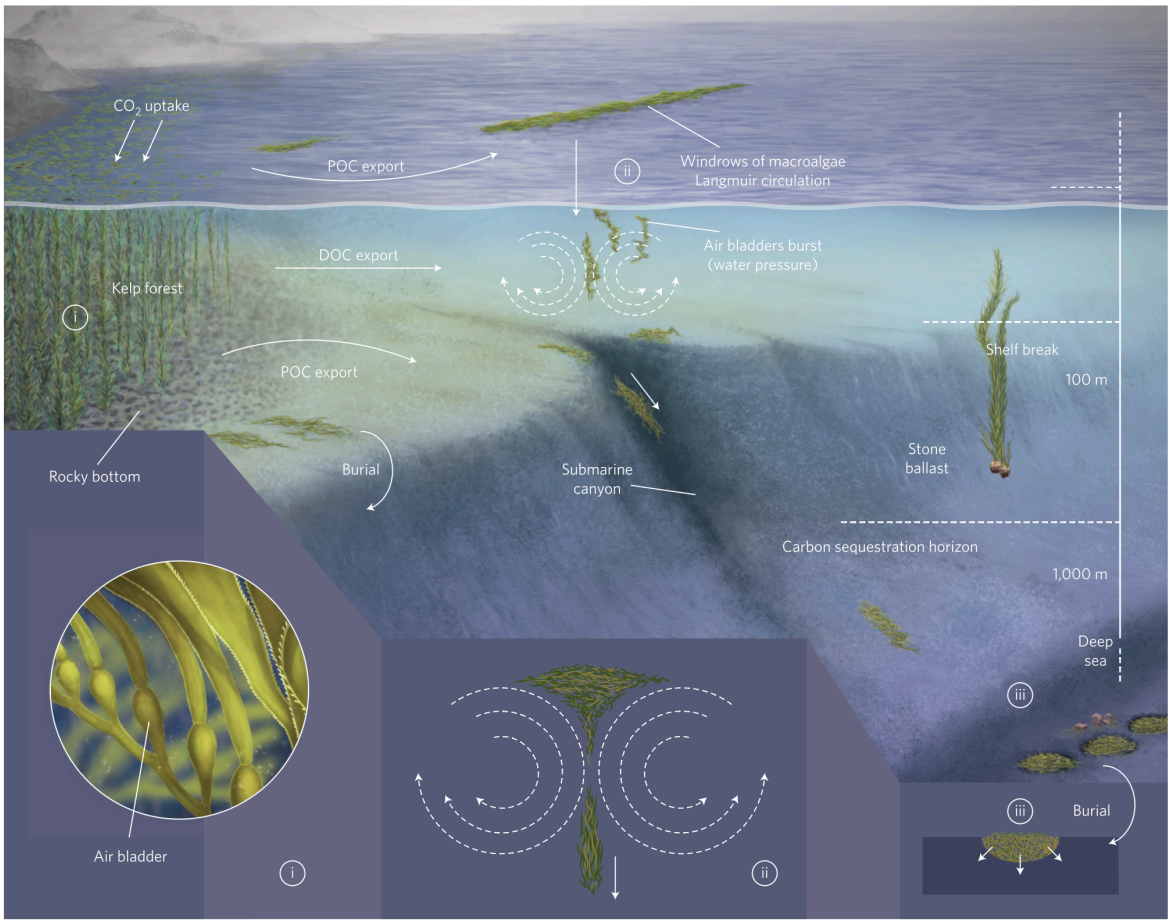


**Figure 5. Diagram of the pathways for export and sequestration of macroalgal carbon. Air bladders can facilitate movement of macroalgae biomass, from production site (i) fragments of macroalgae are transported to depositional environments (ii) and ultimately be either sequestered in the deep sea or buried within deep sediments (iii). From (Krause-Jensen & Duarte, 2016).**

On the other hand, unvegetated coastal sediments have been less investigated in their role on the organic C cycling (Endo and Otani, 2019; Chen and Lee 2022; Kuwae 2021; Riekenberg, 2018). Unvegetated coastal areas are also commonly referred as tidal flats, mudflats and intertidal flats. Coastal intertidal areas are highly productive areas, and they are dominated by microphytobenthos, benthic

macroalgae and phytoplankton primary productivity (Watanabe, et al. 2015; Riekenberg, 2018)

Zhang et al., (2020), compared surface sediment organic C content of 14 intertidal areas in China, by comparing estuarine vs non estuarine intertidal areas it was concluded that estuarine C stocks were comparable with those in shelf areas potentially being important carbon sink areas. Although is clear that more information about organic C in unvegetated ecosystems is required to compare it to vegetated coastal ecosystems recognizing these sites as relevant carbon sinks is an important step.

Opportunistic macroalgae blooms affect intertidal areas with excessive primary productivity, however it is unclear if this type of algae can contribute to sediment C stocks. While some studies have found an increase in organic C after experimental addition of *Ulva* detritus (Corzo et al., 2009), others have not found a significant difference between presence or absence neither after a period of macroalgae addition (Garcia-Robledo, 2011). Additional evidence is needed to clarify whether macroalgal blooming species can contribute to sedimentary organic carbon stocks and to better understand the implications for sediment biogeochemistry.

## 1.3 Thesis outline

The overall aim of this thesis is to investigate the factors controlling macroalgal blooms in UK estuaries and to evaluate how macroalgae blooms impact sediment carbon storage. Indubitable macroalgae blooms are a problem present in coastal ecosystems around the world, however it is valuable to know if this problematic increase in macroalgae production enhanced by eutrophication can be translated into carbon storage.

The present piece of work consists of an introduction chapter, followed by four data chapters and ultimately a synthesis chapter. Next, a brief summary of each data chapter is presented with key research questions. In Chapter 2, historical secondary data was analysed to identify factors contributing to the development of macroalgae blooms in the UK estuaries. The chosen sites for the analysis include estuaries with a history of nutrient enrichment and eutrophication symptoms and persistent macroalgae blooms. Besides, results on historical classifications of eutrophication status and water quality ratios are compared to the degree of impact on the different systems. Research questions addressed in this chapter include:

**RQ1:** How do trends in annual and winter water column nutrient enrichment influence the development of macroalgae blooms in UK estuaries?

**RQ2:** To what extent physical factors such as slope and tidal ranges promote growth of opportunistic macroalgae in UK estuaries?

**RQ3:** Is there a direct link on macroalgae cover and field measurements of biomass with classifications of Eutrophication status and water quality ratios in UK estuaries?

Sediment biogeochemistry of three estuaries in the UK south coast is analysed in Chapter 3. Results from field work conducted in Portsmouth, Langstone and Poole Harbours, are presented to evaluate the impacts of macroalgae blooms in these estuaries from sediment cores and porewaters samples. Research questions in this chapter are:

**RQ4:** Are there major spatial differences in sediment biogeochemistry between sites and macroalgae presence and absence of macroalgae?

**RQ5:** To what extent benthic nutrients promote the persistence of the macroalgae blooms?

**RQ6:** Do macroalgae blooms promote more storage of organic carbon in sediment from intertidal zones?

In Chapter 4, results from seasonal sampling in Langstone Harbour through three different seasons are evaluated to look for sediment biogeochemistry differences in the impacted site. The research questions that motivated this data chapter are:

**RQ7:** To what extent do macroalgae blooms impacts on sediment biogeochemistry change through different seasons?

**RQ8:** Is there an impact of seasonality on sediment carbon storage?

Chapter 5 explores the combination of methods to explore the possibility of identifying macroalgae carbon in sediment carbon stocks. The methods used include CuO oxidation products, triple bulk stable isotopes ($\delta^{13}C$, $\delta^{15}N$ and $\delta^{2}H$), and elemental analysis. Key research questions in this chapter include:

**RQ9:** To what extent is it possible to identify macroalgae derived as a source of organic carbon in sediment carbon stocks with the proposed methods?

**RQ10:** Are there particular CuO oxidation products characteristic of green macroalgae that can potentially be used as biomarkers to track macroalgae carbon in intertidal sediments?

**RQ11:** Are there differences in discrimination by these methods between different groups of macroalgae?

Chapter 2.

# Factors controlling macroalgae blooms in UK south coast estuaries

## 2.1 Introduction

This chapter will present the results of the analysis of secondary data with the aim of identifying factors contributing to the development of macroalgae blooms in south coast UK estuaries. Sites chosen for this analysis are estuaries with different eutrophication status and responses to nutrient enrichment. The research questions that will be addressed in this chapter are:

**RQ1:** Do annual and winter water column nutrient enrichment influence the development of macroalgae blooms in UK estuaries?

**RQ2:** To what extent physical factors such as slope and tidal ranges promote growth of opportunistic macroalgae in UK estuaries?

**RQ3:** Is there a direct link on macroalgae cover and field measurements of biomass with classifications of Eutrophication status and water quality ratios in UK estuaries?

# 2.2 Background

## 2.2.1 Legal framework for monitoring eutrophication in the UK

As previously described in section 1.2.4, the factors that influence development and persistence of macroalgae blooms are a combination of physical, environmental, and anthropogenic stressors in coastal ecosystems. Strategies to prevent eutrophication in the marine environment within UK estuaries started in the early 1990's with the implementation of the Nitrates Directive (ND, 91/676/EEC) and the Urban Wastewater Treatment Directive (UWWTD, 91/271, EEC), both legislative instruments aimed to regulate nutrient pressure on coastal ecosystems.

This chapter will compare the eutrophication status of the UK south coast estuaries from historical OSPAR eutrophication status results, the WFD Ecological Quality Ratio results for available years and records of nutrients and physical parameters from the Environment Agency (EA) to evaluate possible factors that control macroalgae blooms in these sites.

### 2.2.2 Water Framework Directive (WFD)

Another important regulation that requires the assessment of macroalgal bloom for transitional and coastal waters in the UK is the Water Framework Directive (WFD/200/06/EC). WFD was effectively implemented in December of 2000, with the objective of achieving a good biological and ecological status in the UK waterbodies by 2015. This legislation applies for river basins, groundwater, lakes, transitional and coastal waters, the biological elements evaluated for transitional waters include the abundance and composition of phytoplankton, macroalgae, marine angiosperms, benthic invertebrates, and fish. Whereas the abundance and composition of phytoplankton, aquatic flora (marine macroalgae and angiosperms) and benthic invertebrates are considered for the evaluation of coastal waters (Wells, 2010).

The WFD United Kingdom Technical Advisory Group (UK-TAG), helped to stablish the reference conditions (boundary values) for the water bodies so the future deviation from these levels could be assessed (Wells, 2010). Definitions for ecological status related to macroalgae in transitional and coastal waters are presented in (Table 2). To assign a numeric value indicating deviation from reference conditions, the Ecological Quality Ratio (EQR), a multiparameter metric, is used, with scores ranging from 0 (Bad) to 1 (High).

**Table 2. Ecological status as defined in the Water Framework Directive for the evaluation of coastal and transitional waters in relation to the biological element of macroalgae.**

| Ecological status | Coastal Waters | Transitional Waters |
|---|---|---|
| **HIGH** | All disturbance-sensitive macroalgae associated with undisturbed conditions present. The levels of macroalgal cover are consistent with undisturbed conditions. | The composition of macroalgal taxa is consistent with undisturbed conditions. There are no detectable changes in macroalgal cover due to anthropogenic activities. |
| **GOOD** | Most disturbance-sensitive macroalgae associated with undisturbed conditions are present. The level of macroalgal cover shows slight signs of disturbance. | There are slight changes in the composition and abundance of macroalgal taxa compared to the type-specific communities. Such changes do not indicate any accelerated growth of phytobenthos or higher forms of plant life resulting in undesirable disturbance to the balance of organisms present in the water body or to the physicochemical quality of the water. |
| **MODERATE** | Macroalgal cover is moderately disturbed and may be such as to result in an undesirable disturbance in the balance of organisms present in the water body. | The composition of macroalgal taxa differs moderately from type specific conditions and is significantly more distorted than at good quality. Moderate changes in the average macroalgal abundance are evident and may be such as to result in an undesirable disturbance to the balance of organisms present in the water body. |
| **POOR** | Major alterations to the values of the biological quality elements for the surface water body type. Relevant biological communities deviate substantially from those normally associated with the surface water body type under undisturbed conditions. | Major alterations to the values of the biological quality elements for the surface water body type. Relevant biological communities deviate substantially from those normally associated with the surface water body type under undisturbed conditions. |
| **BAD** | Severe alterations to the values of the biological quality elements for the surface water body type. Large portions of the relevant biological communities normally associated | Severe alterations to the values of the biological quality elements for the surface water body type. Large portions of the relevant biological communities normally associated |

| | | |
|---|---|---|
| | with the surface water body under undisturbed conditions are absent. | with the surface water body under undisturbed conditions are absent. |

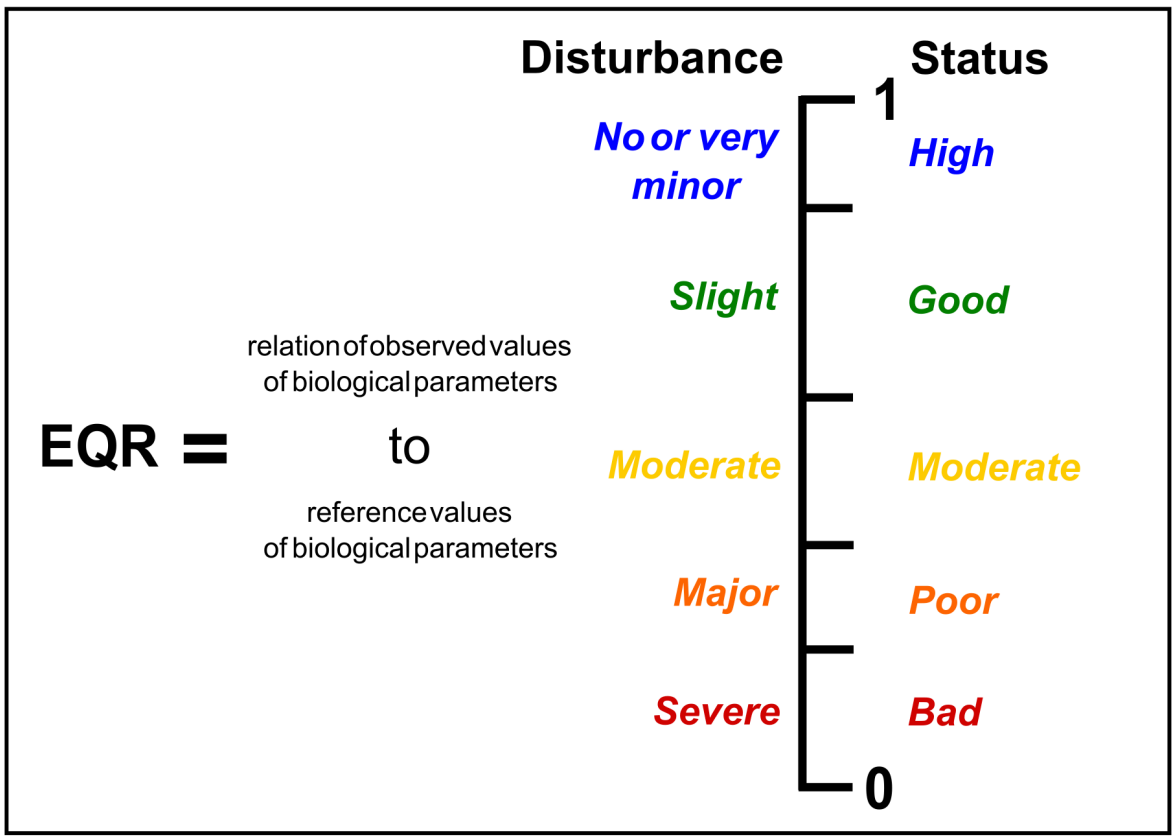


**Figure 6. Suggested Ecological Quality Ratio. The size of the bands differs because the boundaries between classes must align with the normative definitions, not a simple percentage. Modified from (Vincent, 2002).**

### 2.2.2.1 Opportunistic Macroalgal Blooming Tool (WFD).

The Opportunistic Macroalgal Blooming Tool (OMBT) is the guidance document describing the monitoring, assessment and classification of transitional and coastal waters as required by the Water Framework Directive (WFD). The OMBT index includes five metrics:

1. Percentage cover of the available intertidal habitat (AIH %)
2. Total extent of area covered by algal mats (affected area (AA) in hectares) or affected area as percentage of the AIH (AA/AIH, %)

3. Biomass of opportunistic macroalgae in AIH ($g/m^2$)
4. Biomass of opportunistic macroalgae in AA ($g/m^2$)
5. Presence of entrained algae (Percentage of quadrants)

Each variable is equally weighed, and the final result is a value between 0 (Major disturbance) to 1 (minimally disturbed or near reference) and is classified as follows: High= 0.80, Good= 0.60, Moderate= 0.40, Poor= 0.20.

### 2.2.3 OSPAR Common Procedure.

After the Oslo and Paris Commissions (OSPAR) in 1992, the most relevant conclusion was the creation of the Convention for the Protection of the Marine Environment (OSPAR Convention). By 1997, OSPAR established the Strategy to Combat Eutrophication with the Common Procedure for the Identification of Eutrophication Status of the OSPAR Maritime Area (OSPAR, 2017). The first application of the common procedure was carried out in 2003, the second official report was published in 2008 and third common procedure report in 2017.

OSPAR Common Procedure (COMP) is the key guideline for the identification of the eutrophication status in the OSPAR Maritime Area. The application of the COMP consists of two phases, the first phase is an initial screen identification of the areas where it is highly likely that eutrophication is not a problem. The second phase consists in the application of the Comprehensive Procedure which is defined as a

holistic assessment of the eutrophication status by direct assessment of ten parameters (Table 3).

**Table 3. Categories of assessment parameters for OSPAR common procedure for the evaluation of eutrophication status (OSPAR, 2017).**

| | | Assessment parameter |
|---|---|---|
| Category I | | ***Degree of nutrient enrichment*** |
| | 1 | Riverine inputs and direct discharges (area-specific)<br>Elevated inputs and/or increased trends of total N and total P (compared with previous years) |
| | 2 | Nutrient concentrations (Area-specific)<br>Elevated level(s) of winter DIN and/or DIP |
| | 3 | N/P ratio (area-specific)<br>Elevated winter N/P ratio (Redfield N/P = 16) |
| Category II | | ***Direct effects of nutrient enrichment (during growing season)*** |
| | 1 | Chlorophyll-a concentration (area-specific)<br>Elevated maximum, mean and/or 90 percentile level |
| | 2 | Phytoplankton indicator species (area-specific)<br>Elevated levels of nuisance/toxic phytoplankton indicator species (and increased duration of blooms) |
| | 3 | Macrophytes including macroalgae (area-specific)<br>Shift from long-lived to short-lived nuisance species (e.g *Ulva*). Elevated levels (biomass or area covered) especially of opportunistic green macroalgae. |
| Category III | | ***Indirect effects of nutrient enrichment (during growing season)*** |
| | 1 | Oxygen deficiency<br>Decreased levels (< 2 mg l-1 : acute toxicity: 2-6 mg l-1: deficiency) and lowered % oxygen saturation |
| | 2 | Zoobenthos and fish<br>Kills (in relation to oxygen deficiency and/or toxic algae)<br>Long-term area-specific changes in zoobenthos biomass ans species composition |
| | 3 | Organic carbon/organic matter (area-specific) |

| | | |
|---|---|---|
| | | Elevated levels (in relation to III.1) (relevant in sedimentation areas) |
| **Category IV** | ***Other possible effect of nutrient enrichment (during growing season)*** | |
| | 1 | Algal toxins |
| | | Incidence of DSP/PSP mussel infection events (related to II.2) |

COMP classifies the eutrophication status of a particular site into one of the three final categories: non-problem area, potential problem area and problem area. The application of the COMP is responsibility of the contracting parties (Countries with OSPAR Maritime Area designation), the assignment of a category is designated as follows, problem areas are areas showing increased degree of nutrient enrichment alongside direct and/or indirect effects Areas that show direct and/or indirect effects without evidence of increased nutrient enrichment can also be classified as problem areas (Table 4). The areas that show increased degree of nutrient enrichment, but without direct or indirect effects are classified as potential problem areas. Whereas the areas without nutrient enrichment nor direct/indirect effect are considered non-problem areas (Table 4).

**Table 4. Criteria for initial classification of Non-Problem Areas, Potential Problem Areas, and Problem Areas in Common Procedure.**

| | **Category I** Degree of nutrient enrichment Nutrient inputs Winter DIN and DIP Winter N/P ratio | **Category II** Direct effects Chlorophyll a Phytoplankton indicator species macrophytes | **Categories III and IV** Indirect effects/others possible effects Oxygen deficiency Changes/kills zoobenthos, fish kills Organic carbon/matter Algal toxins | **Initial classification** |
|---|---|---|---|---|
| A | + | + | + | Problem area[4] |
| A | + | + | - | Problem area[4] |
| A | + | - | + | Problem area[4] |
| B | - | + | + | Problem area[4 5] |
| B | - | + | - | Problem area[4 5] |
| B | - | - | + | Problem area[4 5] |
| C | + | - | - | Potential problem area[4] |
| C | + | ? | ? | Potential problem area[4] |
| C | + | ? | - | Potential problem area[4] |
| C | + | - | ? | Potential problem area[4] |
| D | - | - | - | Non-problem area[4] |

(+) = Increased trends, elevated levels, shifts or changes in the respective assessment parameters in Table 1

(-) = Neither increased trends nor elevated levels nor shifts nor changes in the respective assessment parameters in Table 1

? = Not enough data to perform an assessment or the data available is not fit for the purpose

Note: Categories I, II and/or III/IV are scored '+' in cases where one or more of its respective assessment parameters is showing an increased trend, elevated level, shift, or change.

Results of eutrophication status are published by OSPAR in a final report for a specific period, the first COMP report published in 2003 comprises data from 1990-2001, second COMP published in 2008 includes data from the period 2001-2005

and the latest third COMP report from 2017 includes data assessed between 2006 and 2014.

# 2.3 Methods

## 2.3.1 Secondary data collection

### 2.3.1.1 Slope

Slope was extracted from the SurfZone Digital Elevation Model 2014 (Environment Agency, 2020) using ArcMap. The Digital Elevation Model (DEM) used is the best currently available covering the inter-tidal zone produced by the Environment Agency. The DEM was delimited only for the areas of interest, using masking tool. Slope was extracted by mask using the “slope” tool in zonal statistics.

Mean slope for the intertidal zone was calculated and used as a constant value in the data set for correlation analysis. A more detailed data set was created extracting slope values for specific locations where biomass data was also available, to test for correlation of slope and biomass.

### 2.3.1.2 Water column nutrients and other physical parameters

Water column nutrients data was obtained from the Environment Agency historical dataset for coastal and transitional waters. This dataset is comprised by 134 water bodies and 17 water quality parameters for the period of 2000-2019. Data was filtered for the sites of interest: Chichester, Christchurch, Langstone, Medway, Poole, Portsmouth and Swale; and parameters total nitrogen, nitrate, nitrite, orthophosphate, N:P ratio, temperature, dissolved $O_2$, salinity and suspended particulate matter. Generally, there was a monthly sample for physical parameters

such as temperature, dissolved $O_2$ salinity, however nutrient sampling was less frequent and variable time gaps in water column data was commonly observed in all sites, these gaps were as little as a single month up to years. Mean annual and winter values will be discussed within this chapter and in most cases, data was enough to confidently calculate these representative means unless stated otherwise. Uncertainties in time gaps with no water column nutrient data will be therefore acknowledged when discussing the results.

Physical parameters of estuaries flushing time, area at high water and tidal ranges were extracted from the Enlaced UK Estuaries database (Manning, 2012).

### 2.3.1.3 Macroalgae biomass

Macroalgae Biomass ($g/m^2$) values were obtained from the remote sensing from the EA monitoring survey a macroalgae patch is comprised by two or more quadrants of 0.25 $m^2$ and each biomass value corresponds to a quadrant (Figure 7).

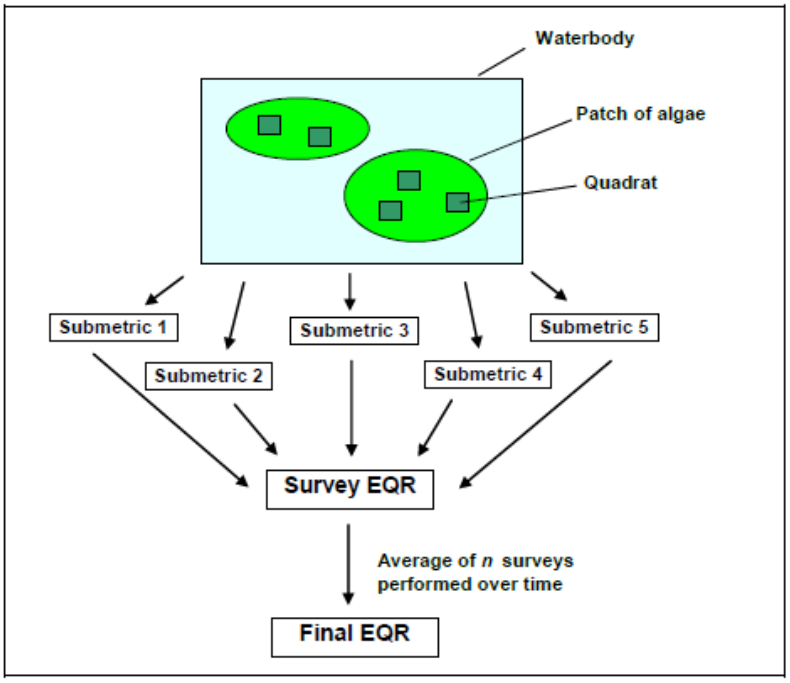


**Figure 7. Sampling scheme for opportunistic macroalgae. (Environment Agency, Confidence of Class for WFD Marine Plant Tools 2013).**

Biomass values were filtered and obtained for the available years of the sites of interest. Peak macroalgae blooms are generally monitored in summer (June to September), although some growth peaks can be developed in spring and occasionally in late summer or early autumn (UKTAG, 2014). Biomass data was within the datasets of macroalgae cover (GIS), the information was exported from these files however biomass data is collected from the field by the Environment Agency as a requirement for eutrophication assessments.

In order to obtain a representative biomass value of the estuaries per available surveyed year, biomass of Affected Area (AA) ($g/m^2$) was selected as it is representative from the biomass production in the impacted areas, rather than the

biomass for the whole Available Intertidal Habitat. Biomass of affected area g/m$^2$ was calculated as stated in the OMBT (UKTAG, 2014) (Equation 1), for the multiple biomass values provided within the dataset corresponding to the quadrants sampled for each macroalgae patch as illustrated in (Figure 7).

**Equation 1. Biomass of AA. As required for the calculation of Ecological Quality Ratio (EQR) for Water Framework Directive (Environment Agency, 2012).**

$$Total\ Biomass\ (g) = \left(\sum patch\ size\ (m^2)\right)\ x\ average\ biomass\ for\ the\ patch\ \left(\frac{g}{m^2}\right)$$

$$Biomass\ of\ AA\ \left(\frac{g}{m^2}\right) = Total\ Biomass/AA$$

## 2.3.1.4 Macroalgae cover

In order to calculate percentage of macroalgae cover, area at high tide (Ha) and the occupied area by macroalgae (Ha) values were utilized. Macroalgae cover was calculated by dividing the area affected for macroalgae (Ha) into the area of the Available Intertidal Area for each estuary and year available. Macroalgae cover density was also extracted from the All_OM_Quads_2008to2017 data source for each estuary using GIS.

### 2.3.2 Data Analysis

Basic statistics were calculated in RStudio using the summarise function within the dplyr package. All plots within this chapter were produced in RStudio with the ggplot2 package except for the macroalgae cover that was within ArcGIS as previously described in Section 2.3.1.4.

Normality and Spearman's rank correlations tests were done in RStudio to explore relationships between water quality variables and physical variables with macroalgae cover and biomass.

# 2.4 Results

## 2.4.1 Eutrophication assessment

The available classifications for the different estuaries in the UK related to eutrophication are presented in Table 5, there is a discrepancy between the available results for different years and sites however comparisons will be made when possible, with emphasis in trends over time. Reports of OSPAR eutrophication status were published on the years 2003, 2008 and 2017 and the estuaries included in this classification include Chichester, Langstone, Poole and Portsmouth Harbours.

Chichester has maintained its status as a problem area in the three available OSPAR reports, whereas Langstone was classified as a problem area in 2003 and 2008 but improved to potential problem area in the latest report of 2017. Poole Harbour worsen its eutrophication status from potential problem area in the first two assessments to problem area in the third application and lastly, Portsmouth maintained its problem area classification on the three applications of the COMP (Table 5).

EQR in Chichester improved from moderate in 2009 to good status in 2018. Likewise, Christchurch improved its good to high status from 2012 to 2013. Langstone has sustained its moderate status since 2009 to the latest measurement in 2019, nonetheless in 2011 recorded a higher classification of good status. On the other hand, Medway has only achieved a good status in the evaluated years of 2008, 2015 and 2018 (Table 5).

Poole Harbour recorded a poor status in the years 2008, 2011 and 2015 although in the latest evaluation in 2022 improved to a moderate status. Portsmouth achieved a moderate status in all the available years except for 2015 where a poor status was obtained. And finally, Swale has maintained its good quality status from 2008 to 2017 (Table 5).

### 2.4.2 Biomass

Mean biomass of AA ($g/m^2$) from the sites evaluated, varied from 25.6 - 1891 $g/m^2$. The lowest biomass was recorded in Christchurch (2013), considerably differing from the previous year 2012 (376 $g/m^2$). In 2008 Swale, registered a biomass of 474 $g/m^2$, the following surveyed year (2012) had the highest biomass in this site, 955 $g/m^2$, however this value decreased substantially to 60 $g/m^2$. In Langstone Harbour, there was a decrease in biomass from 2009 to 2011 (463 to 268.6 $g/m^2$) regardless of this, the most recent record in 2014 has the highest biomass value for Langstone of 603 $g/m^2$. (Table 5).

Lastly, Poole Harbour had the highest biomass of all sites and biomass ranged from 985 - 1891 $g/m^2$, the lowest biomass was in 2009 while the highest biomass was recorded in 2008. The latest years surveyed in Poole Harbour were 2014 and 2015, both with similar biomass of 1141 $g/m^2$ and 1315.5 $g/m^2$ respectively (Table 5).

**Table 5. Table showing macroalgae biomass extension in estuaries biomass of available intertidal area (g/m$^2$), Affected area (Ha), Macroalgae cover of AIH (%), alongside Ecological Quality Ratio (EQR) and OSPAR eutrophication status and for the available years. Christchurch, Medway and Swale are not included in OSPAR evaluation for eutrophication status. EQR classifications are only shown for the specific biological quality element of opportunistic macroalgae as is the focus of this comparison, and therefore is not representative to the whole waterbody.**

| Estuary | Year | Biomass of Affected Area (g/m$^2$) | Affected area (Ha) | Macroalgae cover of AIH (%) | Ecological Quality Ratio | Eutrophication status OSPAR (2003) | Eutrophication status OSPAR (2008) | Eutrophication status OSPAR (2017) |
|---|---|---|---|---|---|---|---|---|
| Chichester | 2009 | 334.5 | 1020.9 | 33.6 | Moderate | Problem Area | Problem Area | Problem Area |
| | 2011 | 322.5 | 1069.5 | 35.2 | Moderate | | | |
| | 2014 | 518.7 | 392.6 | 19 | Moderate | | | |
| | 2018* | | 470.3 | 16 | Good | | | |
| Christchurch | 2012 | 376.2 | 5 | 2.6 | Good | Not assessed | Not assessed | Not assessed |
| | 2013 | 25.6 | 9.4 | 4.8 | High | | | |
| Langstone | 2009 | 463.3 | 476.7 | 24.9 | Moderate | Problem Area | Problem Area | Potential Problem Area |
| | 2011 | 268.6 | 572.3 | 29.9 | Good | | | |
| | 2013 | | | | Moderate | | | |
| | 2014 | 603.8 | 511.2 | 26.7 | Moderate | | | |
| | 2015 | | | | Moderate | | | |
| | 2016 | | | | Moderate | | | |
| | 2018* | | 364.4 | 25.1 | | | | |

| | | | | | | | | |
|---|---|---|---|---|---|---|---|---|
| | 2019 | | | | Moderate | | | |
| Medway | 2008 | 788.1 | 2000 | 32 | Good | Not assessed | Not assessed | Not assessed |
| | 2012 | 419.5 | 386.6 | 6.2 | Good | | | |
| | 2017 | 565.5 | 164.5 | 6.9 | Good | | | |
| Poole Harbour | 2008 | 1890.9 | 202.2 | 3.4 | Poor | Potential Problem Area | Potential Problem Area | Problem Area |
| | 2011 | 984.9 | 141.2 | 2.4 | Poor | | | |
| | 2013 | | | | Moderate | | | |
| | 2014 | 1141 | | | Moderate | | | |
| | 2015 | 1315.4 | 343.4 | 5.7 | Poor | | | |
| | 2016 | | | | Moderate | | | |
| | 2019 | | | | Moderate | | | |
| | 2022 | | | | Moderate | | | |
| Portsmouth | 2007 | | 1189.7 | 73.7 | Moderate | Problem Area | Problem Area | Problem Area |
| | 2009 | 530.4 | 281.9 | 34.4 | Moderate | | | |
| | 2011 | 326.3 | 562.1 | 34.8 | Moderate | | | |
| | 2013 | | | | Moderate | | | |
| | 2014 | | | | Moderate | | | |
| | 2015 | | | | Poor | | | |
| | 2016 | 557.5 | 336.6 | 20.8 | Moderate | | | |

| | | | | | | | | |
|---|---|---|---|---|---|---|---|---|
| | 2019 | | | | **Moderate** | | | |
| | 2022 | | | | **Moderate** | | | |
| **Swale** | 2008 | 474.71 | 710.2 | 22.5 | **Good** | **Not assessed** | **Not assessed** | **Not assessed** |
| | 2012 | 955 | 135.5 | 4.3 | **Good** | | | |
| | 2017 | 60.2 | 91.1 | 2.9 | **Good** | | | |

### 2.4.3 Macroalgae cover

In Chichester the highest macroalgae cover was recorded in 2011 with 35.2%, 2009 had a similar value of 33.6%, by 2014 macroalgae cover decreased to 19% and continued decreasing until it reached 20.1% in 2018 (Figure 8). In 2009, 10.9% of the macroalgae cover was in the range 5-25% whereas a similar portion of 10.2% fell in the 25-50% density (Figure 8a). During 2011 density of macroalgae a greater portion of the cover was of 25-50% while the rest was evenly distributed between the groups (Figure 8b). Finally in 2014 8.9% of the macroalgae cover fell in the range of 5-25% density group (Figure 8c).

Christchurch macroalgae cover was available only for the years 2012 and 2013, both years presented similar macroalgae cover values 2.6% in 2012 and increased slightly in 2013 to 4.8% (Figure 9). There was no density classification for this site, all the available data fell in the range of 5-100%.

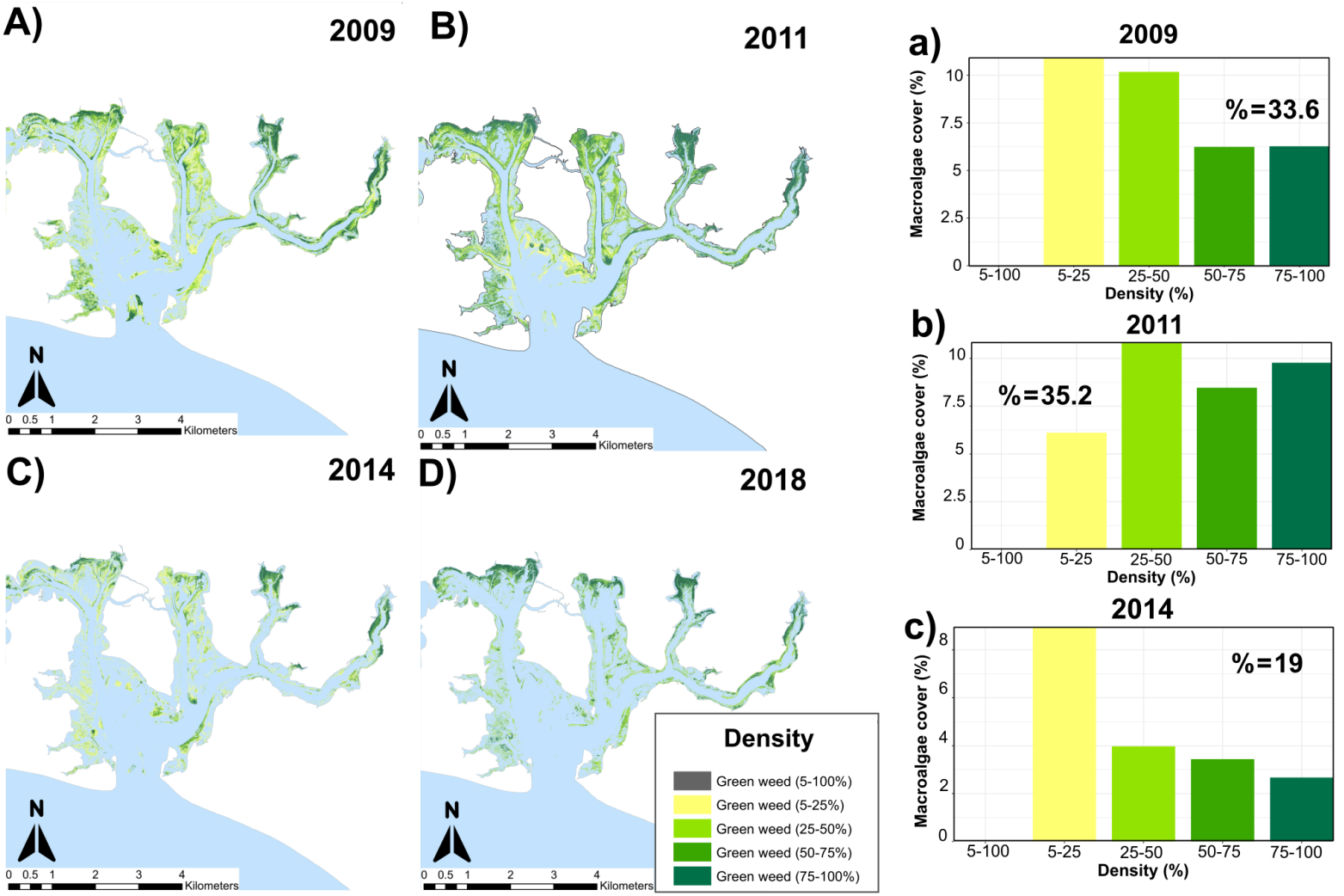


**Figure 8. Maps illustrating the cover area of opportunistic macroalgae in Chichester Harbour and different densities for the years 2009, 2011, 2014, and 2018. Alongside, histograms provide a detailed distribution of density changes over these years.**

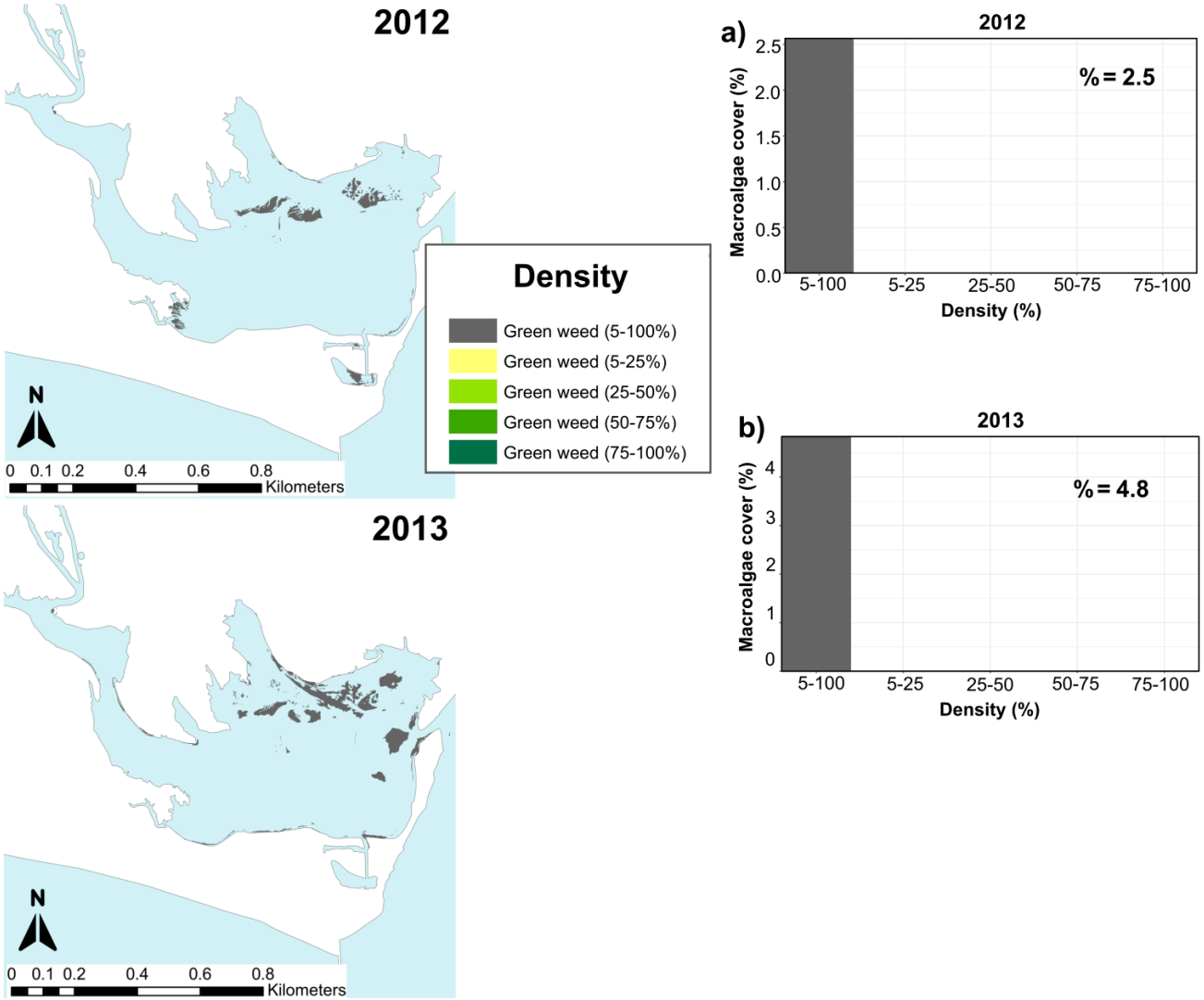


**Figure 9. Maps illustrating the cover area of opportunistic macroalgae in Christchurch and different densities for the years 2012, and 2013. Alongside, histograms provide a detailed distribution of density changes over these years.**

In 2009 Langstone had a macroalgae cover of 24.9%, its highest value was recorded in 2011 with 29.9% and remained high with 26.7% by 2014 (Figure 10). In 2009 10.8% of the macroalgae cover had a density of 5-25%, in 2011 the majority of macroalgae cover had a density of 25-50% (12.2%) and the percentage on the density 75-100% also increased from 2.4 to 4.1% (Figure 10b). By 2014 most of the density was in the range of 5-25% with 10.4% of the macroalgae cover in this category (Figure 10c).

The highest macroalgae cover in Medway was in 2008 with 32%, the following years of 2012 and 2017 presented a sharp decrease to 6.2 and 6.9% respectively (Figure 11). Density data was available for 2008 and 2017, in 2008 the major portion of macroalgae cover (12.8%) was not classified (5-100%) while 6.1% and 5.7% were had a density of 5-25 and 75-100% respectively (Figure 11a). For 2012 all the macroalgae cover was unclassified (5-100%) (Figure 11b). In 2017 2.6% of the macroalgae cover was in the density range of 25-50%, 2.4% in the class 75-100% and 1.8% with a density of 50-75% (Figure 11c).

In Poole Harbour the highest macroalgae cover was in 2014 with 13.7%, 2009 had 9.8% and by 2015 decreased further to 5.7%. Only aerial surveys were performed in this site, therefore there was not density data available (Figure 12).

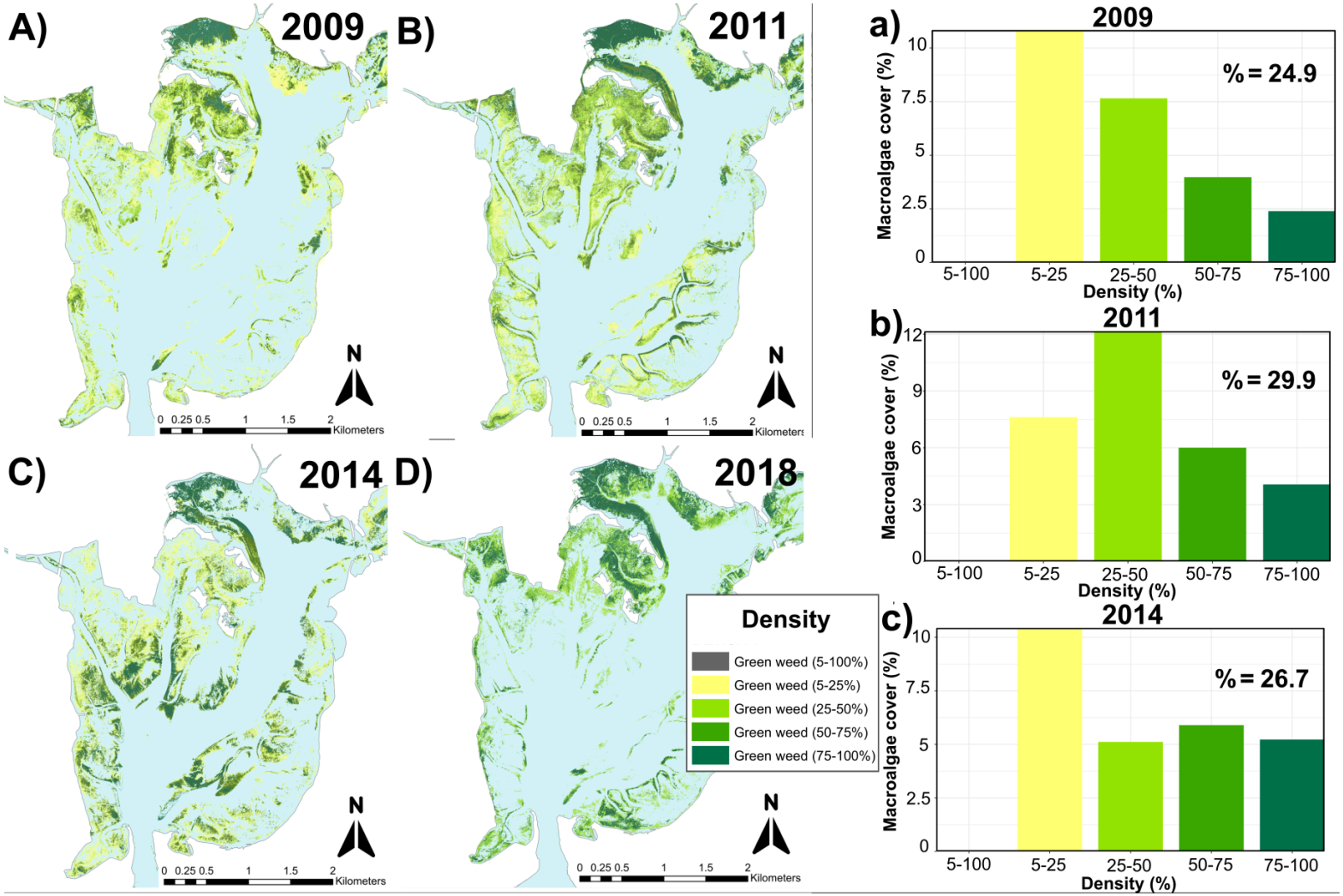


**Figure 10. Maps illustrating the cover area of opportunistic macroalgae in Langstone Harbour and different densities for the years 2009, 2011, 2014 and 2018. Alongside, histograms provide a detailed distribution of density changes over these years.**

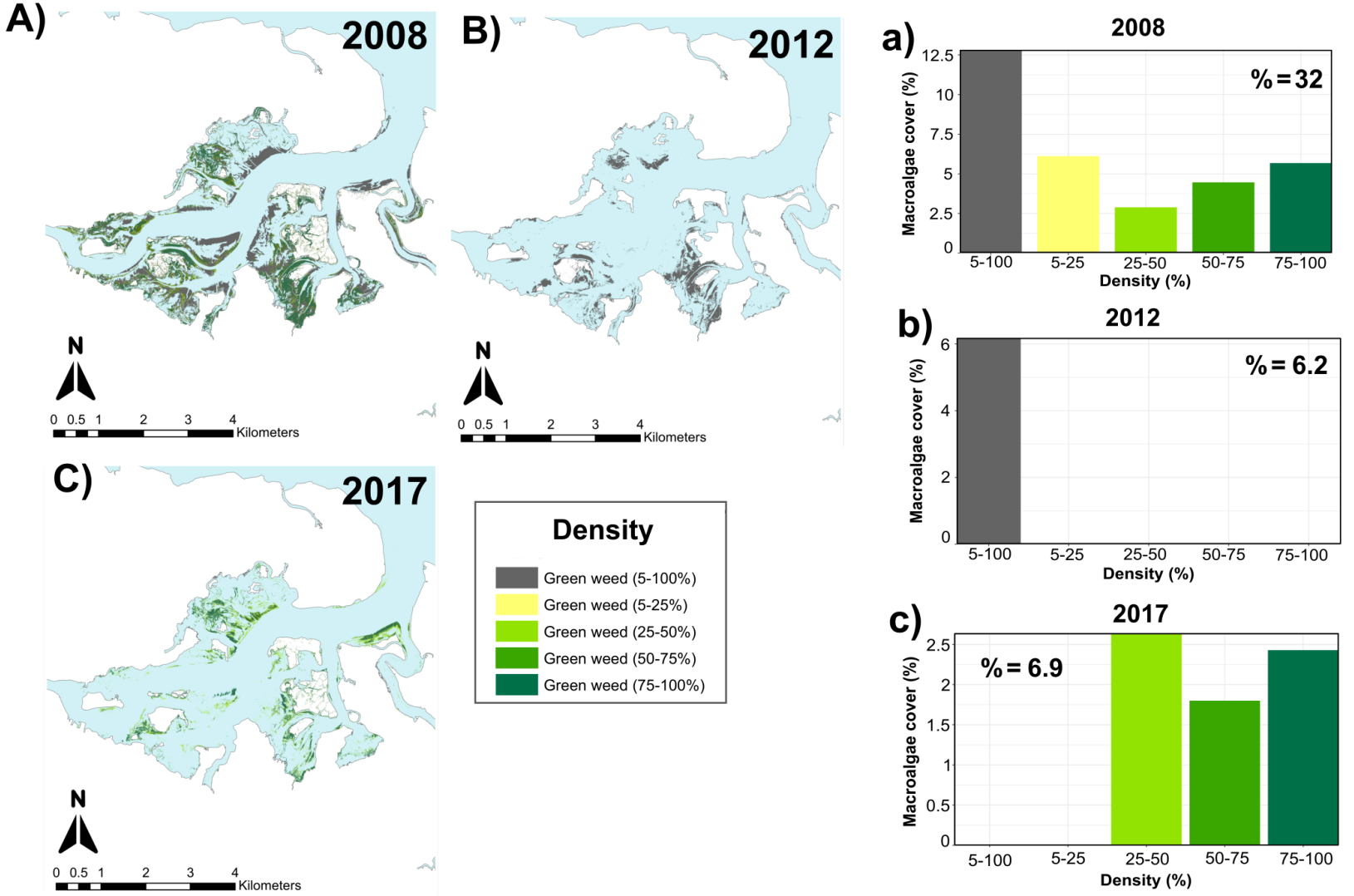


**Figure 11. Maps illustrating the cover area of opportunistic macroalgae in Medway and different densities for the years 2008, 2012, and 2017. Alongside, histograms provide a detailed distribution of density changes over these years.**

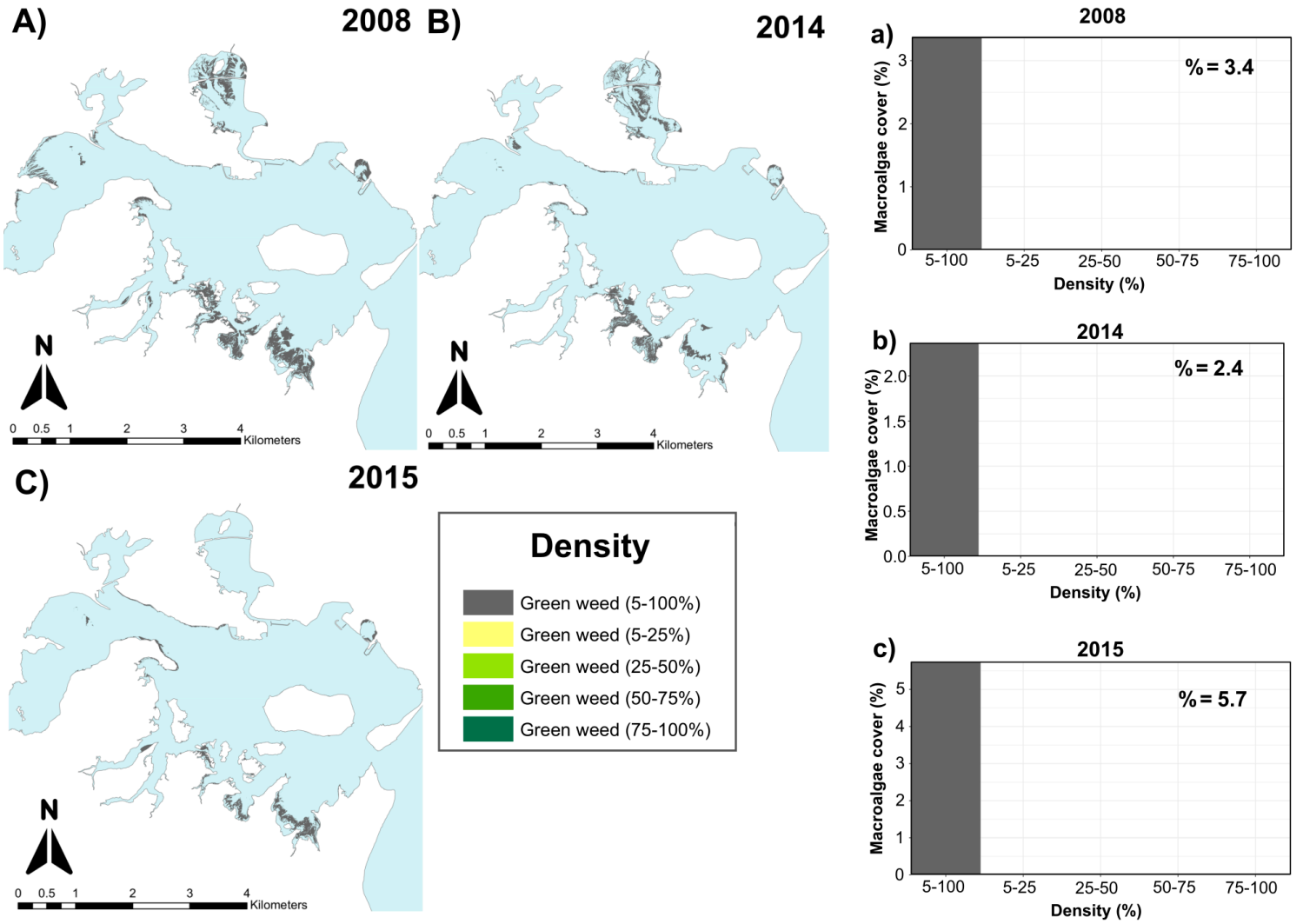


**Figure 12. Maps illustrating the cover area of opportunistic macroalgae in Poole Harbour and different densities for the years 2008, 2014, and 2015. Alongside, histograms provide a detailed distribution of density changes over these years.**

In Portsmouth the highest macroalgae cover was in 2007 with 63.4% decreasing slightly by the following years with 57.7% and 58.3% in 2009 and 2011, by 2016 macroalgae cover decreased to 34.9% of the available intertidal habitat (AIH) (Figure 13). The majority of macroalgae cover density for 2007 (35.8%) was not measured, so fell into the classification 5-100%. In 2011, 15.1% of the macroalgae cover was in the density range of 25-50%. In 2009 and 2016 macroalgae cover was equally distributed among the different density ranges (Figure 13).

Macroalgae cover data for Swale was available for 2008, 2012 and 2017, the highest cover was in 2008 with 25.5% and decreased sharply on the following years with 5.2% and 3.5% respectively (Figure 14). In 2008 macroalgae density was primarily in the 75-100% and 5 - 100%, in 2012 there was not density data (5-100%) and in 2017 most of the macroalgae density was classified in the 25 - 50% range (Figure 14).

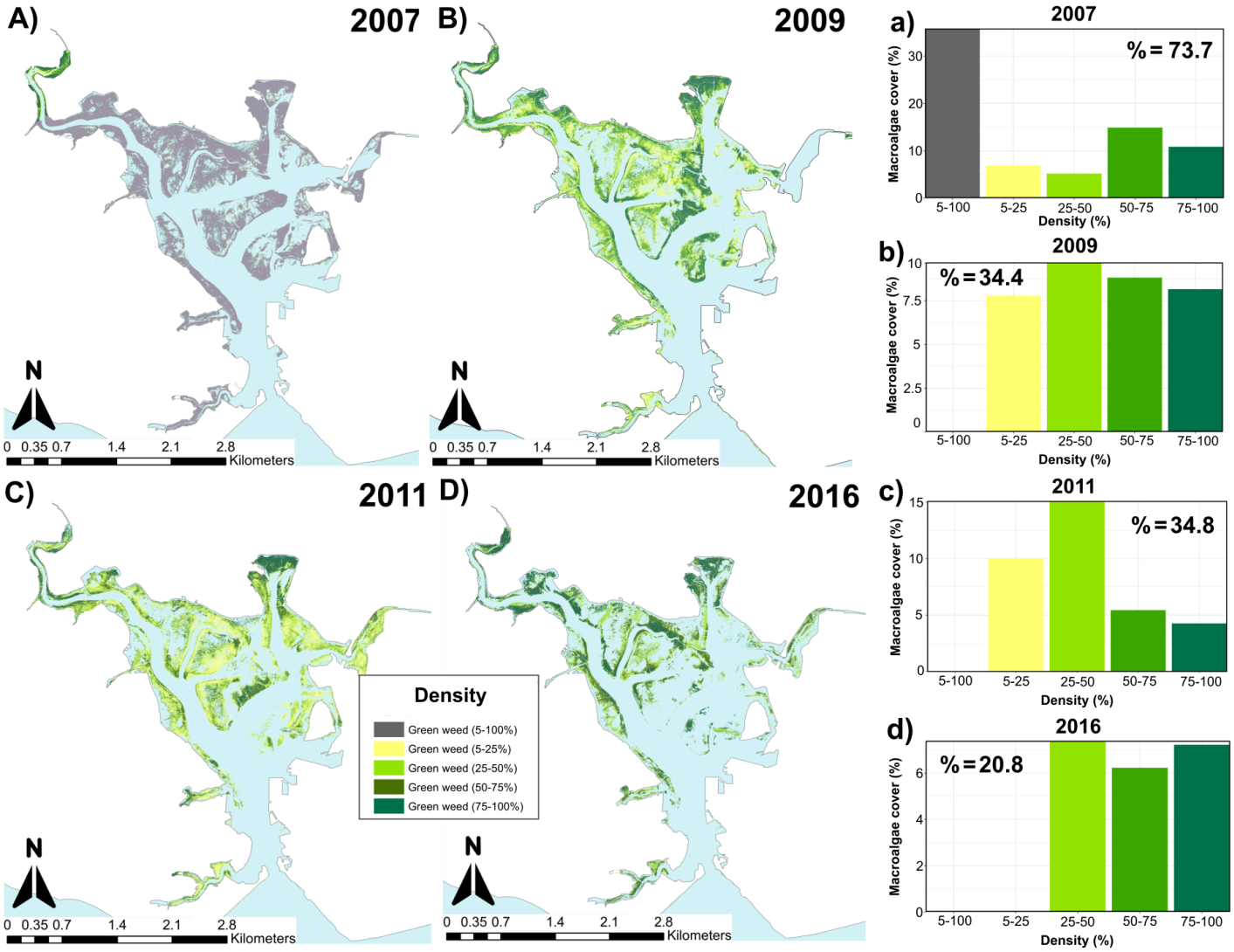


**Figure 13. Maps illustrating the cover area of opportunistic macroalgae in Portsmouth and different densities for the years 2007, 2009, 2011, and 2016. Alongside, histograms provide a detailed distribution of density changes over these years.**

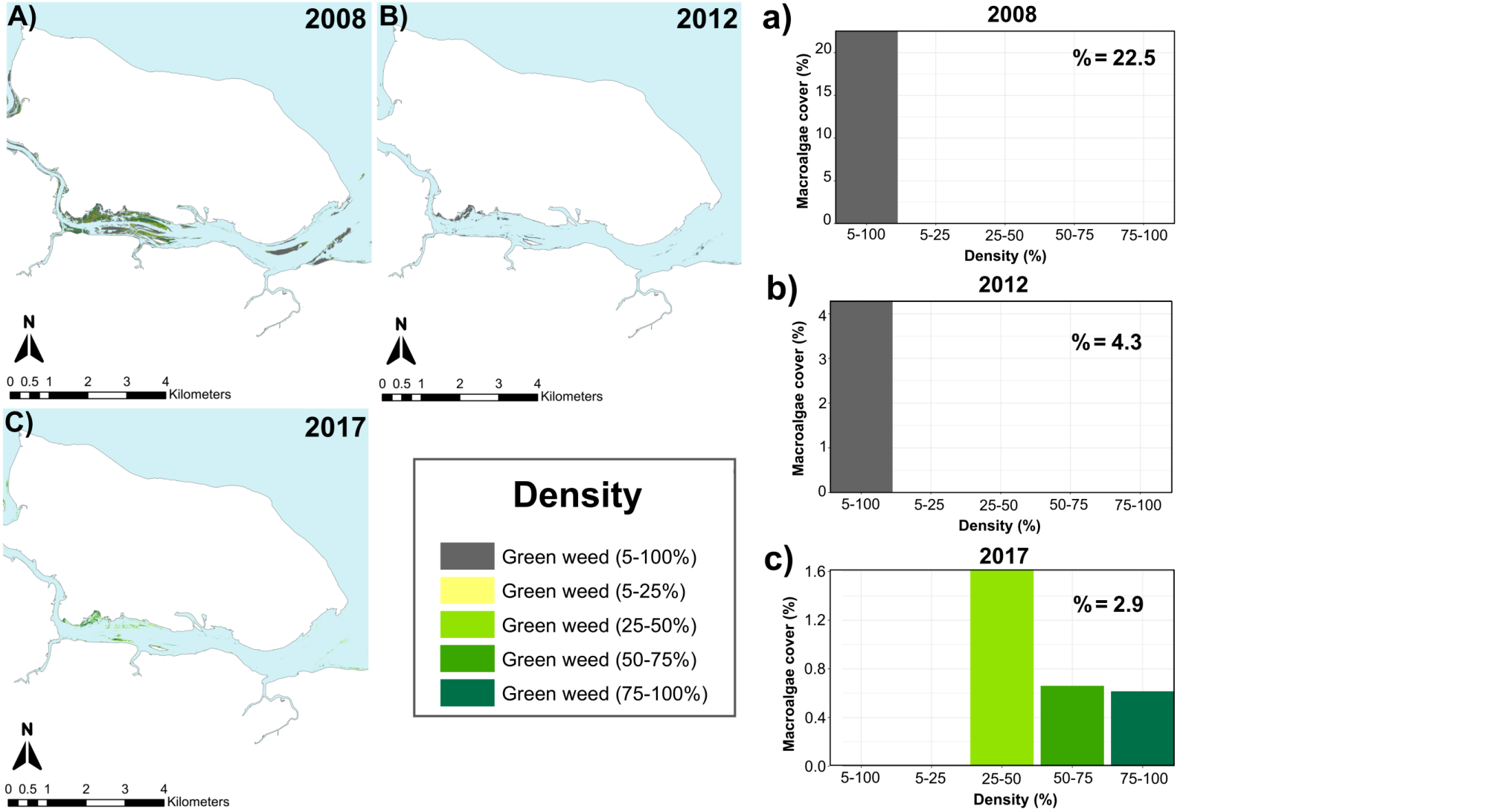


**Figure 14. Maps illustrating the cover area of opportunistic macroalgae in Swale and different densities for the years 2008, 2012, and 2017. Alongside, histograms provide a detailed distribution of density changes over these years**

### 2.4.4 Water column nutrients

Water column nutrient results are presented as annual means and the purpose of this is to evaluate trends over time, thus it is important to note that variation is high and seasonal and interannual trends will not be in annual means or winter means trends. Christchurch stood out with highest mean DIN concentration, 336 ± 158 µmol/L followed by Medway and Swale with 218 ± 132 µmol/L and 104 ± 105 µmol/L respectively. Chichester and Poole had similar lower values of 39.1±145 µmol/L and 27.3 ± 44.2 µmol/L respectively while the lowest values were found in Portsmouth and Langstone with 16.9 ± 32.6 µmol/L and 11.2 ± 14.5 µmol/L (Figure 15).

There were fewer data points for Christchurch compared to the rest of the sites, however it consistently showed the highest concentrations without a consistent decrease over time (Figure 15). Medway declined in DIN concentrations with time, showing its lowest mean concentration in 2019 (87.1 ± 72 µmol/L). Swale had similar mean concentrations over time and the most recent years showed a slight increase. Chichester had generally lower DIN annual means, however there was a considerably high peak in 2005 (192.3 ± 528).

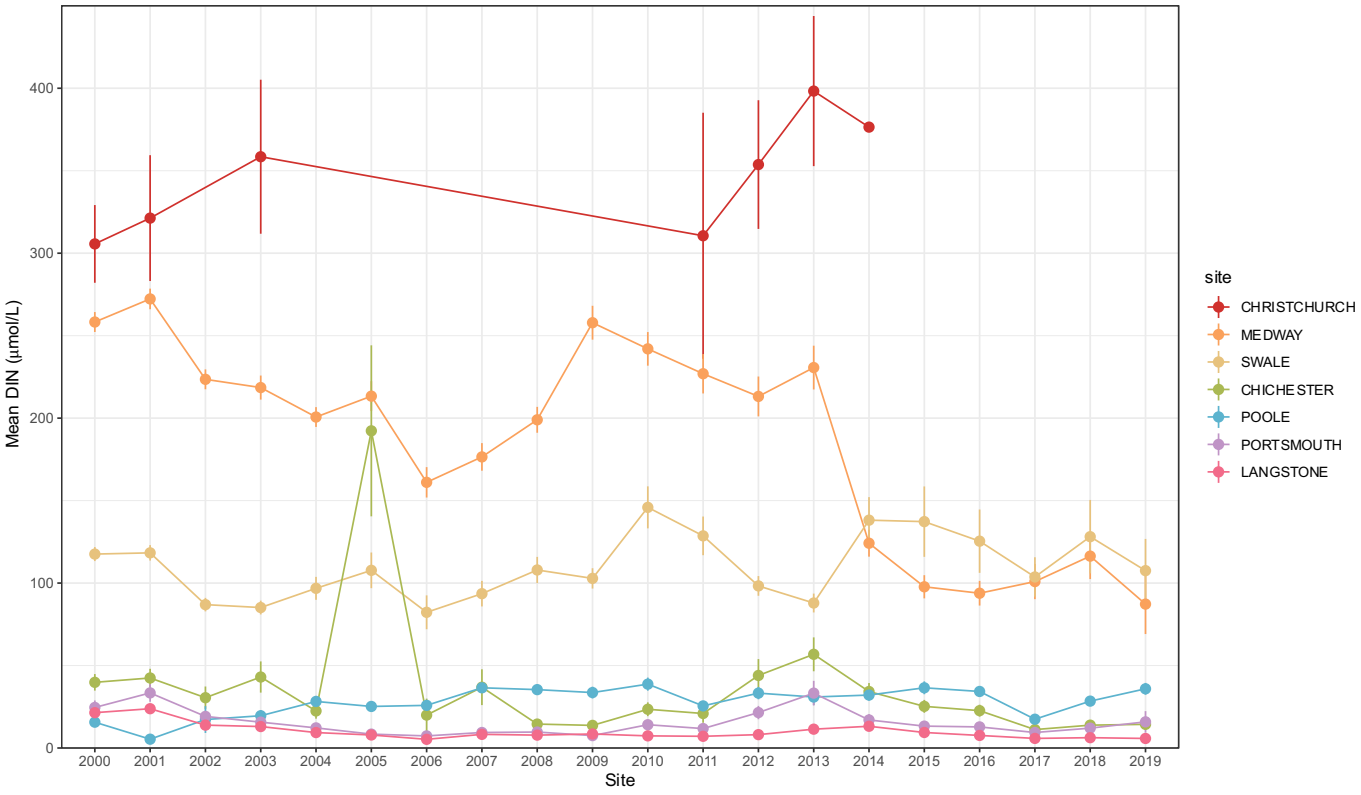


**Figure 15. Dissolved Inorganic Nitrogen (DIN) concentrations (µmol/L) for each estuary from 2000 to 2019. Each point represents the annual mean value and vertical lines indicate standard error for the respective year.**

Ammonium concentrations in water column were relatively low in all sites, however higher values were recorded in Medway and Swale with 14.6 ± 28.3 µmol/L and 13.5 ± 36 µmol/L. Christchurch and Poole had similar mean values 6.6 ± 5 µmol/L and 6.1 ± 28 µmol/L respectively whereas the lowest concentrations were found in Chichester (3.3 ± 4.6 µmol/L), Portsmouth (2.4 ± 3.4 µmol/L) and Langstone (2.3 ± 4.3 µmol/L) (Figure 16).

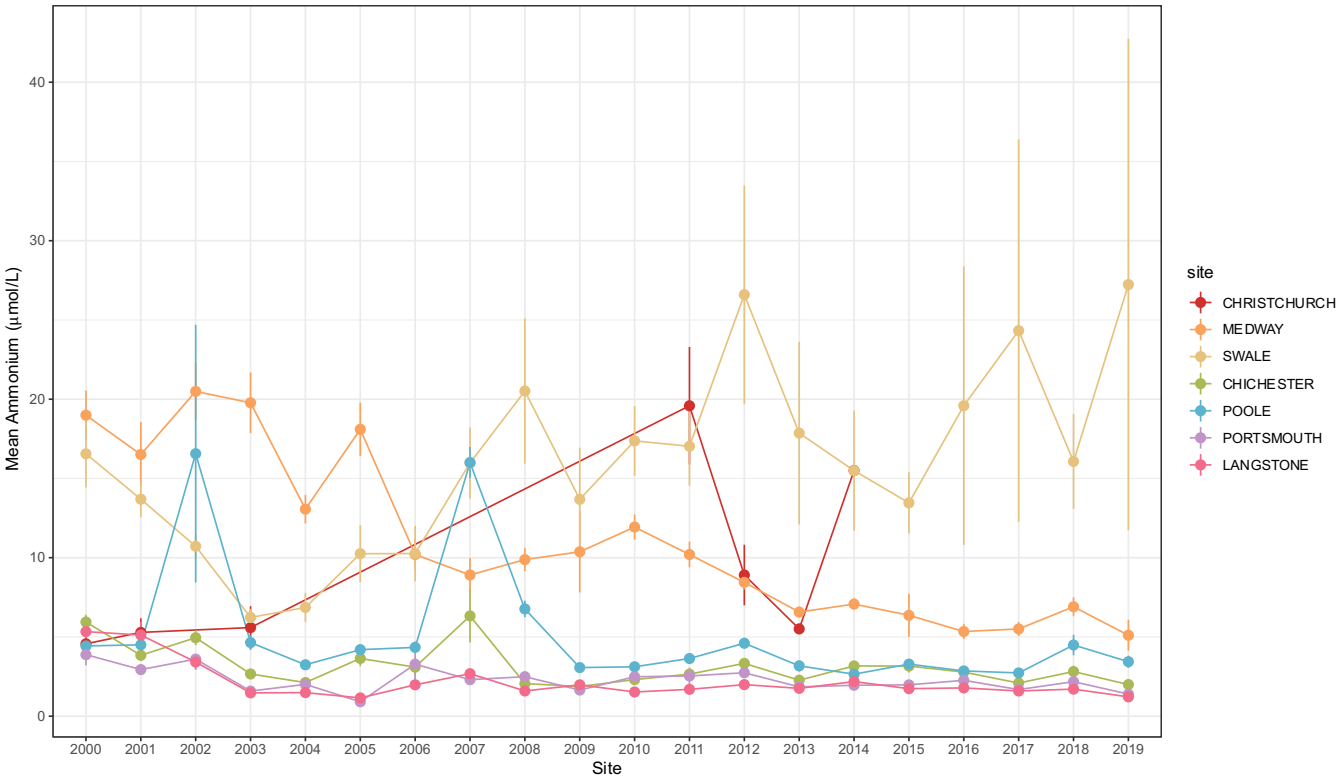


**Figure 16. Ammonium concentrations (µmol/L) for each estuary from 2000 to 2019. Each point represents the annual mean value and vertical lines indicate standard error for the respective year.**

Medway and Christchurch had the maximum nitrate concentrations of all sites, 176 ± 2 µmol/L and 169 ± 7 µmol/L. Swale had relatively high concentrations compared to the rest of the sites with 81.7 ± 1.4 µmol/L, followed by Chichester and Poole with 31.5 ± 3 µmol/L and 27.7 ± 0.7 µmol/L respectively. Portsmouth and Langstone had the lowest mean nitrate mean values 14.4 ± 31.6 µmol/L and 8.5 ± 11.5 µmol/L (Figure 17). Nitrate was the dominant nitrogen form in all the sites.

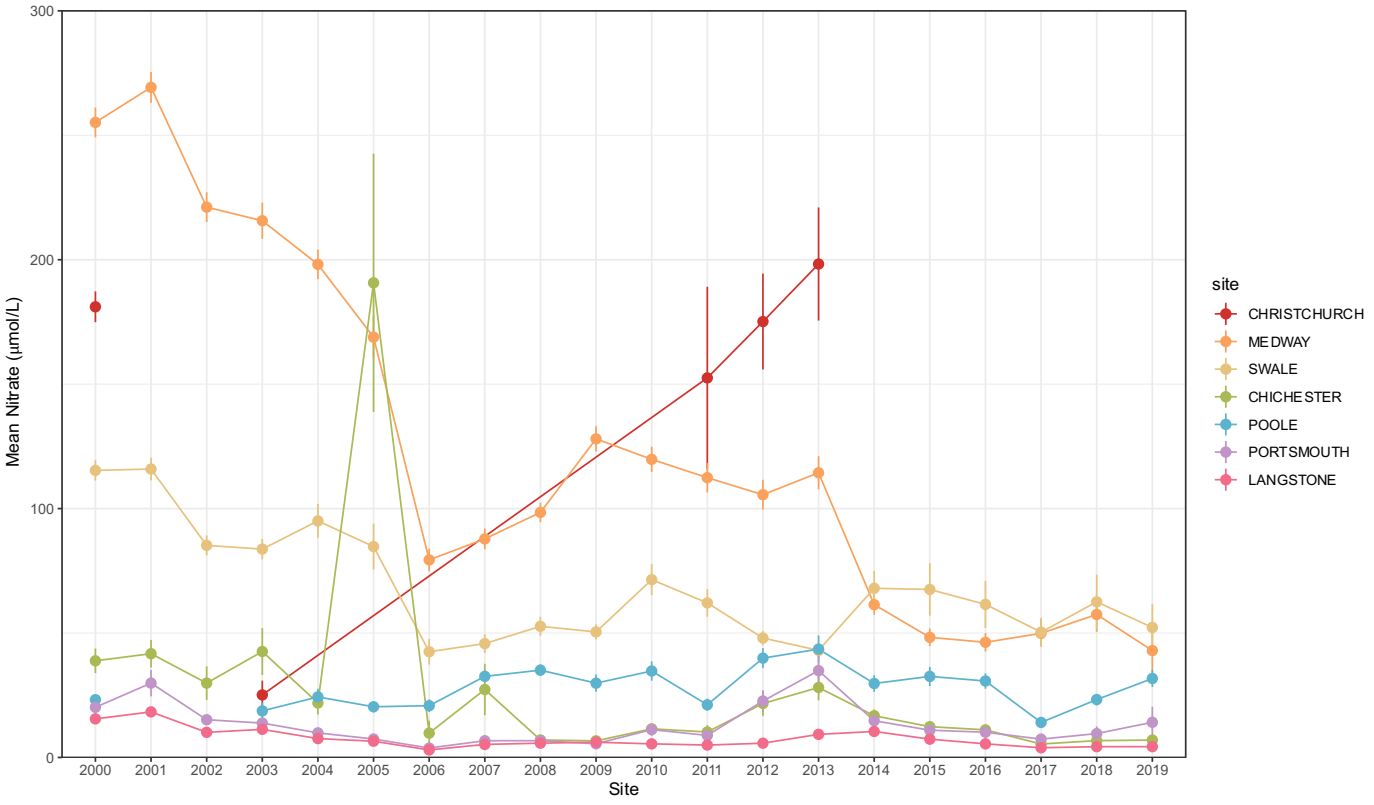


**Figure 17. Nitrate concentrations (µmol/L) for each estuary from 2000 to 2019. Each point represents the annual mean value and vertical lines indicate standard error for the respective year.**

The highest mean nitrite concentrations were in Christchurch and Medway 2.8 ± 1.8 µmol/L and 2.5 ± 2 µmol/L, followed closely by Swale with 2.2 ± 3.7 µmol/L. Poole and Chichester had comparable mean nitrite values with 0.8 ± 0.8 µmol/L and 0.6 ± 0.07 µmol/L respectively, Portsmouth and Langstone had the lowest mean nitrite concentrations with 0.4 ± 0.4 µmol/L and 0.3 ± 0.3 µmol/L (Figure 18).

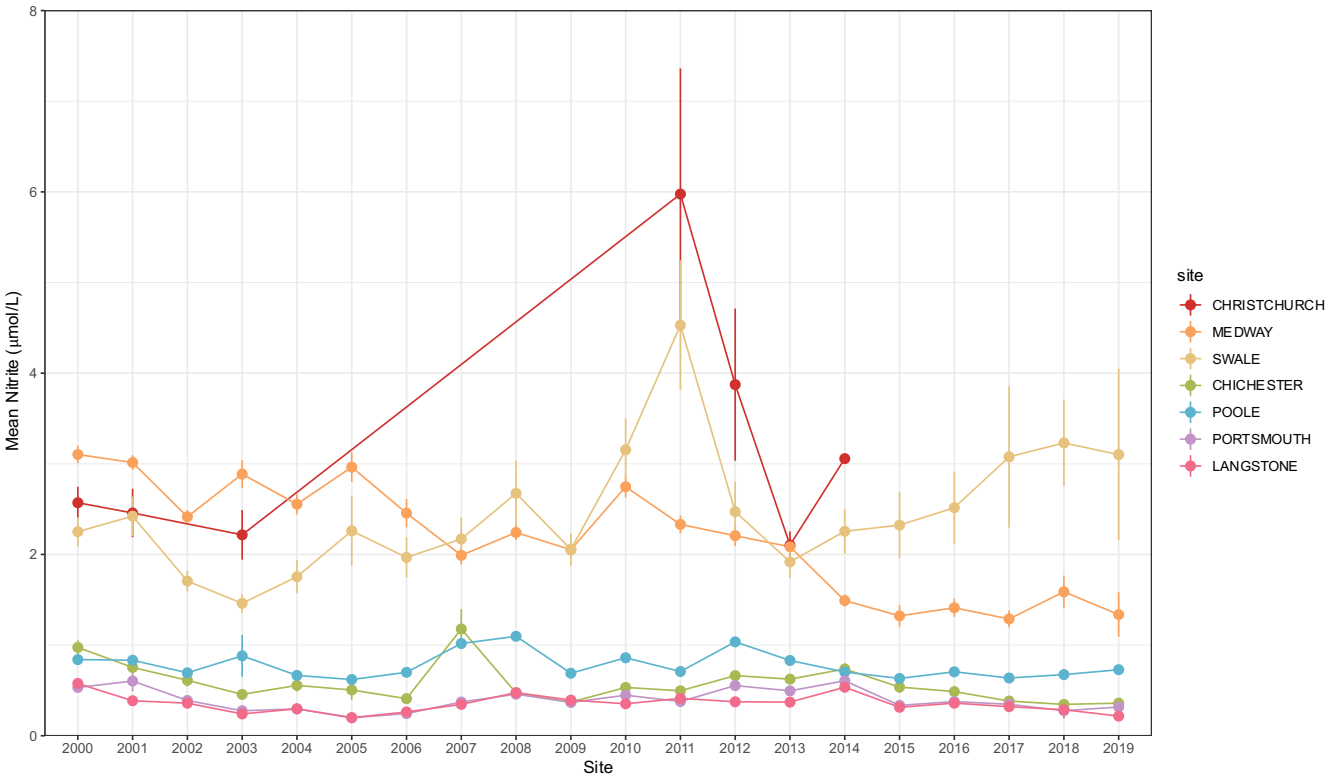


**Figure 18. Nitrite concentrations (µmol/L) for each estuary from 2000 to 2019. Each point represents the annual mean value and vertical lines indicate standard error for the respective year.**

Mean Phosphorus concentrations were also considerably higher in Medway with 12.3 ± 11 µmol/L, Swale and Christchurch followed with 6.9 ± 7 µmol/L and 6.4 ± 6 µmol/L respectively. Chichester and Poole harbours had similar mean phosphorous values, 1 ± 1.7 µmol/L and 0.98 ± 1.6 µmol/L, while Portsmouth and Langstone had the lowest values with 0.5 ± 0.8 µmol/L and 0.5 ± 0.05 µmol/L (Figure 19).

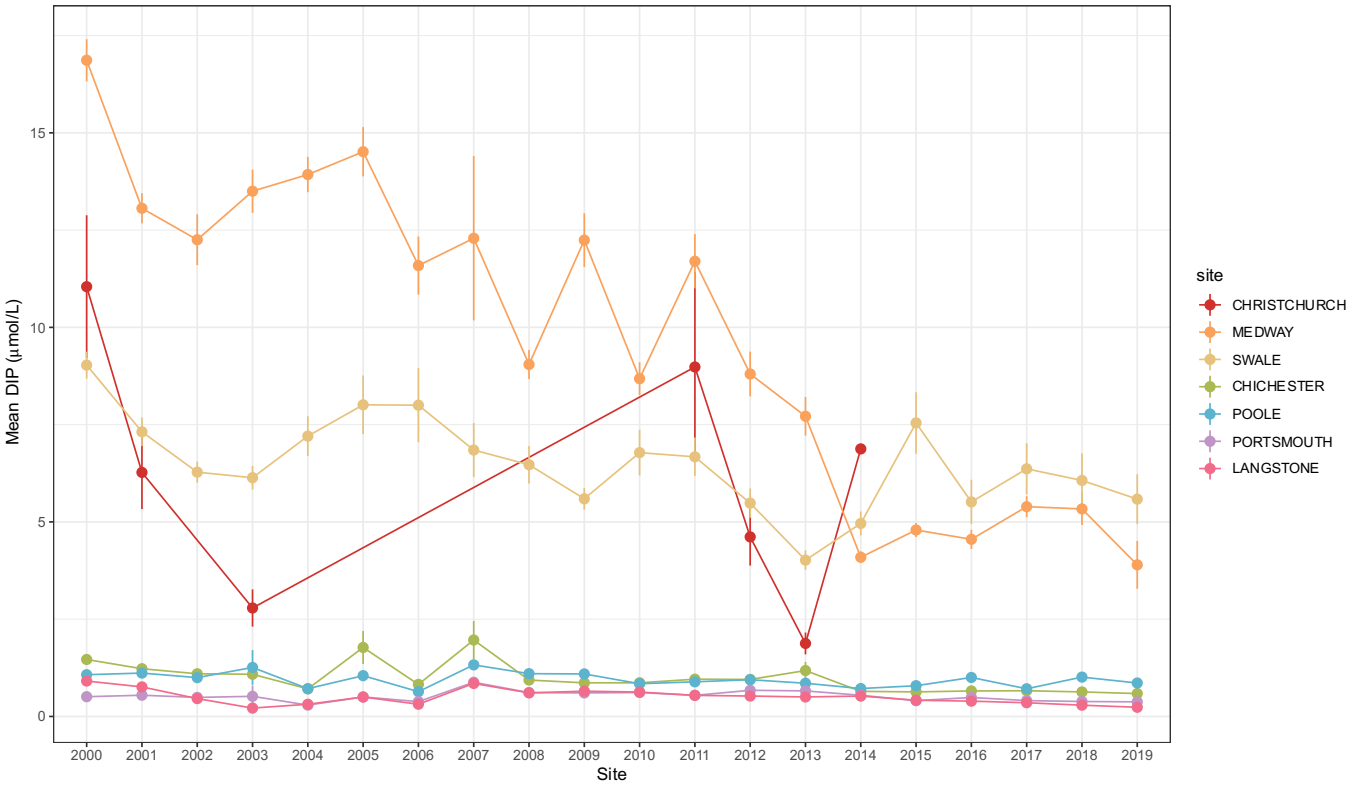


**Figure 19. Dissolved Inorganic Phosphorus (DIP) concentrations (µmol/L) for each estuary from 2000 to 2019. Each point represents the annual mean value and vertical lines indicate standard error for the respective year.**

Annual mean N:P ratios varied substantially from site to site ranging from 17.8 to 93, the highest value was observed in Christchurch 93.9 ± 93 followed closely by Poole Harbour 86.7 ± 218. Chichester had a mean N:P of 49 ± 258 Portsmouth and Langstone had a mean N:P of 45.6 ± 100 and 35.4 ± 87 respectively while the lowest values were found in Medway and Swale, 23.8 ± 41 and 17.8 ± 30 (Figure 20).

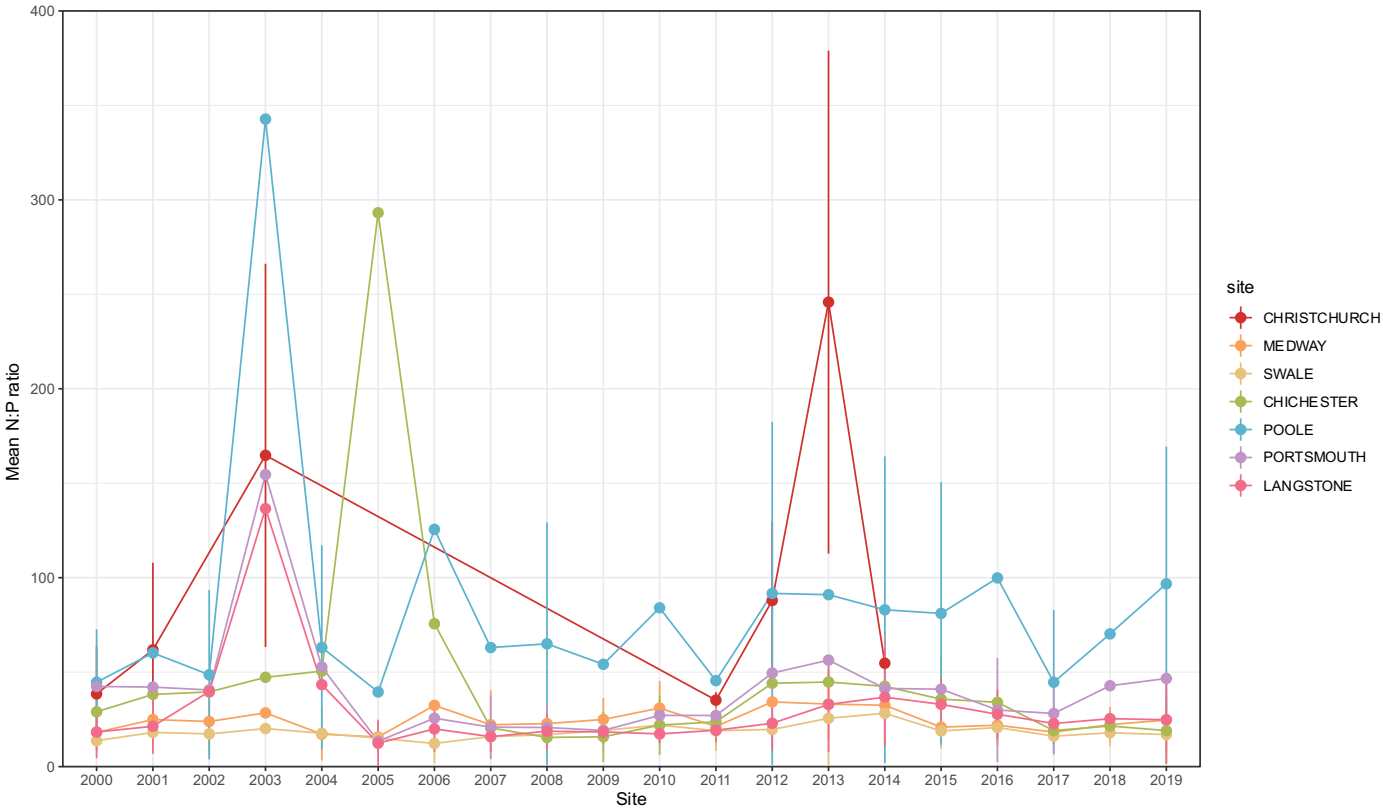


**Figure 20. N:P ratio for each estuary from 2000 to 2019. Each point represents the annual mean value and vertical lines indicate standard error for the respective year.**

### 2.4.5 Winter nutrients

Christchurch and Medway were the sites with the highest winter mean DIN with 405 ± 134 µmol/L and 244 ± 129 µmol/L respectively, followed by Poole Harbour 104 ± 99 µmol/L. Chichester and Portsmouth had similar winter mean DIN values, 59.9 ± 95 µmol/L and 51.3 ± 888 µmol/L respectively. Langstone had a lower value of 22.5 ± 14 µmol/L and Swale was the site with the lowest value of 2.9 ± 3 µmol/L. Christchurch winter DIN data was not available after 2013, however the most recent years showed a gradual increase over time (Figure 21).

Medway had a tendency of decreasing winter DIN concentrations with time while Poole had a less steep decrease over time, and a 2019 value that was slightly higher than the first record in 2000. In the most recent years Portsmouth showed a gradual increase in winter DIN, while Langstone had a small variation overtime. Lastly, Swale maintained a steady winter mean DIN. In 2013 there was a sharp increase in Christchurch, Poole, Portsmouth, Chichester and Langstone (Figure 21).

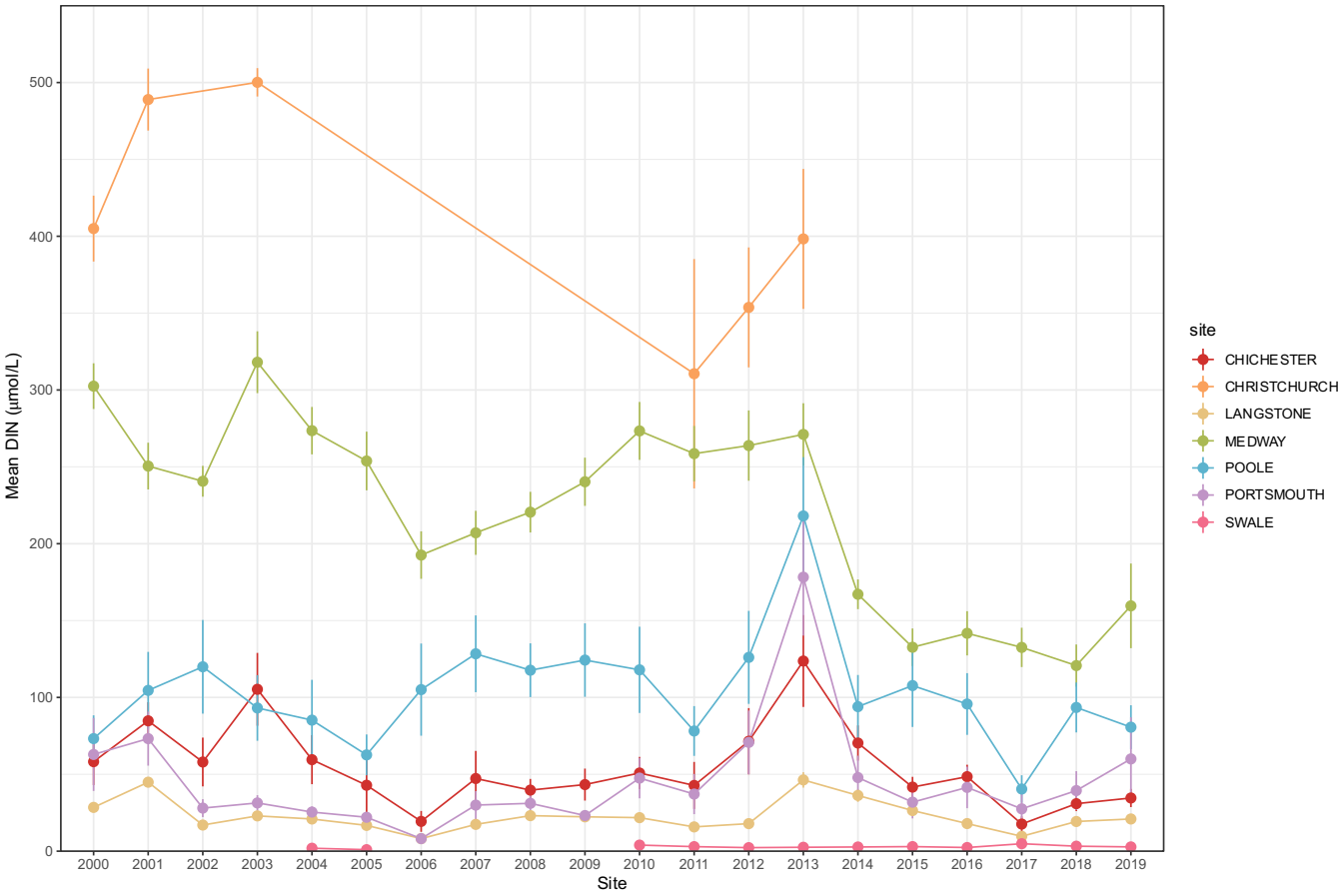


**Figure 21. Winter Dissolved Inorganic Nitrogen (DIN) concentrations (µmol/L) for each estuary from 2000 to 2019. Each point represents the annual mean value for the winter season and vertical lines indicate standard error for the respective year.**

The highest mean winter DIP was of 8.9 ± 6.7 µmol/L in Medway followed closely by µmol/L Swale with 7.3 ± 7.8 µmol/L, Christchurch had the third highest mean winter DIP with 4.3 ± 3.2 µmol/L, these sites had a large variability through time. The rest of the sites had similar lower winter DIP, Chichester and Poole had 1.2 ± 1 µmol/L and 1.05 ± 0.9 µmol/L respectively while Portsmouth and Langstone had the lowest mean winter DIP values with 0.8 ± 0.5 µmol/L and 0.7 ± 0.5 µmol/L (Figure 22).

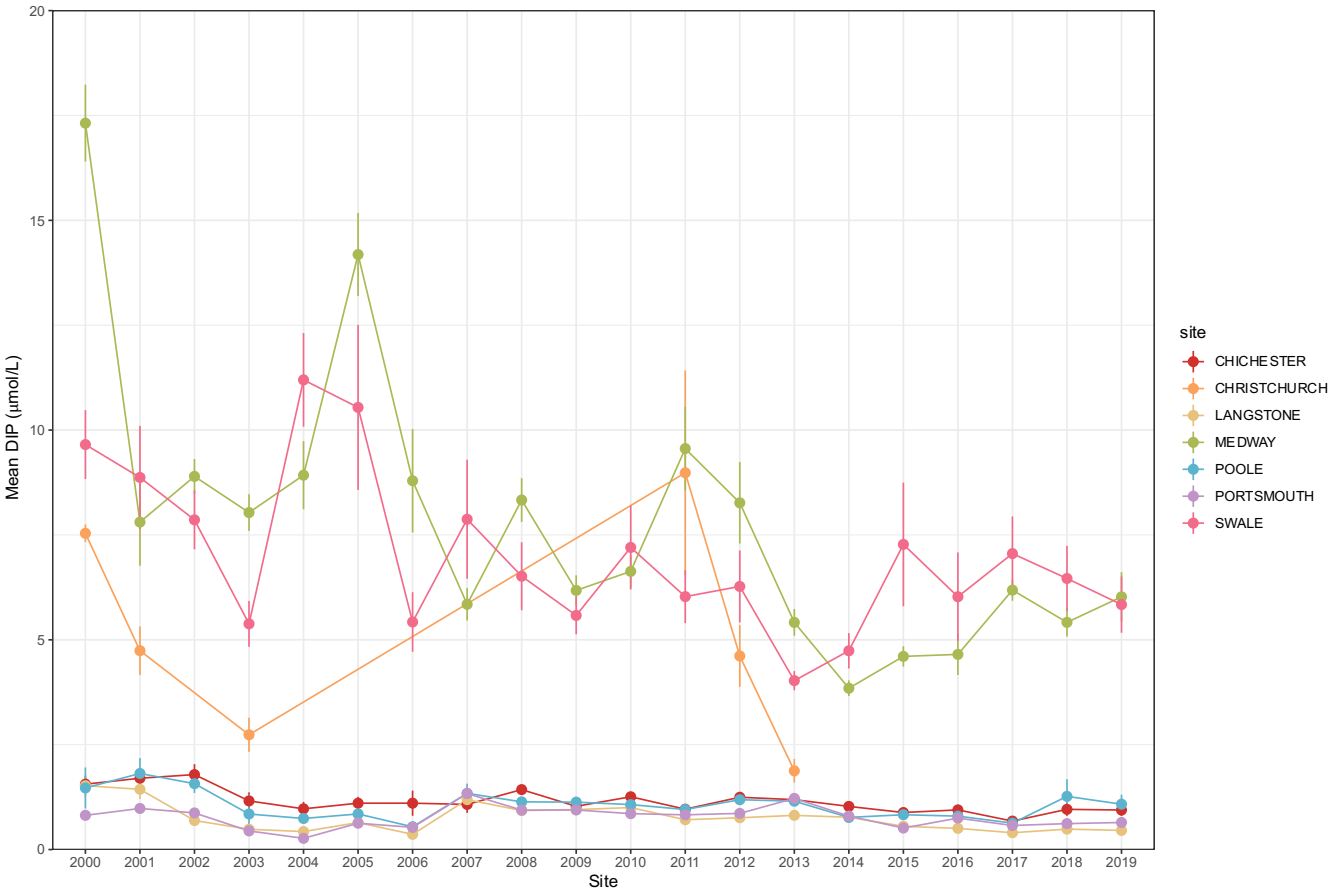


**Figure 22. Winter Dissolved Inorganic Phosphorus (DIP) concentrations (µmol/L) for each estuary from 2000 to 2019. Each point represents the annual mean value for the winter season and vertical lines indicate standard error for the respective year.**

Mean winter N:P ratios were highest in Christchurch, 140 ± 104 and Poole followed with considerably high N:P ratios of 124 ± 165. Portsmouth and Christchurch followed with 64.8 ± 83 and 51.8 ± 70 respectively, whereas Langstone and Medway had slightly lower mean N:P ratios 45 ± 66 and 36 ± 50. Lastly, Swale had the lowest mean winter N:P ratio with 23.3 ± 47 (Figure 23).

Christchurch had a substantial increase of winter N:P ratio in 2003, and 2013 was the last available data for this site. Similarly, Poole presented significant peaks in 2003,

2006 and 2013, and for more recent years maintained considerably higher winter N:P ratios compared to the rest of the sites. Portsmouth and Chichester also presented lower peaks in the same years than Poole. Langstone and Swale had these increases only in 2003 and 2013, while in Medway the relevant highest peak in winter N:P ratios was observed only in 2006 (Figure 23).

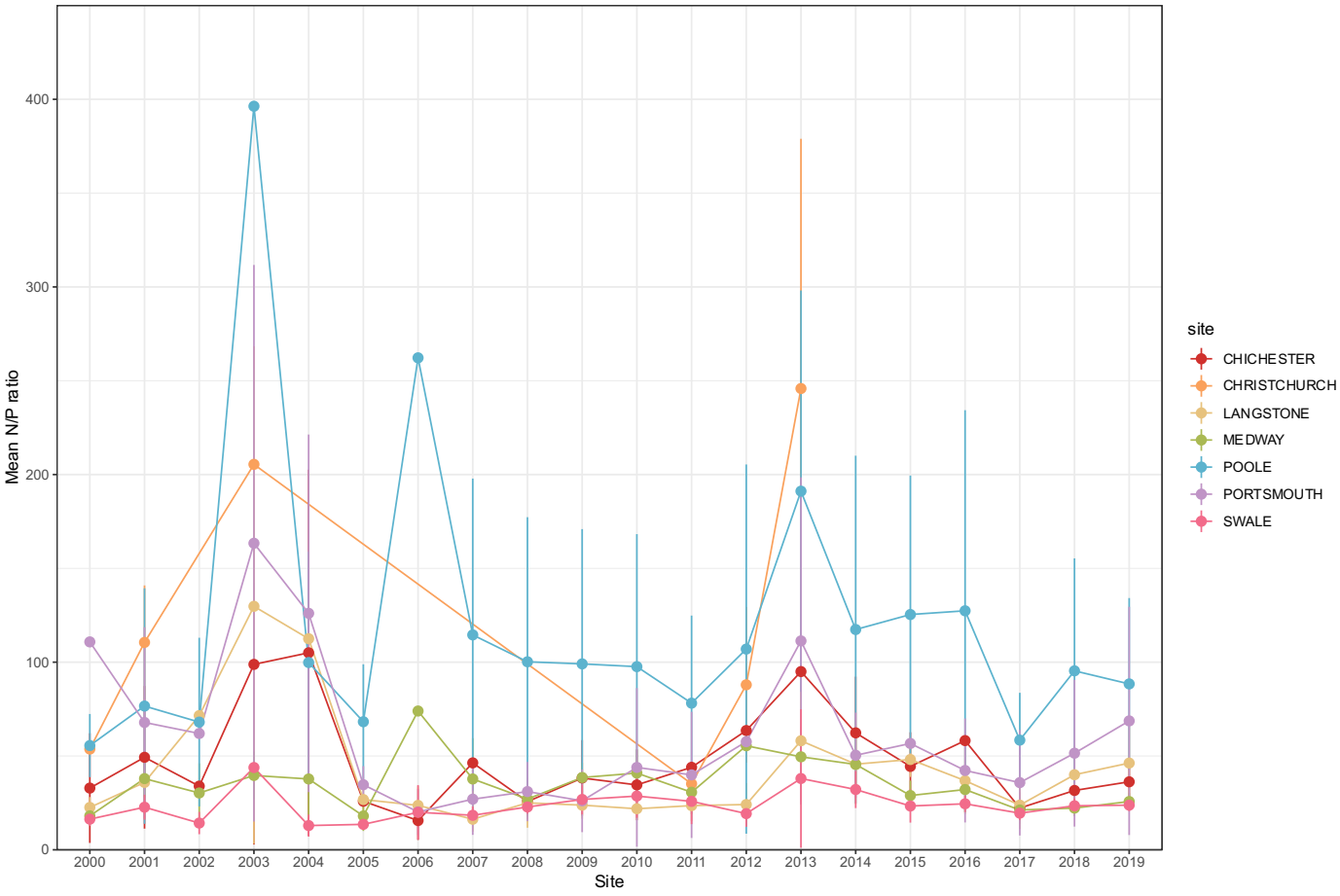


**Figure 23. Winter N:P ratio for each estuary from 2000 to 2019. Each point represents the annual mean value for the winter season and vertical lines indicate standard error for the respective year.**

### 2.4.5.1 Correlation macroalgae cover and biomass

DIN did not show a significant correlation with macroalgae cover but had a weak negative correlation with biomass. Nitrite exhibited a strong negative correlation with macroalgae cover and a moderate negative correlation with biomass. DIP showed a moderate negative correlation with macroalgae cover but showed no significant correlation with biomass. Annual mean N:P ratio showed a weak negative correlation with macroalgae cover and biomass. Dissolved oxygen (DO) had a strong positive correlation with macroalgae cover and a moderate positive correlation with biomass. Salinity did not have a significant correlation with macroalgae cover but had a moderate positive correlation with biomass whereas temperature showed no significant correlation with macroalgae cover or biomass (Table 6).

**Table 6. Spearman correlations of macroalgae cover and biomass, and annual mean water quality variables. Significant Spearman correlations in bold. * p-value<0.05; ** p-value<0.01; *** p-value<0.001.**

| Variable | Biomass | Macroalgae cover |
|---|---|---|
| Nitrate | **-0.43*** | **-0.49**** |
| Nitrite | **-0.53**** | **-0.48*** |
| DIN | -0.07 | **-0.40*** |
| DIP | **-0.38*** | -0.33 |
| N:P | -0.15 | **-0.45*** |
| Dissolved $O_2$ | **0.57**** | 0.29 |
| Salinity | -0.15 | **0.49**** |
| Temperature | 0.33 | 0.31 |

Mean winter DIN and DIP did not show significant correlations with macroalgae cover or biomass. Nitrate had a weak negative correlation with macroalgae cover but no significant correlation with biomass. Nitrite exhibited a strong negative correlation with both macroalgae cover and biomass.

Mean winter N:P ratio displayed a moderate positive correlation with macroalgae cover but no significant correlation with biomass whereas dissolved oxygen had a weak positive correlation with macroalgae cover and a moderate positive correlation with biomass.

**Table 7. Spearman correlations of macroalgae cover and biomass, and winter mean water quality variables. Significant Spearman correlations in bold. * p-value<0.05; ** p-value<0.01; *** p-value<0.001.**

| Variable | Biomass | Macroalgae cover |
|---|---|---|
| Nitrate | -0.19 | **0.03*** |
| Nitrite | **-0.59***** | **-0.51*** |
| DIN | -0.36 | -0.34 |
| DIP | **-0.43*** | -0.25 |
| N:P | 0.53 | **-0.41*** |
| Dissolved $O_2$ | **0.42*** | 0.51 |

"*" Significant variables for ma cover p value <.05

Mean slope showed a moderate positive correlation with biomass and a weak negative correlation with macroalgae cover. Neap tidal range exhibited no significant correlation with biomass but showed a weak positive correlation with macroalgae cover. Spring tidal range had no significant correlation with biomass but showed a moderate positive correlation with macroalgae cover. Flushing time (days) and suspended particulate atter did not show a significant correlation with macroalgae cover or biomass (Table 8).

**Table 8. Spearman's correlations of macroalgae cover and biomass, and physical variables. Significant Spearman correlations in bold. * p-value<0.05; ** p-value<0.01; *** p-value<0.001.**

| Variable | Biomass | Macroalgae cover |
|---|---|---|
| Mean slope | **0.45**** | -0.16 |
| Neap tidal range | -0.36 | 0.26 |

| | | |
|---|---|---|
| Spring tidal range | -0.32 | 0.35 |
| Flushing time (days) | 0.18 | 0.04 |
| Suspended Particulate Matter | 0.27 | 0.06 |

# 2.5 Discussion

## 2.5.1 Eutrophication Assessment

The results from the three applications of COMP are shown in Table 5; From the sites presented here, Chichester, Langstone, Portsmouth and Poole Harbours were evaluated by OSPAR COMP. Portsmouth and Chichester have remained as problem areas whereas Langstone and Poole Harbours had a different classification for the most recent assessment. Langstone, that was classified as problem area for the first two evaluations improved to potential problem area while the opposite happened to Poole Harbour, which worsened to being a problem area in the last evaluation (Figure 24).

When compared with macroalgae cover, the sites with highest nutrient concentrations were usually the ones with lowest macroalgae cover except for Poole Harbour. This is supported by correlation analyses, where statistically significant correlations were present between macroalgal cover or biomass and nutrient parameters the relationships were almost always negative (Tables 6 and 7). Medway, Swale and Christchurch, were categorised with Good and High for the EQR and were not included in the OSPAR eutrophication assessment (Table 5). This also implies that these nutrient enriched sites have not shown other signs of eutrophication.

In the third application of the OSPAR COMP, it was stated that eutrophication is still a problem in 7% of the North-East Atlantic affecting coastal ecosystems. For the United Kingdom, there were identified 21 problem areas and 11 potential problem areas. Problem Areas decreased from 23 to 21 compared to the second assessment, and

Potential Problem Areas increased from 6 to 11, all these with the characteristic of being small, enclosed areas with long water residence times. Although from the first to the third application of the common procedure there is a significant increase in both problem and potential problem areas, this is influenced by the addition of new assessed areas (OSPAR, 2003).

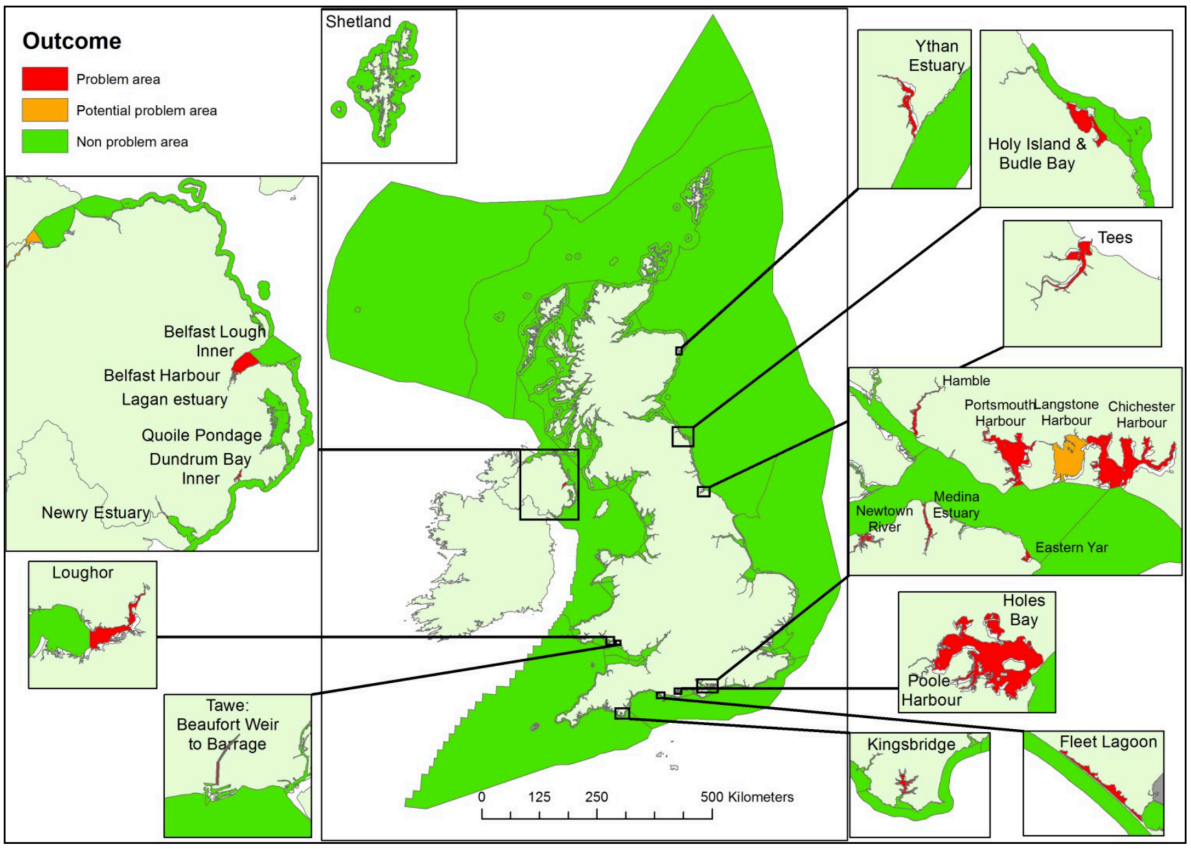


**Figure 24. Coastal sites in the United Kingdom reported as Non-Problem Areas, Potential Problem Areas and Problem Areas in the Third Integrated Report on the Eutrophication Status of the OSPAR Maritime Area (OSPAR, 2017).**

## 2.5.2 Macroalgae cover and biomass

The OMBT states a macroalgae cover greater than 15% of the available intertidal habitat is considered harmful for the ecosystems being the boundary between a good and moderate status. Where macroalgae cover is >75% an area is considered as seriously affected and given the classification of bad status. The upper boundary for a good status determined by macroalgal biomass is set as 500 g/m$^2$ (Table 9). Macroalgal biomass within the range of 110–120 g/m$^2$ have been linked to important detrimental effects on macrobenthic invertebrates (Green et al., 2014). Nonetheless, that same range is set as a good quality status within the WFD boundary (Table 9).

**Table 9. Ecological Quality Ratio (EQR) metrics and boundaries for the Opportunistic Macroalgae Blooming Tool (OMBT), ranges and limits are shown for the different classes of EQR: High, good, moderate poor and bad. (UKTAG, 2014).**

| Quality Status | High | Good | Moderate | Poor | Bad |
|---|---|---|---|---|---|
| **EQR** | **1.0- ≥0.8** | **<0.8 - ≥0.6** | **<0.6 - ≥0.4** | **<0.4 - ≥0.2** | **<0.2 – 0.0** |
| % cover of AIH | ≥0 - <5 | ≥5 -,15 | ≥15 - ,25 | ≥25 - ,75 | ≥75 – 100 |
| Average biomass (gm$^{-2}$) of AIH | ≥0 - <100 | ≥100- 500 | ≥500 – 1000 | ≥1000 – 3000 | ≥3000 (- 6,000) |
| Average biomass (gm$^{-2}$) of AA | ≥0 - <100 | ≥100 – 500 | ≥500 – 1000 | ≥1000 – 3000 | ≥3000 (- 6,000) |
| AA (hectares)* | ≥0 - <10 | ≥10 – 50 | ≥50 – 100 | ≥100 – 250 | ≥250 (- 6,000) |
| AA/AIH (%)* | ≥0 - <5 | ≥5 – 15 | ≥15 – 50 | ≥50 – 75 | ≥75 – 100 |
| % entrained algae | ≥0 - <1 | ≥1 – 5 | ≥5 – 20 | ≥20 – 50 | ≥50 – 100 |

From the available biomass data presented, all the estuaries except for Christchurch surpassed the 500 g/m$^2$ threshold between good and moderate quality status for affected areas at least in one year (Table 5). Nonetheless, Poole Harbour had persistent higher biomass values (985 - 1890 g/m$^2$) classifying as Poor-quality status in 2008, 2014 and 2015. Contrastingly to macroalgae cover data where Poole Harbour

had one of the lowest values, it is the most impacted site of macroalgae biomass production.

This highlights the importance of field surveys for some sites that have significant amounts of biomass but due to their factors this is not reflected in the macroalgae cover data. All surveys in Poole Harbour were performed as aerial surveys which might bias the extent of macroalgae cover at this specific location. These findings suggests that macroalgae cover alone is not sufficient to assess eutrophication impacts in estuaries, however combined with biomass it is a powerful tool to predict impacts on ecosystems (Devlin et al., 2011). Furthermore, it was challenging to compare macroalgae cover and biomass data due to the mismatch between surveyed years and sites.

It is clear that the cost of surveying macroalgae cover and biomass for the legislative requirements is extremely high and multiple efforts are necessary in order to make monitoring programs as accurate as possible. This is particularly challenging in the UK where up to 736275 $Km^2$ of surface area is under the OSPAR region (OSPAR, 2017), being the largest area evaluated for a contracting party (Country) in the third OSPAR COMP and it is therefore acknowledged that there is a large difference between intensity of monitoring in the UK is prioritized only for growing season (OSPAR, 2017).

After an initial assessment when an area is designated as at risk of presenting eutrophication symptoms it is then subject to field campaigns to evaluate biomass and macroalgae cover through aerial survey and GPS manual measurements. This methodology requires significant efforts to obtain the required data for classification

which prevent monitoring of sites with eutrophication to be more frequent and comparable spatially and temporarily.

These field surveys could benefit from the introduction of new technologies for macroalgae cover surveys such as drone imagery which is been proved to be a cost-effective tool for mapping multiple habitats including, Fucales and Kelp (D'Archino and Piazzi, 2021). Giving the opportunity for monitoring field campaigns to be more frequent and comparable both spatially and temporally.

### 2.5.3 Nutrient trends over time

Trends in annual water column nutrients over time were variable for the different estuaries. For example, the Medway was the only site where DIN, $NH^{4+}$, $NO_x$, and DIP concentrations showed a clear decrease pattern. Lower nitrate concentrations in the Swale were recorded in the last years, however ammonium and nitrite concentrations increased. Similarly, in Christchurch trends on DIN, ammonium, $NO_x$ were of increasing over time, while DIP decreased substantially in the period 2000-2003 and 2013 but the last record in 2014 also showed a considerable increase. These three sites recorded the highest nutrient concentrations among all the estuaries presented (Section 2.4.4). On the other hand, the rest of the estuaries (Chichester, Langstone, Portsmouth and Poole) had consistently lower concentrations than Swale, Christchurch and Medway.

Langstone, Chichester and Portsmouth showed a slight decrease in DIN and $NO_x$, while in Poole Harbour the trend was of a slight increase in concentrations. Annual

mean ammonium decreased in Portsmouth and Langstone but was more variable in Chichester and Poole Harbours for instance, Poole had ammonium concentration peaks in 2002, 2007 and less marked in 2012 and 2018. Despite having lower nutrient concentrations, Chichester, Langstone, Portsmouth and Poole Harbours presented higher biomass and macroalgae cover than Swale and Medway. This is also supported by the lack of strong correlations between water column nutrient concentrations and macroalgae cover or biomass with nutrient concentrations (2.3.1.3). Similarly, other studies have not identified a correlation between nutrient concentrations in the water column and either biomass or macroalgae cover (Soulsby et al., 1985).

Although nutrient availability is essential for macroalgae growth, other conditions are required alongside, for example when nutrients are flushed out rapidly from the system it is less likely that eutrophic conditions will develop (Bricker et al., 2008). Furthermore, bloom forming macroalgae (e.g. *Ulva* and *Entheromorpha*) have the capability of storing nutrients internally (Fong, 1994; Kamer et al, 2004), a mechanism that allows macroalgae to proliferate without being dependant on external nutrient availability. These factors could help to explain the lack of observed positive correlations between macroalgae cover and biomass with water column nutrients in this study.

Furthermore, other mechanisms such as nutrient regeneration (Trimmer, et al 2000), would make porewater nutrients more relevant to benthic macroalgae rather than relying on water column nutrients for their growth. The relevance of benthic nutrients on macroalgae will be address with more depth in Chapter 3. N:P ratios have been used as a tool to determine whether a system is nitrogen or phosphorous limited.

Typical N:P ratio for coastal waters is approximately 30:1, whereas estuaries can present a high variability of N:P ratios (Atkinson & Smith, 1983; Lane et al., 2004). According to the results presented above, mean annual N:P ratios were lower in Swale and Medway, <25 suggesting these sites might be nitrogen limited whereas, Portsmouth, Chichester and Langstone and Christchurch had N:P ratios > 30. These higher values are linked to P limited sites (Carstensen et al., 2011).

.

### 2.5.3.1 Winter mean nutrient concentrations

Winter nutrient levels are utilized to assess eutrophication because they provide a reliable indicator of baseline nutrient inputs**,** unaffected by seasonal biological activity. All the estuaries evaluated showed increased DIN mean concentrations in winter compared to the annual means. Although this increase in winter DIN concentrations was observed in every site, it was less pronounced in Christchurch, and Medway, while the highest increase was in Langstone, Portsmouth and Poole Harbours (Figure 21). Swale has not enough data for winter nutrients, therefore it is excluded from this discussion section. Despite the fact that winter mean concentrations are potentially more stable, they still did not show expected positive correlations with macroalgae cover and biomass for their respective years (Tables 6 and 7). Unlike DIN, DIP did not show a clear increase in winter mean concentrations and Medway was the only site where DIN mean concentration decreased in winter from 12.3 to 8.8 µmol/L.

As a result of the increase observed in DIN, N:P ratios increased as well for winter. Chichester, Langstone and Portsmouth winter mean N:P showed an evident increase. Christchurch and Poole mean winter ratios had the highest increase and went from 94

to 139 and 87 to 124 respectively. An increase was observed in Medway as well from 23 to 36 mean N:P in winter however, in this site was associated with the reduction in DIP rather than the increase in DIN.

N:P ratios have been used as a tool to determine whether a system is nitrogen or phosphorous limited. Typical N:P ratio is approximately 30:1 for coastal waters, whereas estuaries can present a high variability of N:P ratios (Atkinson & Smith, 1983; Lane et al., 2004). According to the results presented above, mean annual N:P ratios were lower in Swale and Medway, <25 suggesting these sites might be nitrogen limited whereas, Portsmouth, Chichester and Langstone and Christchurch had N:P ratios >30. These higher values are linked to P limited sites (Carstensen et al., 2011).

In the Venice Lagoon, there was a reported increase in N:P ratio from 40 to 100 in the period of 2000 - 2009. This rise in N:P ratio for this site has been linked to the reduction of P rather than increase in N concentrations (Zirino et al., 2016). Similarly, the sites with highest mean annual N:P ratios reflect generally lower DIP concentrations compared to DIN, whereas lower N:P ratios display considerably higher annual mean DIP. It was proposed that in the Venice Lagoon, $PO_4^{3-}$ and $NO_3^-$ are released during decomposition of organic matter, however $PO_4^{3-}$ is likely being captured by iron oxides while $NO_3^-$ stay dissolved within the water column (Zirino et al., 2016).

## 2.5.4 Physical variables and environmental factors

In sites where nutrient availability is not a limiting factor, physical and environmental factors become more relevant in macroalgae blooms development. These factors

include light availability, wave exposure, flushing time, turbidity, and bed slope (Bermejo et al., 2022; Ni Longphuirt et al., 2016b; Pihl et al., 1999).

In an experiment conducted in Tosa Bay, Japan, where acrylic panels were submerged at 1 m depth in different 0°, 40°, and 90° angles (slope), it was concluded that slope can influence the biomass and composition of bloom forming macroalgae species (Somsueb et al., 2001). From the physical and environmental factors tested here, mean slope of the intertidal area was positively correlated with biomass and ($r_S$= 0.45, $p$= <0.01). While a lower slope could be suitable for macroalgae growth, the range of mean slope in the sites was small (0.8 - 2.4), this can be influencing the positive correlation found (Table 8).

Other factors not tested here, have been proved to influence macroalgae production in estuaries. For example, Aldridge & Trimmer (2009), concluded that in the Medway estuary although nutrient concentrations were higher than in other sites, wave exposure and water mixing were preventing eutrophication signs to develop. This could perhaps be reflected in the data collected here, in that negative correlations were indicated between macroalgae biomass and tidal range. For neap tidal range the relationship was statistically significant (Table 8).

Physical factors evaluated such as slope and tidal ranges play a notable role in promoting the growth of opportunistic macroalgae in UK estuaries. Steeper slopes appear to support higher biomass accumulation, while tidal range, particularly the spring tidal range, is associated with increased macroalgae cover (Table 8). These

results indicate that the physical environment, including the structure of the seabed and tidal dynamics, influences the extent and spread of opportunistic macroalgae in these systems. Site specific factors can influence macroalgae biomass production and generalisation of predictors on macroalgae blooms is difficult to achieve. Future comparisons could be done by grouping estuaries sites with similar responses to e.g. nutrient enrichment or biomass production.

## 2.6 Conclusions

This chapter presented the analysis of secondary data from records of nutrients, macroalgae cover and biomass along with some physical characteristics which could potentially control macroalgae growth. The results presented here, illustrate that solely nutrient enrichment does not control macroalgae blooms in the UK estuaries. Instead, a combination of factors promotes eutrophication symptoms to develop, including sufficient nutrients for algae growth, enough time for the nutrients to be assimilated by the algae and a suitable intertidal area where light is available for photosynthesis to take place. This combination of factors should be considered when identifying potential problem sites and designing mitigation measures.

The trends in mean water column nutrient concentrations over time varied depending on the site. For example, in the Medway, Swale and Christchurch there has been considerable reductions in annual and winter mean nitrate, and DIP, this was reflected in a decrease in biomass and macroalgae covers in recent years in Medway. Whereas the sites with higher macroalgae biomass production had not reflected a decrease in nutrient enrichment over time and their nutrient concentrations are much lower than those observed in other sites; Suggesting that water column nutrients are not solely

responsible for eutrophication signs to develop (RQ1). Furthermore, steeper slopes appear to support higher biomass accumulation, while tidal range, particularly the spring tidal range, is associated with increased macroalgae cover. These results indicate that the physical environment, including the structure of the seabed and tidal dynamics, influences the extent and spread of opportunistic macroalgae in these systems (RQ2).

The data analysis presented also emphasises the importance of the evaluation of eutrophication in the UK estuaries through field campaigns, since eutrophication impacts cannot be predicted solely by aerial imagery. This is particularly of higher importance in sites such a Poole Harbour where macroalgae cover does not reflect the significant biomass production. Field campaigns could benefit from the use of new technologies such as drone imagery in order to reduce costs and get more comparable data between eutrophic estuaries so these sites can be monitored in a regular basis. As the current methodology for recording macroalgae biomass requires a significant amount of time and effort.

With these changes at least macroalgae cover could be monitored in a seasonal/annual basis with reduced cost and effort, making the monitoring of eutrophication in the UK coast more efficient and comparable on a temporal and spatial scale. Nutrient data monitoring in the UK estuaries is a robust data set, and more detail comparisons between nutrient concentrations and macroalgae cover would be beneficial for predicting and identifying mechanisms that enhance eutrophication and macroalgae blooms in these sites (RQ3).

Chapter 3.

# Sediment biogeochemistry from UK southern estuaries

## 3.1 Introduction

Portsmouth, Langstone and Poole Harbours were chosen from the estuaries analysed in Chapter 2 for a more in-depth analysis of sediment biogeochemistry. The aim of this chapter is to evaluate the impacts of macroalgae blooms in these estuaries, with a focus on carbon storage. Research questions for this chapter are:

**RQ4:** Are there major spatial differences in sediment biogeochemistry between sites and macroalgae presence and absence of macroalgae?

**RQ5:** To what extent benthic nutrients promote the persistence of the macroalgae blooms?

**RQ6:** Do macroalgae blooms promote more storage of organic carbon in sediment from intertidal zones?

## 3.2 Background

Estuaries are among the most productive marine ecosystems; they are the connection between land and oceans. Estuarine systems receive inflow from freshwater and organic matter constituting a complex ecosystem where interactions between biological, chemical, and environmental factors fuel primary productivity.

Eutrophication, excess of nutrient availability among other factors, favour condition for green opportunistic macroalgae species to proliferate (Chapter 2). These macroalgae species grow on top of the sediment covering most of the available intertidal areas. Water column nutrient concentrations are normally monitored to evaluate risk of eutrophication; however, sediment biogeochemistry is not commonly evaluated. This can be due to the logistically complicated sampling and processing of sediment samples which makes it costly to regularly monitor.

Macroalgal blooms can modify the biogeochemical cycles of C, N, P and S (Valiela et al., 1997), especially within the benthic ecosystem where they limit oxygen penetration. It is expected that sediment biogeochemistry exhibits pronounced differences in sites where there is more macroalgae deposition. Furthermore, Trimmer et al. 2000, suggested that self-regeneration of macroalgae mats is possible through the utilisation of benthic nutrients. Three of the estuaries in Chapter 2 with different eutrophication status where sampled and the results evaluating sediment biogeochemistry will be presented in this chapter. The sites had a different degree of macroalgal impact and were compared to each other with macroalgae presence and absence sediment cores.

### 3.2.1 Study sites

Three estuaries in the south coast of England were chosen for sampling based on the following eutrophication impact parameters: macroalgae cover, Ecological Quality Ratio (EQR) and Eutrophication status classification by OSPAR Common Procedure (OSPAR CP) (Section 2.2.2.1).


**Figure 25. Study area map showing the estuaries chosen in the south coast of the UK: Poole, Portsmouth and Langstone Harbours.**

#### 3.2.1.1 Portsmouth Harbour

Portsmouth Harbour is an industrialised estuary, which form part of one of the four largest expanses of mudflats on the south coast of the UK. These mudflats support the growing of eelgrass and extensive opportunistic green algae. The total surface area at high tide is 16.597 $km^2$.

The harbour is also part of the estuarine system of the Solent area, and it has been designated as Site of Special Scientific Interest (SSSI) however this area is just the north part of the estuary comprising 12.642 $Km^2$. Portsmouth has been one of the most impacted sites by macroalgae cover in the past decades registering up to 74.7% in 2007, however the most recent survey showed a clear decrease to 21.1% of macroalgae cover in 2016. Biomass also decreased during the register period from 461 $g/m^2$ to 194 $g/m^2$ which suggests that conditions for this site have improved over time.

### 3.2.1.2 Langstone Harbour

Langstone Harbour is a transitional water body located at the southeast of the English coast with a surface area of 19.027 $km^2$ of which 1,449.3 $km^2$ are intertidal areas. At low tide, around ¾ of the total area is completely exposed. The area is designated as a Site of Special Scientific Interest (SSSI) and Special Protection Area (SPA) to its ecological importance supporting migratory bird species. Langstone Harbour biomass reported in (Chapter 2) increased from 463 to 603 $g/m^2$ on the available year whereas macroalgae cover remained in the range of 24-25% through time.

### 3.2.1.3 Poole Harbour

Poole Harbour is a bar-built estuary that has an extent area of 32.239 $km^2$; It is composed by three subsidiary basins: The largest being Holes Bay, Lytchett Bay and the smaller Newton Bay. Although categorised as an estuary (As several rivers flow into it), it has the characteristics of a costal lagoon due to its narrow mouth and characteristic micro-tidal regime (Humphreys, 2005). Poole Harbour biomass showed

a decrease from 1890 to 1315 g/m$^2$ on the last data, although a decrease was observed for this site on biomass, this is still the most impacted site on this regard.

# 3.3 Methods

## 3.3.1 Sampling

Sampling was conducted between the 28th of June and the 2nd of July 2021. A total of 5 sampling sites within the three selected estuaries of Langstone, Portsmouth and Poole Harbours (Chapter 2).

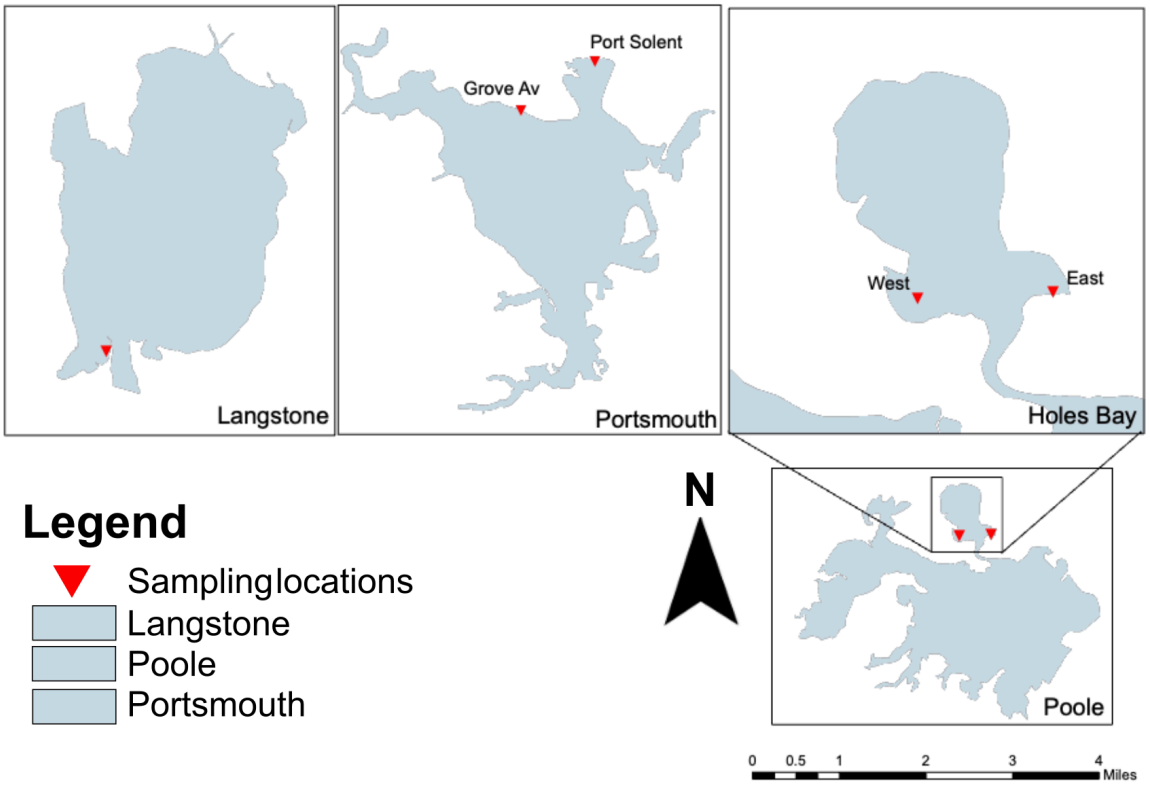


**Figure 26. Sampling locations in Langstone, Portsmouth (Grove Av and Port Solent), and Poole (East and West).**

Sites where distributed the as follows, one sampling site for Langstone, two in Portsmouth (Grove Av and Port Solent) and two for Poole (East and West) see Table 10 for exact coordinates.

**Table 10. Sampling sites coordinates given in latitude and longitude for Langstone, Portsmouth and Poole Harbours.**

| Site | Latitude (N) | Longitude (E) |
|---|---|---|
| **Langstone** | 49.982365 | -0.540438 |
| **Portsmouth Grove Av** | 49.987638 | -0.536399 |
| **Portsmouth Port Solent** | 49.986659 | -0.535996 |
| **Poole East** | 50.71949 | -1.986377 |
| **Poole West** | 50.719032 | -2.002044 |

Sediment cores were collected from the intertidal area of each sampling site at low tide, using 10 cm diameter acrylic tubes. Sampled depth for the sediment cores was of 12 cm, with some exceptions where sediment conditions prevented sufficient penetration. At each site, two cores of sediment below macroalgae mats and two below bare sediment. Due to the spatial extent of macroalgae mats only one macroalgae absent core was collected at each Poole Harbour sites. A total of 18 sediment cores were samples from these sites.

The sediment cores were extruded and sliced at 0.5 cm resolution for the top 2 cm, below that every 1 cm until 10 cm depth, and then 10-12 cm. Sediment was stored in sterilized Whirl-Pak Flat Wire sample bags, and frozen after collection. Samples were kept frozen during transport and placed into a -20°C freezer before processing in the University of Leeds. All sediment was freeze-dried using a Lablyo Mini freeze drier. Sediment bags were weighed before and after freeze-drying and weights were recorded. Once dried, sediment particles were disaggregated and well mixed before subsamples were taken for particle size and elemental CHN analyses.

Porewaters were extracted from separate cores, one for macroalgae absence and another one for macroalgae presence from each sampling site. The core acrylic tubes used were pre-drilled at intervals of 1 cm. 10 mL syringes connected to prerinsed Rhyzons with deionized water (0.15 µm pore size) the porewaters were sampled from the top 10 cm of the sediment cores for subsequent dissolved nutrient and trace metals analyses. Subsamples were transferred pipetting 1 mL in 1.5 mL sterile microcentrifuge plastic tubes and then acidified with 10 µL of concentrated HCl to prevent metal precipitation. The remaining porewater samples were transferred from the syringes to 15 mL centrifuge tubes and frozen for nutrient analysis.

## 3.3.1.1 Sampling sites conditions during fieldwork

### 3.3.1.1.1 Langstone Harbour

In Langstone Harbour there was an evenly spread layer of macroalgae with visible tubular structures in the sediment clear signs of bioturbation (Figure 27). Multiple macroalgae species were observed during sampling, including brown macroalgae attached to rocks on the shore, but green algae were dominant.

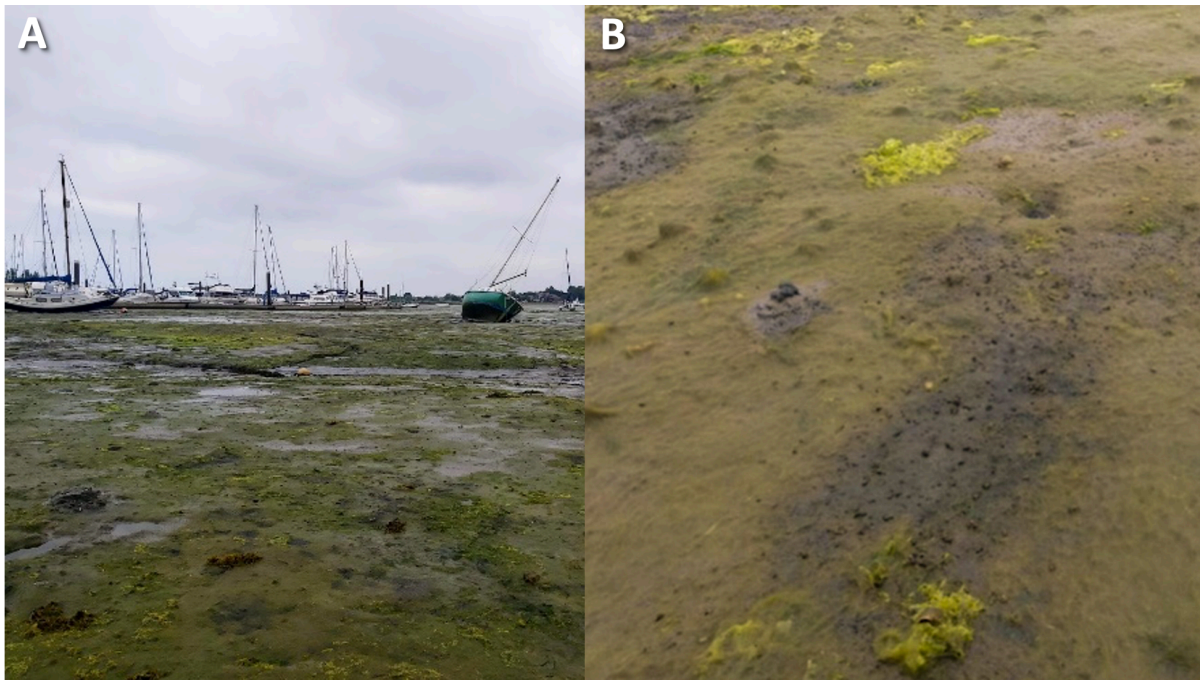


**Figure 27. Field images from Langstone Harbour July 2021. A. Extent of intertidal area covered by macroalgae at low tide, B. Macroalgae absent patch showing multiple burrowing structures on sediment surface.**

### 3.3.1.1.2 Portsmouth Harbour

In Portsmouth Harbour Grove Avenue there was a more uneven distribution of macroalgae and seagrass was also observed during sampling (Figure 28). In Port Solent there was a dense layer of macroalgae covering the sediment and entrained macroalgae biomass was observed within macroalgae present sediment cores (Figure 29). Besides, the surface was visibly darker below the macroalgae mats while sediment from macroalgae absent cores was grey coloured except for the top in the macroalgae cores.

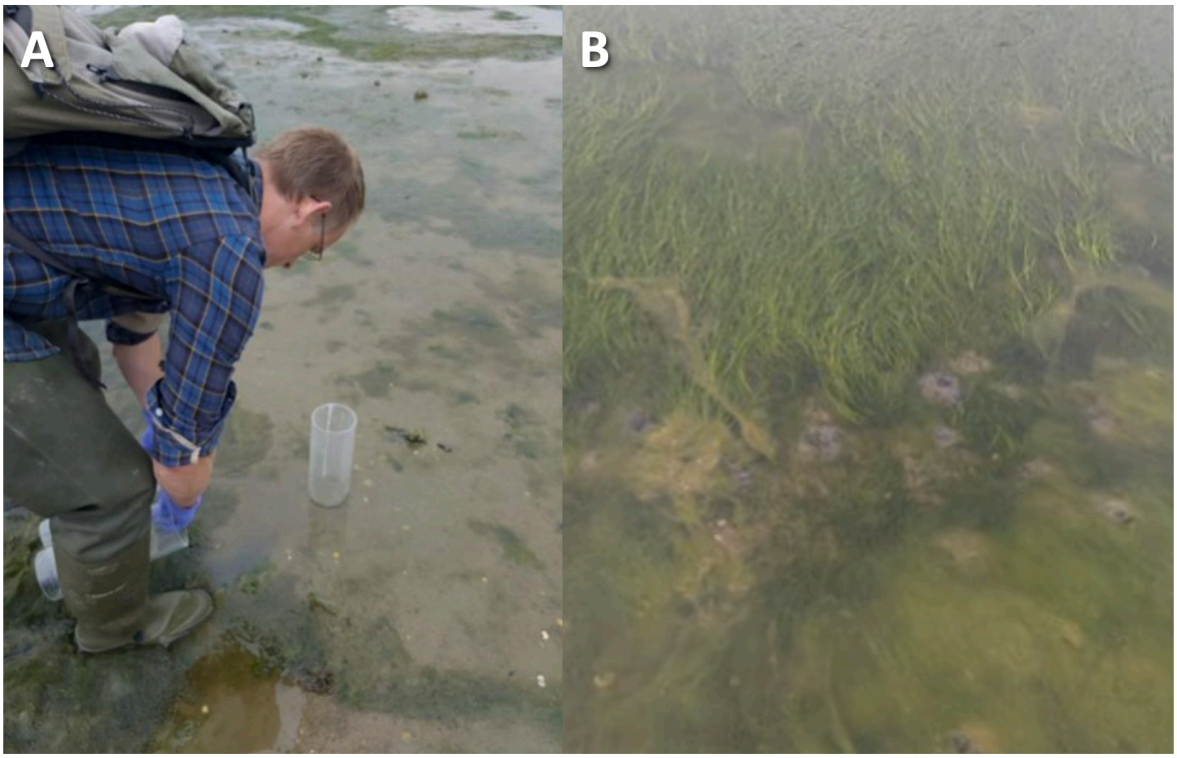


**Figure 28. Field images from Portsmouth Grove Av in July 2021. A. Macroalgae free sediment, B. Seagrass and macroalgae growing on the intertidal area of Grove Av.**


**Figure 29. Field images from Portsmouth Port Solent July 2021. A. Extent of intertidal area covered by macroalgae at low tide, B. Dense macroalgae mat covering macroalgae present sediment cores.**

### 3.3.1.1.3 Poole Harbour

At the Poole Harbour sites, all the exposed intertidal area was covered in macroalgae. Poole Harbour East was surrounded by rocks and there were various types of algae, including brown algae growing attached to the rocks. However, the exposed intertidal area at both sites was entirely covered with opportunistic green algae (Figure 30 and Figure 31).

As highlighted before, there was little to no exposed sediment, therefore it was not possible to extract a replicate core for macroalgae absent sediment at the Poole East and Poole West sites. It can be observed (Figure 30 and Figure 31) that there were patches of algae that were dried by sun exposure. The cored sediment was visibly black all along the sampling tube and had a strong sulfidic smell.

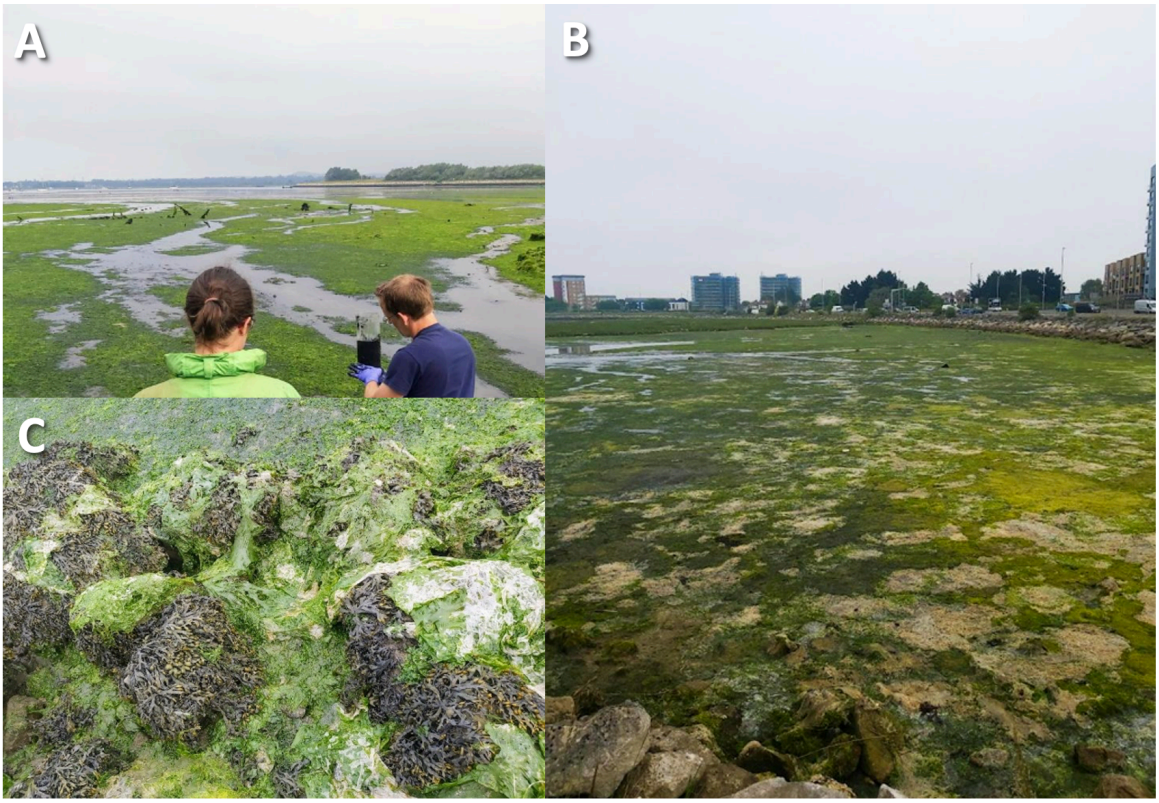


**Figure 30. Field images from Poole Harbour East July 2021. A. Extent of intertidal area covered by macroalgae at low tide, B. Patches of green macroalgae at different stages of decomposition on the intertidal area, C. Brown macroalgae growing attached to the rocky shore.**

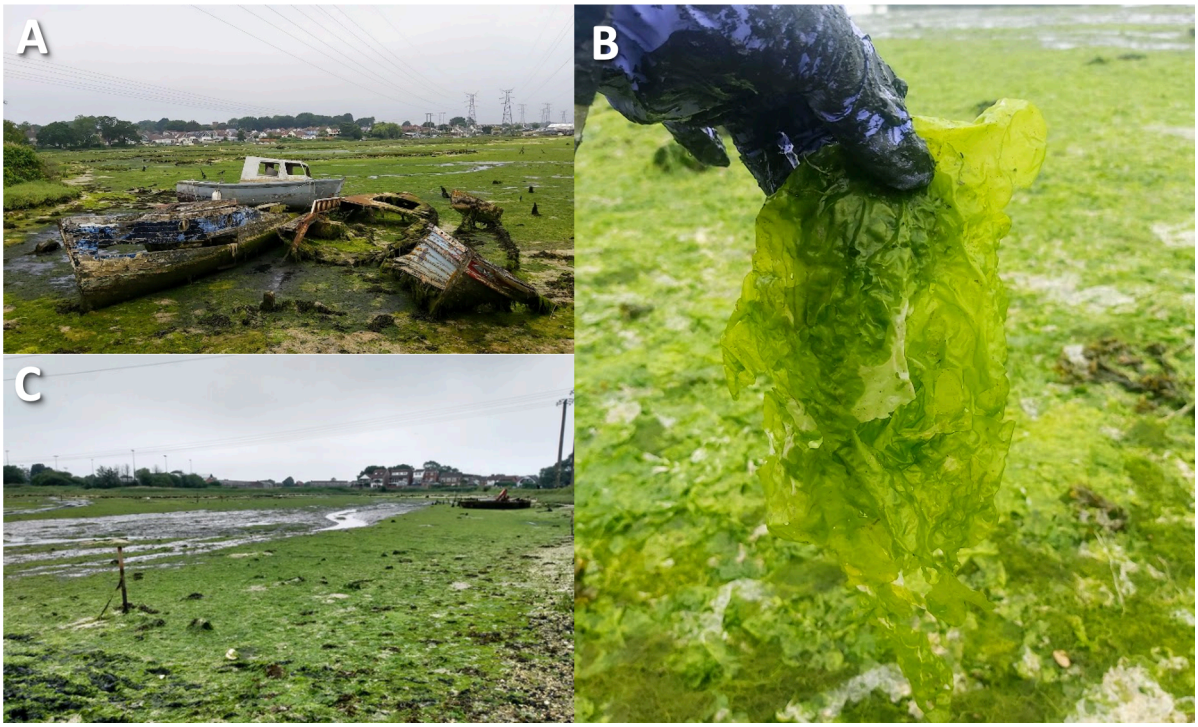


**Figure 31. Field images of Poole Harbour West in July 2021. A. Abandoned boats on the shore of Poole Harbour West, B. Macroalgae (species) and C. Intertidal area at low tide showing the extent of the macroalgae bloom.**

### 3.3.2 ICP-OES

Acidified subsamples were analysed for metals as well as total S, P and Si by Inductively Coupled Plasma-Optical Emission Spectroscopy (ICP-OES). This includes K, Na, Ca, S, Mg, Fe, Mn, Si and P. All results fit in the 95% confidence interval except for Ba and Mn (6.67% and 5.98% uncertainty respectively (Table 11). All results below the limits of detection and quantification were plotted as zero concentrations. DIP in Portsmouth Harbour was measured by ICP-OES just at one of the sites as the extracted volume of porewater was insufficient for both analyses.

DSi was measured as total sulphur by the ICP-OES instrument, however when discussing these results, it is assumed that total sulphur is primarily DSi as samples where immediately acidified. Results of K, Ca, S and Mg are presented as ratios of Na concentrations, this to account for Na variability in the different sites, to make it comparable these ions were normalised to Na concentrations.

**Table 11. Limits of detection and quantification for ICP-OES method alongside % of uncertainty.**

| | K | Na | Ca | S | Mg | Fe | Mn | Si | P |
|---|---|---|---|---|---|---|---|---|---|
| LOD ($mgL^{-1}$) | 5.44E+00 | 1.11E+01 | 8.15E-01 | 5.40E+00 | 2.34E+00 | 1.86E-03 | 1.10E-04 | 4.95E-03 | 2.40E-03 |
| LOQ ($mgL^{-1}$) | 1.81E+01 | 3.71E+01 | 2.72E+00 | 1.80E+01 | 7.79E+00 | 6.20E-03 | 3.67E-04 | 1.65E-02 | 8.01E-03 |
| Uncertainty (%) | 1.05 | 0.42 | 0.52 | 0.80 | 0.60 | 2.47 | 5.98 | 5.09 | 3.16 |

LOD = Limit of detection (The concentration below which the analyte cannot be detected). Calculated as 3x stdev of 6 blank measurements.

LOQ = Limit of quantification. (The concentration below which the analyte cannot be quantified). Calculated as 10x stdev of 6 blank measurements.

% Uncertainty = The 95 % confidence interval of 6 repeated standard measurements related to the mean as a percentage.

### 3.3.3 Dissolved nutrients

The non-acidified subsamples were analysed for total nitrogen, ammonium, nitrite, (nitrite+nitrate), phosphate and silicate. Samples were analysed with a continuous flow analyser (SAN++, Skalar) in the analytical laboratory in the School of Geography (University of Leeds). Nitrate fraction was calculated by subtracting nitrite values from the nitrite+nitrate data. Results were given in mg/L and compared with certified values. Certified reference material used for N species and P concentrations was Simple Nutrients in Seawater-QC3179 (Table 12). 15% replicates were run alongside with the samples. Results in mg/L were converted to µmol/L using their respective conversion factor for each nutrient.

**Table 12. Comparison between nutrient certified concentrations of the CRM Simple Nutrients in Seawater-QC3179.**

| | $NH_4$_N | NO2_N | ($NO_2$_N+$NO_3$_N) | $NO_3$_N | PO4_N |
|---|---|---|---|---|---|
| QC3179 | (mg/L) | (mg/L) | (mg/L) | (mg/L) | (mg/L) |
| Certified values | 14.3 | 1.99 | 9.04 | 7.05 | 1.46 |
| Comparison with CRM (%) Duplicate 1 | 96 | 81 | 101 | - | 102 |
| Comparison with CRM (%) Duplicate 2 | 95 | 81 | 100 | - | 103 |

### 3.3.4 Elemental CHN

Sediment samples were freeze-dried using a Lablyo Mini freeze-dryer until constant weight was reached. Sample bags were weighed before and after freeze-drying, and the weight was recorded working out the average weight of the bags. Once dried, sediment samples were gently disintegrated by hand while inside the bags and subsamples were taken out. Macroalgae, seashells, pebbles and other visible components were extracted using clean tweezers prior to grinding of the remaining subsample with an agate pestle and mortar.

8 mg of sample was weight out in Elemental Microanalysis 5x8 mm silver capsules. Peaty soil was used as CRM and Sulfanilic Acid as standard and for calibration. Replicates were runed for 10% of the samples and blank capsules were measured Samples and CRM capsules were acidified with 30 µl of 15% HCl to remove inorganic C, oven-dried at 80°C until dry. Capsules were folded and packed into small cubes prior to analysing them in an Elementar vario EL cube.

### 3.3.5 Particle Size Analysis

Subsamples of 3 g from the original bags were weight into 125 mL shaking bottles. Subsequently, 50 ml of Calgon 5% was added to the bottles to disperse the sediment particles. The shaking bottles were placed on a shaker table at 95 rpm for 2 hrs for proper disaggregation and dispersion of the sediment in the solution. After preparation, a shaking bottle was poured into a beaker with a stir bar and ~ 1 mL of sample slurry was introduced into the laser diffraction particle size analyser (Coulter TM LS230), this procedure was repeated 3 times for each sample. All 9 curves were

integrated to produce an average before exporting the data. Particle size results for Poole Harbour East are not presented as macroalgae fragments at multiple depths were interfering with sediment PSA.

### 3.3.6 Data analysis

Significant differences between organic carbon tested between estuaries and presence and absence of macroalgae with Kruskal-Wallis statistical test. Spearman's correlation test was also performed to explore relationship between particle size and organic carbon for the different sampling sites.

Results for dissolved nutrients, dissolved metals, organic carbon, C:N ratios and particle size data are presented in graphics as line plots representing the changes with depth. All plots were made using RStudio and ggplot2 package. Basic statistics, mean, min, max, standard deviation and ranges were obtained in RStudio, using "dplyr" package and the function summarise.

# 3.4 Results

## 3.4.1 Porewater nutrients general trends

### 3.4.1.1 Dissolved Inorganic Nitrogen (DIN), Ammonium, Nitrite and Nitrate

DIN concentrations in Langstone ranged from 175 to 1100 µmol/L, the minimum value was found at 1 cm in the macroalgae absent cores and the maximum at the top of the macroalgae present core (Figure 32A). Differences between macroalgae presence and absence will be presented in the next section (Figure 32).

Minimum and maximum DIN concentrations were very similar for both sites 27.1 and 30.3 µmol/L; 357 and 376 µmol/L for Grove Av and Port Solent respectively. However, distribution down core was the opposite. While maximum concentrations where at the top in Port Solent, Grove Av had minimum concentrations at the top of the core with a tendency to increase with depth (Figure 32B &C).

Poole East DIN concentrations ranged from 70.5 – 976 µmol/L, likewise Poole West concentrations fell in the range of 77.4 – 911 µmol/L, distributions downcore where similar in both sites of Poole Harbour, starting with considerably high concentrations at the top and a sharp decrease between 2-3 cm to start increasing gradually with depth again (Figure 32D & E).

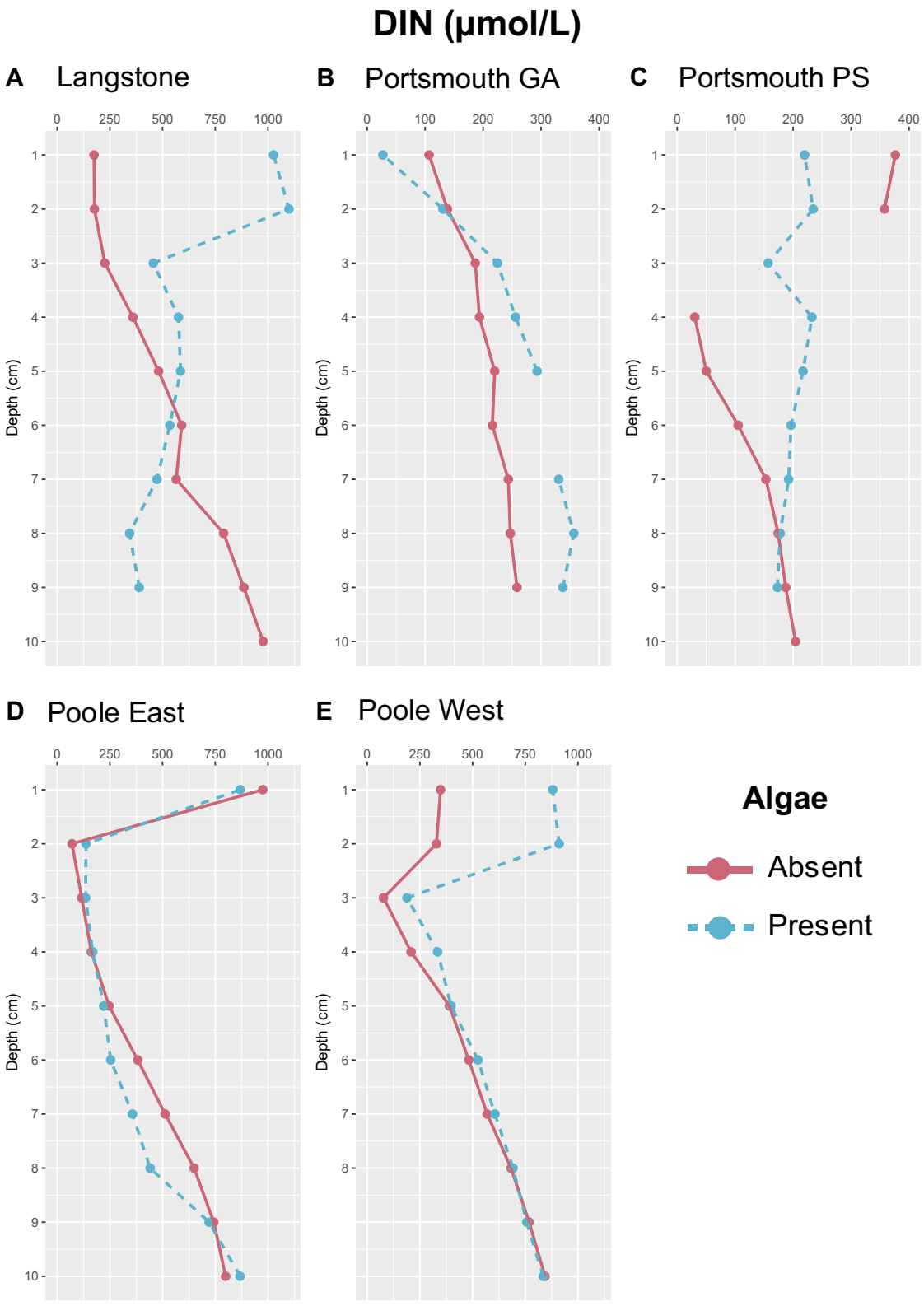


**Figure 32. Dissolved Inorganic Nitrogen (DIN) profiles (µmol/L) in the porewaters of the top 10 cm sediment for each sampling site. Red line represents the core where macroalgae was absent while blue dotted line represents macroalgae present cores.**

Ammonium was the major component of the DIN and represented more than 93% of the measured DIN all sites. Poole East had the greatest ammonium fraction with 97.7%, Langstone followed with a similar 97.5%, and Poole West 97.4% (Figure 33). Portsmouth Harbour sites had a slightly lower fraction of ammonium than the rest of the sites with 94.5% and 93.7% in Port Solent and Grove Av respectively (Figure 33).

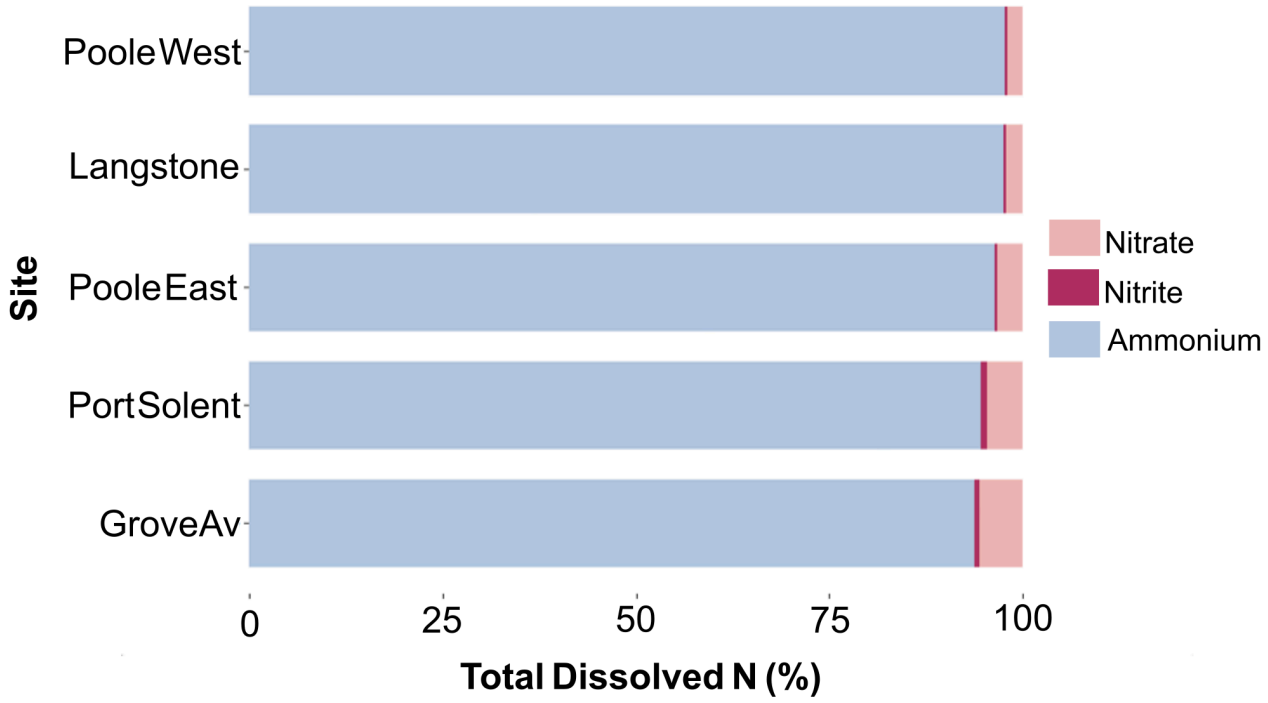


**Figure 33. Bar plot showing the different fractions (Nitrite, nitrate and ammonium) of the dissolved inorganic nitrogen. Each bar is the result of the mean of the cores for the respective site.**

In Langstone ammonium concentrations ranged from 159.6 to 1093.4 µmol/L, the minimum concentration was on the macroalgae absent core at 2 cm depth whereas the maximum was at the same depth on the macroalgae present core (Figure 34A). Distribution downcore differ from present and absent cores, the absent core had lower concentrations at the surface and increased progressively with depth. On the other hand, the macroalgae present core had a subsurface peak at 2 cm depth and

decreased sharply by 3 cm from 1093.4 µmol/L to 449.9 µmol/L until it reached its minimum at 8 cm depth (Figure 34A).

In Portsmouth Harbour Grove Av ammonium concentrations ranged between 19 and 348 µmol/L, minimum concentrations for both macroalgae present and absent cores were found at the surface, 88.4 µmol/L and 19.1 µmol/L respectively. In both cores ammonium concentrations increased with depth, however the enrichment was higher in the macroalgae present core with a minimum concentration at 8 cm depth of 348.1 µmol/L whereas the absent core reached its minimum of 251.3 µmol/L at 9 cm depth (Figure 34B).

In Port Solent, slightly higher values than in Grove Av were observed 24–366 µmol/L. Concentrations were lower at the top for the macroalgae present cores. However, differences arose as depth increased. In Port Solent the absent core decreased its minimum concentration sharply by 4 cm depth and slightly increased again with depth while the macroalgae core reached its maximum value at 2 cm, but concentrations decreased slightly with depth (Figure 34C).

In Poole Harbour sites ammonium concentrations ranged 61.2 - 964.5 µmol/L and 73.9 – 902.6 µmol/L for East and West respectively (Figure 34D & E). In Poole East the presence or absence of macroalgae did not affect the distribution of ammonium downcore, in both cores there was a surface peak with maximum concentration for the absent core 964.4 µmol/L and 854.8 µmol/L for the present core. By 2 cm depth both concentrations decreased significantly to 612 µmol/L and 135.3 µmol/L for the absent and present cores respectively to start increasing downcore (Figure 34).

In the case of Poole West in the west site there was a clear difference between macroalgae presence and absence at the surface where the present core had up to 3 times more ammonium (880.2 µmol/L) than the absent core (333.9 µmol/L). Both cores decreased to its minimum concentrations at 3 cm depth, 73.9 µmol/L and 173.5 µmol/L and started increasing progressively with depth after (Figure 34E).

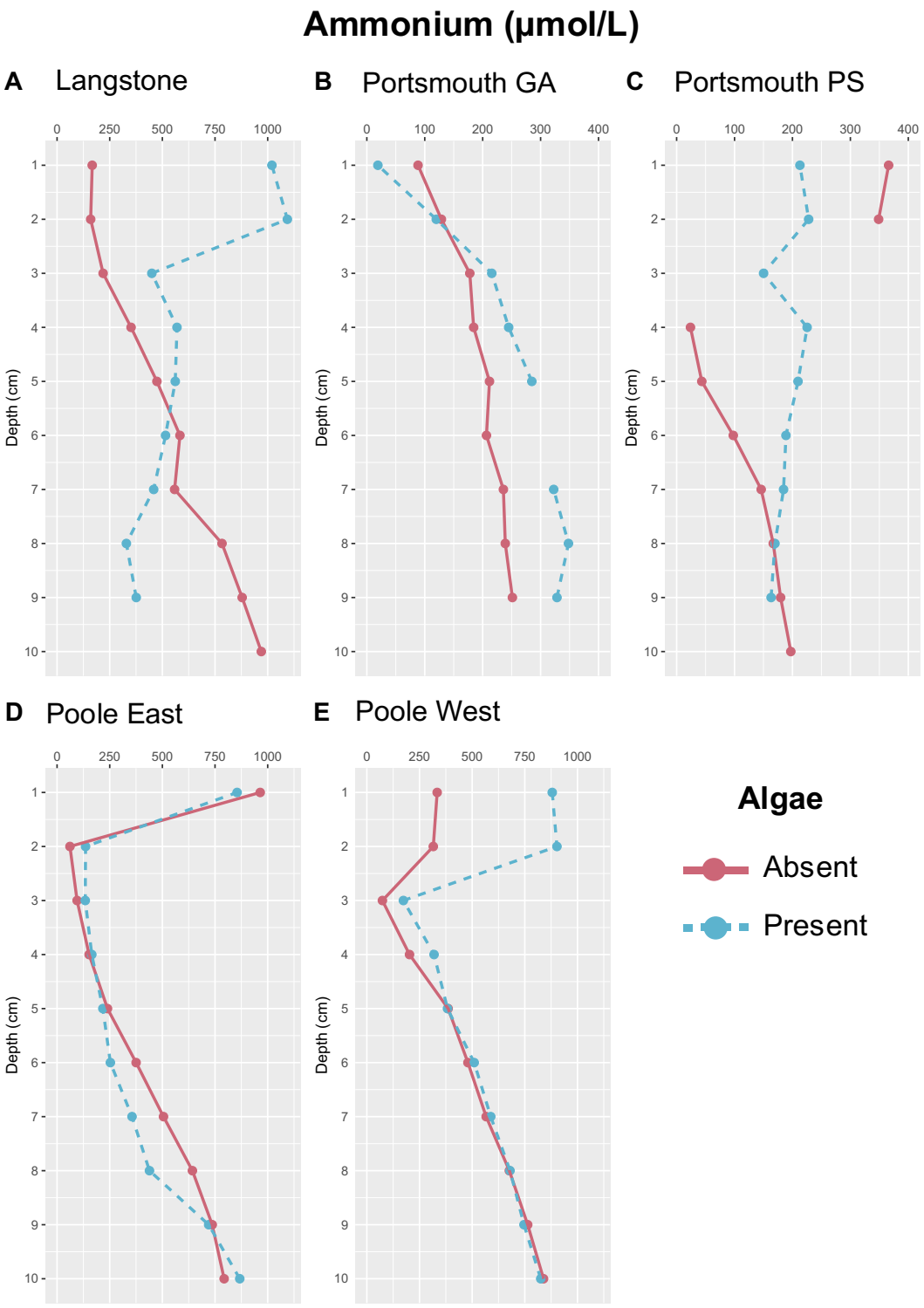


**Figure 34. Ammonium profiles (µmol/L) in the porewaters of the top 10 cm sediment for each sampling site. Red line represents the core where macroalgae was absent while blue dotted line represents macroalgae present cores.**

In Langstone nitrate had a minimum concentration of 5.14 µmol/L and a maximum of 23.2 µmol/L. Distributions downcore were different for macroalgae presence and absence (Figure 35A). The macroalgae absent core had a subsurface peak at 2 cm depth with its maximum concentration of 15.4 µmol/L and decreased by 3 cm (5.4 µmol/L), after this depth concentrations had little variation. On the macroalgae present core the opposite pattern was observed where constant values were found up to 4 cm depth with a peak at 5 cm (23.2 µmol/L) to decrease with depth again reaching 6.5 µmol/L at 10 cm depth (Figure 35A).

In both Portsmouth sites, nitrate was more abundant than the other locations. Nitrate concentrations ranged from 6.1 – 16.9 µmol/L and 5.4 – 9.2 µmol/L for Grove Av and Port Solent respectively (Figure 35B & C). In Grove Av surface nitrate concentrations were higher on the macroalgae absent core 16.9 µmol/L, than on the present core 6.9 µmol/L. The minimum concentration at the macroalgae absent was reached at the bottom of the core (6 µmol/L). On the other hand, the macroalgae present core reached its maximum at the 4 cm depth (Figure 35B).

In Port Solent, nitrate was more abundant at the surface on the macroalgae absent core compared to present core, 9.2 µmol/L and 5.9 µmol/L respectively, by 3 cm depth both cores had similar concentrations and remained comparable for the rest of the core (Figure 35C).

Poole East nitrate concentrations ranged from 0.4 – 20.5 µmol/L while in Poole West 1.4 – 17.1 µmol/L. Maximum concentration in the East was detected at 3 cm depth on the macroalgae absent core whereas the minimum concentration was on the

macroalgae present core at the same depth (Figure 35D & E). In Poole West, the maximum concentration was found at 7 cm depth on the macroalgae present core and minimum was on the absent core at 6 cm depth (Figure 35E).

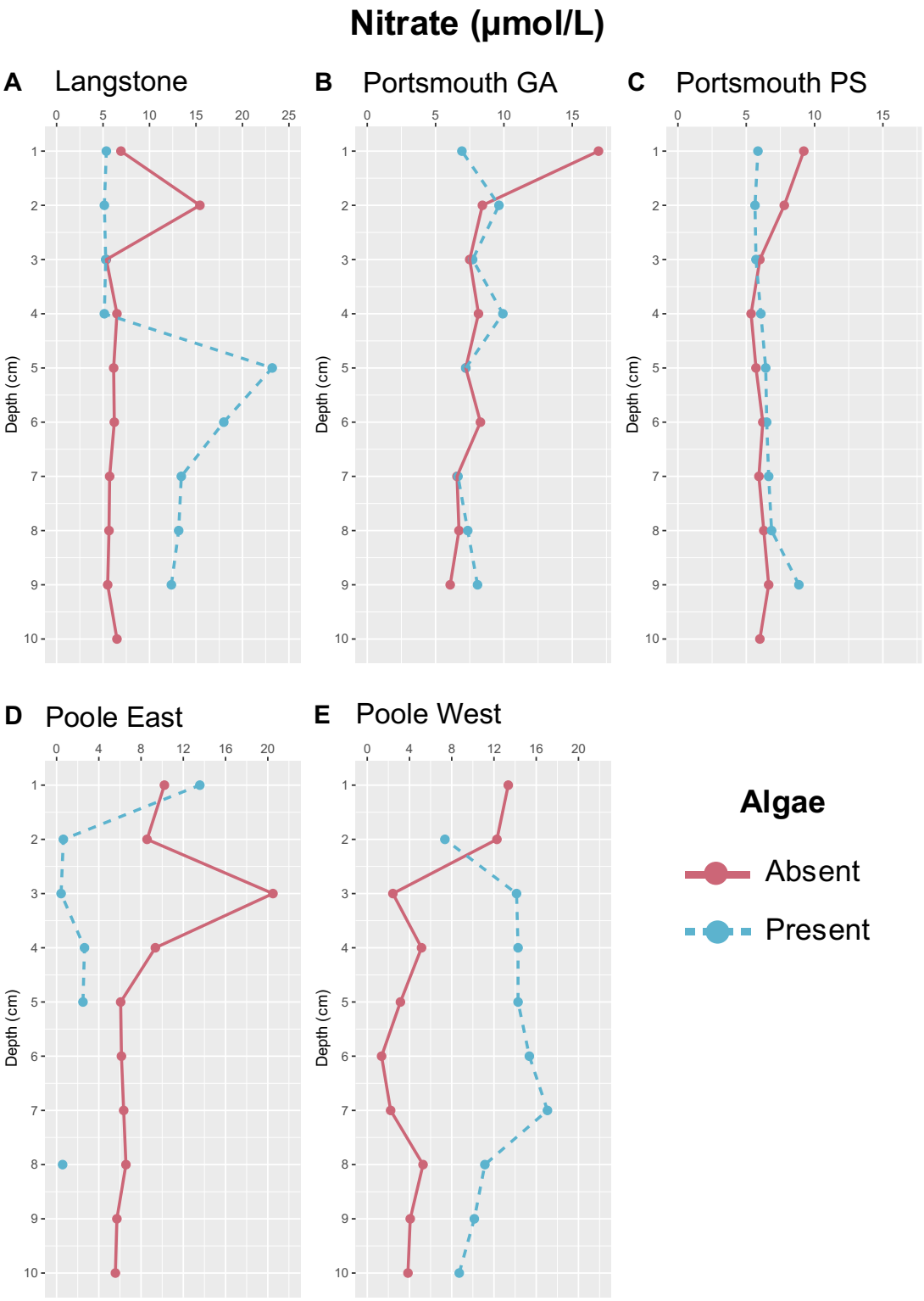


**Figure 35. Nitrate profiles (µmol/L) in the porewaters of the top 10 cm sediment for each sampling site. Red line represents the core where macroalgae was absent while blue dotted line represents macroalgae present cores.**

In Langstone nitrite concentrations ranged between 0.9 – 1.9 µmol/L the minimum concentration was at 4 cm depth in the macroalgae present core while the maximum was found in the absent core at 3 cm depth (Figure 36A). Downcore distribution for the macroalgae absent core showed a sub-surface peak at 2 and 3 cm (Max= 1.9 µmol/L) depth and decreased at 5 cm again, to have less variable concentrations below. The macroalgae present core had similar concentrations on the top 5 cm and concentrations peaked at 7cm depth (1.4 µmol/L).

Nitrite concentrations in Grove Av ranged 1.1 – 1.4 µmol/L minimum concentration was at the surface of the macroalgae present core and maximum at the surface of the absent core (Figure 36B). Nitrite was more abundant in the macroalgae absent core with the higher concentration found at the surface (1.4 µmol/L), concentrations for this core decreased with depth and reached its minimum at 5 cm depth (1.1 µmol/L). On the contrary the presence of macroalgae resulted in less nitrate at the top 2 cm and minimum concentration was detected at the surface (1.07 µmol/L) and increased slightly with depth reaching its maximum at 9 cm (1.2 µmol/L) (Figure 36B).

The range of nitrite concentrations in Port Solent was 1 – 1.2 µmol/L, minimum values were at multiple depths in the present core while maximum was observed in the absent core at 2 cm (Figure 36C). The greatest differences were observed at the top of the cores where the macroalgae absent core had higher concentrations than the macroalgae present core with 1.1 µmol/L and 1 µmol/L respectively and both cores slightly decreased concentrations with depth (Figure 36B).

In Poole East nitrite concentrations 0.5 – 1.4 µmol/L, the minimum concentration was recorded at the surface of the macroalgae present core (0.5 µmol/L) and 10 cm of the absent cores (5.6 µmol/L), whereas the maximum at 8 cm on the present core (Figure 36D). The macroalgae present core had lower concentration in the top 0.5 µmol/L and compared to the absent core (0.9 µmol/L). Downcore distribution where also contrasting, while the macroalgae present core increased concentrations with depth the opposite was true for the absent core (Figure 36D).

On the other hand, Poole West nitrite concentrations fell between the range of 0.6 – 1.1 µmol/L. Minimum concentration on this site was observed at 10 cm of the macroalgae absent core while the maximum at 3 cm on the same core (Figure 36E).

The macroalgae present core started with lower concentrations at the top 3 cm with its minimum concentrations found at the surface (0.6 µmol/L) and remained similar for the rest of the core, while the macroalgae absent core has higher concentrations at the top 3 cm and peaked at that depth with a concentration of 1.1 µmol/L, after that it decreased progressively with depth (Figure 36E).

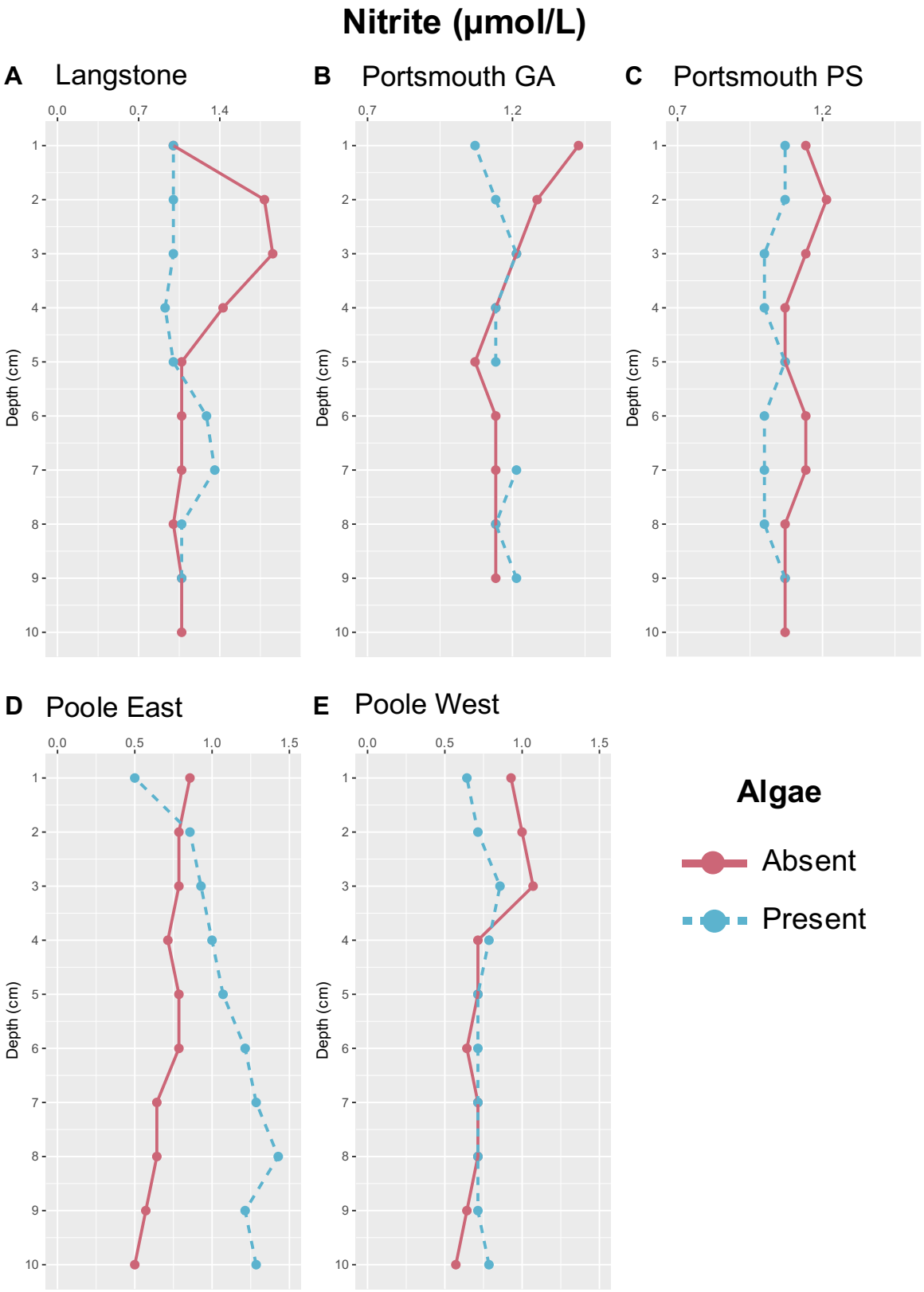


**Figure 36. Nitrite profiles (µmol/L) in the porewaters of the top 10 cm sediment for each sampling site. Red line represents the core where macroalgae was absent while blue dotted line represents macroalgae present cores.**

### 3.4.1.2 Dissolved Inorganic Phosphorus

Langstone had a range of Dissolved Inorganic Phosphorus (DIP) concentrations between 28.7 – 275.3 µmol/L, the maximum value was observed at the bottom of the macroalgae absent core whereas the minimum was reached at 6 cm depth on the macroalgae present core (Figure 37A). Surface concentrations However, there is insufficient data points on the macroalgae present core to identify any downcore patterns (Figure 37A).

In Portsmouth Harbour DIP was only measured in Port Solent as the extracted volume of porewater was insufficient for ICP analyses of Grove Av samples. Therefore, in Port Solent DIP values ranged from 3 to 42 µmol/L, top 4 cm of the macroalgae present core had higher concentrations reaching its maximum at 4 cm with 24.9 and decreased again with depth. DIP was not detected on the surface of the absent core and below the surface started to increase concentration with depth until reached its maximum value of 40.1 µmol/L at 10 cm (Figure 37B).

In Poole Harbour mean DIP concentrations for the East were in the range of 14.2 – 138.7 µmol/L. In Poole East the minimum concentration was found at the surface of the macroalgae present core and maximum at the 10 cm depth in the absent core. Concentrations on both cores for the top 4 cm was similar and below that depth (Figure 37BC).

DIP concentrations in Poole West 39.5 – 284.6 µmol/L, the minimum value was found at the surface of the absent core and maximum at the bottom of the macroalgae present core (Figure 37D). The macroalgae absent core had lower

concentrations at all depths, and had its minimum at the surface 39.5 µmol/L and increased with depth until it reached its maximum at the 10 cm depth 183.4 µmol/L. The macroalgae present core had a similar distribution started with the lowest concentration at the top cm 77.5 µmol/L, there was a subsurface peak at 2 cm depth (198.4 µmol/L) and reached its maximum at the bottom with 284.6 µmol/L (Figure 37E).

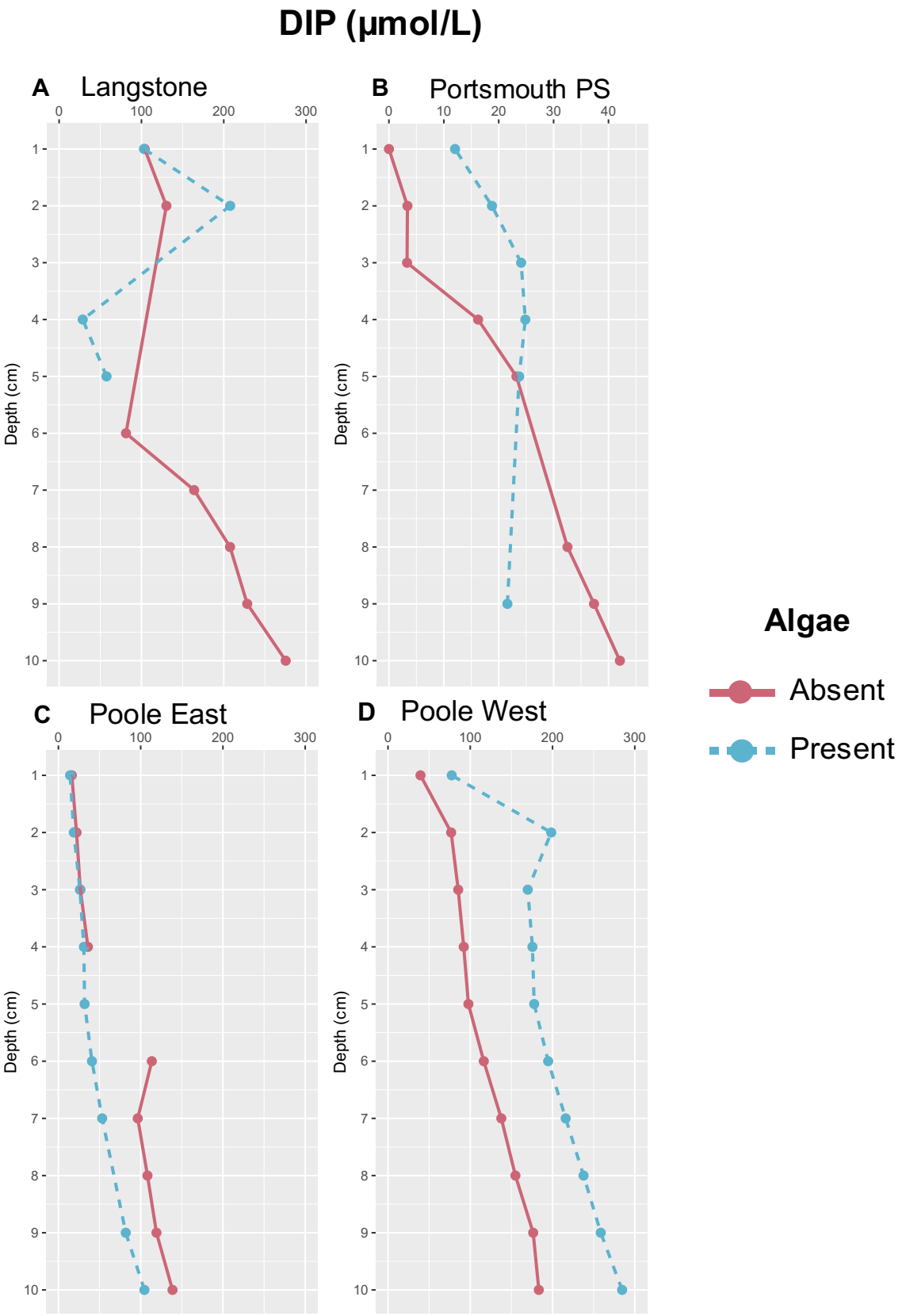


**Figure 37. Dissolved Inorganic Phosphorus (DIP) profiles (µmol/L) in the porewaters of the top 10 cm sediment for each sampling site. Red line represents the core where macroalgae was absent while blue dotted line represents macroalgae present cores.**

### 3.4.1.3 Dissolved Silicon

Dissolved silicon (DSi) in Langstone ranged 320.4 – 685.4 µmol/L, the minimum concentration was at the surface in the absent core (Figure 38A). There were not enough data points to compare downcore trends between cores, however there was higher concentrations at the top of the macroalgae present core (508.1 µmol/L) and the absent core starts with low concentrations at the top (320.4 µmol/L) that progressively increased with depth until it reached its maximum at the bottom of the core (685.4 µmol/L).

In Port Solent DSi concentrations went from 30.8 to 552.7 µmol/L, minimum value was again at the surface of the absent core while the minimum was observed at the 10 cm depth from the same core. The macroalgae present core had a higher concentration at the top of the core 164.3 µmol/L and increased with depth and reached its maximum at 9 cm depth 389.9 µmol/L. On the macroalgae absent core there was a lower concentration at the top, 30.8 µmol/L but concentrations increased sharply at 2 cm depth (266.4 µmol/L) and another sharp increase at 5 cm (506.5 µmol/L), until it reached the maximum concentration at 10 cm depth with 552.7 µmol/L (Figure 38B).

DSi in Poole East ranged between 120.2 – 561.8 µmol/L, minimum value was observed on the first cm in the absent core while the maximum concentration was measured at 6 cm depth in the same core (Figure 38C). While the macroalgae present core presented a slight increase with depth, the absent core had a marked increase at 6 cm and concentrations remained higher for the rest of the core.

In Poole West DSi concentrations were higher than in the East ranging between 172.5 and 700.5 µmol/L. Minimum DSi concentration was at the surface of the macroalgae absent core and the maximum was found at the 10 cm in the macroalgae present core (Figure 38D). Both cores displayed an increase in concentrations with depth, however the macroalgae present core had higher concentrations in the top 6 cm.

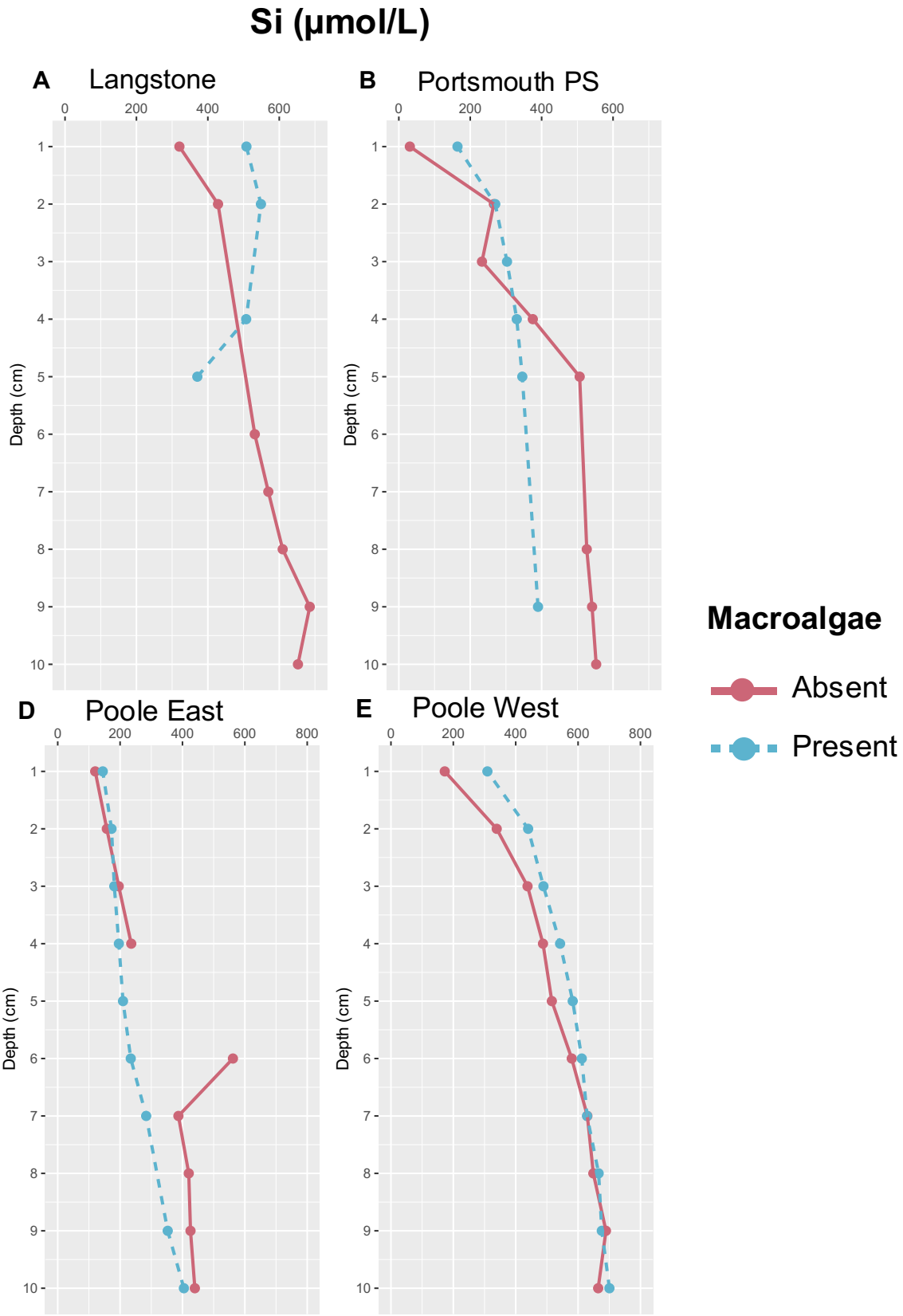


**Figure 38. Dissolved silicon profiles (µmol/L) in the porewaters of the top 10 cm sediment for each sampling site. Red line represents the core where macroalgae was absent while blue dotted line represents macroalgae present cores.**

## 3.4.2 Dissolved metals

### 3.4.2.1 Iron

Langstone stood out significantly from the other estuaries with the highest Fe concentrations ranging 36.6 – 406.4 µmol/L. The highest concentration was detected at the top of the macroalgae absent core (406.4 µmol/L), concentrations decreased with depth and reached its minimum at 10 cm depth (49.3 µmol/L). The macroalgae present core was less enriched and started with a surface concentration of 50.9 µmol/L by 4 cm depth Fe was not detected and at 5 cm depth Fe concentration peaked to 125.5 µmol/L (Figure 39A). In Port Solent a similar pattern was observed where Fe was not detected in the macroalgae present core, and the absent core had its maximum concentration at the surface 2.9 µmol/L but was not detected below 3 cm depth (Figure 39B).

Fe in Poole East was at its highest concentration at the top of the absent core 6.55 µmol/L, by 2 cm depth declined to 2.2 µmol/L and was not detected below this depth. On the present core, Fe was only detectable at 3 cm depth with a concentration of 1.3 µmol/L (Figure 39C). On the other hand, in Poole West there was Fe detected in both present and absent cores at the top 2 cm of the cores. In this case both cores were enriched at the top cm with 52 µmol/L and 58.2 µmol/L for the absent and present core respectively, by 2 cm depth both concentrations declined for the absent core to 1.5 µmol/L and 14.3 µmol/L in the present core. No Fe was measured below this depth in any of the cores (Figure 39D).

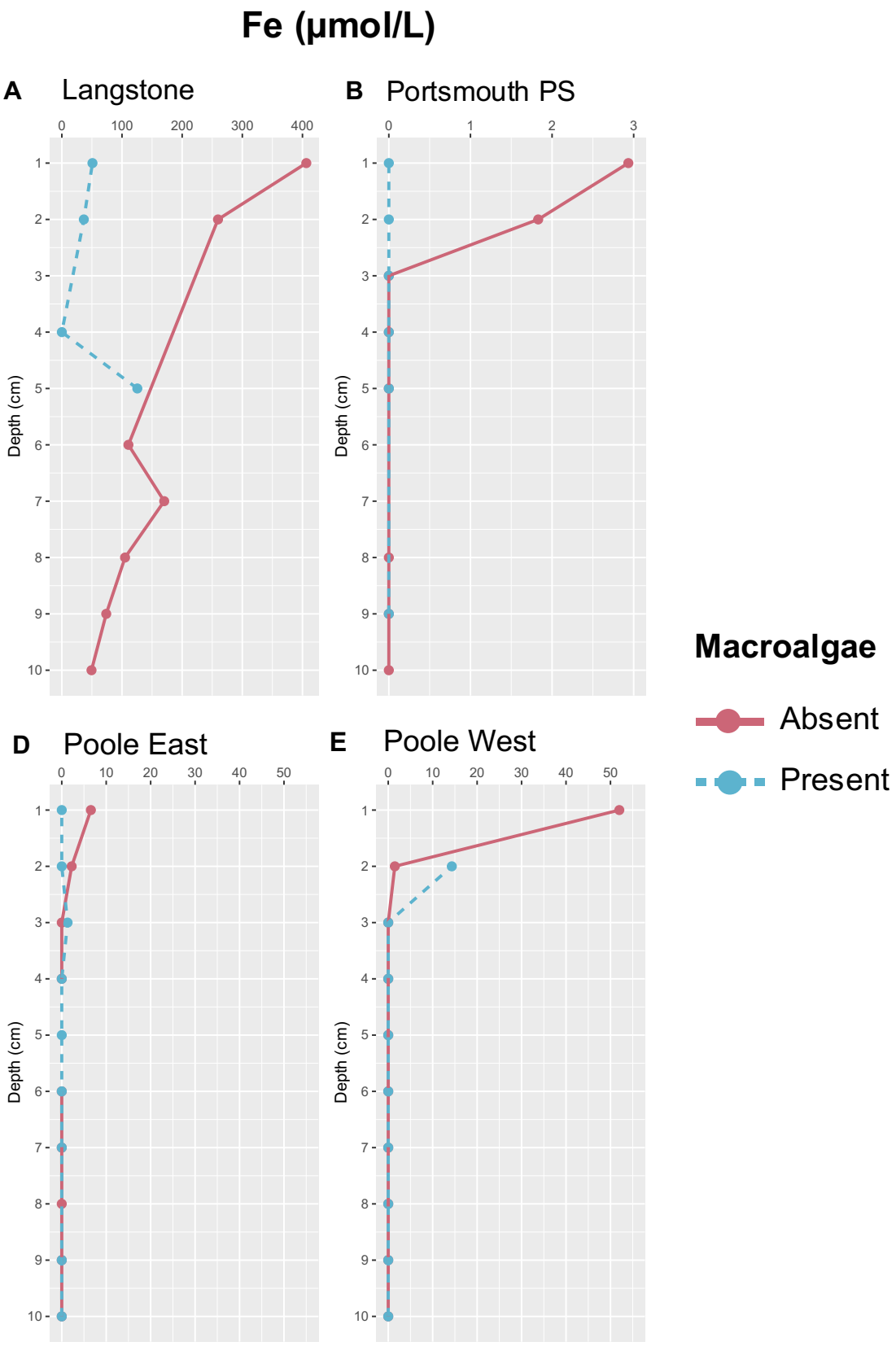


**Figure 39. Dissolved Iron profiles (µmol/L) in the porewaters of the top 10 cm sediment for each sampling site. Red line represents the core where macroalgae was absent while blue dotted line represents macroalgae present cores.**

### 3.4.2.2 Manganese

Mn concentrations in Langstone ranged from 1.6 – 14.6 µmol/L. There was a tendency for the absent core to increase concentrations with depth, reaching its maximum at the bottom of the core (14.6 µmol/L). In the present core the maximum concentration was found at 2 cm depth (9.7 µmol/L) and peaked again at 5 cm depth (8.6 µmol/L) however a pattern downcore was no detected on the macroalgae present core (Figure 40A).

In Port Solent, Mn concentrations went from 0.5 µmol/L to 4.3 µmol/L. Distributions downcore where contrasting, while concentrations in the macroalgae present core tended to increase with depth and had its maximum value at the bottom (4.3 µmol/L), the absent core peaked at 2 cm depth (1.8 µmol/L) and decreased with depth until it reached its minimum at 10 cm depth (0.5 µmol/L) (Figure 40B).

Poole East Mn concentrations for both cores had the maximum concentration at the surface, with 0.3 µmol/L in both the macroalgae present and absent cores. This concentration declined and Mn was no longer detected below 3 cm depth (Figure 40C). In Poole West Mn concentrations were higher in the macroalgae present core with a subsurface maximum of 7.5 µmol/L concentrations declined and was not detected at 4 cm and below 6 cm depth. In the macroalgae absent core, the top cm had a concentration of 1.1 µmol/L, concentrations decreased with depth and Mn was not detected below 5 cm depth (Figure 40D).

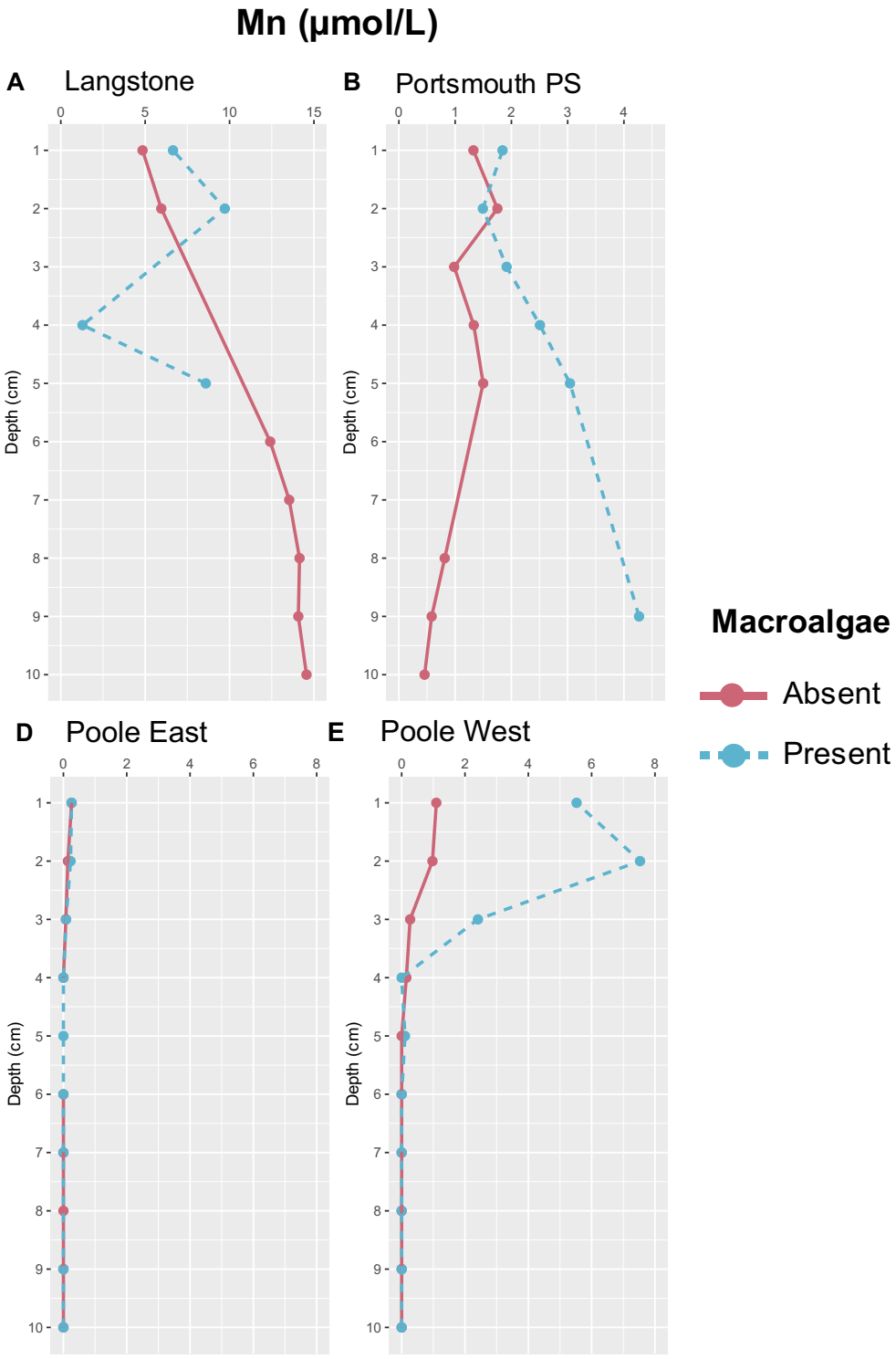


**Figure 40. Dissolved Manganese profiles (µmol/L) in the porewaters of the top 10 cm sediment for each sampling site. Red line represents the core where macroalgae was absent while blue dotted line represents macroalgae present cores.**

### 3.4.2.3 Sodium

Langstone Na concentrations ranged 411 to 450 mmol/L, concentrations were more stable in the macroalgae absent core, but the present had a decline at 4 cm where the minimum concentrations was detected (Figure 41A). In Port Solent, concentrations of Na went from 347 to 472 mmol/L concentrations in both cores decreased with depth, however the macroalgae present core had slightly lower concentrations but the same distribution than the absent core (Figure 41B).

Poole East Na concentrations ranged between 379.4 and 735 mmol/L concentrations were decreasing downcore but overall, the variation was not much except for the absent core that peaked with 735 mmol/L at 6 cm depth (Figure 41C).

A similar pattern was observed in Poole West where Na concentrations were less variable downcore and values ranged between 360 mmol/L to 393 mmol/L (Figure 41D).

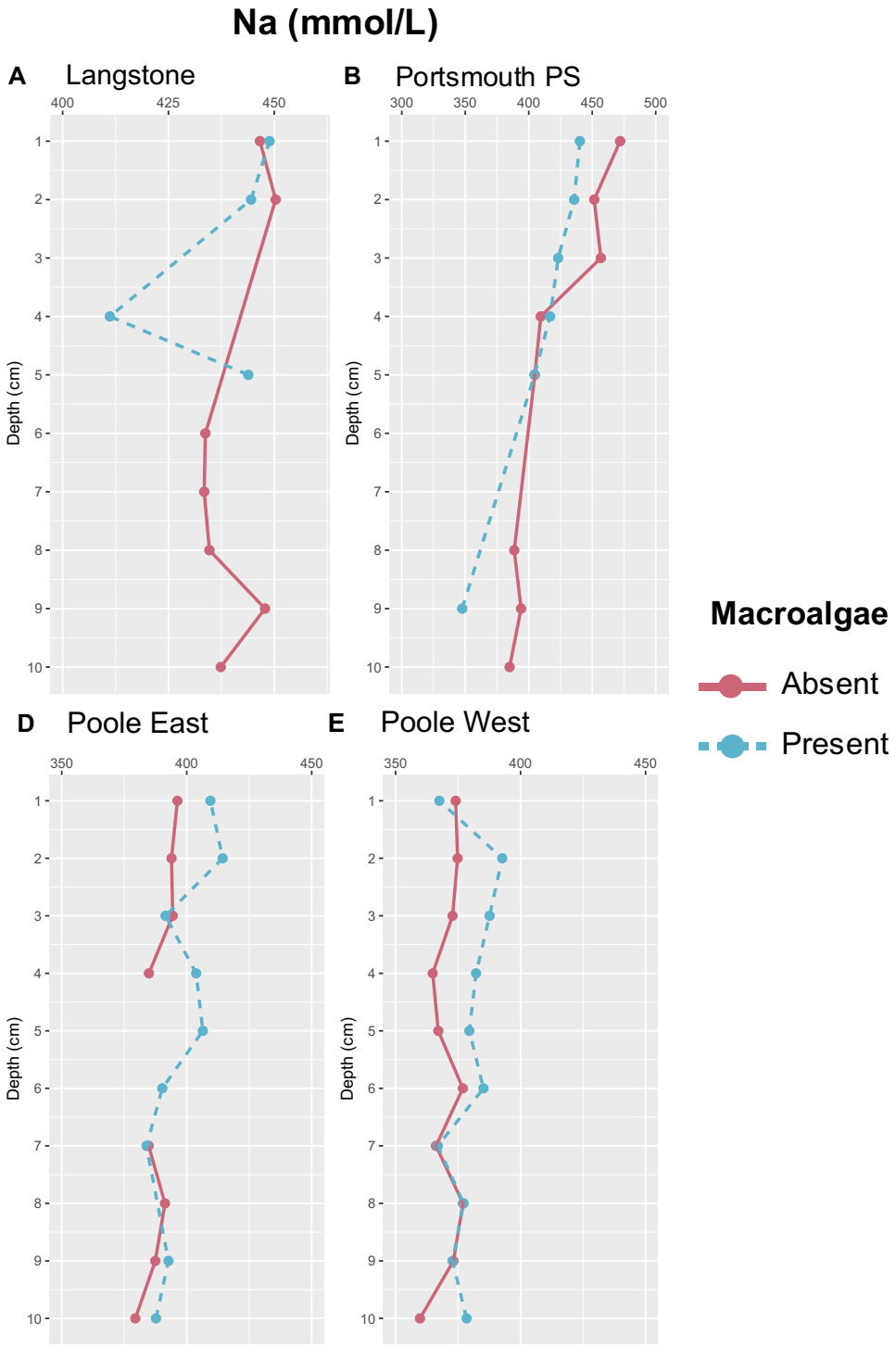


**Figure 41. Dissolved Sodium (mmol/L) in the porewaters of the top 10 cm sediment for each sampling site. Red line represents the core where macroalgae was absent while blue dotted line represents macroalgae present cores.**

### 3.4.2.4 S/Na ratio

Langstone S/Na ratios ranged from 0.04 to 0.06, the macroalgae absent core had a slightly higher concentration at the surface comparted to the present core. Distributions downcore showed a decrease in both macroalgae absent and present cores (Figure 42A).

In Port Solent S/Na ratios were between 0.056 and 0.064, similarly to Langstone the trend downcore was of decreased concentrations as depth increased, macroalgae absent core decreased gradually with depth and the macroalgae present core had a less steep decrease (Figure 42B).

S/Na ratios in Port East were between 0.043 and 0.065. S/Na ratios decreased downcore for both macroalgae absent and present cores (Figure 42C). Similar distribution downcore was observed in Poole West were S/Na ratios ranged 0.041 and 0.065, however in this site the macroalgae present core had lower values than the macroalgae absent core (Figure 42D).

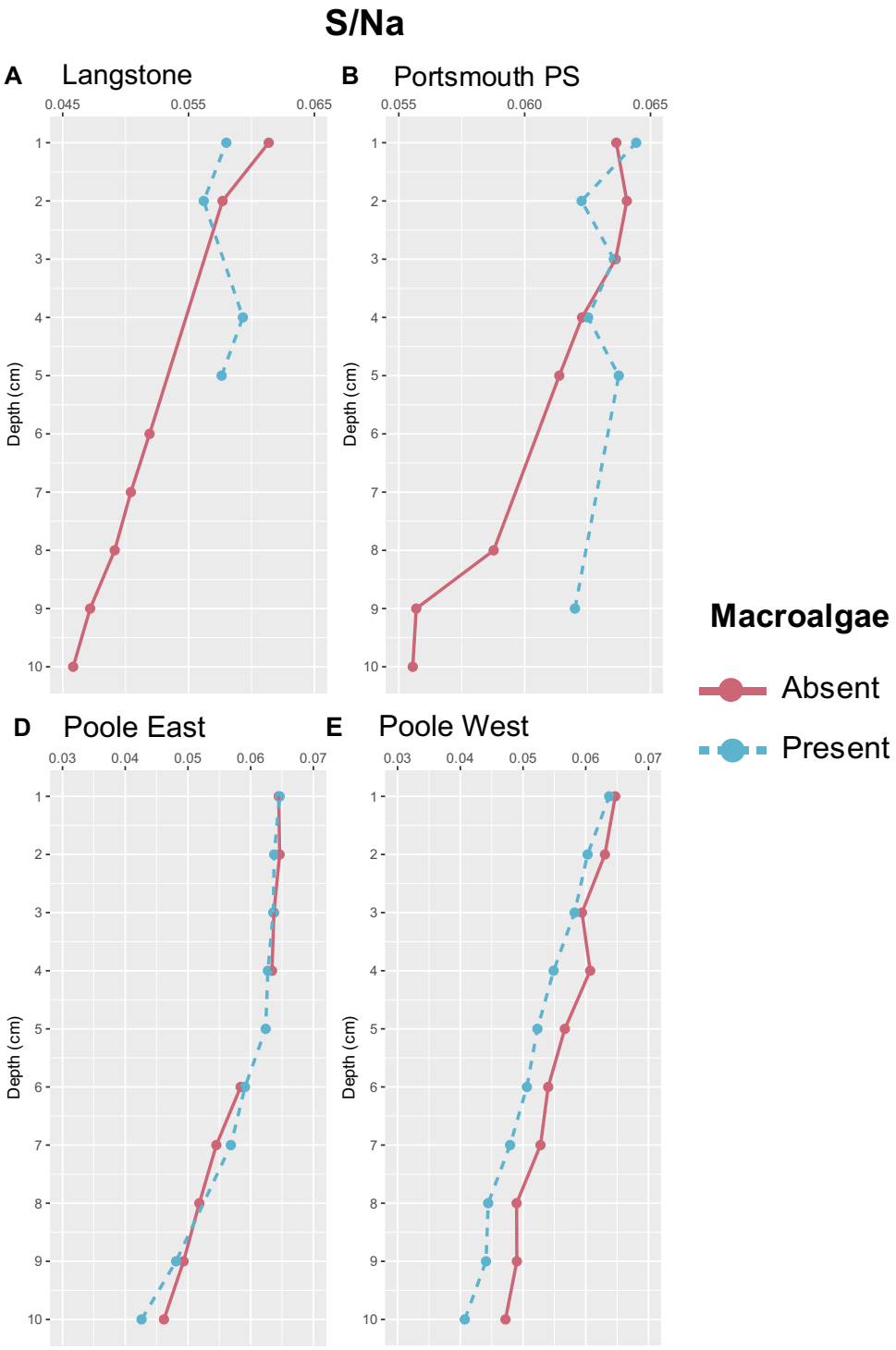


**Figure 42. S/Na in the porewaters of the top 10 cm sediment for each sampling site. Red line represents the core where macroalgae was absent while blue dotted line represents macroalgae present cores.**

### 3.4.2.5 K/Na and Ca/Na ratios

K/Na ratios in Langstone and Port Solent did not change with depth. constant whereas in Poole Harbour sites had 2 points with higher ratios than the rest of the cores. In Poole East has this peak at 4 cm depth in the macroalgae absent core (0.032) and Poole West had it in the macroalgae presence core at 9 cm depth (0.037) (Figure 43).

Ca/Na mean ratios in all sites had very similar values, Port Solent (0.023 ± 0.001), Langstone (0.026 ± 0.002), Poole East (0.023 ± 0.0003) and Poole West (0.024 ± 0.001). Distributions downcore were generally constant. In Port Solent there was a slight increase with depth only in the macroalgae present core at 9 cm depth (0.026). In Langstone the opposite happened where the macroalgae absent core tended to increase Ca/Na ratio with depth, having its maximum value at 7 cm depth (0.03). In Poole Harbour sites on the other hand, Ca/Na ratios maintained constant concentrations with depth in all cores (Figure 44).

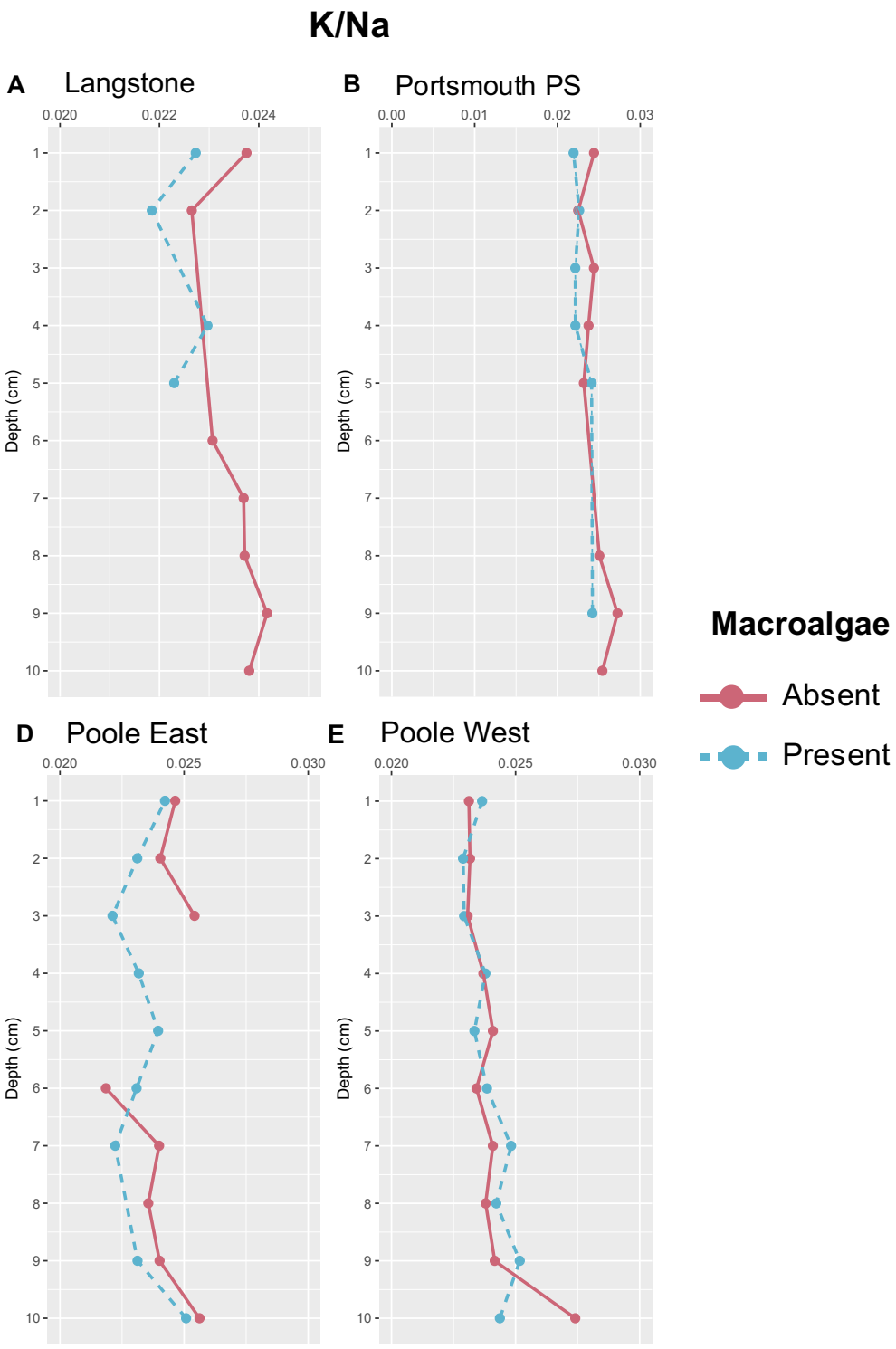


**Figure 43. K/Na in the porewaters of the top 10 cm sediment for each sampling site. Red line represents the core where macroalgae was absent while blue dotted line represents macroalgae present cores.**

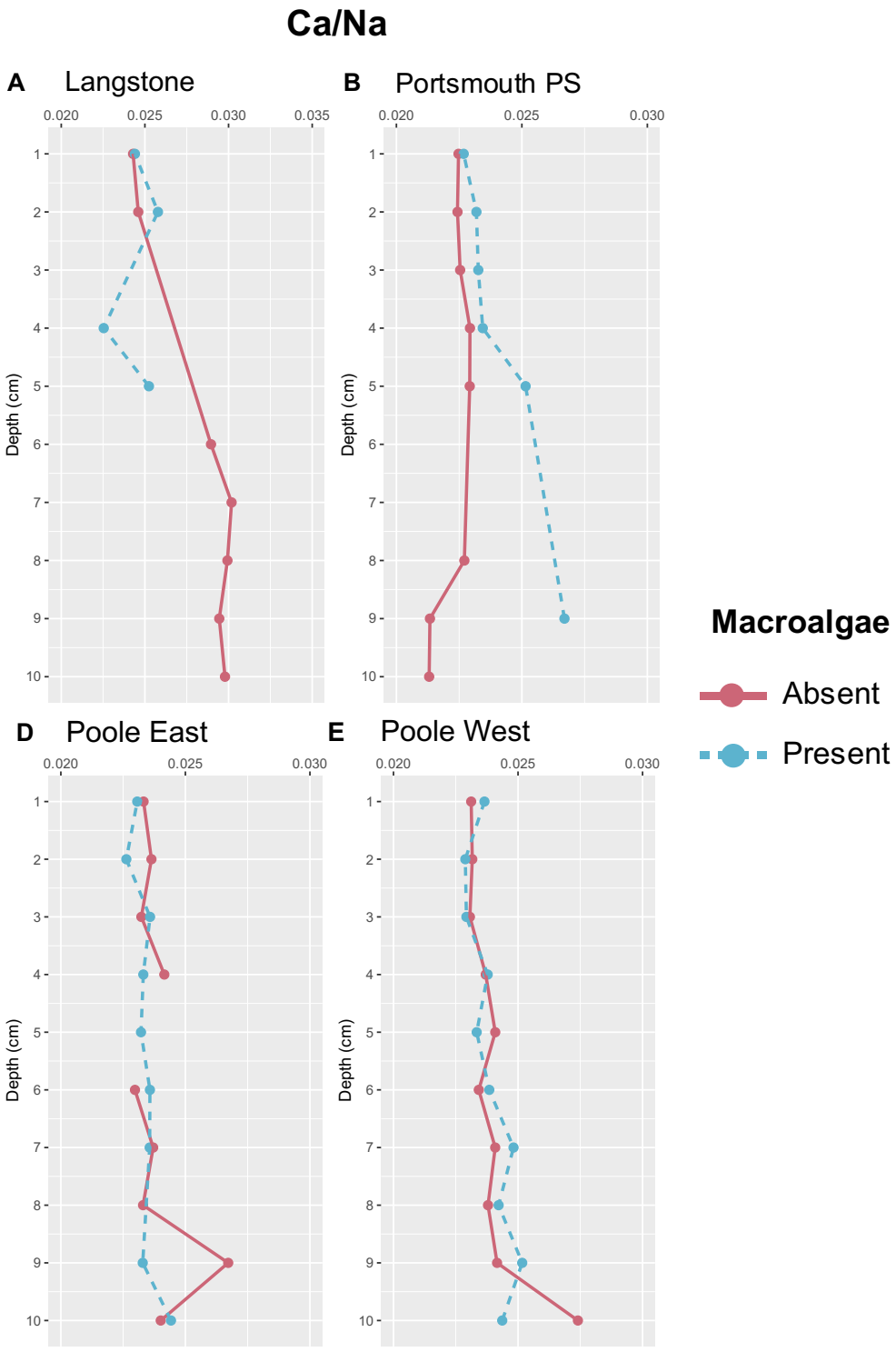


**Figure 44. Ca/Na in the porewaters of the top 10 cm sediment for each sampling site. Red line represents the core where macroalgae was absent while blue dotted line represents macroalgae present cores.**

### 3.4.3 Organic Carbon

The organic C results from the three sampled sites displayed a great variability between sites, with values ranging from 0.2 - 6.6%. In contrast, organic C content remained consistent between sediment cores from the same site. Mean sediment organic C values varied from site to site, Grove Av being the site with the lowest (0.72 ± 0.16%) followed by Langstone (1.36 ± 0.23%) and Port Solent (1.74 ± 0.6%). While Poole Harbour sites had the highest mean organic C values with 3.74 ± 0.24% and 4.64 ± 0.85% in Poole West and East respectively.

In Portsmouth sites, distributions downcore where different for each site. organic C in Grove Av maintained constant with depth whereas Port Solent despite having more organic C in the top of the core, the tendency was to decrease substantially with depth (Figure 45). Distribution downcore in Langstone Harbour was similar than in Grove Av, having little to no variations downcore.

Within Poole Harbour sites, Poole East organic C decreases considerably within the top 2 cm and then remains mostly constant. In the macroalgae present core D from this site, organic C increased with depth and reached comparable amounts from the surface off the core. On the other hand, in Poole West organic C within the sediment was mostly constant with depth.

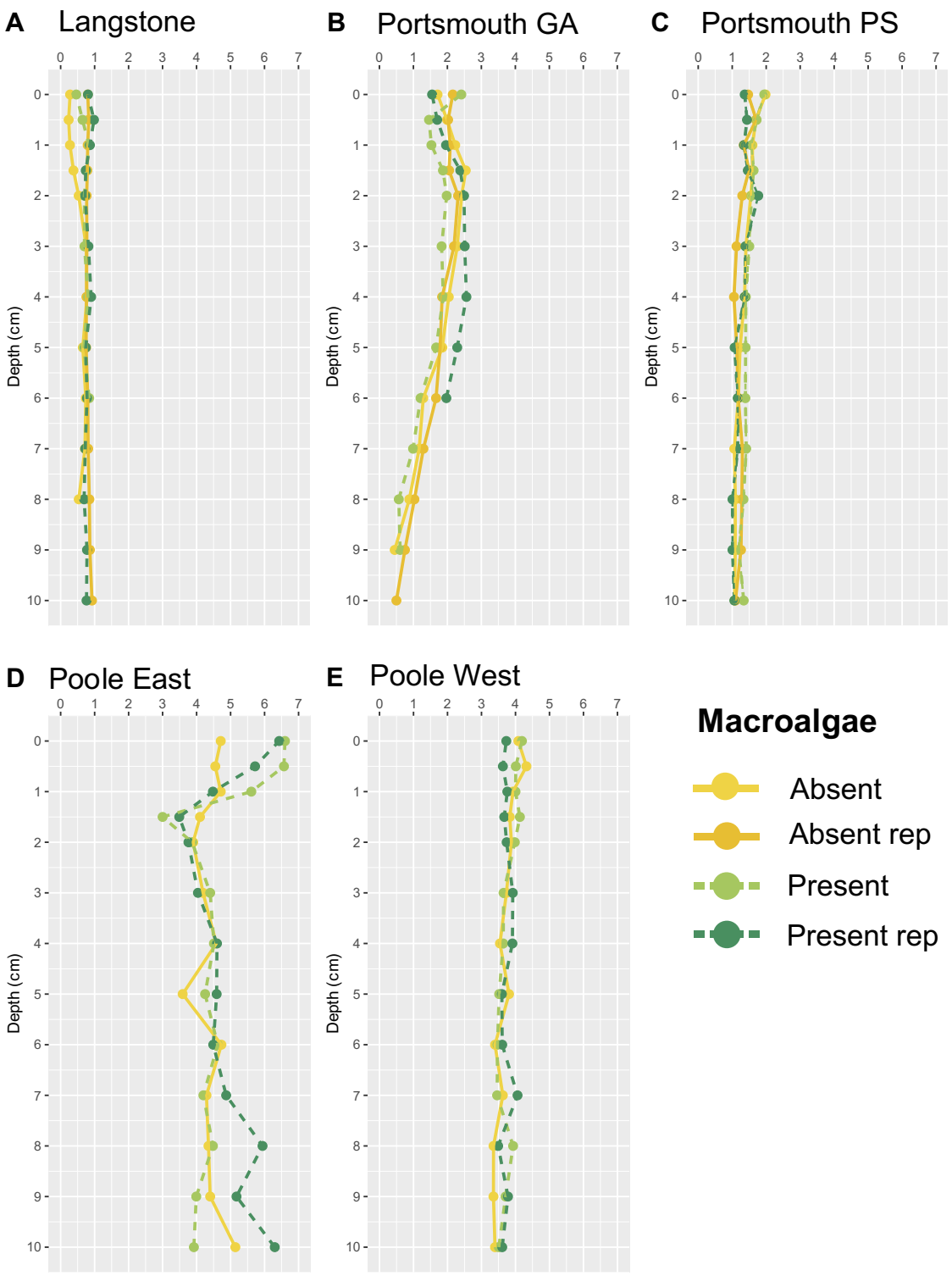


**Figure 45. Total organic carbon (%) in sediment from different sites, comparing cores with presence and absence of macroalgae for the top 12 cm of sediment. The dashed line represents cores with macroalgae presence, while the solid line represents cores without macroalgae. Plot all y-axes are the same in every plot for comparison.**

### 3.4.4 Differences of organic carbon storage/content between presence and absence of macroalgae

Portsmouth sites showed slight differences between absence and presence of algae. Grove avenue macroalgae absent cores had a mean organic C of 0.68 ± 0.2% while the present sediment cores 0.76 ± 0.1% (Figure 46). In Port Solent, the absent cores had a mean organic C value of 1.7 ± 0.6% while the present cores 1.78 ± 0.6%. The same pattern was observed in Langstone Harbour where mean organic C from absent and present cores were quite similar, 1.33 ± 0.2% and 1.38 ± 0.2% respectively.

In Poole West mean organic C content in sediments cores was similar for absence and presence of macroalgae. Mean organic C for the macroalgae absence cores was 3.71 ± 0.3%, while in the present cores was 3.76 ± 0.2%. Poole East mean cores had more variation between absence and presence of macroalgae compared to other sites, 4.4 ± 0.4% and 4.7 ± 0.9% respectively.

Each organic C data set for their respective site was tested for statistical differences between presence and absence of macroalgae using the non-parametric test Kruskal-Wallis. There was not a significant difference between presence and absence of macroalgae in any of the tested data sets.

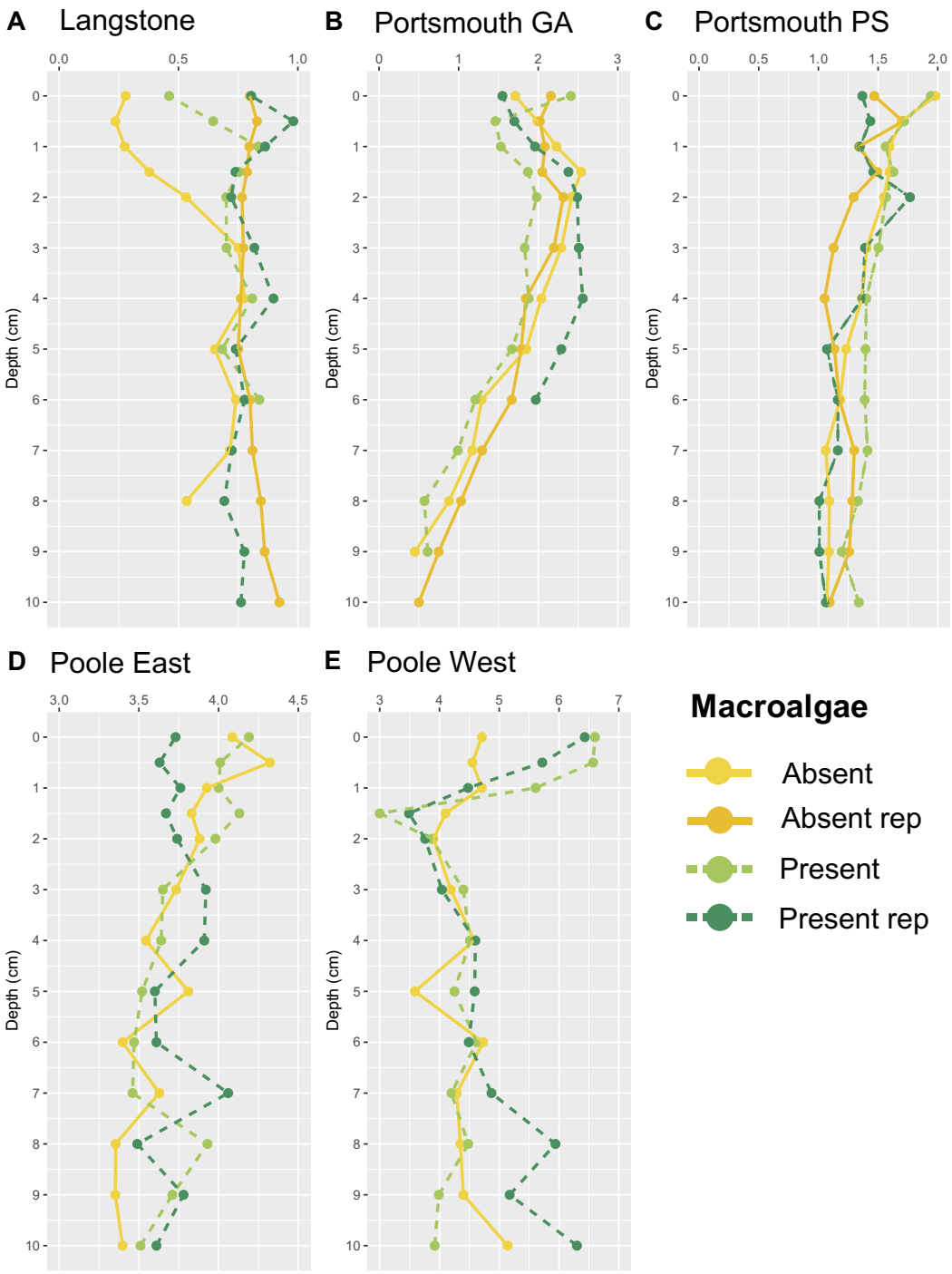


**Figure 46. Total organic carbon (%) in sediment from different sites, comparing cores with presence and absence of macroalgae for the top 12 cm of sediment. The dashed line represents cores with macroalgae presence, while the solid line represents cores without macroalgae. Each plot has different y-axis scales for comparison between presence and absence of algae.**

**Table 13. Table showing results for the non-parametric *Mann-Whitney* test ing for differences between total organic carbon with presence and absence of algae (A test was performed for each site).**

| Estuary | Site | *P*-value |
|---|---|---|
| **Portsmouth** | Grove Avenue | 0.53 |
| | Port Solent | 0.1 |
| **Langstone** | Langstone | 0.3 |
| **Poole Harbour** | Poole East | 0.46 |
| | Poole West | 0.51 |

### 3.4.5 C:N ratio in sediments

All sites C:N ratios were found in the range of 6.7-16. The sampled sites in Portsmouth Harbour showed different values, mean C:N ratio in Grove Av for instance was 6.7 ± 0.9 whereas Port Solent C:N ratio was 7.4 ± 2 (Figure 47). Langstone harbour mean C:N ratio was 7.11±1. On the other hand, Poole Harbour sites had higher C:N ratios compared to other sites. Mean C:N ratios in these sites were 10.9 ± 2.5 and 9.2 ± 1.3 for Poole East and West respectively.

The C:N ratio variation in Grove Avenue is observed on the top 2 cm, while in Port Solent there is a single core that stands out with high C:N ratios, rest of the cores fell in the 3.6-7.9, the outlier presented a range of 8.7-12.8. In Langstone there is an overall constant C:N ratio of 6-8 downcore, with the highest value found at 9 cm depth (Figure 47).

Poole West on the other hand, displayed a slight increase with depth in C:N ratio and Poole East presented a considerable increase downcore. Both maximum values are found at the deepest part of the core. In both sites, macroalgae present cores presented higher C:N values compared to absent cores (Figure 47).

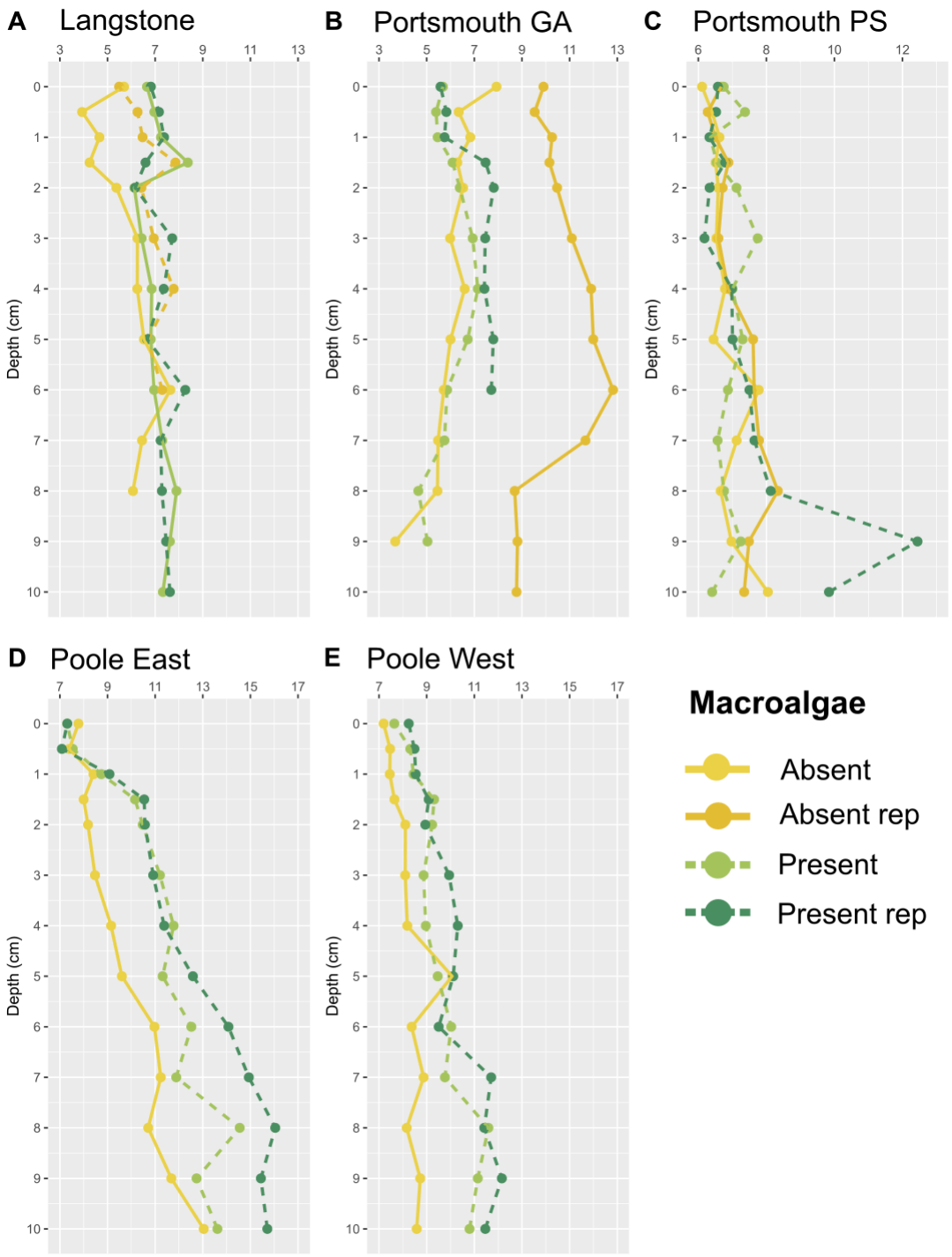


**Figure 47. Sediment C:N ratios from different sites, comparing cores with presence and absence of macroalgae for the top 12 cm of sediment. The dashed line represents cores with macroalgae presence, while the solid line represents cores without macroalgae. Each plot has different y-axis scales for comparison between presence and absence of algae.**

### 3.4.6 Particle size distribution

Clay content in Langstone harbour was higher than all the other sites accounting for 34-37% of the particles in the 4 sediment cores, while Silt was the most abundant fraction for this site 57-63%. This site stood out with the least Sand fraction in the cores, only ranging from 2-6% (Figure 48).

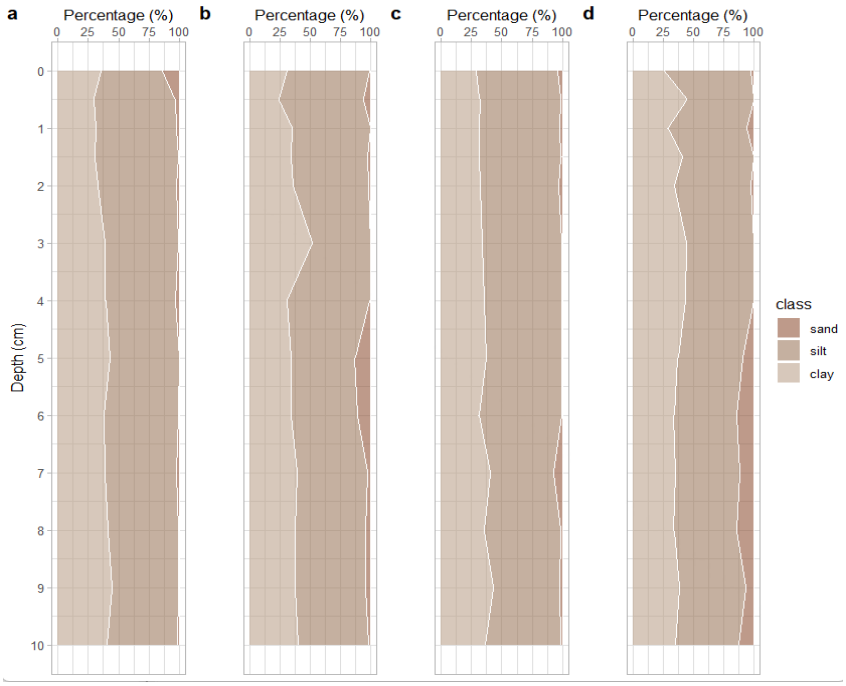


**Figure 48. Vertical profiles of particle size distribution presented as the percentage of clay, silt, and sand for the top 12 cm of sediment cores from Langstone Harbour.**

Portsmouth clay mean content per core was slightly lower than in Langstone (21-31%), the same is observed for Silt than ranged between 45-59%. However, the Sand fraction was higher than in the rest of the sites (13-31%) (Figure 49 & Figure 50).

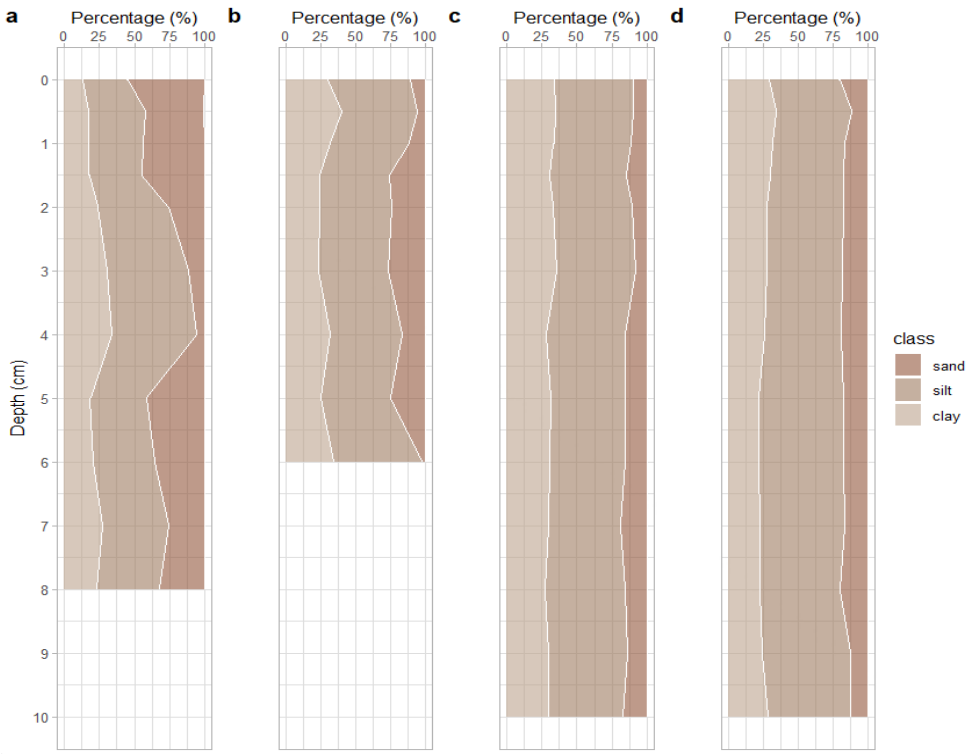


**Figure 49. Vertical profiles of particle size distribution presented as the percentage of clay, silt, and sand for the top 12 cm of sediment cores from Portsmouth Grove Av.**

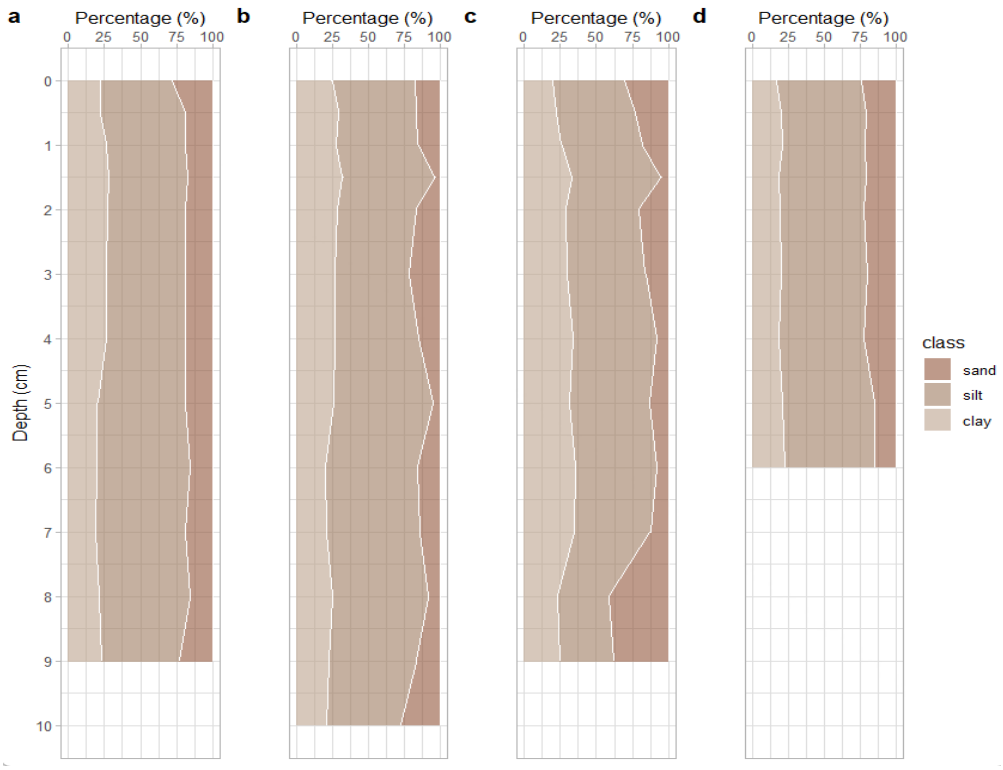


**Figure 50. Vertical profiles of particle size distribution presented as the percentage of clay, silt, and sand for the top 12 cm of sediment cores from Portsmouth Port Solent.**

Poole Harbour clay fraction was higher than Portsmouth but lower than in Langstone, accounting for 21-31%. As in the rest of the sites, silt was the greatest fraction in Poole Harbour (57-60%) and the Sand fraction accounted for the least 8-24% of the cores (Figure 51).

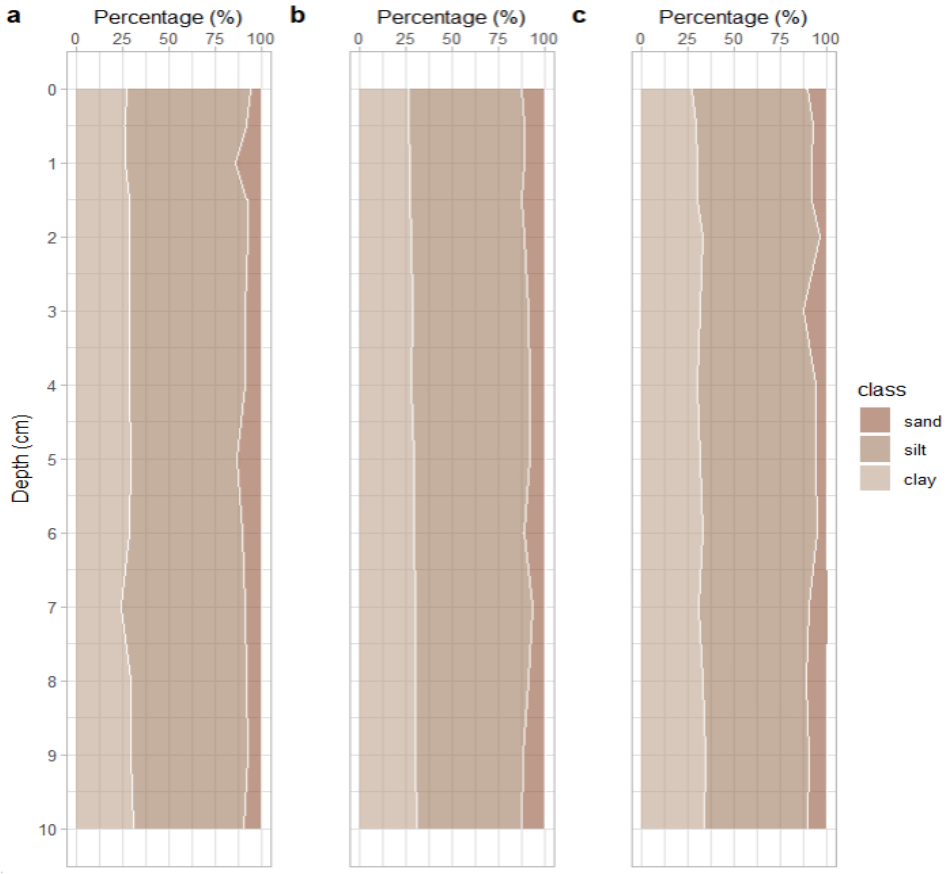


**Figure 51. Vertical profiles of particle size distribution presented as the percentage of clay, silt, and sand for the top 12 cm of sediment cores from Poole Harbour West.**

Mean particle size for all sites ranged between 4.6 – 7.5 µm, being Langstone the site with the lowest value and Poole East the highest (Table 14). It is suspected that the increase in Poole East larger particles were caused by fragments of macroalgae that where present in the sediment during the analysis.

The mean particle size varied among the different sites, with the smallest mean size observed at Langstone (4.65 ± 0.6µm), and the largest at Poole East (7.5 ± 1.5µm). The other sites had mean particle sizes of 5.85 ± 1.3µm at Grove Avenue, 6.7 ± 1.1µm at Port Solent, and 5.45 ± 0.4µm at Poole West (Table 14).

**Table 14. Mean particle size, min and max values among the different sites.**

| Site | Mean particle size (µm) | StDev | Min | Max |
|---|---|---|---|---|
| Grove Avenue | 5.85 | 1.32 | 3.86 | 11.01 |
| Port Solent | 6.66 | 1.06 | 4.60 | 8.74 |
| Langstone | 4.65 | 0.62 | 3.28 | 6.44 |
| Poole West | 5.45 | 0.39 | 4.67 | 6.54 |

When examining the correlation between mean particle size and organic carbon content across all depths, significant negative correlations were found at Grove Avenue ($r = -0.65$, $p < 0.001$). Conversely, a positive correlation was observed at Poole West ($r = 0.35$, $p = 0.027$) and Langstone ($r = 0.38$, $p = 0.005$). No significant correlation was detected at Port Solent ($r = -0.01$, $p = 0.946$).

**Table 15. Correlation results for mean particle size (µm) vs organic carbon (%) content all depths.**

| Site | Coef | *p*-value |
|---|---|---|
| Grove Avenue | -0.65 | <0.001 |
| Port Solent | -0.01 | 0.946 |
| Poole West | 0.35 | 0.027 |
| Langstone | 0.38 | 0.005 |

Additionally, the correlation between silt content and organic carbon content revealed strong and significant relationships at Port Solent ($r = -0.06$, $p < 0.001$) and Langstone ($r = 0.516$, $p < 0.001$). However, no significant correlations were found at Grove Avenue ($r = 0.61$, $p = 0.686$), Poole West ($r = 0.152$, $p = 0.354$).

**Table 16. Correlation results for Silt (%) vs organic carbon (%) content all depths**

| Site | Coef | *p*-value |
|---|---|---|
| Grove Avenue | 0.61 | 0.686 |
| Port Solent | -0.06 | < 0.001 |
| Poole West | 0.152 | 0.354 |
| Langstone | 0.516 | < 0.001 |

# 3.5 Discussions

## 3.5.1 General biogeochemical state of sites

### 3.5.1.1 Nutrient dynamics in macroalgae dominated environments.

Opportunistic macroalgae species such as *Ulva, Cladophora* and *Enteromorpha* can negatively impact benthic biogeochemistry. Macroalgae mats from these species increased the abundance of inorganic nutrients within the sediment porewater, this has been demonstrated in numerous studies including microcosm experiments (Corzo et al., 2009; García-Robledo & Corzo, 2011) and field measurements (Lapointe, 1989; Ratmaya et al., 2022; Spivak, 2015).

One of the most affected is Dissolved Inorganic Nitrogen, more specifically the ammonium fraction which is typically the principal N species in the DIN, it can be observed that the ammonium fraction of the total dissolved nitrogen within the sediment porewaters represented 93-97% (Figure 33) in the three sites of this study. This is consistent with other estuarine environments in the literature where ammonium is the main nitrogen form present in the porewaters (Caffrey J. M., 2002; Trimmer, 2002; Garcia-Robledo et al., 2008; Chang et al., 2023).

Increases of ammonium concentrations in sediment below macroalgae mats have been linked to the decomposition of algae detritus (Garcia-Robledo et al., 2013) and in an active macroalgae bloom release of nutrients to the overlying water can be reutilized by growing algae (Trimmer et al., 2000). The ammonium profiles presented here, displayed greater concentrations on the top 3 cm in the macroalgae

present cores from Langstone and Poole West site while Poole East showed same pattern for macroalgae present and absent cores. This could be explained by the uniform macroalgae cover found in this site and the nature of the field sampling where it became challenging to establish an absolute absence of macroalgae. Therefore, despite taken as a macroalgae absent core could be representing macroalgae present conditions.

In contrast, none of the cores in Grove Av displayed ammonium enrichment within the surface sediment, besides ammonium profiles were less variable between the presence and absence of macroalgae. On the other hand, Port Solent sediment cores displayed 2x and 4x the concentrations observed in Grove Av in the top 3 cm, being the macroalgae absent core the one that presented the higher concentrations of both. This was consistent with the lowest abundance of macroalgae in Portsmouth sites, therefore the less ammonium within porewaters could be linked to minor decomposition of macroalgae detritus within the sediment.

It should also be noted that the highest porewater ammonium concentrations were observed in the estuaries with greater macroalgal biomass (Poole and Langstone (Table 5). Considering previous findings in the literature, it is likely that in Portsmouth, Langstone and Poole estuaries macroalgal cover contributes to elevated porewater ammonium concentrations, and that that ammonium could have a role in sustaining bloom conditions.

Oxidized forms of N, $NO_3^-$ and $NO_2^-$ were also impacted by the presence of macroalgae mats. Sediment cores from all sites where macroalgae was absent had consistently a surface enrichment of $NO_3^-$ and $NO_2^-$, besides not substantial increases were observed in deeper parts of the cores; pattern that was not observed for the macroalgae present cores, (Figure 35 & Figure 35). Microcosm experiments have previously shown reduced oxygen penetration and reduced $NO_x^-$ fluxes from the water column into sediment impacted with *Ulva* detritus (Garcia-Robledo, 2013). It is therefore possible that macroalgae mats act as a physical barrier preventing diffusion of nutrients as well as $O_2$ penetrations.

Depletion in $O_2$ depth penetration has been observed linked as a consequence of Ulva affected sediment, reporting a significant inverse correlation ($r = –0.71$, $p < 0.01$, Pearson correlation) between oxygen penetration depth and $NO_3^-$, which favours denitrification of water column $NO_x^-$ (Garcia-Robledo et al., 2013). Although when water column $NO_x^-$ are low, it is highly likely that minimum benthic denitrification and increase in ammonification can sustain macroalgae growth during low water column nutrient periods (Trimmer et al., 2000).

Dissolved silicon (DSi) is an essential nutrient for phytoplankton growth, DSi often becomes the limiting nutrient for phytoplankton growth in coastal ecosystems (Conley & Malone, 1992; Howarth et al., 2011). Si in the marine environment thus, is present in a biological form (Biogenic Si), dissolved in seawater or in a mineral form.

In shallow coastal ecosystems Si is deposited in a biogenic form and can be regenerated within the sediment, this DSi regeneration can sometimes be greater than riverine inputs (Anderson, 1986). DSi profiles presented here, showed a pattern of increasing concentration with depth in all sites and cores, higher concentrations of DSi were also found in the surface of macroalgae present cores from Langstone, Port Solent and Poole West (Figure 38). The increase in DSi concentrations downcore can be attributed to biogenic Si deposition and some diffusion back to the water column at the surface. Nonetheless, higher concentrations at the surface of the macroalgae present cores might be an indication of less diffusion.

### 3.5.1.2 Redox state on southern estuaries sediment

Oxygen is the primary oxidation agent of organic matter within marine sediments, however as depth increases $O_2$ is naturally depleted and other oxidation agents such as $NO_3^-$, $Mn^{2+}$, $Fe^{2+}$, $H_2S$ and $CH_4$ take the role in organic matter mineralization (Caffrey, 2002), therefore redox zonation is typically classified as oxic, sub-oxic and anoxic in the absence of $O_2$ (Figure 52). Dissolved minerals play an important role on biogeochemical processes taking place within benthic ecosystems. They provide insight into the redox conditions within sediment profiles, which at the same time are controlled oxygen penetration in the sediment and the amount of organic carbon in the system (Emerson, 1985). Coastal areas have characteristic conditions oscillating redox geochemistry in the sediments that at the same time are subject to seasonal or periodical oxic and anoxic conditions (Burdige, 2007). These mixed redox conditions are relevant to organic carbon preservation because remineralization efficiency is diminished when reducing $O_2$ availability (Corzo et al., 2009; Hartnett et al., 1988).

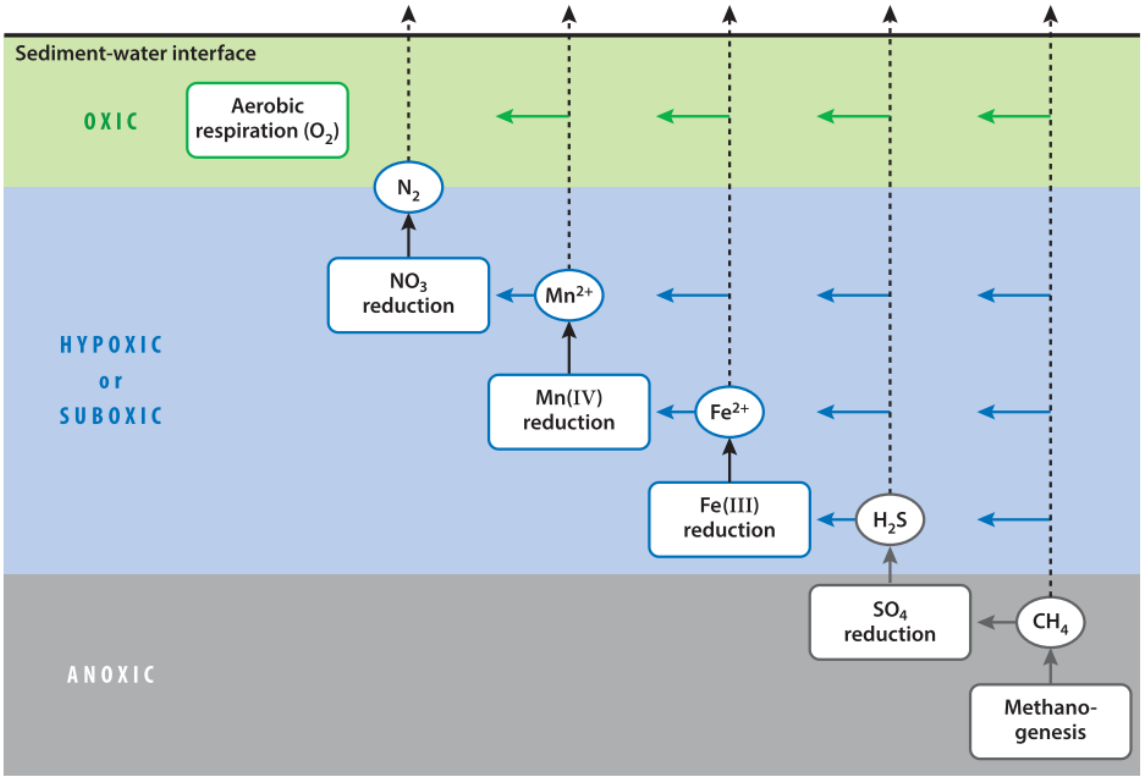


**Figure 52. Conceptual illustration of different redox zones (Oxic, hypoxic or suboxic and anoxic), oxidation agents and reduction reactions taking place in organic matter remineralization, by Bianchi et al 2016.**

In Portsmouth Port Solent, Fe was absent at all depths in the macroalgae present core, while in the macroalgae absent core was depleted at 3 cm. General decrease in Mn was also observed in the absence of macroalgae while the presence of macroalgae seemed to increase Mn availability downcore. This Mn accumulation downcore can be the result of organic carbon decomposition in which promotes accumulation of dissolved Mn in porewaters rather than precipitating as a sulphide (Luther 1988, Burdige and Nelson 1985). The Mn concentrations therefore suggest lower oxygen availability for the macroalgae present core.

Benthic fauna plays a key role in oxygenating sub-oxic layers by sediment bioturbation promoting Fe and Mn redox reactions (Burdige, 2007). Multiple

burrowing structures were observed in Langstone Harbour, indicating there was a high bioturbation activity that could have been mixing sediment and promoting oxygenation deeper than in other sites (Figure 27). This was also translated into less consumption of Fe in Mn, where penetration depth of Fe and Mn in Langstone was deeper than in any other site. However, the same pattern is observed downcore where concentrations decreased with depth for Fe profiles in both presence and absence of macroalgae.

Mn on the other hand was accumulating for the macroalgae absent core with depth, while it is unclear if Mn is either increasing or decreasing downcore for the macroalgae present core due to the lack of data below 5 cm. Poole Harbour sites presented less Fe in the East site than in the West but again, macroalgae presence reduced Fe availability compared to the absent cores in both cases, even being absent in the East site at all depths. In the macroalgae present core in Poole West, Fe was not detected below 3 cm, and Mn was not detectable from 4 cm depth.

Furthermore, all sediment cores showed a clear decrease with depth in S/Na ratios in porewaters. S/Na ratio decrease downcore from initial surface ratio in Port Solent was 28.8 and 24.01% in macroalgae absent and present cores respectively. Langstone Harbour had similar average decrease downcore (26.1%). Whereas Poole Harbour sites showed a steeper decrease, Poole West having a reduction from surface S/Na ratio of 30.2 and 34.2%; Poole East 31.5 and 37.57% for absent and present cores respectively. The observed pattern in S/Na ratios alongside the Mn and Fe profiles suggest sulphate reduction could be occurring in these sites,

which becomes a relevant oxidation process in low oxygen eutrophic sediments (Valdemarsen et al., 2010).

Anoxic sediments are characterized with a darker almost black colour; The observed depth of oxidised sediment from Portsmouth Grove Av was visibly greater than in other sites (Figure 28 & Figure 29), Langstone sediment was sub-oxic where only the fine layer of sediment was oxygenized and Portsmouth Port Solent and Poole Harbour sites where completely visibly dark and anoxic (Link to sampling pictures). Field observations alongside with

Phosphorus (P) is an essential nutrient for primary productivity, benthic P cycling is strongly influenced by Fe redox state (Kraal, 2014). Under oxic conditions, the formation of Fe oxides is an important mechanism that promotes preservation of P in marine sediments (Jensen, 1995). However anoxic conditions on the contrary, lead to the release of phosphate to sediment porewaters translating in les P retention within marine sediments (Rozan, 2002).

Macroalgae present profiles for DIP showed consistent enrichment on the sediment surface compared to absent macroalgae (Figure 37). This pattern was clearly observed in Port Solent and Poole West, in Langstone the difference was less clear but a subsurface peak for DIP was found at 2 cm depth whereas in Poole East this pattern was not detected for either macroalgae presence or absence. Surface DIP enrichment during summer has been linked to productive season of macroalgae mats as sulfidic and anoxic organic matter decomposition take place during the summer months (Rozan, 2002).

This decomposition process takes place at the same time as more macroalgal biomass is growing, the absence of enrichment in Poole East would more likely be due to the reutilization of DIP by macroalgae to produce biomass rather than indicating more oxic conditions. This can be deducted by the particular redox conditions within this site where absence of Mn and Fe within porewaters in both presence and absence of macroalgae are indicator of highly anoxic conditions within this site. These mechanisms that allow macroalgae to obtain nutrients from porewaters is an example of the tight benthic-pelagic coupling within these shallow estuarine systems.

### 3.5.2 Organic C storage in intertidal sediments

The mechanisms for organic carbon preservation in marine sediments involve complex interactions between benthic, pelagic, and terrestrial sources which are yet to be fully understood. We do have knowledge on some factors that can enhance organic carbon storage, for example high sedimentation rates promotes higher burial rates coupled with sub-oxic and anoxic remineralization and therefore more organic C is stored within the sediments (Burdige, 2007). These are common conditions in most coastal areas, where not only autochthonous production is happening, but they are also receiving land-derived allochthonous organic carbon inputs resulting in higher organic C burial than in the deeper ocean (Berner Robert A., 1982; Chen & Lee, 2022).

Organic C in marine sediments varies widely spatially depending on the ecosystem. For example, values reported in the literature for organic carbon content in open

ocean sediments typically fall in the range of ~0.1-0.2% and it is suspected that almost all the organic C reaching the seafloor in these ecosystems is ultimately remineralised (Burdige, 2007). There are exceptions to this such as oxygen minimum zones basins that can average around ~3% and maximum values can reach up to ~10% (Burdige, 2007; Woulds & Cowie, 2009). Fjords ecosystems have recorded mean organic C of 2.6% (Smith et al., 2015). While on the other hand, more productive coastal and estuarine sediments normally have organic C 1-3% (Burdige, 2012).

Within coastal areas the focus on investigation organic carbon has been primarily on blue carbon ecosystems (mangroves, salt marshes and seagrasses) (Kindeberg et al., 2018; Toru Endo & Sosuke Otani, 2019). Comprehensive studies analysing data from 88 seagrasses meadows and 219 core sites have concluded that the median organic C value for seagrass sediments is 1.2% and 1.4% respectively (Fourqurean et al., 2012; Kennedy et al., 2010) and mangrove sediments organic C content have typical median values ~7% (Breithaupt et al., 2012; Toru Endo & Sosuke Otani, 2019).

The organic C reported found in the intertidal sediments from Langstone, Portsmouth and Poole Harbour estuaries range between the 0.24-6.6%, exceeding values reported for coastal ecosystems. We hypothesize that some of this organic C could be macroalgae-derived carbon, as macroalgae were the dominant primary producers in these sites. Possible sources contributing to the organic C sedimentary pool will be evaluated in Chapter 5.

Differences in organic C were not significant between macroalgae present and macroalgae absent cores within any of the estuaries, therefore presence of macroalgae does not appear to increase organic C concentration at small spatial scales, or within a season. This reflects the fact that the exact pattern of macroalgal patches will vary between seasons and may even be changed substantially by each tidal cycle. However, the data do show higher sediment organic C concentrations in estuaries with higher macroalgae cover and biomass, which leads support to our hypothesis that occurrence of macroalgae contributes to sediment organic C storage.

Most studies evaluating macroalgae detritus decomposition, have been done by replicating dead macroalgae decay in microcosm experiments and taking measures of $O_2$ consumption rates as an indicator of mineralisation/decomposition (Zimmerman et al., 1984; Kristensen et al., 1994; Hansen et al., 1998; Lomstein et al., 2006; Garcia-Robledo et al 2009; Garcia-Robledo, 2011). This approach has some limitations like the challenge for replicating natural environment conditions. The amount of macroalgae detritus that is added to the mesocosm sediment, can be variable between experiments. Thus, modifying sediment biogeochemical conditions. Lastly, field measures of organic C content in the sediment considering depth are rarely coupled with the $O_2$ consumption rates. This can lead to a situation where it is assumed that all the mineralisation is attributed to be macroalgal detritus (García-Robledo et al., 2008).

Another common assumption is that macroalgae derived carbon is mineralised rapidly and therefore not preserved within the production site. However, scientific literature on carbon storage within tidal mudflats (Typically macroalgae dominated sites) is currently very scarce (Chen & Lee, 2022; Toru Endo & Sosuke Otani, 2019). The potential contribution of macroalgae derived carbon has been recently acknowledged, and efforts are being focused on looking for macroalgal carbon in depositional environment and its possible contribution to blue carbon stocks.

C:N ratios ranged between 6.7-10.9 among the sampling sites. Variation downcore for Grove Av, Port Solent, Langstone and Poole West was generally small. On the other hand, Poole East C:N ratio increased considerable with depth with 2x higher C:N ratios in deeper sediment compared to the surface. Mean C:N ratios in Portsmouth ($C:N_{gav}$= 6.7; $C:N_{port}$= 7.4) and Langstone ($C:N_{lan}$= 7.1) fall into the range of 5-8 associated with marine derived organic material (Meyers, 1994) while Poole Harbour sites had higher C:N values ($C:N_{west}$= 9.2; $CN_{east}$= 10.9) linked to a combination of marine and land derived organic carbon (Lamb et al., 2006). The interpretation of C:N ratios for identification of sources in sediment organic C needs to be done cautiously, therefore complementary analyses of organic C provenance in these sediments will be discussed in Chapter 5.

## 3.5.3 Changes over time in nutrient concentrations

### 3.5.3.1 Dissolved nutrient concentrations in sediment

A recent survey conducted by Cefas (Unpublished data 2020) in Portsmouth harbour evaluated the status of this site with nutrient discharges and macroalgae biomass as parameters, concluding that Portsmouth has seen a significant improvement in water quality and eutrophication status compared to data from 20 years ago as a baseline. Despite the lack of sediment biogeochemistry data presented in the report, it is recognised that water quality and less biomass are early signs of recovery and changes in sediment nutrient biogeochemistry are expected almost a decade later.

Spivak, (2015), conducted an experiment where sediment cores from an eutrophic system were transplanted into an oligotrophic site (And vice versa) and sediment biogeochemistry data was compared to mesocosm experiments from the same sites with high and low nutrient treatments. Suggesting that trophic history of the sediment played a crucial role in ecosystem biogeochemistry than solely nutrient availability.

Nonetheless, when dissolved ammonium concentrations are compared with a CEFAS survey from 2002 (Unpublished) it is observed that all sites have increased ammonium porewater concentrations in 2021. This increase is more pronounced for Poole Harbour, whereas Portsmouth and Langstone were comparable with previous measurements (Figure 53).

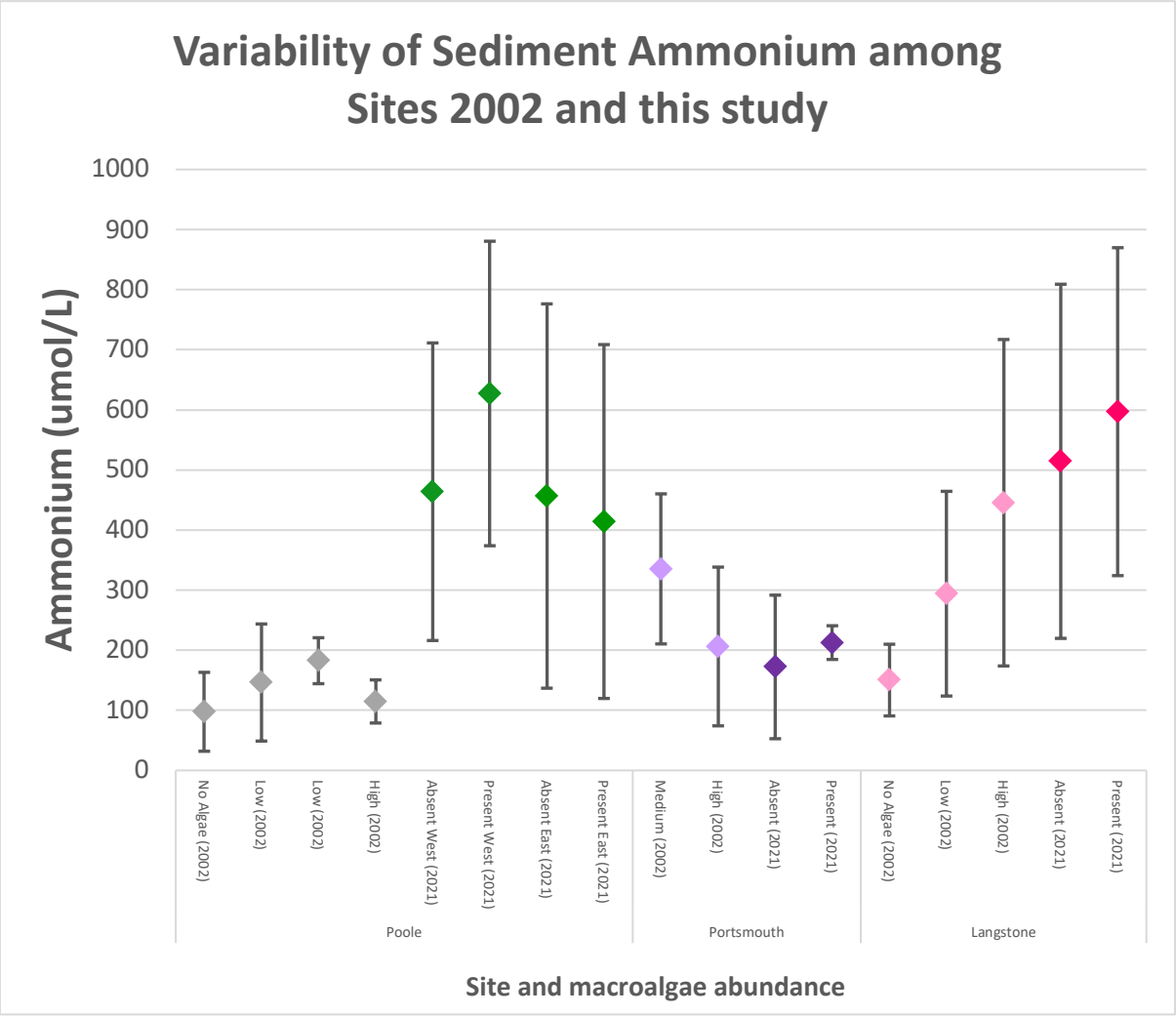


**Figure 53. Comparison between dissolved ammonium concentrations between CEFAS (2002) and this study (2021). In CEFAS (2002) cores were divided in NA= No Algae, L= Low, M= Medium and H= High, in here we separated cores in abs= Absence and pst= Presence of macroalgae.**

It is interesting in Portsmouth harbour that despite having a recent improvement in water column nutrient concentrations and macroalgae cover dissolved ammonium within the sediment remains quite similar specially in the High (206 µmol/L) and Macroalgae Present (2012 µmol/L) (Figure 53).

This suggest that dissolved ammonium concentrations in the sediment take longer to reflect signs of recovery from eutrophication, and trophic history of this site could

be playing a part in the slower decrease in ammonium concentrations in the sediments (Spivak, 2015).

### 3.5.3.2 Temporal changes in water column nutrient concentrations

The role of nutrient concentrations entering estuarine systems is well established, and it does play a crucial part in the development of macroalgae blooms. This excess of availability in nutrient inputs fuel the benthic macroalgae in the sediments (Robertson & Savage, 2018; Smetacek & Zingone, 2013).

Long term monitoring programs in estuaries can give an insight of the ecosystem health and likelihood of development of a bloom. However, this is not a straightforward cause-effect process and other factors such as low tidal stress (Aldridge & Trimmer, 2009) and water residence time (Howarth et al., 2011) influence the likelihood of a macroalgae bloom to proliferate. Historical data from the environment agency database comprising 20 years between 2000-2019 was compared with the available results from this study, to evaluate trends in sedimentary vs water column nutrient enrichment (Section 2.3.1.2).

Mean DIN concentrations in the water column ranged 5.2-38.7 µmol/L for all estuaries. Langstone Harbour mean DIN fall between 5.2-23.8 µmol/L, and concentrations have decreased within the las 20 years from 21 to 5.7 µmol/L, a reduction of 75%. Portsmouth Harbour values were between 33-7.3 µmol/L and are

generally lower for the recent years. However, there is an increase since 2017 and concentrations raised up to 15.8 µmol/L by 2019 (Figure 54).

On the other hand, Poole Harbour has experienced a considerable increase since the first record. While in 2001 mean DIN concentrations were at their lowest (5.3 µmol/L) by 2019 this was 7 times higher (35 µmol/L) This trend is consistent with field observations where Poole Harbour was the most impacted site with macroalgae cover and sediment total dissolved nitrogen concentrations elevated (Figure 54).

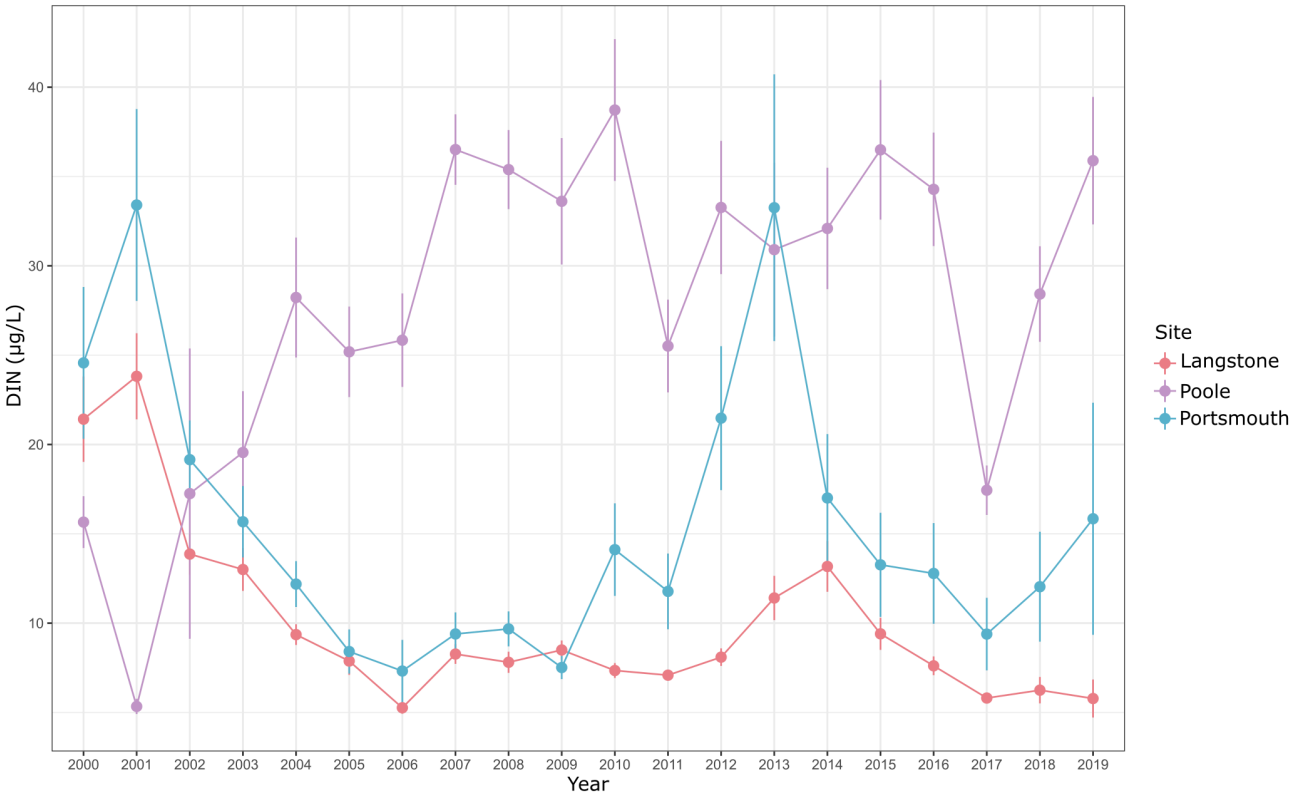


**Figure 54. Water column Dissolved Inorganic Nitrogen (DIN) concentrations (µmol/L) for Langstone, Poole and Portsmouth Harbours from 2000 to 2019. Each point represents the annual mean value and vertical lines indicate standard error for the respective year (Chapter 2 data).**

Unlike the sediment where almost the entire DIN was in the form of ammonium, in the water column nitrate seems to be the main contributor Whilst mean ammonium concentrations for the water column remained relatively low, typically falling in the range of 0.9-6.7 µmol/L, with only two peaks in 2002 and 2007 that exceeded 16 µmol/L (Figure 54). Nonetheless, once again Poole Harbour has generally more ammonium (2-16 µmol/L) than Langstone and Portsmouth that were both comparable in trend and concentrations (0.9-5.3 µmol/L) (Figure 55). The concentration difference between porewaters and water column, together with the general downcore increase in concentrations in porewaters suggest that ammonium fluxes out of the sediment to the water column.

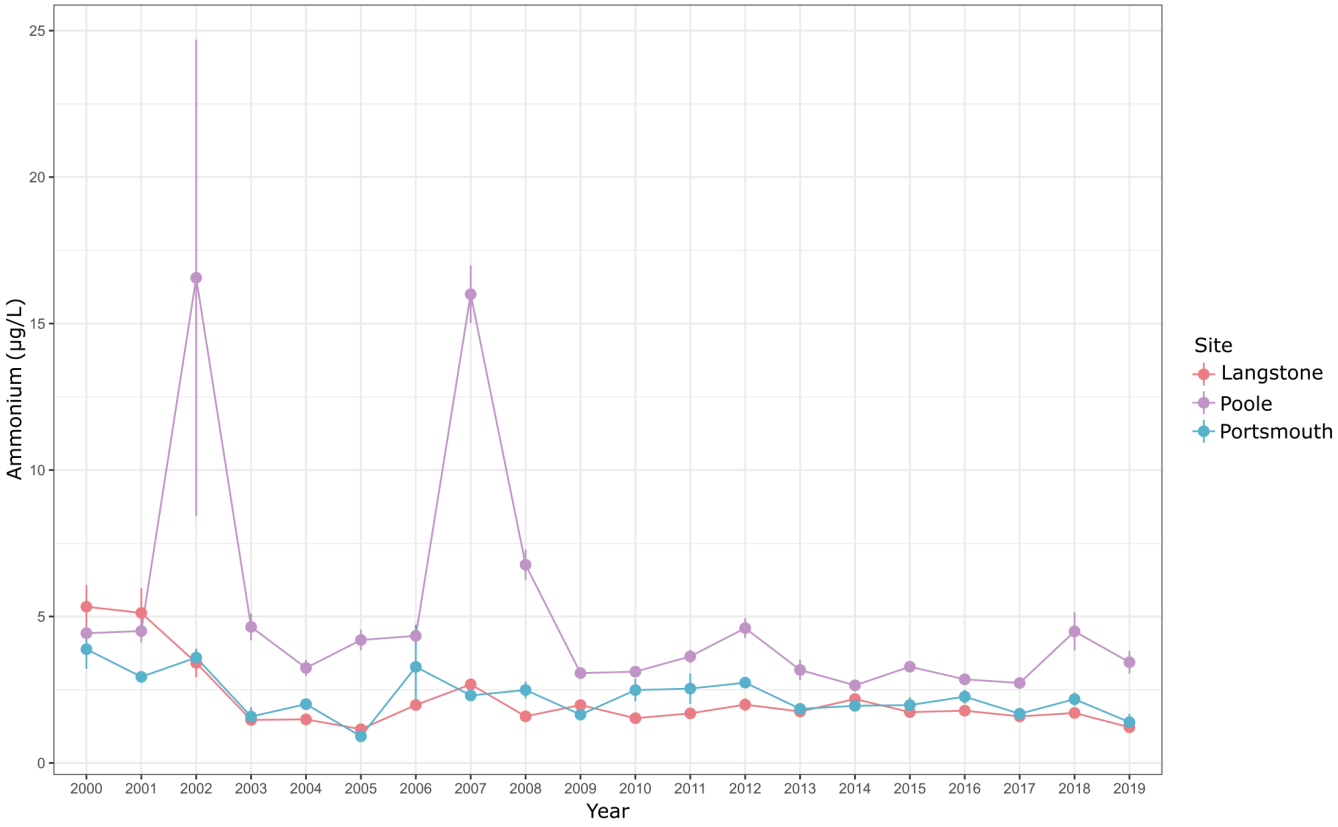


**Figure 55. Water column ammonium concentrations (µmol/L) for Langstone, Poole and Portsmouth Harbours from 2000 to 2019. Each point represents the annual mean value and vertical lines indicate standard error for the respective year (Chapter 2 data).**

Nitrate concentrations on the other hand, were more variable both spatially and temporally. Poole Harbour was the site with higher concentrations generally increasing with time (14 - 43µmol/L) (Figure 56). Portsmouth nitrate concentrations on the other hand were generally lower (3 - 34 µmol/L) with the exception if two substantial peaks in 2001 and 2013. This 2013 peak was also observable in Langstone nitrate concentrations (3 - 18 µmol/L), although it was less pronounced than in Portsmouth (Figure 56).

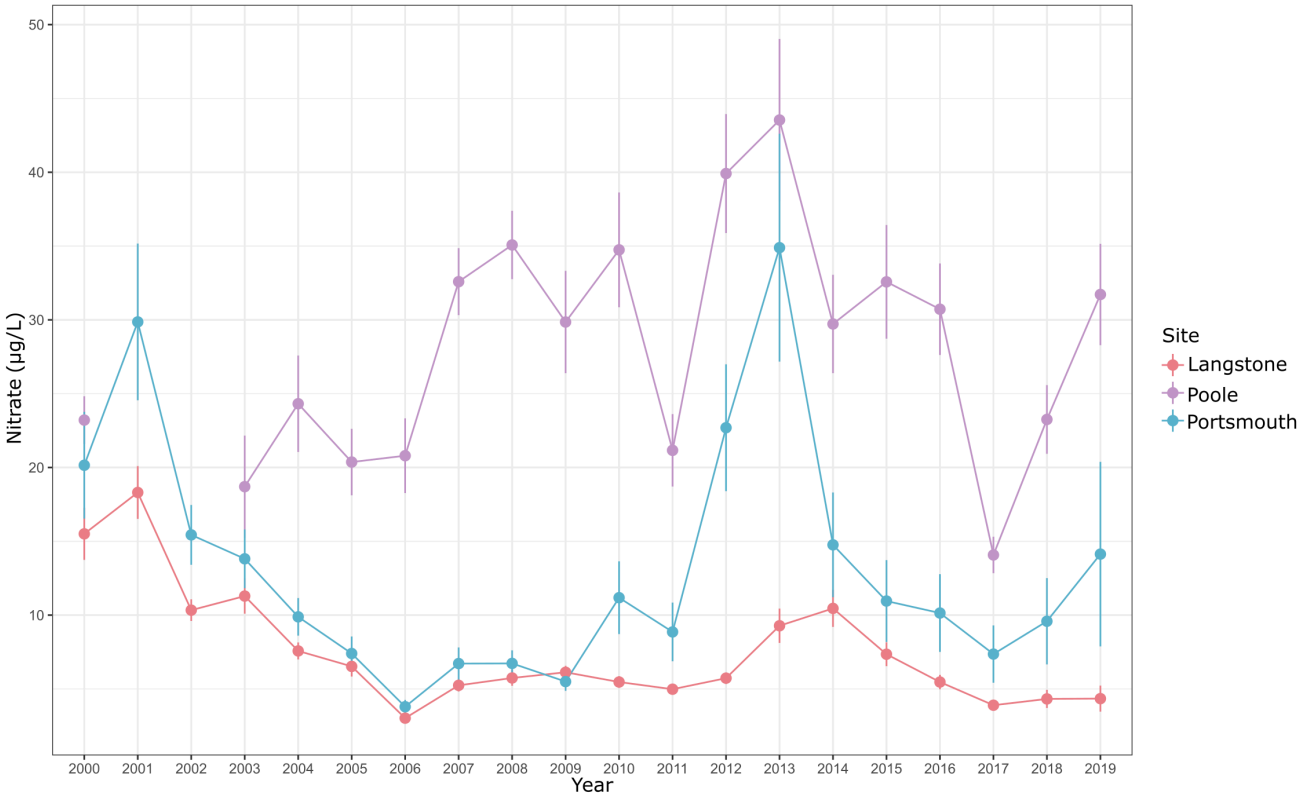


**Figure 56. Water column nitrate concentrations (µmol/L) for Langstone, Poole and Portsmouth Harbours from 2000 to 2019. Each point represents the annual mean value and vertical lines indicate standard error for the respective year (Chapter 2 data).**

Mean nitrite concentrations in the water column ranged between 0.1 - 1.09 µmol/L these are comparable with the dissolved fraction in the porewaters that fell between 0.4 - 1.8 µmol/L, suggesting that the sediment is not a major source for nitrate to the

water column. Again, Poole Harbour stood out with the highest concentrations (0.6 - 1.09 µmol/L) whereas Portsmouth and Langstone Harbours remained close to another in concentrations with 0.1 - 0.6 µmol/L and 0.1 - 0.6 µmol/L respectively. In the timeframe displayed in, Poole Harbour maintained similar concentrations in the las 20 years while Portsmouth and Langstone presented a slight decrease (Figure 57).

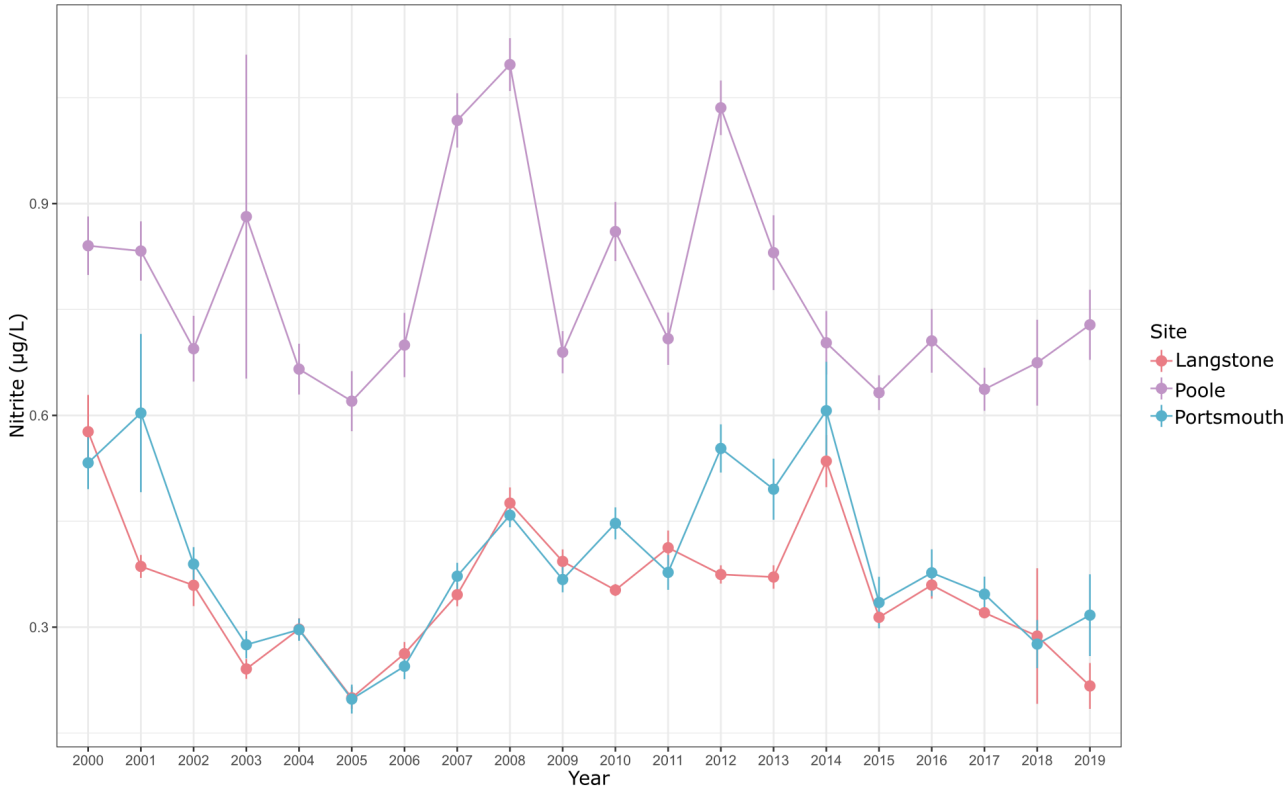


**Figure 57. Water column nitrite concentrations (µmol/L) for Langstone, Poole and Portsmouth Harbours from 2000 to 2019. Each point represents the annual mean value and vertical lines indicate standard error for the respective year (Chapter 2 data).**

Lastly, phosphate concentrations in the water column were in the range of 0.2 - 1.3 µmol/L being significantly lower than the ones found in the sediments (0.7 - 280 µmol/L) (Figure 58). Concentrations of phosphate in the water column through time follow a similar pattern to other nutrients, with Poole Harbour being the site with more phosphate (0.6 - 1.3 µmol/L). On the other hand, Portsmouth and Langstone

generally displayed similar concentrations 0.2-0.8 and 0.2-0.9 µmol/L respectively. However, Langstone started in the year 2000 with higher concentrations than Portsmouth. All three sites have relatively lower concentrations in more recent years than in the start of 2000 (Figure 58).

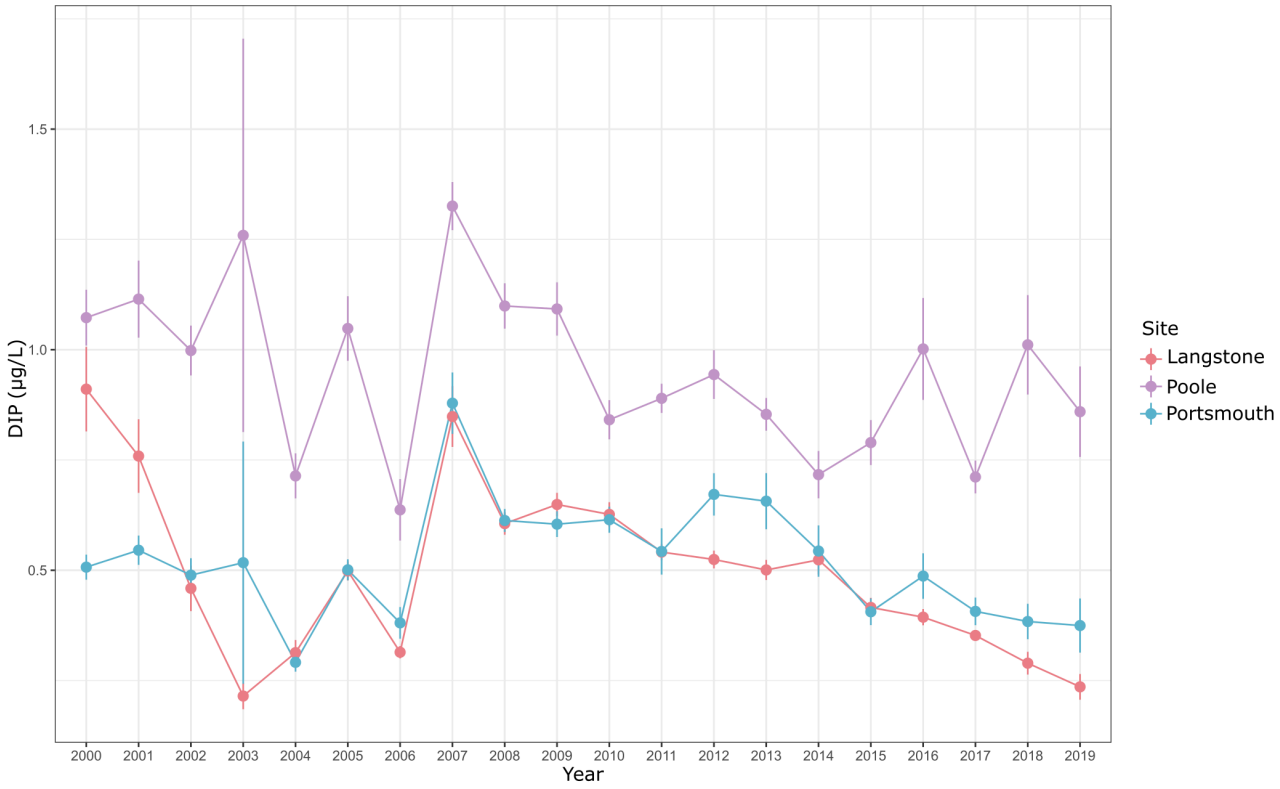


**Figure 58. Water column Dissolved Inorganic Phosphorus (DIP) concentrations (µmol/L) for Langstone, Poole and Portsmouth Harbours from 2000 to 2019. Each point represents the annual mean value and vertical lines indicate standard error for the respective year (Chapter 2 data).**

Porewater data for DIP presented in section 3.4.1.2 does not match the water column trend for Portsmouth and Langstone Harbours as Portsmouth had the lowest DIP (20 ± 12.5 µmol/L) compared to 144 ± 78.1 µmol/L in Langstone. Whereas water column DIP concentrations are quite similar for both sites. Nonetheless, water column DIP trend does agree with dissolved DIP sediment concentrations in Poole Harbour as the West site had the highest mean concentration 158 ± 66.2 µmol/L and lower for Poole East 56.8 ± 43.6 µmol/L.

## 3.6 Conclusions

It is clear that the presence of dense macroalgae mats can heavily modify sediment biogeochemistry, impacting directly the nutrients cycling, sediment redox conditions and organic C storage. Concentrations of oxidized forms of N ($NO_x$) where considerably low in all sites and ammonium was the dominant N form always accounting for 93-97% of the total DIN in sediment porewaters. Differences in ammonium porewater nutrients between macroalgae presence and absence cores were most macroalgae present cores had higher concentrations of ammonium. Probably due to the ammonium release happening as a consequence of mineralisation of the macroalgal detritus.

Redox biogeochemistry was also impacted by macroalgae, as discussed for Portsmouth, Langstone and Poole Harbours. Porewaters Fe, Mn, DIP and S/Na trends downcore showed that redox conditions in these sites was sub-oxic and anoxic in most impacted sites. These trends coupled with ammonium enrichment provided evidence of the limited oxygen penetration within these sediments especially when dense macroalgae was on top of the sediment, more anoxic remineralisation of organic carbon could be occurring at the same time.

The organic C present in the top 12 cm of these sediments is considerable compared to other marine ecosystems (Section 3.4.3) with 0.25-6.6%. No significant differences in organic C were observed between presence and absence of macroalgae, however variability in sediment organic C content was more evident between sampling sites and estuaries. Grove Av was the site with the lowest mean

organic C (0.72 ± 0.16%) followed by Langstone (1.36 ± 0.23%) and Port Solent (1.74 ± 0.6%). While Poole Harbour sites had the highest mean organic C values with 3.74 ± 0.24 % and 4.64 ± 0.85 % in Poole West and East respectively.

There was no correlation found between organic C sediment content and particle size nor presence or absence of macroalgae. However, the amount of organic carbon was generally constant downcore for Langstone and Poole sites, suggesting more efficient storage and probably less degradation due to the more anoxic conditions present at these sites (RQ6).

The data presented also demonstrates the spatial variability of macroalgae blooms impact within the same estuary. This was observed in Portsmouth Harbour where the impacts on macroalgae blooms was higher in Port Solent site compared to Grove Av. Organic C storage was higher in Port Solent (1.74 ± 0.6%) compared to Grove Av (0.7 ± 0.16%). Although seagrass was observed during fieldwork in Grove Av this was not reflected in more organic C storage within these sediments. Nonetheless, there was more organic C loss with depth in Port Solent compared to Grove Av. Therefore, impacts of macroalgae blooms on sediment biogeochemistry are more evident at estuary or site scales than a smaller (mat/patch) scale (RQ4).

The presence of dense macroalgae mats act as a physical barrier, the “cap” on the sediment surface of sites with dense macroalgae mats prevents diffusion of oxygen in the sediment and preventing diffusion of nutrients back to the water column. These conditions promoted more organic C storage in these sediments as observed from the more impacted sites. Observed surface enrichment for ammonium and DIP

can be directly utilised benthic macroalgae supporting more biomass production (RQ5), creating anoxic conditions that favoured the accumulation of more organic C, by less effective remineralisation.

Findings presented in this chapter, provided evidence on the relevance of intertidal unvegetated coastal areas impacted with macroalgae in sedimentary carbon storage. Describing some mechanisms that can be promoting this accumulation of organic C in more impacted sites, the possible contribution of macroalgae on sedimentary organic C will be explored in detail in Chapter 5.

Chapter 4.

# Influence of seasonality of macroalgae blooms on sediment biogeochemistry

## 4.1 Introduction

Langstone Harbour was selected from the group of estuaries in Chapter 3, with the aim of further investigate the influence of seasonality on sediment biogeochemistry in three different seasons. The research questions that will be addressed in this chapter are the following:

**RQ7:** To what extent do macroalgae blooms impacts on sediment biogeochemistry change through different seasons?

**RQ8:** Is there an impact of seasonality on sediment carbon storage?

# 4.2 Background

## 4.2.1 Langstone Harbour history with eutrophication and macroalgae mats

Langstone Harbour is an area of biodiversity interest due to the large amount of wader bird species that feed in these ecosystems. Eutrophication and macroalgae mats in Langstone Harbour were reported in the literature since the 1980's. The spread of green macroalgae on the intertidal sediment was since attributed to the increase of effluent treated and untreated sewage being discharged into the system (Tubbs and Tubbs, 1980). Early studies identified the effect of increasing opportunistic macroalgae (green seaweed) on bird populations and food availability (macro invertebrates), findings highlighted that waders and wildfowl birds avoided areas with macroalgae for feeding purposes (Nicholls et al.,1981).

Another important change that occurred in Langstone Harbour is the loss of seagrasses species. Den Hartog (1994), analysed the monitoring data available for two seagrass species (*Zostera marina* and *Zostera noltii*) growing in an area of 10 Ha for the period 1986-1992 in Langstone Harbour. For the period of 1986-1990 no change in the distribution of the seagrass was observed, however what they report as a "thick blanket" of *Enteromorpha radiata* suffocated most of the living seagrass (Den Hartog 1994).

In later years, more detailed analyses of the effects of eutrophication and macroalgae mats on sediment biogeochemistry. Trimmer et al., (2000), evaluated the contribution of macroalgae mats on N availability during a seasonal cycle with

field measurements of organic C, nutrient concentrations, C:N ratios and N demand by the macroalgae biomass in Langstone and Chichester harbours. They concluded that macroalgae mats increased overlying water concentrations of $NO_3^-$ and $NH_4^+$ on a seasonal pattern (Trimmer et al., 2000).

### 4.2.2 Seasonal changes on sediment biogeochemistry

Estuaries are naturally dynamic environments and sensitive to external changes. nutrient loads into coastal areas are impacted by the amount of rainfall and freshwater runoff into coastal ecosystems (Kamer & Fong, 2000). And seasonal differences on the amount of nutrients delivered to coastal ecosystems have been previously observed, specially linked to precipitation extreme or scarcity events (Nedwell, et al., 2002).

Another important seasonal factor is temperature, light exposure during warmer months and consequently temperature variations create seasonal patterns in macroalgae growth (Valiela et al., 1997). Seasonal variation on macroalgal biomass production has been identified in all macroalgal groups such as *Fucus, Kelp, Rhodophyta, Ulva and Enteromorpha* (Bermejo et al., 2019; Broch & Slagstad, 2012; Graiff et al., 2020; Kregting et al., 2008; Wheeler & Bjornsater, 1992).

Furthermore, temperature variations can also affect coastal benthic ecosystem, and it has been reported that sediment temperature differences between cold and warmer seasons can be as high as 20°C (Burdige, 2006) and consequently, rates

of faunal activity and organic C reactivity which ultimately impacts sediment biogeochemistry (Burdige, 2012).

Another consequence of the seasonal patterns is that as biomass production varies, oxygen and N demand from the macroalgae mats are also variable through the seasons. Trimmer et al., (2000), identified that in summer N demand by macroalgae reached its maximum (55%) and $NO_3^-$ and $NH_4^+$ concentrations in the overlying water where macroalgae mats were covering the sediment were at its minimum. Furthermore, minimum rates of denitrification were reported in these sediments which promotes the accumulation of inorganic N in the sediment (Trimmer et al., 2000).

Langstone Harbour was chosen among previous sites in Chapter 3 to evaluate seasonality of benthic biogeochemistry in an environment impacted by eutrophication and opportunistic macroalgal mats. The previous published data, accessibility to this site and proximity with University of Portsmouth facilities where some of the reasons why this site was chosen.

On the previous chapter, there was a pattern identified for DIN where an increased was observed in macroalgae present cores; In addition, the amount of organic carbon was variable between estuaries. Therefore, it is expected that during the different seasons as macroalgae abundance change this could modify the previously observed trends in sediment biogeochemistry on a seasonal basis.

.

# 4.3 Methods

## 4.3.1 Study site

Langstone Harbour was selected to resample for the next two seasons (Autumn and winter) in order to have a seasonal perspective on the biogeochemical changes that continuous macroalgae blooms could be inducing on this system. Resampling for autumn was carried out in autumn the 1st and 2nd of October exactly 3 months after the summer sampling. And the winter sampling took place the 2nd of February.


**Figure 59. Map of Langstone Harbour showing the seasonal sampling locations, marked by red triangles.**

### 4.3.2 Sampling.

As described for the previous sampling in July (Chapter 3), a total of four sediment cores with a 12 cm depth were taken, 2 with macroalgae presence and 2 absent for solid phase analysis including TOC and N. Furthermore, 2 sediment cores where taken (presence and absence of macroalgae) with a 10 cm depth. Pore waters were extracted for these 2 cores using 10 ml syringes connected to prerinsed Rhizons (0.15 μm pore size).

Sediment cores were sliced horizontally as previously described and placed into plastic bags. Immediately after they were placed into a -20°C freezer located in the Institute of Marine Sciences of the University of Portsmouth. 1 mL of each porewater sample was transferred into 1.5 mL microtubes and were acidified with 10 μL of concentrated HCl to prevent metal precipitation. The rest of the porewater was frozen at -20°C until further shipping to Leeds.

### 4.3.2.1 Field observations

During summer sampling there was a high macroalgae cover, with small patches of bare sediment. And at least two species of green algae and one of brown algae attached to hard substrata were observed on the shore. There were visible signs of benthic bioturbation, where structures within the sediment were observed in the surface (Figure 60).

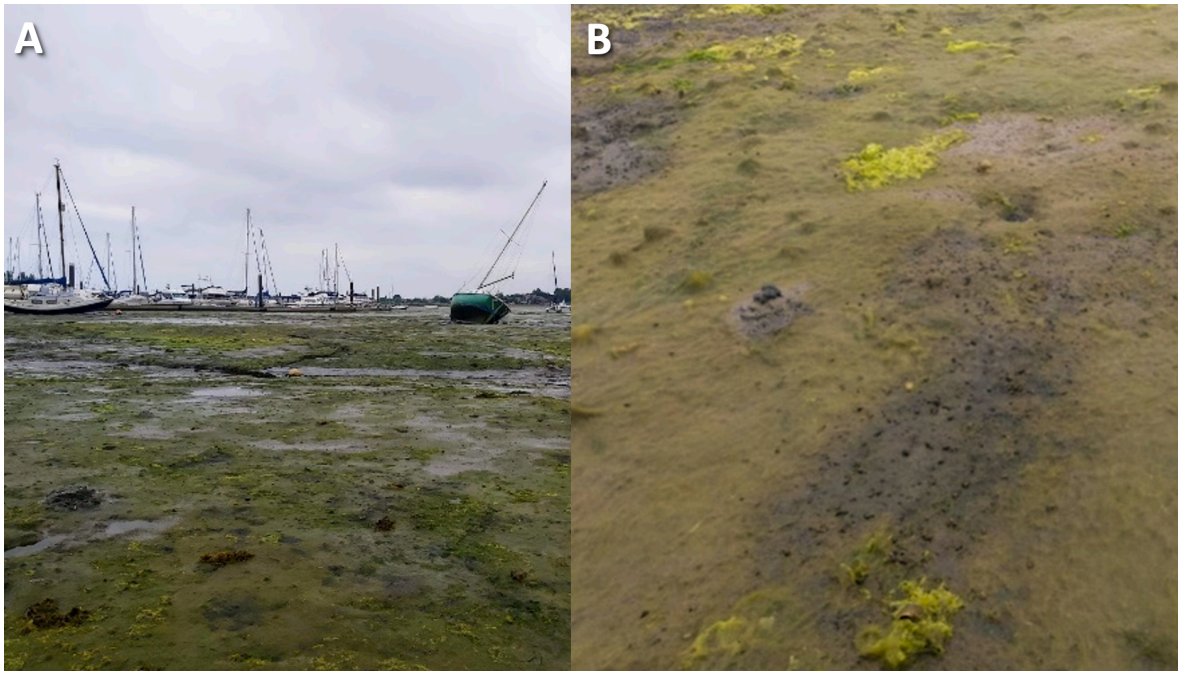


**Figure 60. Field images from Langstone Harbour July 2021 (Summer). A. Extent of intertidal area covered by macroalgae at low tide, B. Macroalgae absent patch showing multiple burrowing structures on sediment surface.**

In autumn, macroalgae was still present in almost all the visible intertidal and most of the sediment clearly black with or without algae on top. Brown algae was attached to the rocks on the shore (Figure 61). In the winter there was macroalgae still present, although the layer covering the sediment was thinner (Figure 62).


**Figure 61. Field images from Langstone Harbour October 2021 (Autumn). A. Extent of intertidal area covered by macroalgae at low tide. B. Sediment core showing the extent of anoxic depth within the core.**

**Figure 62. Field images from Langstone Harbour February 2021 (Winter).**

#### 4.3.2.2 Data analysis

Results for dissolved nutrients, dissolved metals, organic carbon, C:N ratios and particle size data are presented in graphics as line plots representing the changes with depth. Plots were made using RStudio and ggplot2 package. Basic statistics, mean, min, max, standard deviation and ranges were analysed in RStudio, using “dplyr” package and the function summarise.

Previously presented secondary data (Chapter 2) was also grouped in different seasons for Langstone to evaluate water column trends during the different seasons and compare them to porewater nutrients.

# 4.4 Results

## 4.4.1 Porewater Nutrients

### 4.4.1.1 Nitrogen

#### 4.4.1.1.1 Dissolved Inorganic Nitrogen (ammonium + nitrate + nitrite)

Mean values of DIN differed from season to season, in summer, mean DIN was at its highest 564 ± 278 µmol/L and declined with colder months. Autumn mean DIN was 437 ± 348 µmol/L while in winter dropped to 242 ± 132 µmol/L (Figure 63).

Differences between presence and absence of macroalgae where clear among the different seasons. During summer there where major differences observed between presence and absence cores, macroalgae present core was enriched in DIN (mean= 609 ± 269 µmol/L) compared to the absence core (mean = 522 ± 293 µmol/L) (Figure 63A). The maximum concentration for the macroalgae present core was at 2 cm depth (1099 µmol/L) with a pronounce decline by 3 cm to continue a smooth decrease downcore. On the contrary the absent core had its minimum concentration at the top 1cm (174 µmol/L) and gradually increased with depth until reaching the maximum at the 10 cm depth (977 µmol/L) (Figure 63A).

By autumn changes in DIN concentrations between presence and absence of macroalgae are more evident. Mean concentration for the macroalgae core was 193 ± 258 µmol/L, while the absent core mean concentration reached 681 ± 238 µmol/L. Nonetheless, the highest concentration is found at the 1 cm on the macroalgae core (899 µmol/L) right after depleting to the minimum at 2 cm depth (5 µmol/L) and then started increasing slightly again.

The macroalgae absent core has its minimum concentration at 2 cm depth as well, however it was much higher than in the present core, 95 µmol/L. DIN concentrations increased with depth until it reached its maximum at the bottom of the core (884 µmol/L) (Figure 63B).

In winter DIN concentrations were at its lowest compared to autumn and summer, the macroalgae present core had a mean of 314 ± 155 µmol/L while the absent core 177 ± 57 µmol/L. In this season there was a similar distribution downcore in both cases, however the macroalgae present core had higher concentrations. Minimum concentrations were at 2 cm for the macroalgae present core (78 µmol/L) and at 3 cm for the macroalgae absent core (94 µmol/L) (Figure 63C). Concentrations increased downcore for both cores to reach their maximum values at the 9 cm depth (absent= 257 µmol/L; present= 543 µmol/L) (Figure 63C).

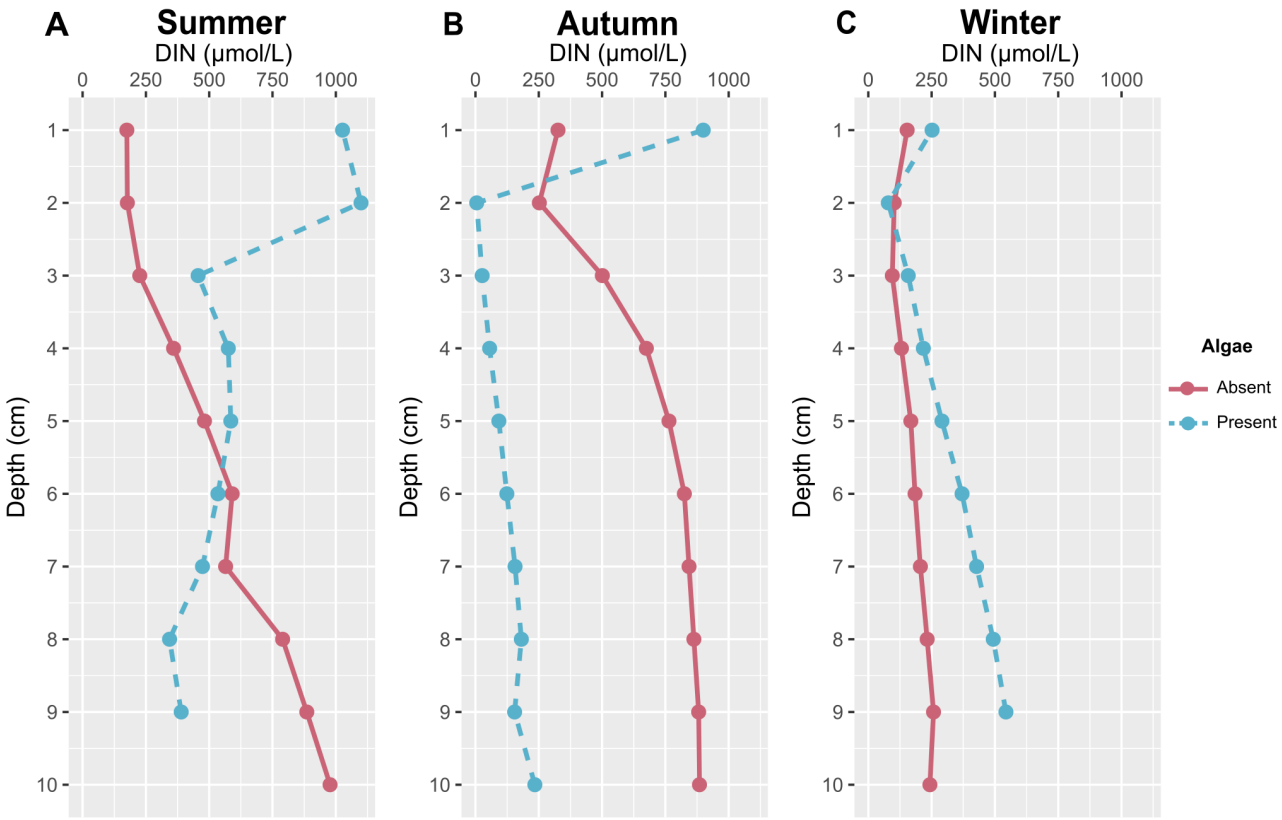


**Figure 63. Dissolved Inorganic Nitrogen (DIN) profiles (µmol/L) in the porewaters of the top 10 cm sediment for each season (A. Summer, B. Autumn, C. Winter). Red line represents the core where macroalgae was absent while blue dotted line represents macroalgae present cores.**

During summer the ammonium fraction of the DIN represented 98%, followed by nitrate 1.6% and nitrite 0.2%. By autumn, ammonium increased making 99% of the DIN, while nitrate and nitrite accounted for 0.4% and 0.5% respectively. And in winter, nitrate fraction increased to 3% and nitrite 1.3%, while ammonium remained the major component with 96% (Figure 64).

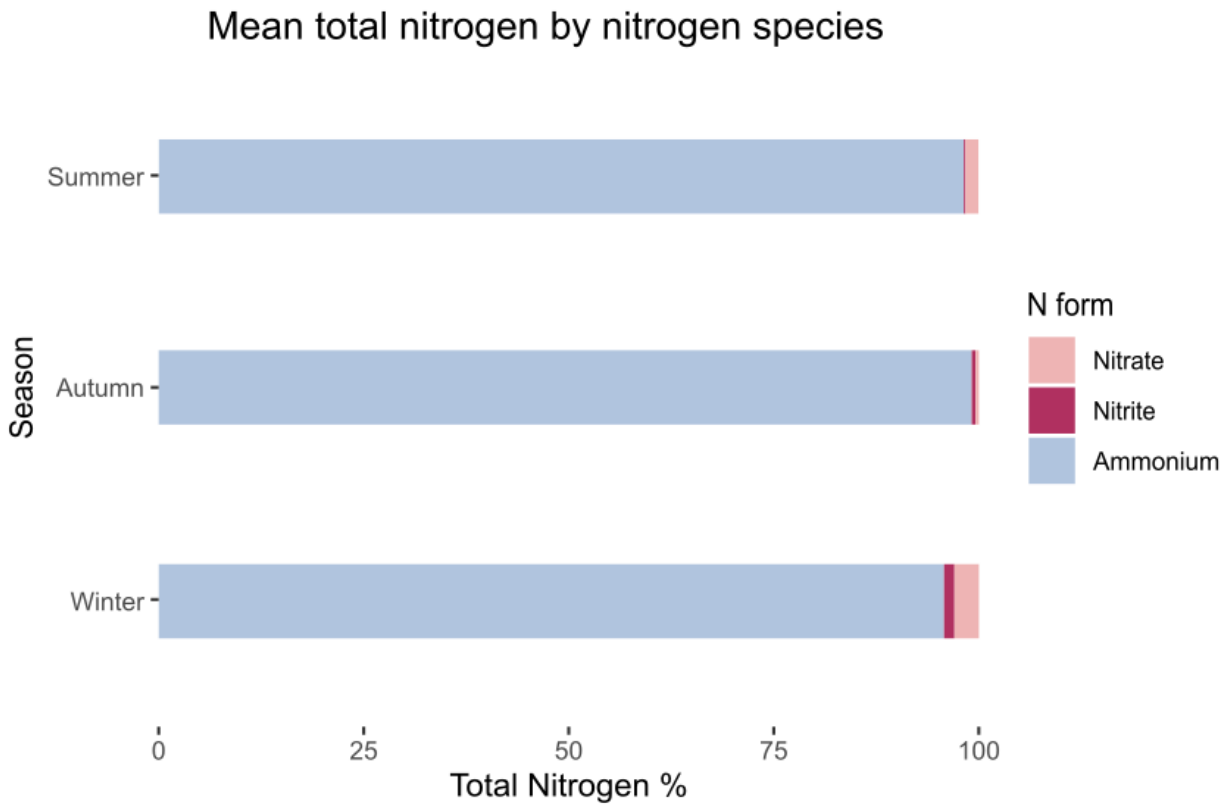


**Figure 64. Mean percentage of total dissolved inorganic nitrogen (DIN) by nitrogen species (nitrate, nitrite, and ammonium) for each season (summer, autumn, winter). The stacked bar chart shows the relative contributions of each nitrogen form to the total nitrogen pool.**

#### 4.4.1.1.2 Ammonium

Porewater ammonium concentrations were close to those found within DIN, making it in all seasons the main contributor of the nitrogen species. Mean ammonium concentration during summer was of 564 ± 278 µmol/L, decreasing with each season. In autumn mean ammonium was 437 ± 348 µmol/L and in winter 242 ± 132 µmol/L (Figure 65).

In summer mean ammonium concentrations in macroalgae present and absent cores were similar, absence= 514 ± 294 µmol/L and presence= 596 ± 272 µmol/L (Figure 65A). By autumn, differences became more marked with the macroalgae

absent core having a mean concentration of ammonium of 677 ± 240 µmol/L and the present core 189 ± 258 µmol/L (Figure 65B). In winter mean ammonium concentrations were 164 ± 64 µmol/L for the macroalgae absent core and 306 ± 155 µmol/L in the macroalgae present core (Figure 65C). Distribution downcore in all cases are the same than for DIN concentrations (Figure 65).

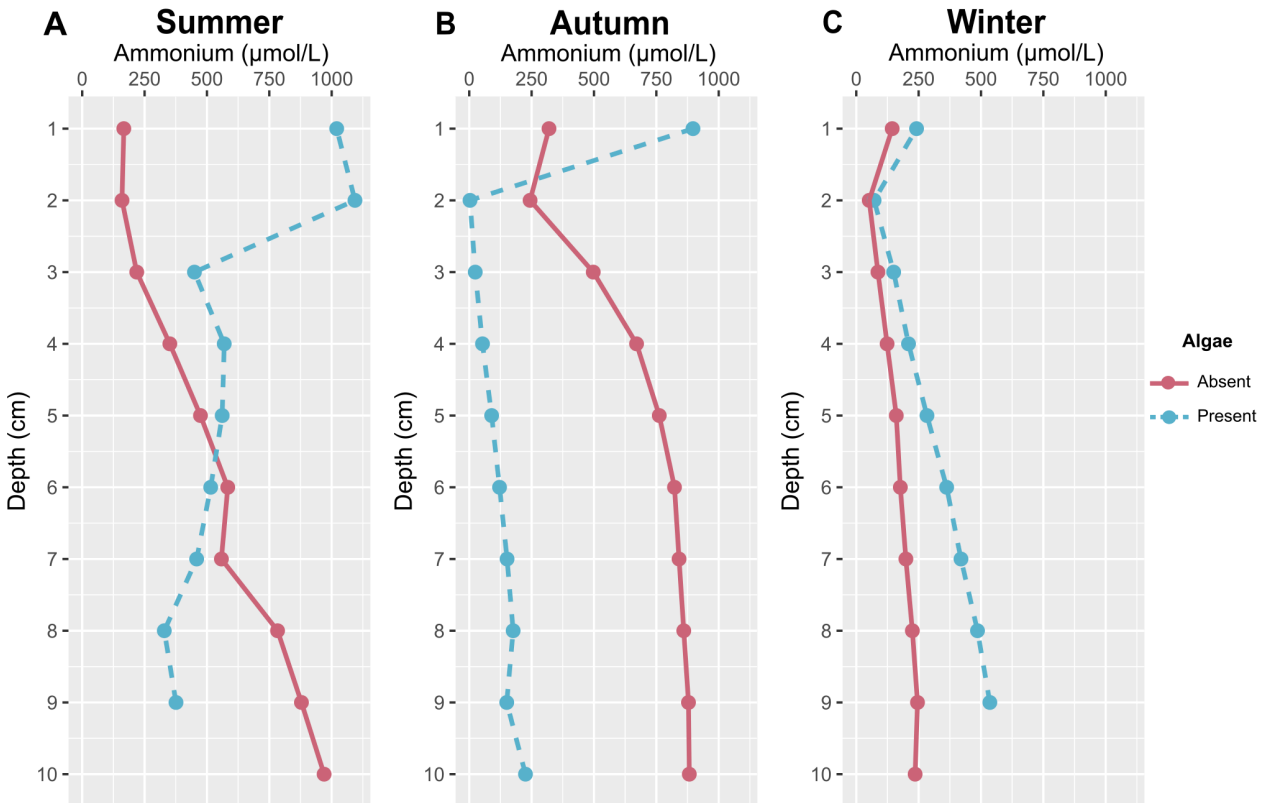


**Figure 65. Dissolved ammonium profiles (µmol/L) in the porewaters of the top 10 cm sediment for each season (A. Summer, B. Autumn, C. Winter). Red line represents the core where macroalgae was absent while blue dotted line represents macroalgae present cores.**

#### 4.4.1.1.3 Nitrate

Porewaters nitrate concentrations varied significantly from each sampling visit. In summer mean nitrate concentration was 9 ± 5.3 µmol/L by autumn went down to 1.71 ± 2.3 µmol/L and finally in winter it increased again to 7.22 ± 8 µmol/L (Figure 66). In summer, there was greater variability between macroalgae present and absent cores. The macroalgae absent corer had a mean nitrate concentration of 7 ± 3 µmol/L while the present core has 11.2 ± 6.5 µmol/L. Macroalgae absent core maintained mostly constant nitrate concentrations downcore, except for the 2 cm where the max peak was observed at 15 µmol/L. On the macroalgae present core constant lower concentrations remained at the top 4 cm with the maximum concentration at 5 cm (23 µmol/L) and slightly decreased with depth (Figure 66A).

During autumn both cores had similar mean nitrate values, 1.78 ± 2.5 µmol/L for the absent core and 1.71 ± 2.2 µmol/L in the present core. Nonetheless, maximum value for the macroalgae absent was found at the top 2 cm (8 µmol/L) and declined to a minimum below 5 cm. On the other hand, macroalgae present core reached its maximum concentration at the bottom of the core 7 µmol/L, staying constant on the top 6 cm to start increasing with depth (Figure 66B).

Winter mean nitrate concentration was higher for the macroalgae with 8.8 ± 11 µmol/L than in the present core, 5.3 ± 0.8 µmol/L. Both cores had constant nitrate values with depth, ranging between 4 - 8 µmol/L with the only exception being found at 2 cm on the macroalgae absent core (40 µmol/L) (Figure 66C).

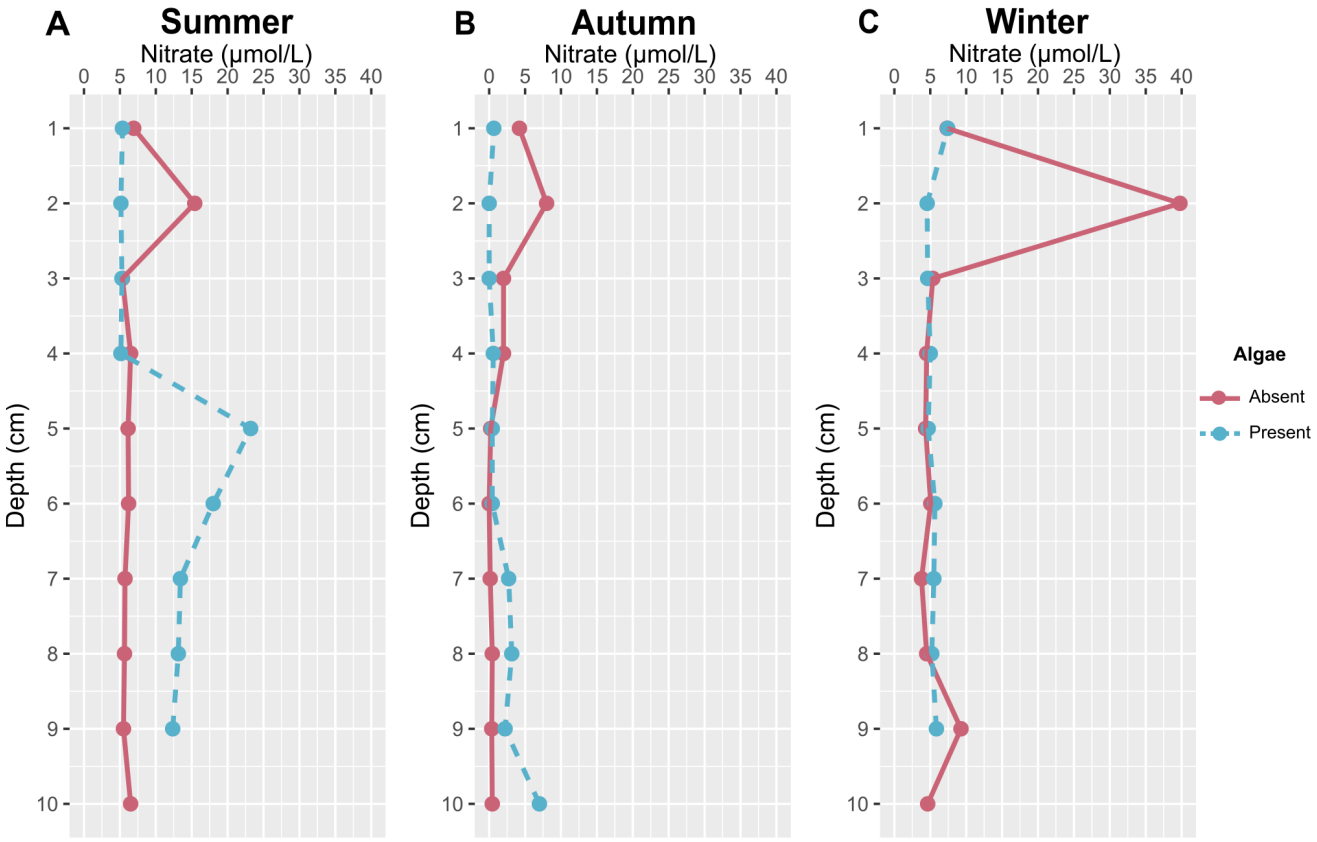


**Figure 66. Dissolved nitrate profiles (µmol/L) in the porewaters of the top 10 cm sediment for each season (A. Summer, B. Autumn, C. Winter). Red line represents the core where macroalgae was absent while blue dotted line represents macroalgae present cores.**

### 4.4.1.1.4 Nitrite

Nitrite concentrations generally increased with every season. Summer mean nitrite concentration was 1.16 ± 0.26 µmol/L, in autumn 2 ± 0.43 µmol/L and reached its maximum by winter with 3 ± 1.9 µmol/L (Figure 36). During summer, macroalgae absent core had a slightly higher mean nitrite concentration, 1.24 ± 0.32 µmol/L compared to 1.08 ± 0.14 µmol/L in the macroalgae present core. The increase in the absent core is observed between 2-4 cm depth, while values for the macroalgae present core remained constant downcore (Figure 67A).

In autumn mean nitrite concentration for the macroalgae present core was 2.16 ± 0.2 µmol/L, similarly the macroalgae absent core has 1.98 ± 0.57 µmol/L. All values downcore were very similar except for 2 cm depth where a difference was observed between macroalgae presence and absence. While macroalgae present core reached its maximum value at 2 cm depth (2.64 µmol/L), the opposite occurred in the absent core where minimum concentration was also at 2 cm depth (0.35 µmol/L) (Figure 67B).

Winter nitrite concentrations where slightly more variable than in the other seasons. Mean nitrite concentration for the macroalgae present core was 2.5 ± 0.34 µmol/L while the absent core had 3.5 ± 2.5 µmol/L. The macroalgae present concentrations downcore where constant ranging between 2.1-3 µmol/L compared to the absent core where maximum value reached 10.6 µmol/L at 2 cm depth (Figure 67C).

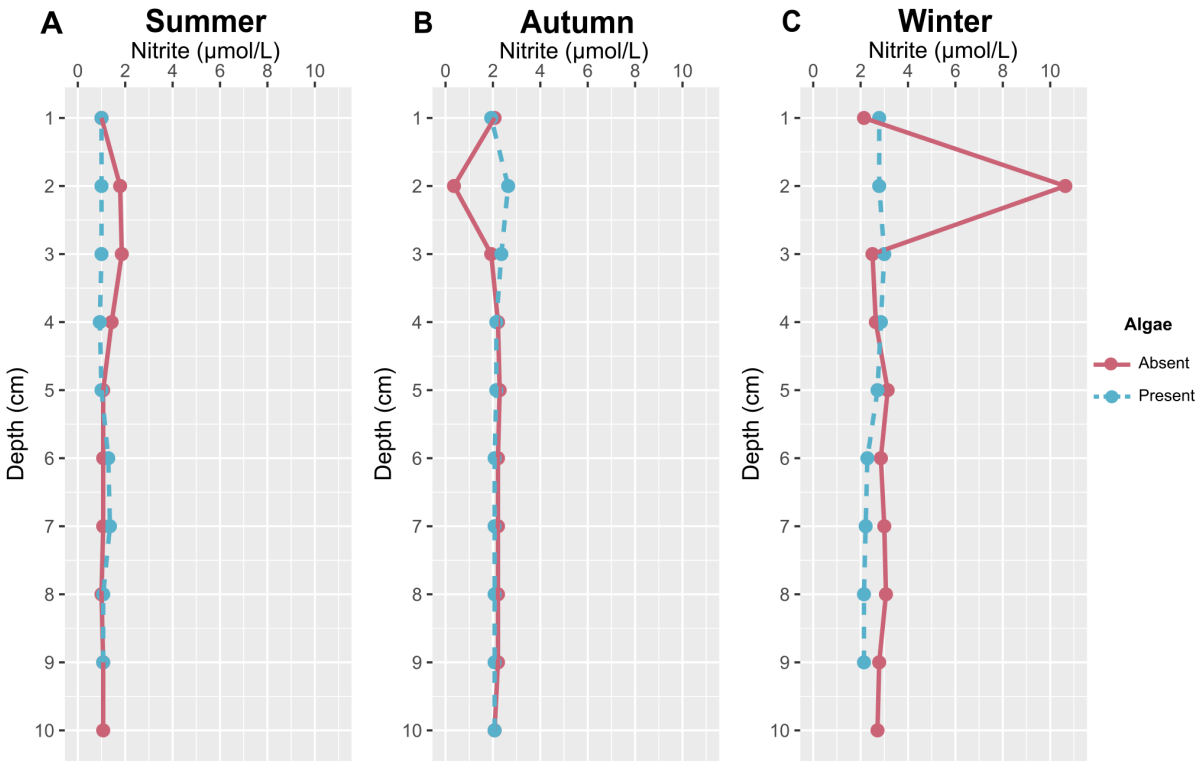


**Figure 67. Dissolved nitrite profiles (µmol/L) in the porewaters of the top 10 cm sediment for each season (A. Summer, B. Autumn, C. Winter). Red line represents the core where macroalgae was absent while blue dotted line represents macroalgae present cores.**

### 4.4.1.2 Phosphate

Phosphate concentrations were varying from season to season. Mean concentration in summer was 148 ± 81 µmol/L, during autumn mean phosphate decreased to 55.4 ± 41.5 µmol/L and by winter it reached its maximum value with 313 ± 94 µmol/L (Figure 68).

Differences between macroalgae presence and absence were clearly observed in all seasons. In summer, macroalgae absent cores had a mean phosphate concentration of 181 ± 70 µmol/L, while the macroalgae present core has a mean of 99.3 ± 78.5 µmol/L. Macroalgae absent core phosphate concentrations were generally increasing with depth and had its maximum concentration at the deeper

end of the core (275 µmol/L); the minimum at 5 cm depth (81.2 µmol/L). Downcore patterns for the macroalgae absent for macroalgae presence could not be determined because sample limitation meant there was no data points below 4 cm depth (Figure 68A).

Autumn mean phosphate concentration in absence of macroalgae was 19.2 ± 12.6 µmol/L while in presence of macroalgae the value increased to 95.6 ± 15.7 µmol/L. Both cores present constant value down core with a barely noticeable increase with depth. Maximum value for the absent core was found at the end of the core (41 µmol/L) and in the macroalgae present core at 5 cm depth (110 µmol/L) (Figure 68B).

During winter mean phosphate concentration was higher in the macroalgae absent core with a value of 357 ± 96.4 µmol/L than in the macroalgae present, 258 ± 56.8 µmol/L. The maximum concentration in the macroalgae absent core (456 µmol/L) was reached at 10 cm depth, whereas in the present core at 7 cm depth (318 µmol/L). In both cases, can be observed a general increase downcore (Figure 68C).

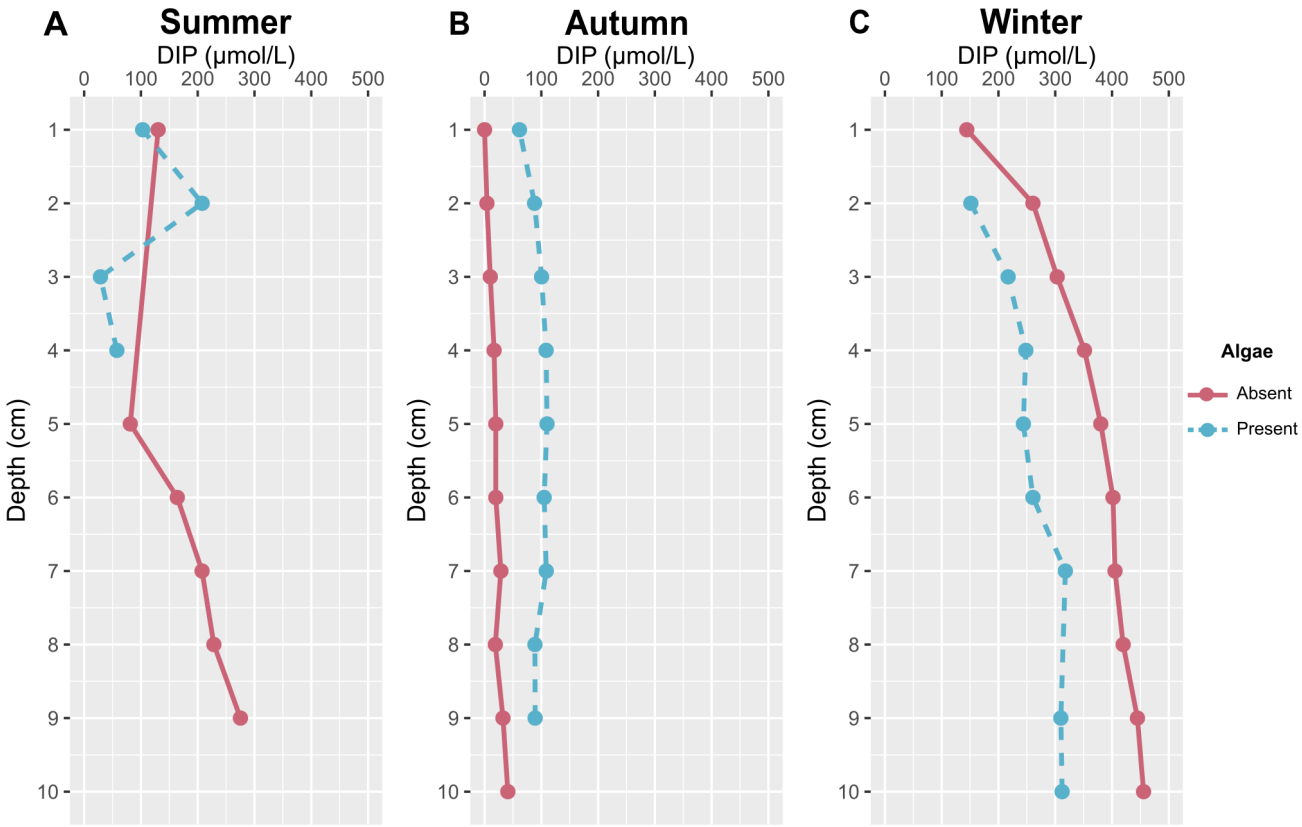


**Figure 68. Dissolved Inorganic Phosphorus (DIP) profiles (µmol/L) in the porewaters of the top 10 cm sediment for each season (A. Summer, B. Autumn, C. Winter). Purple line represents the core where macroalgae was absent while blue dotted line represents macroalgae present cores.**

## 4.4.1.3 Dissolved silicon

Mean concentrations of dissolved silicon (DSi) were less variable from season to season than other nutrients. Summer mean DSi concentration was 541 ± 96 µmol/L, decreasing gradually in the next seasons. In autumn mean DSi went down to 369 ± 137 µmol/L and by winter had a smaller decrease to 345 ± 104 µmol/L (Figure 69). There were noticeable differences between macroalgae presence and absence for all seasons. In summer mean DSi concentrations for the macroalgae absent core was 579 ± 92.3 µmol/L and 484 ± 78 µmol/L in the macroalgae present core. The absent core showed an increase with depth and the maximum concentration (685 µmol/L) was observed at 8 cm depth (Figure 69A).

Mean autumn DSi concentrations were 272 ± 122 µmol/L and 476 ± 25.8 µmol/L for the absent and present cores respectively. The macroalgae absent core had its minimum concentration at the top (63 µmol/L) and progressively increased with depth reaching its maximum at 10 cm depth (480 µmol/L). On the other hand, the macroalgae present core started with the lowest concentration also at the top of the core (293 µmol/L) but had its maximum at 5 cm depth (504 µmol/L). DSi concentrations for macroalgae presence were less variable with depth (Figure 69B).

In winter macroalgae absence core had a lower mean concentration than in the presence core, 393 ± 106 µmol/L and 284 ± 62.6 µmol/L respectively. In absence of macroalgae, DSi concentration had its minimum at the top cm (159 µmol/L) and increased with depth until it reached its maximum at the bottom (502 µmol/L). Prescence of macroalgae had a similar pattern downcore, starting with the lowest concentration at the top (167 µmol/L), however reached its maximum at 7 cm depth (350 µmol/L) (Figure 69C).

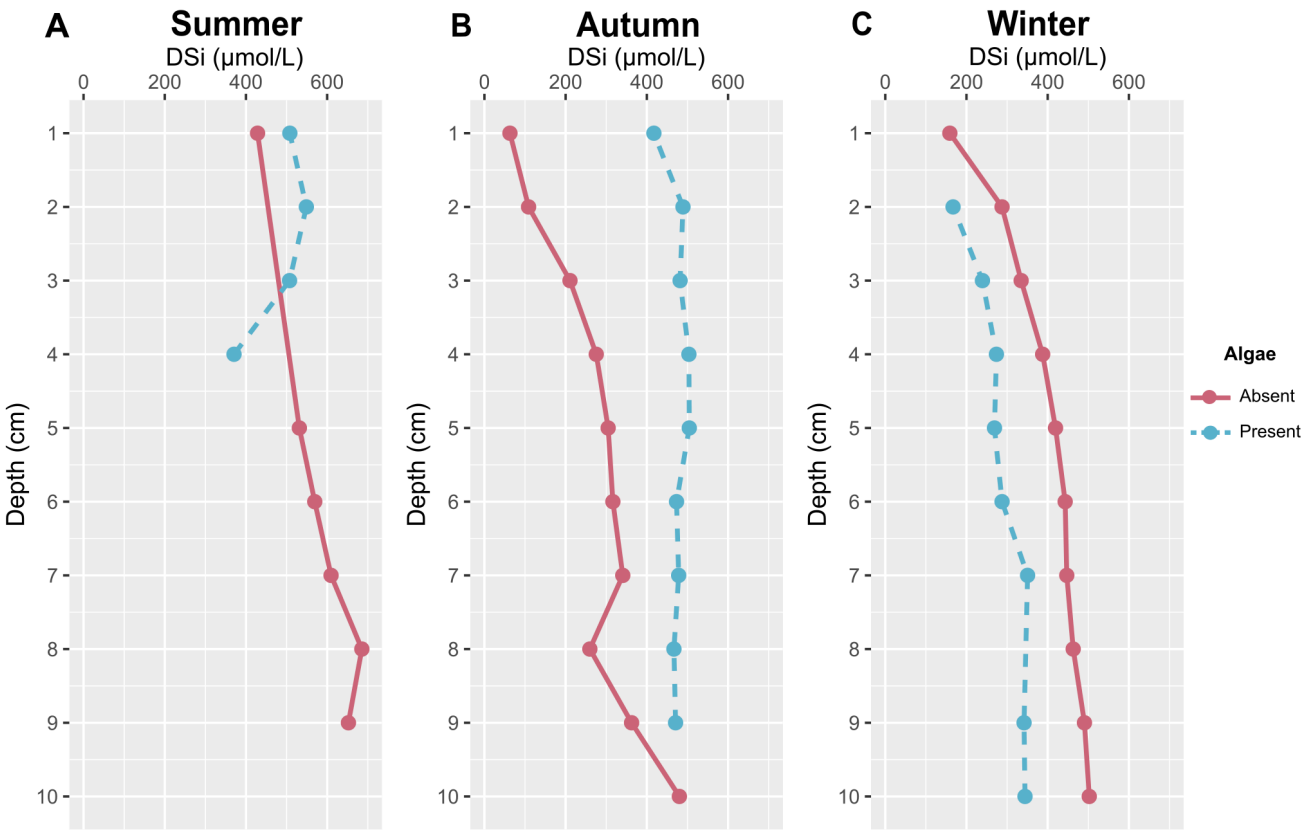


**Figure 69. Dissolved silicon profiles (µmol/L) in the porewaters of the top 10 cm sediment for each season (A. Summer, B. Autumn, C. Winter). Purple line represents the core where macroalgae was absent while blue dotted line represents macroalgae present cores.**

## 4.4.2 Dissolved metals

### 4.4.2.1 Iron

Mean Fe concentration in summer was 98.2 ± 129 µmol/L, this value declined in autumn to 65.9 ± 75.2 µmol/L and increased significantly during winter reaching 331 ± 239 µmol/L (Figure 70). In summer mean Fe concentration in the macroalgae absent core (128 ± 16.2 µmol/L) was almost three times greater than in the present core (53.2 ± 52.7). Fe concentrations in the macroalgae absent core decreased with depth starting with 260 µmol/L while its minimum value observed at 9 cm (49.3 µmol/L). Trends for the present core couldn't be observed as there was a lack of data, however it had its maximum value at 4 cm depth (125 µmol/L) (Figure 70A).

During autumn, there were significant differences between mean Fe in macroalgae presence and absence. While in presence of algae there was mean Fe of 0.42 ± 1.2 µmol/L the absence of macroalgae increased this value up to 125 ± 158 µmol/L. In absence of macroalgae the top cm was enriched with Fe (Max= 517 µmol/L), decreasing exponentially with depth. On the other hand, the macroalgae present was depleted in Fe, having the maximum concentration at the top 1 cm (3.8 µmol/L) and was not detected at other depths (Figure 70B).

In winter the absent core has a mean Fe concentration of 200 ± 238 µmol/L while the present had a greater mean of 496 ± 103 µmol/L. In the macroalgae absent core the maximum concentration was found at the subsurface 2 and 3 cm (max= 591 µmol/L) and then decreased sharply until it couldn't be detected below 6 cm depth. On the contrary the macroalgae present core maintained high Fe concentrations at

all measured depths. The minimum value was observed at the first cm (306 µmol/L) with the peak value found at 7cm (629 µmol/L) (Figure 70).

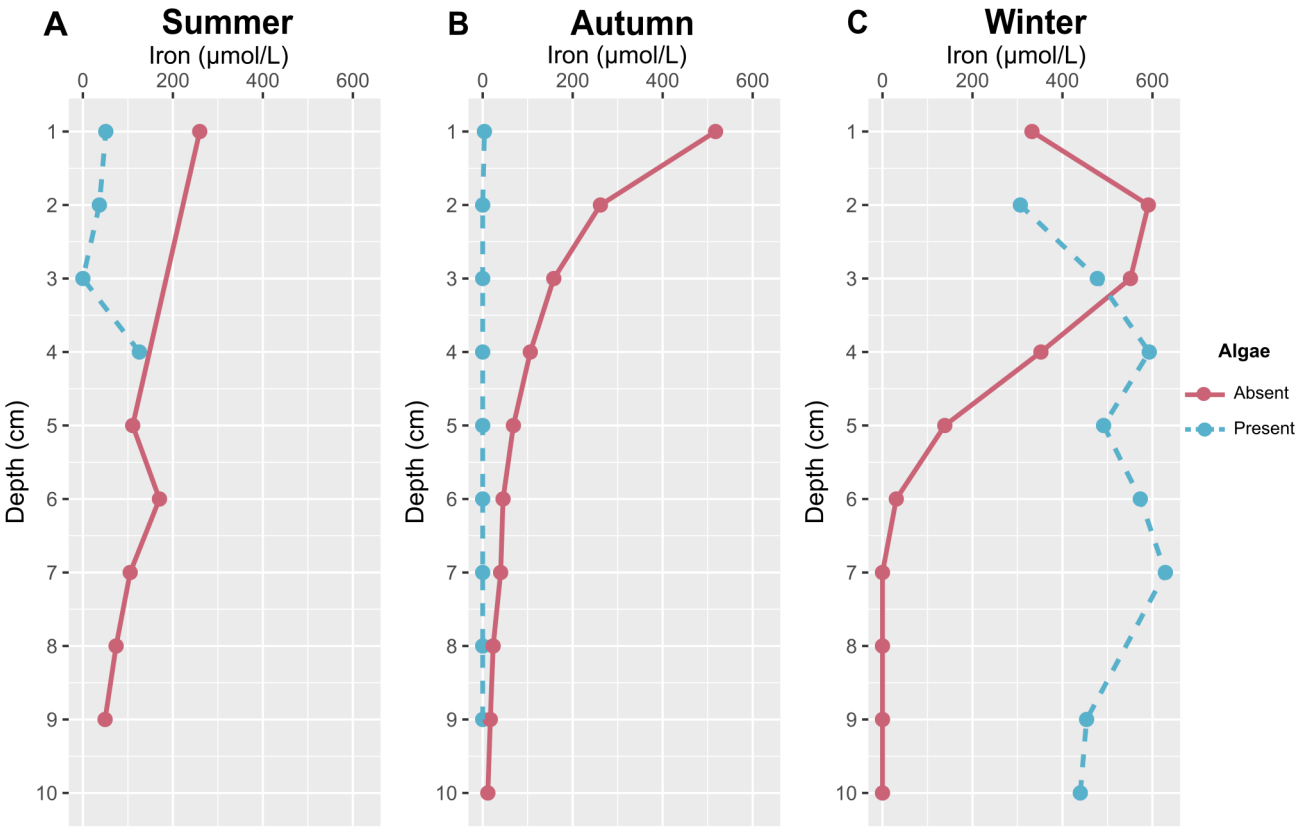


**Figure 70. Dissolved iron profiles (µmol/L) in the porewaters of the top 10 cm sediment for each season (A. Summer, B. Autumn, C. Winter). Red line represents the core where macroalgae was absent while blue dotted line represents macroalgae present cores.**

### 4.4.2.2 Manganese

Mn concentrations in summer where the highest of all the seasons, with an average of 10.1 ± 4.45 µmol/L, by autumn this value dropped significantly to 1.36 ± 1.37 µmol/L and during winter increased slightly to 1.97 ± 2.6 µmol/L.

In summer there were clear differences between macroalgae presence and absence, macroalgae absence core has a mean Mn concentration of 12.4 ± 3.27 µmol/L (Figure 71). Minimum value for this core was at the top cm (5.96 µmol/L), progressively increasing with depth until it reached its maximum at 9 cm depth (14.6 µmol/L). In the macroalgae present core there was a mean Mn concentration of 6.56 ± 3.74 µmol/L, however not clear distribution downcore could be observed (Figure 71A).

Autumn Mn concentrations in the macroalgae absent core where higher than in the macroalgae present core, with a mean of 2.56 ± 0.62 µmol/L and 0.035 ± 0.1 µmol/L respectively. In both cases concentrations were uniform with depth, however in the macroalgae present core Mn was only detected at the 1 cm depth and in the macroalgae absent core the maximum concentration was also at the top (3.48 µmol/L) while the minimum was reached at 8 cm depth (1.63 µmol/L) (Figure 71B).

By winter mean Mn concentrations in macroalgae presence and absence where similar, 2.17 ± 2.8 µmol/L and 1.72 ± 2.4 µmol/L respectively, however their distribution downcore was contrasting. Whilst the macroalgae absent core had a subsurface peak at 2 cm depth (6.21 µmol/L) and Mn was not measured below 4 cm in the macroalgae present core there was the opposite distribution, Mn was not

detected until the 7 cm depth with the maximum concentration of 4.81 µmol/L (Figure 71C).

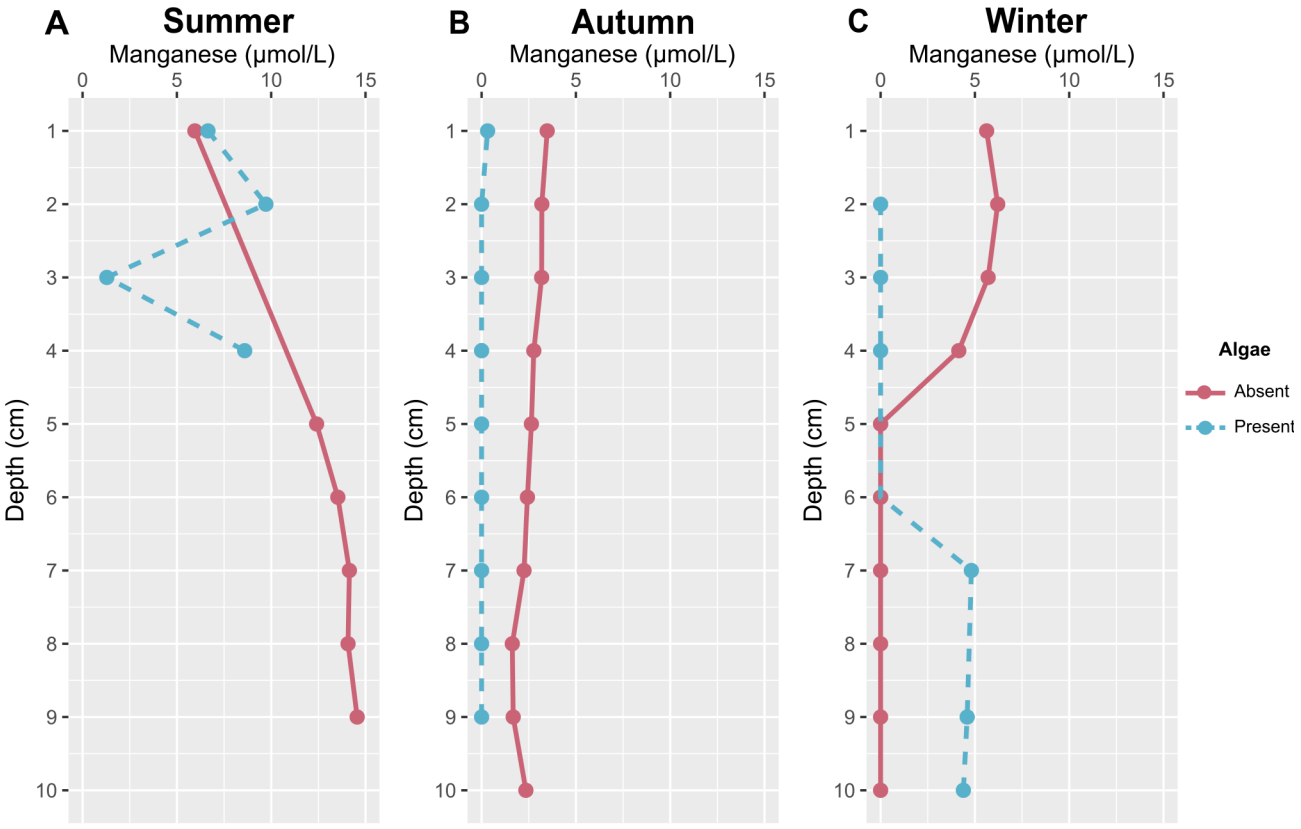


**Figure 71. Dissolved manganese profiles (µmol/L) in the porewaters of the top 10 cm sediment for each season (A. Summer, B. Autumn, C. Winter). Red line represents the core where macroalgae was absent while blue dotted line represents macroalgae present cores.**

## 4.4.2.3 Sodium

In summer, Na concentrations were at their lowest with a mean value of 439 ± 11.6 mmol/L (Figure 72A) and the maximum mean concentration was in autumn 483 ± 29.6 mmol/L (Figure 72B). During winter, a mean Na of 459 mmol/L was measured cm (Figure 72C).

Distribution of Na concentrations downcore was similar between presence and absence of macroalgae core in most seasons. In autumn and winter there was slightly more Na in the macroalgae present core, while in summer this couldn't be observed as there wasn't enough data cm.

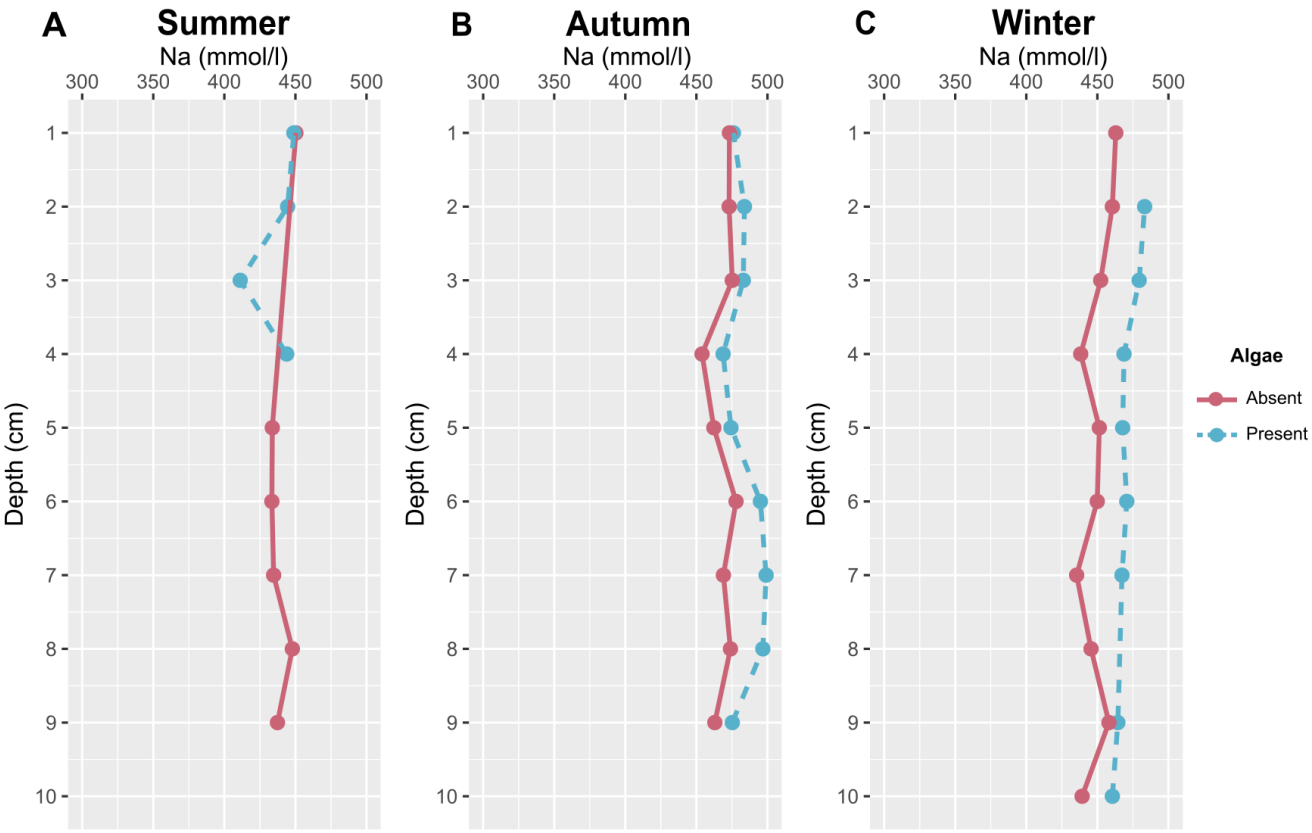


**Figure 72. Porewaters Na (mmol/L) concentrations in macroalgae present and absence cores during the three seasons, measured by ICP-OES method A. Summer, B. Autumn, and C. Winter.**

## 4.4.2.4 S/Na ratio

Mean S/Na during summer was lower 0.053 ± 0.005 increasing gradually by season, summer mean S/Na was 0.059 ± 0.004 and the maximum value was observed in winter 0.066 ± 0.002. There were not major differences between S/Na presence and absence of algae (Figure 73A).

In autumn and winter there was a clear difference between presence and absence of macroalgae, during autumn the macroalgae present core had generally lower S/Na values downcore (0.055 ± 0.002) compared to the macroalgae present core (0.063 ± 0.001) both decreasing gradually downcore (Figure 73B). While in winter macroalgae present had lower S/Na ratio only at the top 6 cm with a mean ratio of 0.066 ± 0.0007 and macroalgae absent core had a slightly higher mean S/Na ratio 0.067 ± 0.003 (Figure 73C). Distributions downcore in autumn where decreasing with depth in both cores whereas in winter the macroalgae present core increased slightly with depth and the opposite occurred in the absent core.

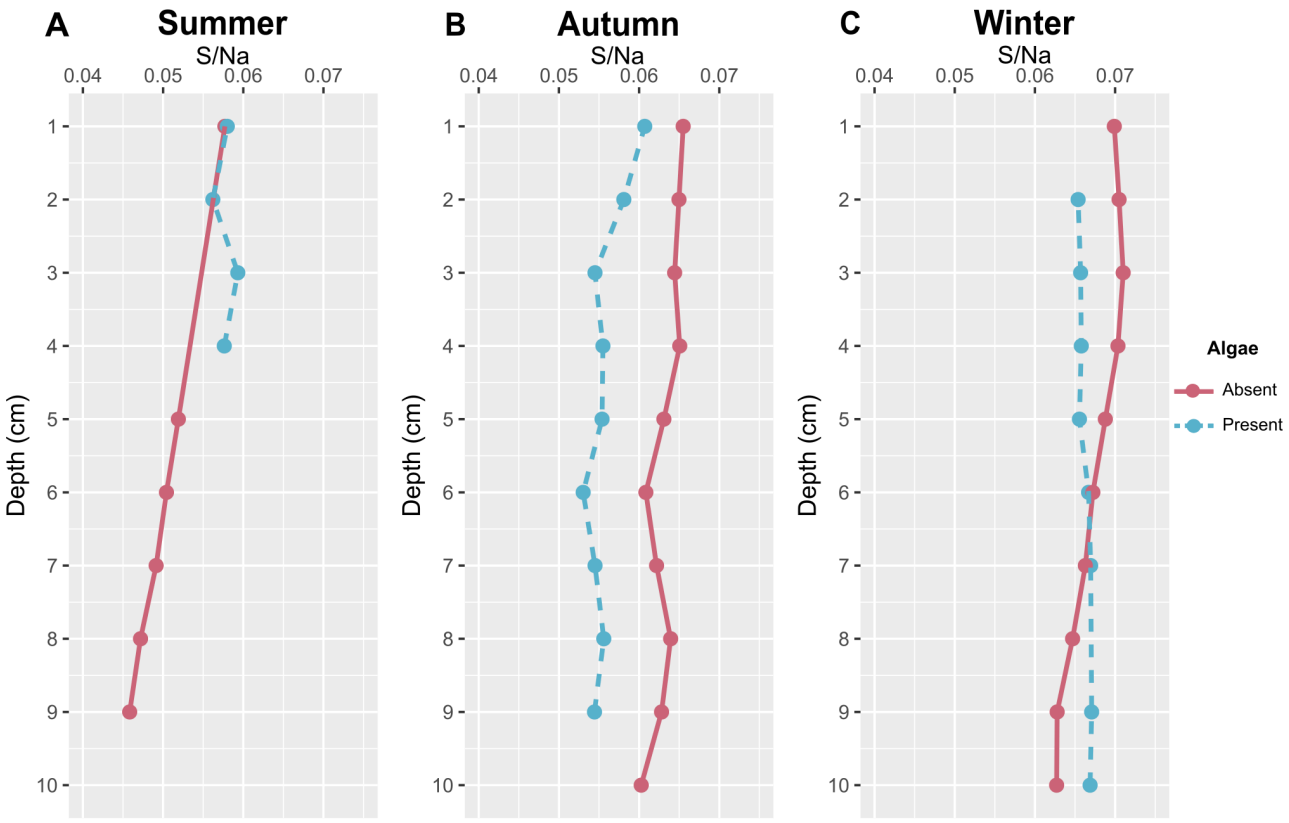


**Figure 73. S/Na ratio profiles in the porewaters of the top 10 cm sediment for each season (A. Summer, B. Autumn, C. Winter). Red line represents the core where macroalgae was absent while blue dotted line represents macroalgae present cores.**

### 4.4.2.5 K/Na ratio

K/Na concentrations throughout the different seasons where constant in all seasons. Mean K/Na during summer was 0.022 ± 0.001, in autumn 0.023 ± 0.0007 and in winter 0.024 ± 0.0008. There were not differences in K/Na between the presence and absence of macroalgae (Figure 74).

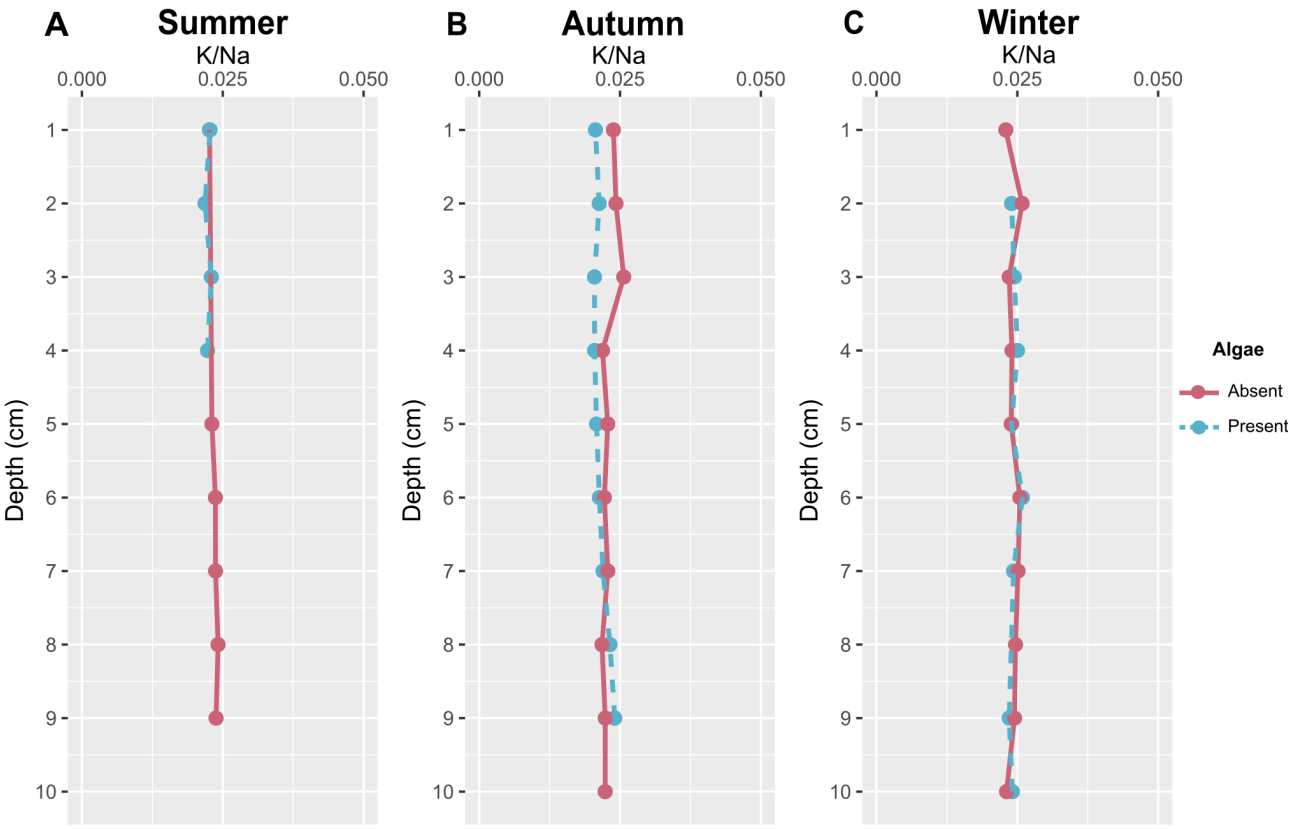


**Figure 74. Porewaters K/Na in macroalgae present and absence cores during the three seasons, measured by ICP-OES method A. Summer, B. Autumn, and C. Winter.**

### 4.4.2.6 Ca/Na ratio

Mean Ca/Na in summer was 0.027 ± 0.003, in autumn 0.024 ± 0.002 and during winter, 0.03 ± 0.004. Differences in Ca/Na values between the presence and absence of macroalgae were minimal and only visible in autumn and winter, where in both cases macroalgae absent cores had slightly higher values in the top 5 cm (Figure 75).

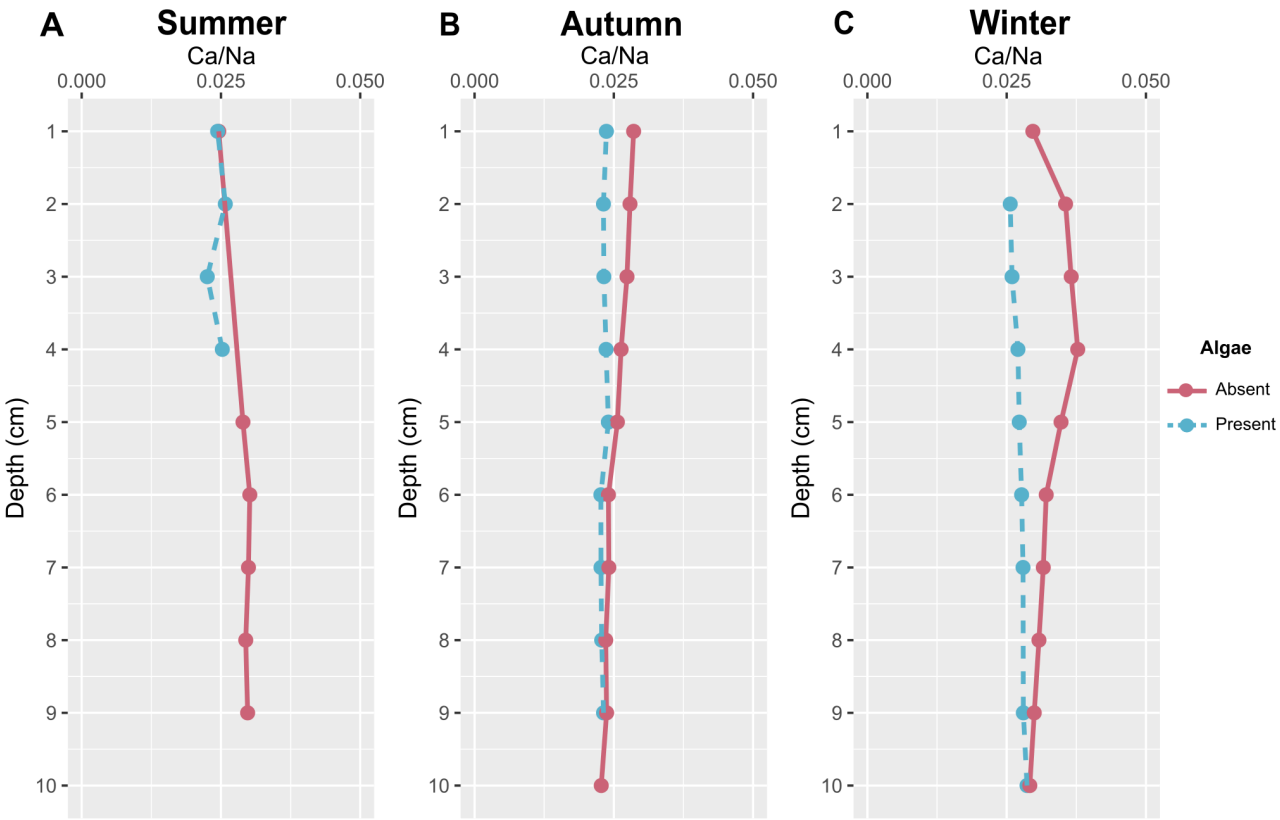


**Figure 75. Porewaters Ca/Na in macroalgae present and absence cores during the three seasons, measured by ICP-OES method A. Summer, B. Autumn, and C. Winter.**

### 4.4.3 Total Organic Carbon

Mean organic C content in the sediment varied from season to season, in summer mean organic C was at its lowest 1.36 ± 0.2% and increased with each seasonal sampling. During autumn mean organic C increased to 1.62 ± 0.2% and by winter it reached 2.27 ± 0.17%. However, macroalgae presence and absence sediment cores for each season had similar values of organic carbon (Figure 76).

In summer mean organic carbon in macroalgae absent cores was 1.33 ± 0.4% while present cores had 1.38 ± 0.23%. Distribution downcore in all sediment cores cases had a tendency of decreasing with depth, remaining more constant below 5-6 cm depth (Figure 76A). Autumn means organic carbon were 1.33 ± 0.2% and 1.38 ± 0.2% for the macroalgae absent and present cores respectively. The macroalgae absent cores had constant organic carbon downcore, with core A at 6 cm depth having noticeable higher organic C content. In the macroalgae present cores a different pattern was observed, where the top cm had slightly more organic C than the rest of the core and it reaches pretty much constant values below 1.5 cm (Figure 76B).

In winter, mean organic carbon increased to 2.3 ± 0.2% in the macroalgae absent cores and 2.2 ± 0.1% for the present cores. More variability is observed in the macroalgae absent cores at the top and bottom sediment while the macroalgae present cores display a more constant distribution downcore (Figure 76C).

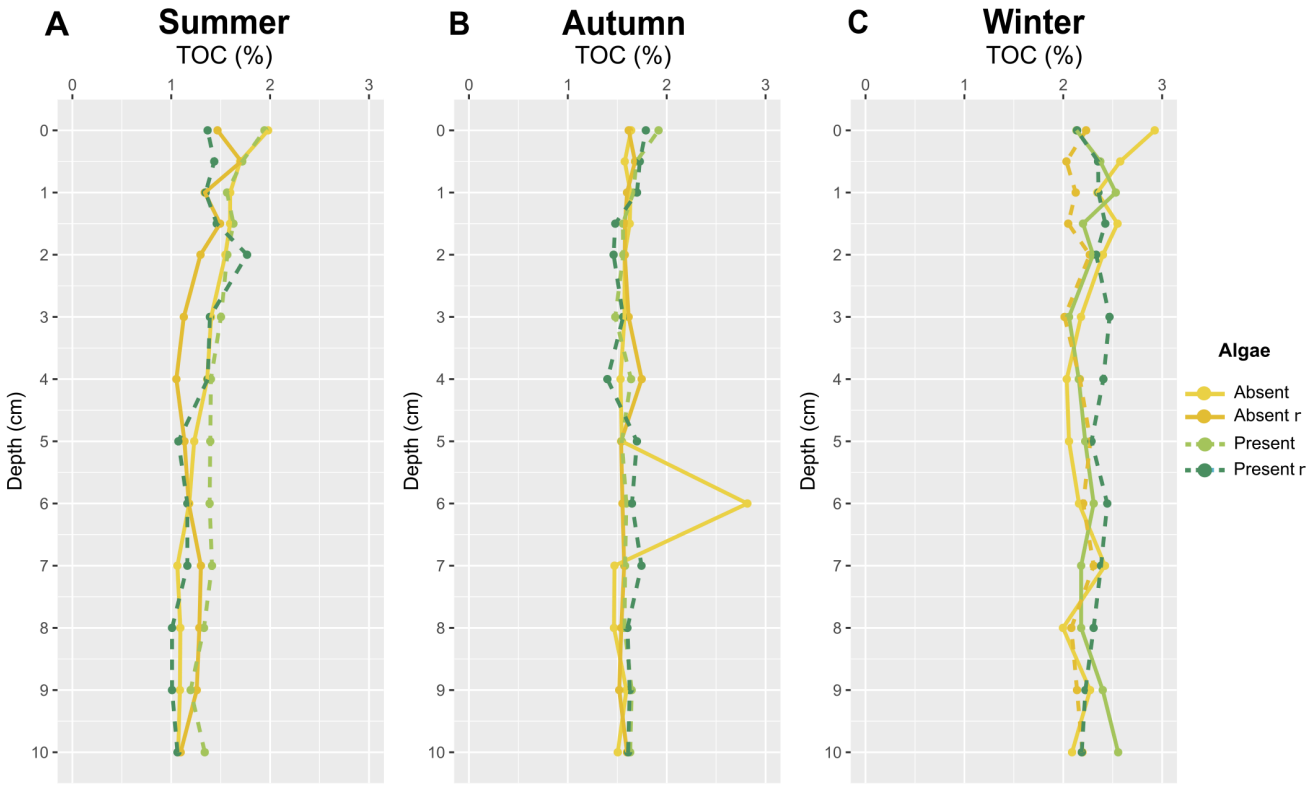


**Figure 76. Total organic carbon (%) in sediment from each season (A. summer, B. Autumn and C. Winter), comparing cores with presence and absence of macroalgae for the top 12 cm of sediment. The dashed line represents cores with macroalgae presence, while the solid line represents cores without macroalgae.**

Values of organic C were tested for significant differences using *Kruskall-Wallis* finding a significant differences between the seasons ($p$<0.001). Following a post-hoc analysis it indicated that the mean values for total organic C for every season where significantly different from each other (Figure 77).

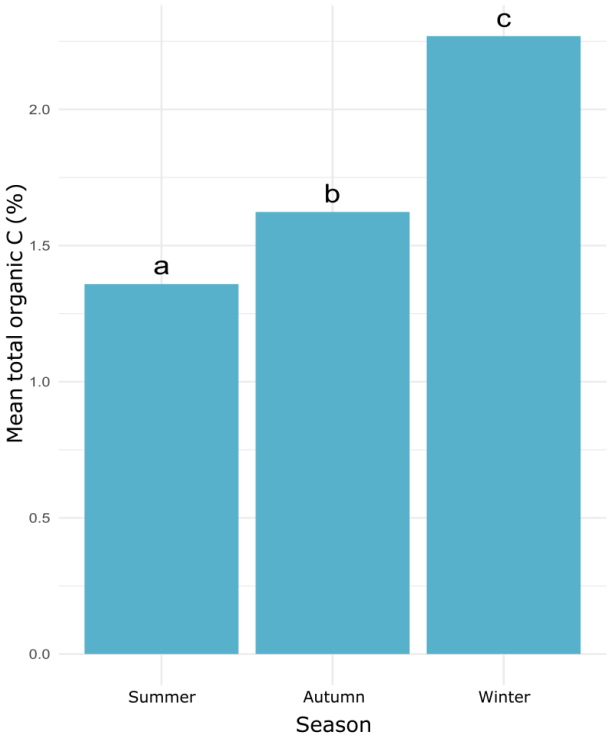


**Figure 77. The barplot displays the mean total carbon (Total C) values for three different seasons: Autumn, Summer, and Winter. The letters above the bars indicate the results of the post-hoc Dunn's test with Bonferroni correction, performed following a *Kruskal-Wallis* test. Different letters signify significant differences between the groups at a significance level of 0.05.**

### 4.4.4 C:N ratios

Mean C:N ratios varied from season to season. In summer mean C:N ratio was 7.1 ± 1, by autumn this value increased slightly to 7.4 ± 0.4 and in winter mean C:N ratio decreased to 4.2 ± 0.4. All sediment cores during all three seasons had a uniform distribution downcore, except for core D in summer that had the highest C:N ratio with 12.4 only at 9 cm depth (Figure 78).

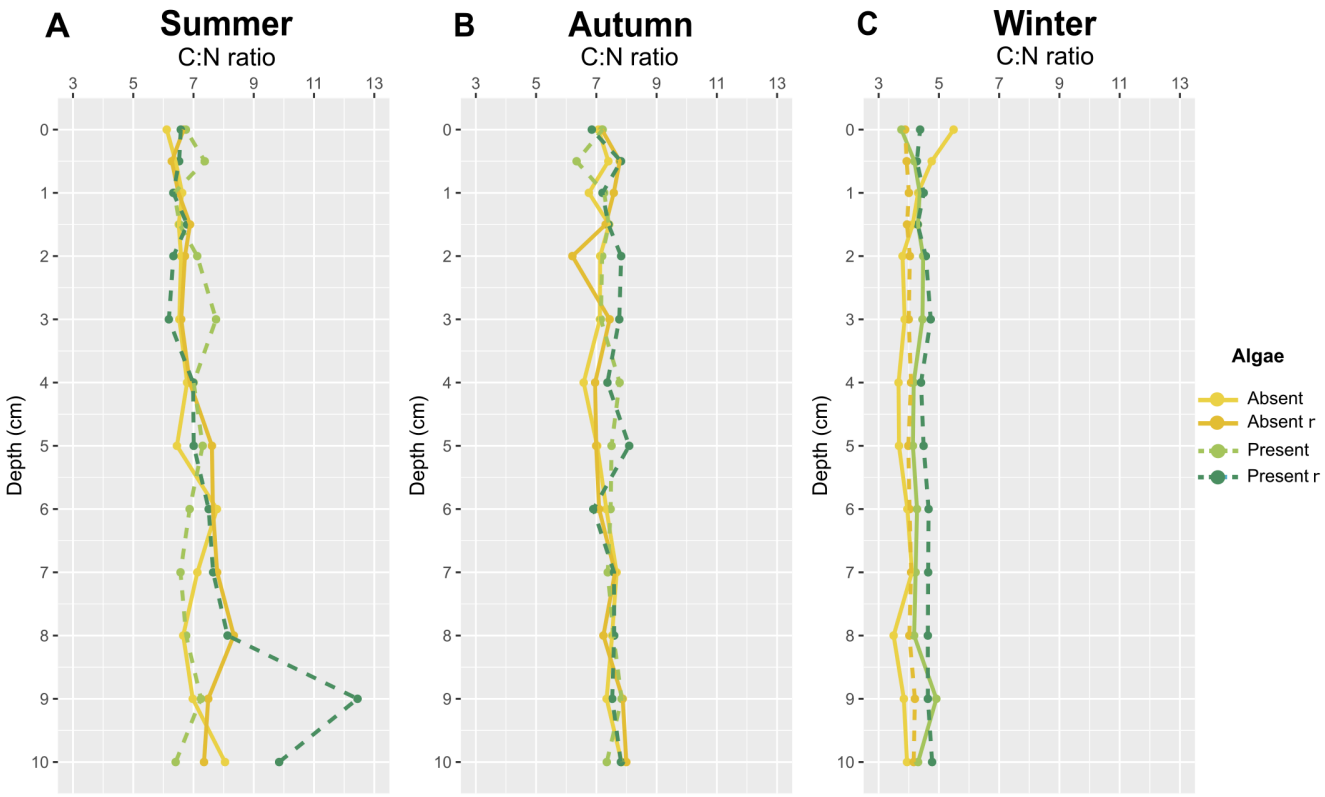


**Figure 78. C:N sediment ratios from each season (A. summer, B. Autumn and C. Winter), comparing cores with presence and absence of macroalgae for the top 12 cm of sediment. The dashed line represents cores with macroalgae presence, while the solid line represents cores without macroalgae.**

There were not significant differences between presence or absence of macroalgae in C:N ratios (Kruskal-Wallis, *p*= 0.469), and distribution downcore is uniform which suggest the top 12 cm of these sediments is well-mixed. Significant differences were

observed in C:N ratios between seasons (Kruskal-Wallis, $p<0.001$), having higher ratios on the summer and lowest during winter.

# 4.5 Discussions

## 4.5.1 Seasonal patterns in nutrients

Dissolved inorganic nitrogen in the sediments (mainly ammonium), had the highest concentrations in summer and autumn compared to winter. Greatest differences between macroalgae presence and absence were observed in summer and autumn. During winter DIN concentrations were higher for the macroalgae presence core compared to the absent and they both increased with depth (Figure 63). The winter enrichment at the top of the macroalgae present core, might be caused by the benthic regeneration of nutrients fuelling the remaining biomass mat in winter (Sundback et al., 2003; Trimmer et al., 2000).

Nitrate concentrations in porewaters were lowest in autumn and highest in winter, while there was a consistent enrichment on the top 2 cm for the macroalgae absent cores in all seasons. On the other hand, nitrite concentrations generally increased being lowest in summer and highest in winter. This seasonal pattern is consistent with the fact that respiration rates tend to correlate positively with temperature in coastal sediments (Thamdrup et al., 2009), resulting in greater rates of nutrient regeneration in the sediment during warmer seasons.

The macroalgae absent cores displayed a pattern of increasing DIN concentration with depth with lower surface concentrations than in the present cores in summer, this same pattern was observed in autumn and more uniform concentrations downcore were present during winter (Figure 63). Increasing porewater DIN concentrations downcore can be explained by accumulation of porewater

ammonium with time, coupled with diffusion upwards across the sediment-water interface down the concentration gradient. This downcore pattern has been previously described as “pre algal mat” (Zimmermann & Montgomery, 1984) suggesting it is a state not impacted by macroalgae.

On the contrary, the macroalgae present cores had a consistent enrichment at the top more pronounced in summer and autumn. Inorganic nutrients are released during the decomposition process of macroalgal detritus (Zimmermann & Montgomery, 1984). Furthermore, anaerobic decomposition of organic carbon under sulfidic conditions releases 16 times more $NH_4^+$ than phosphate (Rozan et al., 2002). These conditions can promote the accumulation of ammonium at the top of the macroalgae cores.

Consequently, phosphate is immediately used by the macroalgae leading to the lowest concentrations of phosphate during summer observed in some porewaters (Rozan et al., 2002). Phosphate concentrations in Langstone did not display a clear seasonal pattern in Langstone. However, there was a clear tendency of lower concentrations at the surface and further increase with depth in all the cores (Figure 68). Which could suggest diffusion of benthic phosphate to the overlying water.

### 4.5.1.1 Water column nutrients

Water column nutrients were potted seasonally in order to identify seasonal patterns. Water column DIN concentrations in winter tend to be higher than in all other seasons, with summer minima followed closely by spring and autumn (Figure 79). Nitrate concentrations had a similar distribution to DIN being the main nitrogen species of the dissolved nitrogen pool (Figure 80). Likewise, for DIP with a winter maximum and summer minimum concentrations (Figure 81).

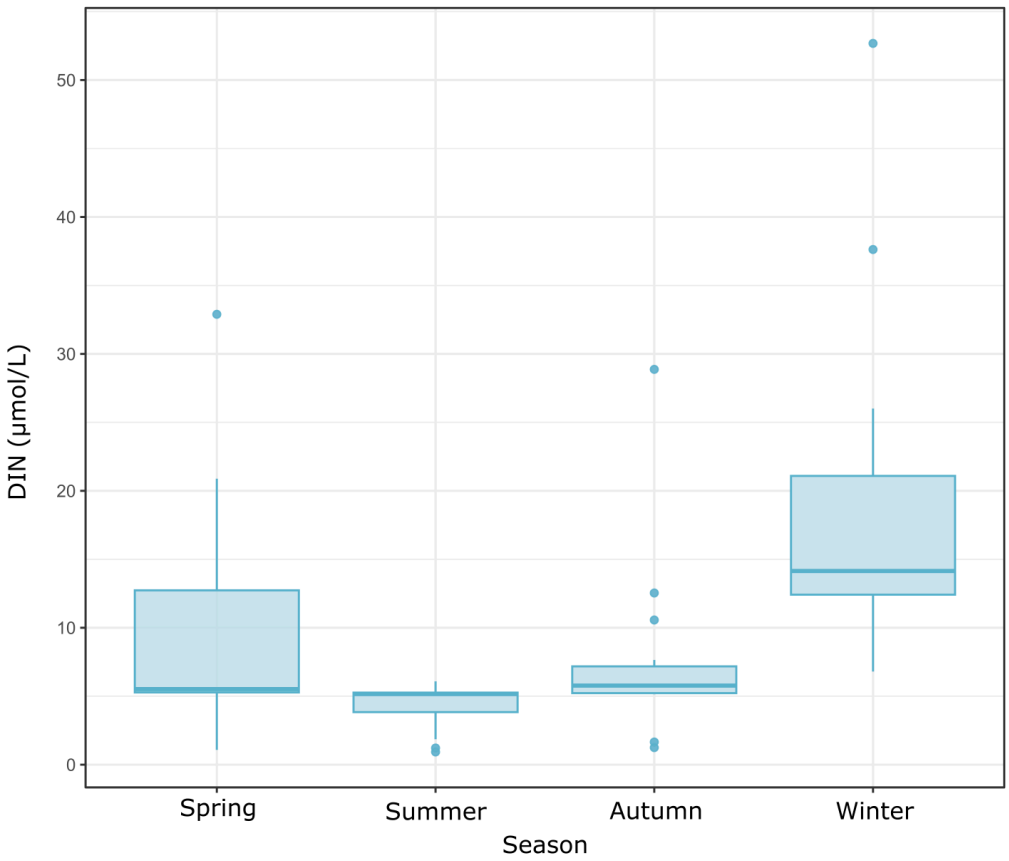


**Figure 79. Seasonal variation of Dissolved Inorganic Nitrogen (DIN) concentrations (µmol/L) across different seasons from water column data from Langstone (2000-2019) (Chapter 2). The central line in each box represents the median DIN concentration, the edges of the box indicate the interquartile range (IQR), and the vertical lines extend to the range of the data, excluding outliers, which are plotted as individual points.**

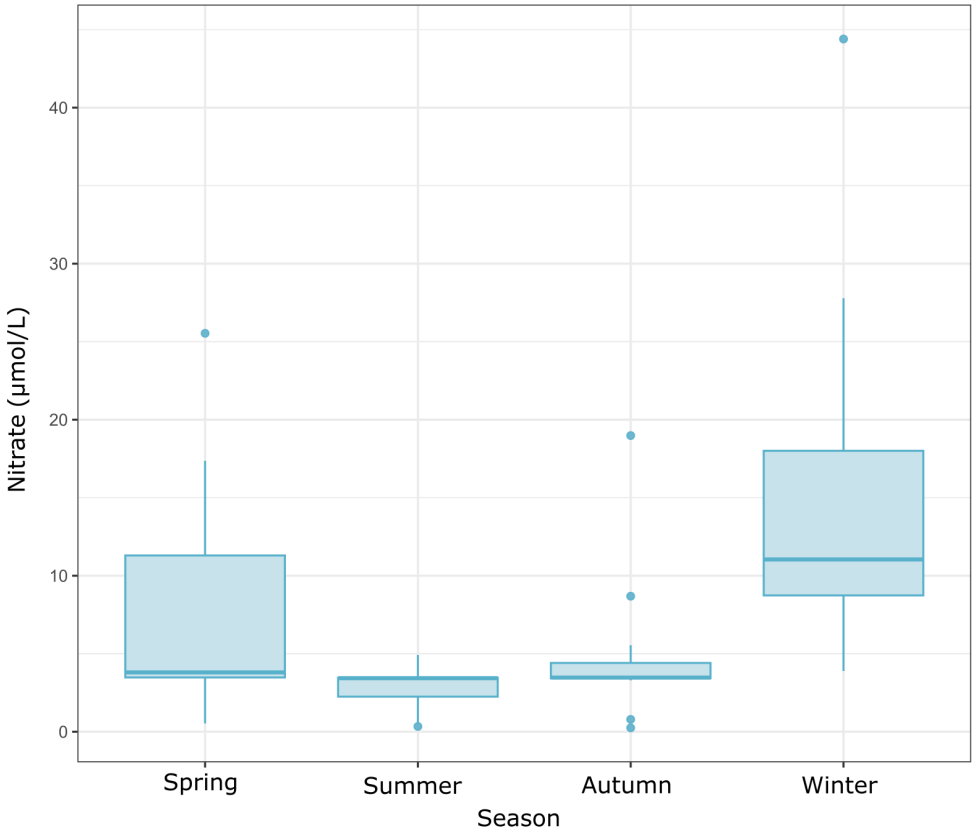


**Figure 80. Seasonal variation of Nitrate concentrations (µmol/L) across different seasons from water column data from Langstone (2000-2019) (Chapter 2). The central line in each box represents the median DIN concentration, the edges of the box indicate the interquartile range (IQR), and the vertical lines extend to the range of the data, excluding outliers, which are plotted as individual points.**

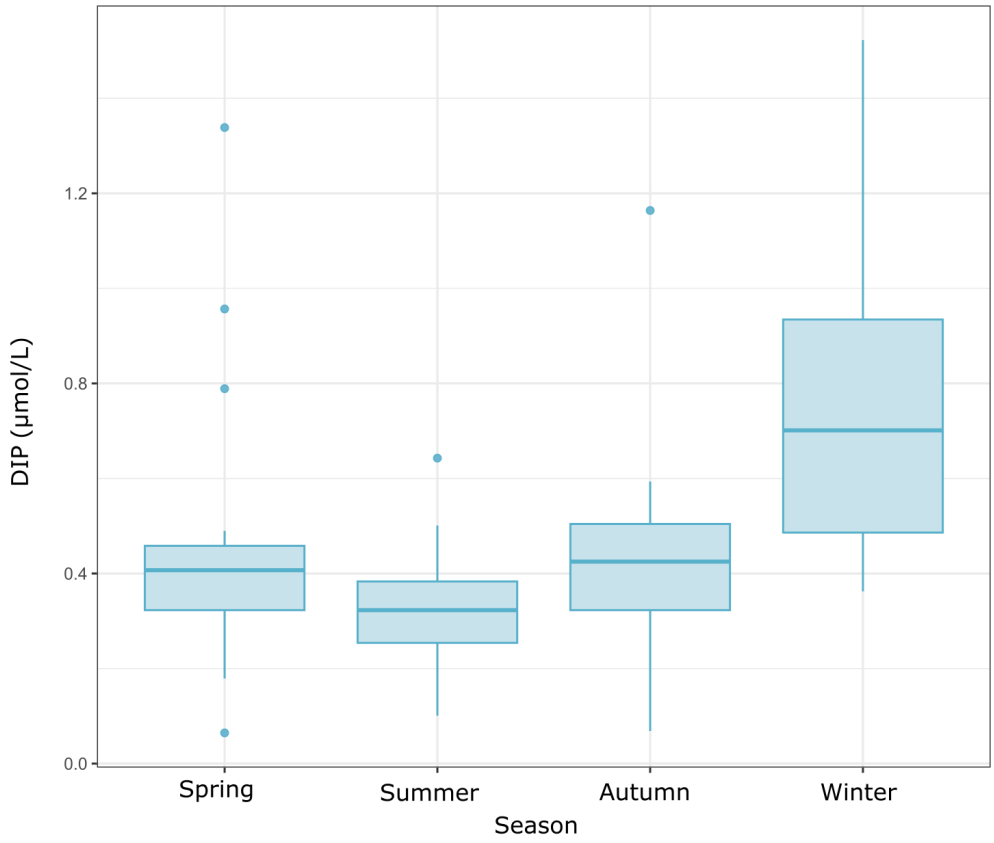


**Figure 81. Seasonal variation of Dissolved Inorganic Phosphorus (DIP) concentrations (µmol/L) across different seasons from water column data from Langstone (2000-2019) (Chapter 2). The central line in each box represents the median DIN concentration, the edges of the box indicate the interquartile range (IQR), and the vertical lines extend to the range of the data, excluding outliers, which are plotted as individual points.**

Opportunistic macroalgae species usually peak their biomass production during summer when water column nutrient concentrations are at their minimum (Trimmer et al., 200). This is the opposite pattern observed for benthic nutrient concentrations where surface DIN concentrations were higher in the summer and declined sharply by winter. This seasonal maxima in benthic nutrients, especially DIN has been previously observed in other estuarine systems with opportunistic macroalgae (Yasui et al., 2020).

### 4.5.2 Seasonal redox state

Iron concentrations on the surface during all seasons were greater on the macroalgae absent cores than on the present cores. In summer Fe was present at all depths within the absent core whereas the present core was depleted in Fe, with a peak at 4 cm depth of 125 µmol/L, by autumn the macroalgae present core had no Fe measurable on the top 10 cm of the sediment while during the winter the macroalgae present core was enriched in Fe with generally high concentrations at all depths.

Dissolved Fe within the porewaters in the macroalgae present cores had a mean minimum concentration during autumn, 65.9 µmol/L and summer had a slight increase to 98.2 µmol/L and increased significantly during winter to 331 µmol/L (Figure 70). Similarly, Mn displayed generally higher concentrations in the absent cores during all seasons. And for the present cores, concentrations were not detected during autumn and by winter Mn was present from the 7 cm depth (Figure 71). The presence of macroalgae diminished Fe concentrations in summer and autumn, while by winter Fe was present at higher concentrations downcore. Furthermore S/Na ratios showed a steeper decrease downcore in summer and autumn compared to the winter cores that present minimum variation downcore. S/Na ratios trends also suggests more oxygen penetration during the winter months.

Rozan et al. (2002) presented a schematic diagram illustrating phosphate cycling changes as redox conditions shift from anoxic in summer to more oxic in winter (Figure 82). During summer, higher DIP concentrations were observed in the upper sediment in Langstone, corresponding to phosphate release under anoxic conditions. The low iron concentrations in this season suggest the reduction of iron

oxides, which further contributes to phosphate release. The S/Na profiles showed slight increases during summer, suggesting sulfate reduction and hydrogen sulfide formation under anoxic conditions.

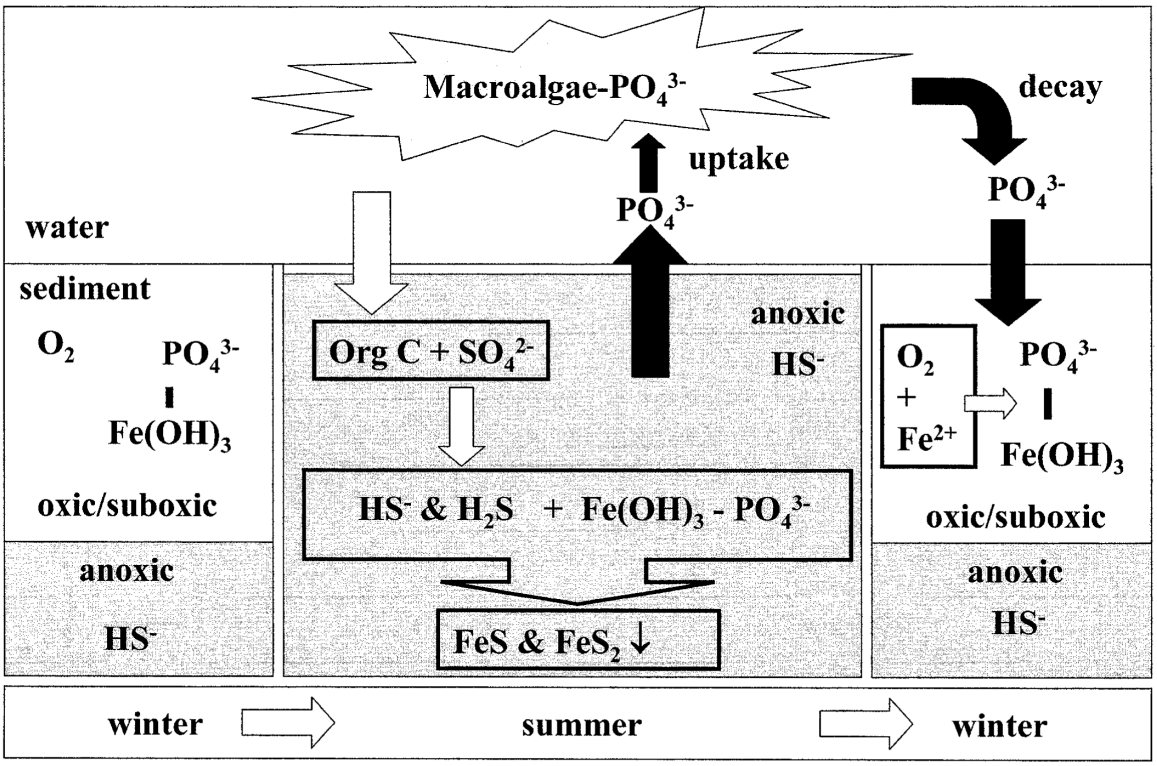


**Figure 82. Seasonal schematic of phosphate cycling (black arrows) as redox state changes with seasons in sediment. Phosphate ad Phosphate adsorbed to Fe(III) solid phases is stored in oxic and suboxic sediments in the winter and early spring (lower left), then is converted to the dissolved phase and taken up by macroalgae (with a N: P of 20) in the summer as sulfate reduction occurs in the sediments (center and top) and finally is readsorbed to and stored on Fe(III) phases as oxic conditions are reestablished in the sediments in late fall and winter (lower right) (Rozan et al., 2002).**

In contrast, Fe profiles in winter showed surface enrichment compared to other seasons, stabilizing iron oxides and preventing phosphate release. As a result, DIP profiles in winter at Langstone display increasing concentrations with depth, reflecting the more oxic conditions.

In autumn, however, the DIP and iron profiles may indicate a delayed onset of oxic conditions. This pattern could be influenced by the presence of macroalgae, as

shown by the absence of dissolved Fe in the cores where macroalgae were present, compared to the surface enrichment in cores where macroalgae were absent. Overall, the seasonal pattern observed in Langstone agrees with the results presented by Rozan et al., (2002).

Evidence presented suggest that macroalgae contributes to the extreme anoxic conditions observed and is supported when compared to other studies where macroalgae is not a factor. (Bally et al., 2004), investigated changes in porewaters biogeochemistry in an intertidal estuary and Fe and Mn concentrations significantly increased in summer, which was attributed to oxide and hydroxide reduction at the sediment-water interface.

### 4.5.3 Seasonal implications for sediment organic carbon

Organic C content in the sediment from Langstone fluctuated through the different seasons. Starting with the lowest mean organic C in summer 1.4 ± 0.2% then gradually increased with time. In autumn mean organic C was1.6 ± 0.2% and it reached 2.3 ± 0.2%. Coupled with the reduction of nutrient concentrations observed in winter. This increase is probably due to the slower remineralisation rates as temperature decreased, coupled with the still active macroalgae production in winter. Lower temperatures have been shown to reduce microbial activity (Kristensen & Hansen, 1995) and decrease benthic fauna bioturbation (Lopez & Levinton, 1987) processes that can favour organic C preservation.

Whether this excess accumulation will be easily remineralised by spring, is still unclear. However, it is possible that as other factors such as an increase in bacterial and benthic fauna activity as temperatures rise will decrease the organic C content in winter.

Trimmer et al. (2000), reported sediment organic carbon for Langstone and Chichester harbours along the different seasons in 1995. Samples were taken in 5 intertidal sites in Langstone all with different levels of macroalgal impact (*Enteromorpha* and *Ulva*). Results were available for 0-1 and 4-5 cm depth. These results were compared to the ones measured in this study for the same depths available for Langstone in summer, autumn, and winter. Presence and absence of macroalgae cores were included. The seasonal pattern identified previously, where

organic carbon increasing within the colder months was not found in (Trimmer et al., 2000).

Results showed significantly more organic carbon (Kruskal-Wallis, $p<0.001$) in the more recent results from 2021-2022 than those in Trimmer et al. (2000) (Figure 83).

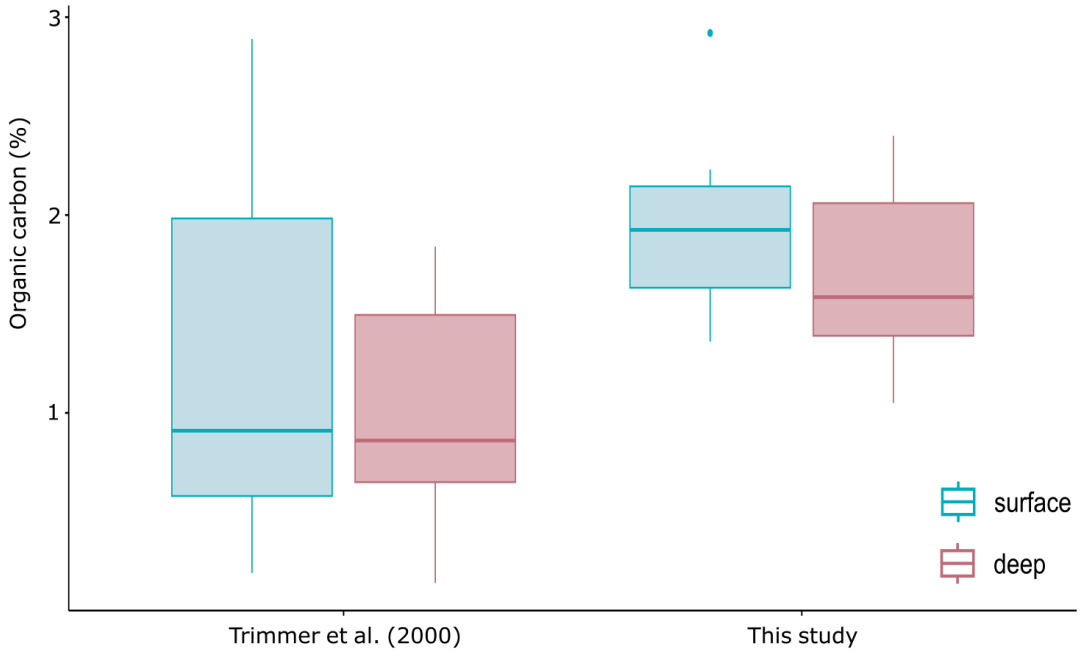


**Figure 83. Box plot showing mean and standard deviation comparison in sediment organic carbon from Langstone Harbour. Blue boxes represent surface sediment 0-1 cm and red boxes represent 4-5 cm depth sediment. Data comparisson from Trimmer et al. (2000) and this study.**

Although there could be other factors influencing these differences in sediment organic C such as spatial variability, macroalgae impact and other external sources of organic C, this comparison provides a good representation of the current state of Langstone Harbour after almost 30-year difference. Whether the origin of the organic carbon in Langstone is a result of an increase in primary productivity or other land-derived sources will be explored in Chapter 5.

### 4.5.4 C:N ratios

C:N ratios are traditionally believed to be conservative in sediments and consequently reflect the relative contribution of different end members to the sediment mixture (Thornton and McManus, 1993). Based on this, C:N ratios could suggest the origin of the organic material within a sediment complex mixture, however the transformations and degradation of organic matter as sediment depth increases modifies C:N ratios and complicates its use to predict organic C provenance (Lamb et al., 2016).

Values in the range 5-8 are typically linked to algae derived organic carbon while higher values between 25-35 are associated with unaltered vascular plants derived material (Emerson & Hedges, 1988; Hedges et al., 1986). C:N ratios reported here for Langstone during summer and autumn are consistent with other marine derived material 7-10 (Cowie et al., 2009; Trimmer et al., 2000). Nonetheless, significantly lower ratios observed in winter (mean= 4.2) could suggest more algal/phytoplankton-derived material, this due to the abundance of proteins and absence of cellulose in marine algae (Meyers, 1997).

This seasonal lowering of C:N ratios in winter has been observed in the Pearl River estuary in China, where a mean value of 7.1 ± 0.9 from particulate organic carbon was observed and attributed to phytoplankton origin (Yu et al., 2010). However, Yu et al., (2010) did not present winter data for sediment organic C. Trimmer et al., (2000) presented seasonal data for sedimentary C:N and organic C from Langstone and Chichester Harbours, C:N ratios reported were generally more variable

seasonally and with depth, a pattern not observed within this study were C:N. ratios were more uniformly distributed downcore (Except for a sharp increase in a macroalgae present core at 9cm depth in summer (Figure 78)).

The contribution of terrestrial organic matter, particularly during winter, is also possible due to increased freshwater runoff and stormwater inputs, which can carry organic materials from land into coastal systems (Rabalais et al., 2002). However, this seem not to be the case in Langstone where low winter C:N ratios from are indicative of marine-derived organic C even though phytoplankton and macroalgae blooms are more likely to develop during summer (Section 1.2.4). It is likely that a combination of processes in Langstone favour preservation of marine origin in winter.

# 4.6 Conclusions

Langstone Harbour has a long history with eutrophication and opportunistic macroalgae mats that can be tracked back to the early 1980's. Seasonality is an important factor influencing the sediment biogeochemistry in Langstone Harbour, as evidenced by the clear seasonal variations observed in this chapter. Additionally, the presence of macroalgal biomass at the site contributed to unique conditions that further altered sediment biogeochemistry, highlighting the important role of macroalgae in shaping nutrient cycling and organic C dynamics in the sediment.

Within pore waters nutrients, total dissolved nitrogen was one of the most variable between seasons and presence or absence of algae. Ammonium was the major component of the dissolved nitrogen pool within the sediment in all seasons, with a decrease in winter where more oxidized forms of N were observed.

Redox conditions were sensible to seasonal changes for example, dissolved metals profiles alongside the increase in NOx concentrations in winter reflected more oxic conditions in this season compared to more anoxic/suboxic in summer and autumn.

Macroalgae presence appears to reduce iron and manganese concentrations in summer and autumn due to the creation of anoxic conditions, as evidenced by the lower concentrations in the macroalgae-present cores. However, by winter, iron concentrations increased, indicating a shift to more oxic conditions. However, more oxic conditions during winter did not translate to more remineralisation. Instead, significantly greater amounts of organic C were measured during winter compared to summer and autumn (Kruskall-Wallis $<0.001$).

Despite the potential for terrestrial organic matter input through freshwater runoff in winter, low C ratios suggest that Langstone sediments remain dominated by marine-derived organic matter throughout the year. Evidence presented in this chapter support the hypothesis of autochthonous contribution to the sediment organic C, especially during the winter were lower C:N ratios of 4.2 ± 0.4 being indicative of marine produced organic matter. This extra organic C accumulated during winter could be easily remineralised by the start of spring season as higher temperatures promote more bacterial activity and consequently remineralisation still needs to be explored.

Some historical data could suggest that the organic C is accumulating overtime in the intertidal zone of Langstone, for example when compared to organic C data from Trimmer et al., (2000) it is clear that there is more organic C sediment being stored within Langstone sediments. However, more evidence would be required to be certain that some of the organic C remains within the sediment on the next seasonal cycle. Additionally, there is the need to identify the provenance of this autochthonous material deposited during winter, and more in-depth analysis of the possibility for macroalgae derived C to be responsible for this increase, from the available evidence no other study has reported this accumulation of organic C on a seasonal basis.

This chapter explores the impact of seasonality on sediment biogeochemistry in Langstone Harbour across summer, autumn, and winter. It also explores the link between macroalgae blooms and various factors such as dissolved nutrients,

metals, redox conditions, and organic carbon, that collectively shape sediment biogeochemistry (RQ6). Furthermore, presents new evidence of seasonal accumulation of organic C during winter which can presumably be of autochthonous origin, highlighting the relevance of estuarine environments for sediment carbon storage (RQ7).

Chapter 5.

# Investigation of macroalgae derived carbon in sediment carbon stocks

## 5.1 Introduction

The present chapter explores the viability of different methods to identify macroalgae carbon in sediment. The methods utilised for this purpose are CuO oxidation products, triple bulk stable isotopes ($\delta^{13}C$, $\delta^{15}N$ and $\delta^{2}H$), and elemental analysis. The sites evaluated in this work include the three estuaries from the UK from Chapter 3, and samples from the Baltic Sea to compare different macroalgae groups (Green and brown). Key research questions for this chapter include:

**RQ9:** To what extent is it possible to identify macroalgae derived as a source of organic carbon in sediment carbon stocks with the proposed methods?

**RQ10:** Are there particular CuO oxidation products characteristic of green macroalgae that can potentially be used as biomarkers to track macroalgae carbon in intertidal sediments?

**RQ11:** Are there differences in discrimination by these methods between different groups of macroalgae?

# 5.2 Background

## 5.2.1 Macroalgal carbon in marine sediments

Carbon storage in the ocean has gained major attention within the research community in recent years, especially in blue carbon areas, in response to ongoing climate change. Blue carbon ecosystems are defined as vegetated coastal areas where significant amounts of organic carbon are stored within their biomass and sediment below (Nellemann, et al., 2009). Therefore, angiosperm macrophytes such as seagrass, mangroves and saltmarshes are better understood ecosystems in terms of organic carbon content (Fourqurean et al., 2012; Lima et al., 2020; Kindeberg et al., 2018; Kennedy et al., 2010; Sanders et al., 2014). More recently however, there is growing recognition that macroalgae are could also be an important setting for blue carbon storage (Hill et al., 2015; Hardison 2010; Krause-Jensen et al., 2018; Raven et al., 2018)

Macroalgae is recognized to be the most abundant and productive among the benthic marine primary producers (Hill et al., 2015; Krause-Jensen & Duarte, 2016). While macroalgae production and its causes have been widely studied, little is known about the fate of this production, and its role in long term marine carbon storage is currently a topic of scientific debate. Unlike angiosperm macrophytes, most macroalgae species grow attached to a hard substrate or free floating (Luning, 1990), without the possibility to directly transfer organic carbon to the sediments via their roots.

Coastal unvegetated areas (non-angiosperm dominated), are believed to act as sources of organic C within the cycling. This is mainly because although presenting higher productivity rates by a variety of primary producers, including macroalgae, microalgae and microphytobenthos; the lack of structural complexity of their cell walls and thus, higher decomposition rates make them more easily remineralised and therefore it is less likely that the organic C is stored for long-term in the underlying sediment (Hill et al., 2015).

In a comprehensive review Hill et al. (2015), concluded that despite the inefficiency of macroalgae dominated areas to store carbon long-term, macroalgal detritus plays an important role in blue carbon by acting as carbon donors to depositional areas where organic carbon can be sequestered for longer timescales. They propose three possible fates for macroalgal derived carbon: 1) Particulate and dissolved C is stored for prolonged periods until it is either 2) Assimilated by microbial biomass or 3) Respired as $DCO_2$ back to the water column and possibly the atmosphere.

It is also recognised that there is insufficient evidence to neglect macroalgae contribution within production areas (Hill et al., 2015). Specially in drifting algal mats, where conditions influencing the amount and quality of the organic C introduced to the sedimentary pool. More recently, it has been discussed the possibility of macroalgae derivate organic carbon to contribute to the blue carbon stocks, this contribution is mainly believed to occur as macroalgae is fragmented and exported from the production site to some sites like continental margins where organic C can be sequestered and stored for longer time scales (Krause-Jensen & Duarte, 2016).

Although it can be exported, C donors it has been assumed that macroalgae biomass can simply not contribute significantly to carbon storage in the production sites because this biomass is not attached to the sediments via roots as it is the case for other marine macrophytes like seagrasses or mangroves, and the algal detritus is rapidly consumed by benthic organisms and bacteria.

Corzo et al (2009), found that mean annual sediment content of C and N increased for sediment covered in opportunistic green macroalgae. The presence of macroalgae influenced oxygen penetration which translated to a lower aerobic respiration rate compared to bare sediment even with relatively low biomass. These findings suggest that anaerobic conditions occurring below macroalgae mats can contribute to the preservation of some of the macroalgal production.

In order for organic carbon to “escape” remineralisation certain conditions need to be met. First, anoxic conditions within the sediments are necessary because this reduces the oxidation rate of the organic carbon. Depending on the extent, and biomass present on top of these sediments this condition is achievable where thick macroalgae mats prevent the oxygen to penetrate as it occurs as a consequence of eutrophication. Another condition is that burial rates must be high so the freshly produced organic carbon can be trapped in the sediments.

Macroalgae carbon storage has been previously detected in the marine environment, however there are few studies reporting presence of macroalgae in marine sediments. Of all the reported studies, only 10% of them were in coastal areas (water depth below 10 m), and more than 60% in the deep sea (>1000 m)

(Krausen-Jensen and Duarte, 2016). Although macroalgae presence in marine sediment has been reported in the scientific literature, evidence is still scarce, especially in coastal environments where sources of the organic carbon contributing to the sedimentary organic carbon pool are diverse. Methods for this detection varied from isotope signatures, observation of macroalgae fragments in these sediments, algal fragments in sediment cores, lipids and sterols analysis.

## 5.2.2 Methods to detect macroalgal carbon in marine sediments.

### 5.2.2.1 CuO oxidation products

The CuO oxidation method produces derivatives of organic molecules by reaction in the presence of CuO and in the absence of oxygen. The method was originally used for lignin characterisation in plant tissues (Pearl & Dickey, 1952; Prahl et al., 1994). Thirty years later, Hedges & Ertel (1982), adapted this method for use in environmental samples including soil and sediment. Then, (Goni & Hedges, 1995) used this method in the context of fingerprinting different organic carbon sources in marine sediments, including primary producers like bacteria, phytoplankton and macroalgae.

However, it wasn't until recent years, that macroalgal derived carbon started to gain interest in the scientific community again (Geraldi et al., 2019; Krause-Jensen et al., 2018a, 2018b; Krause-Jensen & Duarte, 2016). This due to the increasing interest in the study of blue carbon. It has been suggested that macroalgae carbon could be prevalent from coastal areas to the deep sea. Nonetheless, the great majority of

studies that have reported presence of macroalgae in marine sediments are from the deep sea (Krause-Jensen & Duarte, 2016).

### 5.2.2.2 Bulk stable isotopes

Isotopes are atoms from the same element whose nuclei is formed by the same number of protons is the same but a different number of neutrons. Stable isotopes are naturally present in the environment and most of the elements of interest in geochemistry such as C, H, O, N, P and S have at least two stable isotopes (Hoefs, 1980). Stable isotopes are commonly expressed as delta (δ) values, δ values are the difference in the ratio of a rarer (usually heavier) isotope to the more common isotope, between a sample and a reference material. Using C as an example, the equation used for calculating isotope δ values was defined by McKinney et al. (1950) as follows:

$$\delta C^{13} = \frac{(C^{13}/C^{12})_{sample} - (C^{13}/C^{12})_{standard}}{(C^{13}/C^{12})_{standard}} \times 1000$$

Stable isotope geochemistry is widely used to express isotopic composition in delta values. Carbon and Nitrogen isotopic compositions has been used to study different resources entering food webs in both fresh (Cole et al., 2011; Gudasz et al., 2017) (Cloern et al., 2002) by analysing animal tissue and food sources. In addition, isotopes can also differentiate between marine and terrestrial organic carbon that is deposited in marine sediments (Tan & Strain, 1979; Zetsche et al., 2011). This can be achieved as $\delta^{13}C$ and $\delta^{15}N$ values are distinct for marine and terrestrial sources.

For example, $\delta^{13}C$ values for marine autochthonous organic carbon generally ranges from -24‰ to -18‰ (Zetsche et al., 2011) while terrestrial C3 material is characterised for more depleted values -32‰ to -21‰ (Deines, 1980). Nonetheless, results of a single stable isotope not enough to identify particular sources. This becomes particularly difficult in coastal environments (Xia et al., 2019) where multiple sources contribute to the sediment organic carbon.

C:N ratios have been utilised alongside $\delta^{13}C$ to evaluate the fate of terrestrial organic carbon in coastal and marine sediments (Hedges & Parker, 1976; Tan & Strain, 1979). Given the chemical composition of terrestrial plants with depleted nitrogen and predominantly lignin and cellulose content, significantly higher C:N ratios are observed for terrestrial organic carbon. C:N ratios as high as 35 have been reported for land-derived organic carbon whereas pure marine algae range between 5-8 (Hamilton & Hedges, 1988).

Organic matter remineralisation within the sediment could influence $\delta^{13}C$ and C:N thus using them in isolation can lead to ambiguous results specially in coastal areas (Lamb et al., 2006). Incorporation of $\delta^{13}C$ and $\delta^{15}N$ stable isotopes with C:N ratios have been previously used to increase preciseness in distinguish organic carbon provenance (Middelburg & Herman, 2007). However, complications arise when trying to identify different autochthonous sources.

Hondula et al. (2014), evaluated the use previously published isotopic ratios of $\delta^{2}H$ of a variety of primary producers from fresh and marine environments, including

phytoplankton, benthic microalgae, macrophytes, macroalgae and terrestrial vegetation. Finding significant differences between terrestrial vegetation and macrophytes. Similar results were found for the samples of primary producers from the Red Sea, where macroalgae and seagrasses values of $\delta^{13}C$ and $\delta^{15}N$ overlapped but $\delta^{2}H$ was distinctive between sources. Seagrasses $\delta^{2}H$ averaged -56.6 +/-2.8‰ and macroalgae -97.7 +/- 3.4‰ (Duarte et al., 2018), highlighting this promising addition for food web studies and less investigated contribution of different autochthonous sources in sediment organic carbon.

The use of bulk $\delta^{2}H$ to discriminate between different primary producers is a promising tool for the investigation of the autochthonous organic carbon provenance in the marine environment. However, complications arise when measuring $\delta^{2}H$ in bulk sediment samples due to nature of the mixture, which includes H linked to organic carbon and mineral H (Geraldi et al., 2019; Gudasz et al., 2017). To overcome this, demineralisation of sediment and soil samples prior $\delta^{2}H$ analyses has been successfully used for measuring bulk $\delta^{2}H$ without significant loses of organic carbon (Ruppenthal et al., 2013).

### 5.2.2.3 Environmental DNA

Environmental DNA analyses (eDNA) refers to the DNA that can be extracted from environmental samples such as sediment, soil, water, and air with no target organism (Taberlet et al., 2012). eDNA analyses have been widely used for microbial diversity studies and had become a popular tool in monitoring invasive and endangered species (Pawlowski et al., 2020).

eDNA has been identified as a powerful tool for identifying and quantify primary producers contributing to the marine sedimentary organic carbon pool (Geraldi et al., 2019). Ortega et al., (2020) evaluated mangrove and seagrasses sediment samples from the Red Sea looking for macroalgal contribution to the organic carbon pool. Macroalgae represented 33% of the marine macrophytes within the eDNA reads of coastal sediments, *Rhodophyta* (red algae) was the major contributor with 64.5%, followed by *Phaeophycean* (Brown algae) 19.1% and *Chlorophyta* (Green algae) 16.3%. Furthermore, macroalgae DNA has been detected in the open ocean (Ortega et al., 2019), highlighting the importance of these macrophytes for organic carbon sequestration.

# 5.3 Methods

## 5.3.1 Sampling Gulf of Finland

Some of the sediment and macroalgae samples included in this chapter were collected from a field campaign in the Gulf of Finland (Northern Baltic Sea) in 2021. Sediment cores, suspended matter, porewaters and sedimenting material was collected from 3 different sites within distance of a *Fucus vesiculosus* canopy (Figure 84). Fieldwork was conducted on the *Augusta* research vessel from the Tvärmine Zoological Station (University of Helsinki) from the 30$^{st}$ of August to 3$^{rd}$ of September 2021.

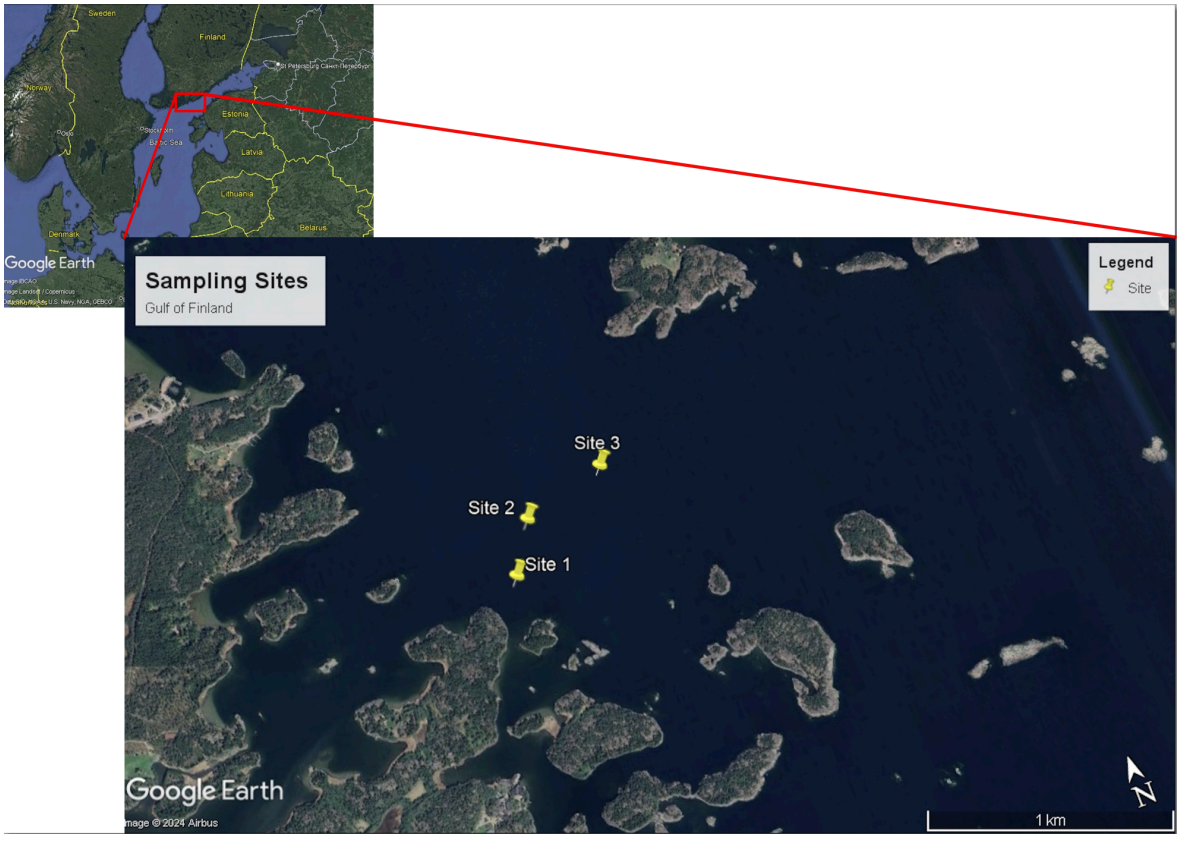


**Figure 84. Map showing the sampling sites in the northern Baltic Sea. Site 1 being the one with most proximity to the *Fucus vesiculosus* canopy and site 3 is the furthest site.**

10 cm diameter and 30 cm long sediment cores were collected one per site and processed on deck. Sediment was sectioned using a core extruder, acrylic rings (1 and 2 cm) and an acrylic slicer, sediment was sectioned in 1 cm resolution for the top 10 cm and 2 cm resolution for the remaining length of the cores and placed into sterile pre labelled sampling bags. Once sliced, sediment samples were stored frozen at -20°C in Tvärmine Zoological Station until freeze dried and sent to Leeds for analyses. Subsamples for CuO oxidation products and isotopes analyses were also separated.

An extra sediment core from each site was retrieved for porewaters extraction. Porewaters were recovered using rhizons attached to 10 mL syringes at 2cm resolution including overlying water. Porewater samples were stored frozen in Tvärmine Zoological Station at -20°C and transported to Leeds (Still frozen) for nutrient analysis.

For suspended material, glass fibre filters were placed in a muffle furnace for combustion at 500°C for 4 hours to remove any organic material, after that weights were recorded for each filter prior filtering sea water. An approximate volume of 2 L was filtered for each filter, having a total of nine, eight and seven filters for each site 1, 2 and 3 respectively. Once the suspended material was on the filters, they were oven dried at 80°C until constant weight. They were stored in Tvärmine Zoological Station and sent back to Leeds.

### 5.3.2 CuO oxidation

Among the southern estuaries' sediment samples, a set of 15 subsamples were selected for the CuO oxidation treatment. This subset was selected from each estuary to represent presence and absence of macroalgae on the sediment surface, as well as surface and deep sediment. Sediment sub samples from 0-0.5 cm depth were selected as surface and 9-10 cm for deep. In the case of Poole Harbour an extra sample was analysed in a macroalgae present core at 4-5 cm, due to an organic carbon peak detected in the sediment profile at that depth (Section 3.4.3).

Previously freeze dried and ground sediment and algae were processed for CuO oxidation as described in (Kaiser & Benner, 2012). Sample and reagents were weighed in glass vials as follows, 1g of sediment sample, 0.1 g of Ammonium Iron (II) sulphate and 1g of Cu oxide. In an inert atmosphere glove box (Ar), the sample reagent mix was transferred into metal bombs and 7mL of NaOH were added. The bombs were sealed, after letting the oxygen being replaced by Ar. The bombs were placed into an oven for 3 hours at 155 °C and were constantly mixed through being mounted on a vertical rotating disk.

Once the bombs were cooled, cinnamic acid and ethylvanillin were added as internal standards For Batch 1 CINACID: 15.3 µg, EVAN: 4.08 µg; Batch 2 Langstone: 30.6 µg, EVAN: 8.16 µg; Batch 2 Poole: CINACID: EVAN: the mix and centrifuged at 7000 rpm for 8 min, 3.5 mL of NaOH and 3.5 mL of water were added, and the samples were centrifuged again. Samples were decanted into PTFE/FEP centrifuge tubes, and samples were acidified with 6N HCl until they reached a pH of 1. After

pH adjustment, the organic material was extracted by solvent extraction in ethyl acetate.

Sodium sulphate powder was added to the liquid samples to absorb all remaining moist. Then, samples were passed through glass columns with activated silica, and oven dried for 2 hours at 50 °C. Once dried, samples were derivatized with pyridine and BSTFA prior to GC-MS analysis. Samples were analysed in Agilent 6890GC with 5973 MSD, column length 30m x 0.25mm x 0.25µm film thickness and flow rate of 1.5ml/min. The instrument was set in SCAN mode for CuO oxidation products results.

### 5.3.3 Stable isotopes analysis ($\delta^{13}C$, $\delta^{15}N$ and $\delta^{2}H$)

A total of 12 sediment samples (6 from Southern estuaries and 6 from Finland), 4 macroalgae samples (3 green macroalgae collected from southern estuaries and 1 brown macroalgae from Finland), 3 samples of particulate matter from Finland and 5 phytoplankton samples (1 Finland and 4 from Langstone).

The 25 samples of sediment, phytoplankton, particular matter and macroalgae samples were analysed by the National Environmental Isotope facility (Elementar UK Ltd, Cheadle, SK8 6PT, UK). Isotope ratio analysis was performed using a Pyrocube elemental analyser coupled to a PrecisION isotope ratio mass-spectrometer (EA-IRMS).

For $\delta^{15}N$ and $\delta^{13}C$ determination the instrument was operated in CN mode. Sample was weighed into a tin capsule before combustion in the elemental analyser, with

resultant $N_2$ and $CO_2$ separated via a GC column and passed to the IRMS for measurement. Data was normalised using traceable Sucrose and Glutamic acid standards ($\delta^{13}C$). IAEA-N1 and IAEA-N2 ($\delta^{15}N$). $\delta^{15}N$ data is expressed in as the ratio $^{15}N/^{14}N$ in ‰ relative to air. $\delta^{13}C$ data is expressed in as the ratio $^{13}C/^{12}C$ in ‰ relative to PDB (Pee Dee Belemnite).

$H_2$ was analysed for $\delta^2H$ was analysed using the same instrument but in pyrolysis mode. $\delta^2H$ is expressed the ratio $^2H/^1H$ in ‰ relative to VSMOW (Vienna Standard Mean Ocean Water).

### 5.3.3.1 Sediment demineralisation prior $\delta^2H$ analyses

Demineralisation of sediment was carried out to eliminate the mineral fraction of the samples. 50 mg of sediment was weighed into 50 mL centrifuge tubes, 4 mL of the demineralisation reagent (HF 20% vol). The tubes with sediment and reagent mixture were centrifuged overnight (~14h) at 3000G. Solids were resuspended in 4 mL of 0.1 M HCl centrifuged and decanted three times, followed by resuspension in deionised water.

SPE Bond Elut PPL cartidges (5 mL) were preconditioned with acetone and methanol (1 volume each), followed by one cartridge volume of 0.1 HCl. The eluted solubilised organic matter solution was recombined with the solid and oven dry at 40°C.

### 5.3.3.2 Data analysis

Analysis of the CuO oxidation products data was carried out in OpenChrom, open-source software for chromatographic data (Wenig & Odermatt, 2010). The first step was to import the chromatograms into OpenChrom, files were read in .D format, once imported, the “Base line detector” function was applied followed by the “Baseline subtract filter”. By following these steps, the baseline was fixed to avoid over estimation of the abundance of the peaks. In order for OpenChrom to be able to recognize the peaks, the peak detector>first derivative function was applied to the chromatograms. After the peaks identification, the irrelevant peaks with minimal abundance were discarded. Following the removal of peaks with minimal abundance, peak areas were calculated using the peak integrator>peak integrator trapezoid and subsequently the peak scan table was exported to excel to have scan list with information about peak areas and retention time.

To determine whether the CuO oxidation products (knowns and unknowns), present in the macroalgae were equally detectable in the sediments, five major ions were recorded from the m/z chart for each relevant peak. These numbers were recorded from left to right from highest abundance to the less abundant ion in a new spreadsheet. After having all the ions, a column was created for combining the cells using =CONCAT function in excel, to have a single number that represented each CuO product for every sample.

Major ions codes were exported to R and by using the intersect function data sets were tested for common values. Each macroalgae dataset was tested for common

compounds against other macroalgae samples and sediment samples and if identical values were found each test generated a new data set with these common values. Finally, the generated common compounds of every interaction were used to identify these peaks in the chromatograms that were subsequently categorised as relevant compounds, following the identification of relevant compounds their peak areas were used for an attempt of quantitative and qualitative analysis of surface and deep sediment. Different macroalgae species of green, and brown algae species along with macroalgae collected from the sampling estuaries sites were also tested for common compounds to explore if there was either a particular compound or group of compounds distinctive for a specific macroalgae group.

The number code for each relevant CuO product was assigned taking the macroalgae from Poole Harbour as a reference as this was the sample with the highest amount of CuO oxidation products. The rest of relevant compounds from the southern estuaries green macroalgae were added at the end of the numbers sequence in order of appearance. It was assumed that compounds in common from the macroalgae samples found in the sediment samples were sourced from the macroalgae of the same site.

### 5.3.3.3 Statistical analysis

Differences of isotopic values from primary producers and sediment samples were tested using ANOVA and *Kruskall-Wallis* methods depending on the results of normality. Statistical analyses were performed using RStudio built-in functions.

#### 5.3.3.3.1 Principal Components analysis

After analysis of concentrations from the CuO oxidation products produced by the green macroalgae and sediment samples from the southern estuaries' sites. Relevant compounds were compared to those previously reported by (Goni & Hedges, 1995) using the major ions obtained from the chromatograms. Of the 22 relevant compounds initially identified, 6 of them were also found in the previous study Table 6.

Port Solent samples were excluded from this analysis as there is suspicion of relative concentrations not being accurate, although the calculations were rechecked multiple times. We suspect there was an error on labelling, however there is no way of confirming this. CuO oxidation products pattern was still presented as is representative of the distribution and abundance.

# 5.4 Results

## 5.4.1 CuO oxidation products from macroalgae samples

### 5.4.1.1 Green macroalgae from southern estuaries

A relevant compound was defined as a CuO product present in macroalgae and sediment samples from the southern estuaries, chromatograms are presented as an illustration of the number of CuO products and relative abundance to the internal standard (Cinnamic acid). A total of 79 CuO oxidation products were produced by the oxidation of the green macroalgae collected from Poole Harbour. This sample had the highest number of CuO oxidation products from all the green macroalgae samples of which 18 of them were categorized as relevant (Present in sediment samples). The most abundant compounds from Poole harbour macroalgae sample were compounds 5, 16 and 9 (Figure 85).

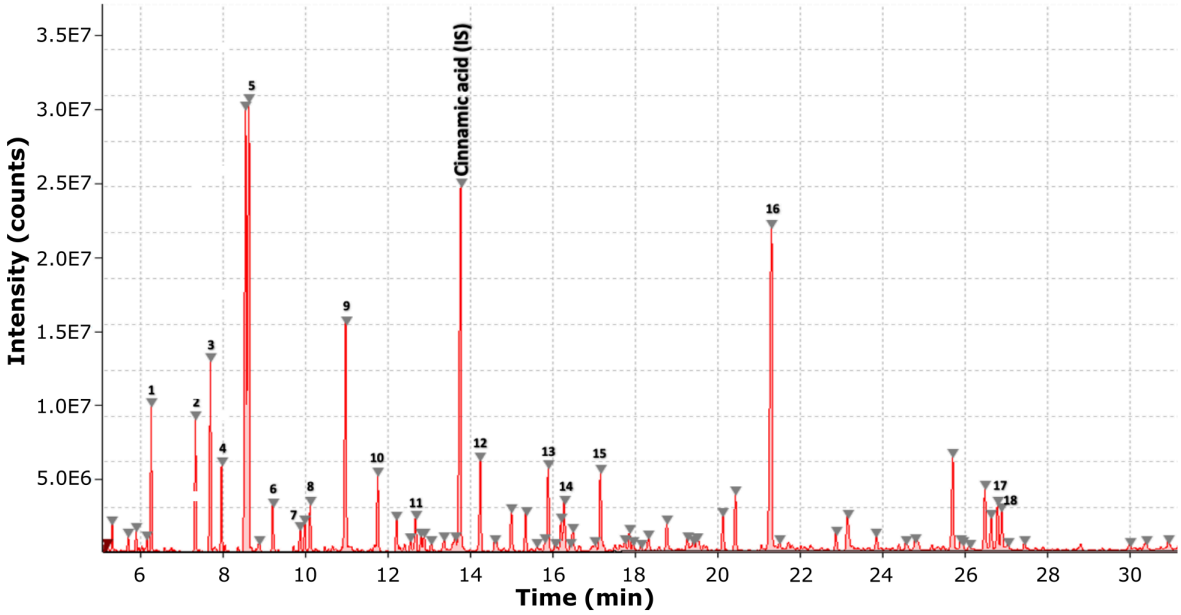


**Figure 85. Chromatogram showing relevant CuO oxidation products peaks from Poole East macroalgae compared to the internal standard. Only peaks from compounds in common with sediment samples are labelled (More information about identity of relevant compounds in Table 18).**

Langstone Harbour macroalgae had 40 CuO oxidation products, from which 9 were relevant compounds. The highest concentration for this macroalgae sample was from the internal standard cinnamic acid, then compounds 5 and 16 were the most abundant CuO oxidation products (Figure 86).

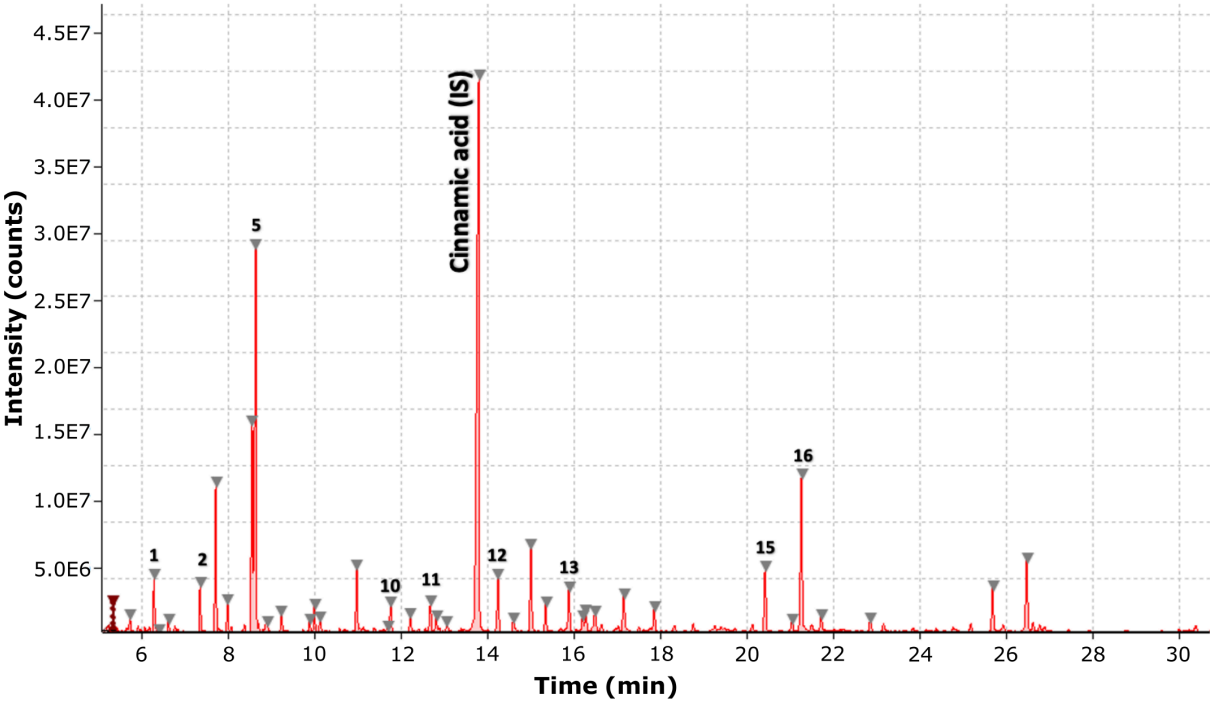


**Figure 86. Chromatogram showing relevant CuO oxidation products peaks from Langstone macroalgae compared to the internal standard. Only peaks from compounds in common with sediment samples are labelled (More information about identity of relevant compounds in Table 18).**

There were 55 CuO oxidation products from Portsmouth Port Solent macroalgae and 9 of them were relevant. Compounds 5 and 16 stood out for their higher abundance compared to the rest of the compounds. Compounds 20, 21 and 22 were added to relevant CuO oxidation products from this sample as they were unique to Port Solent macroalgae and sediment samples. Compunds 5 and 16 stood out as the most abundant in this sample as well (Figure 87).

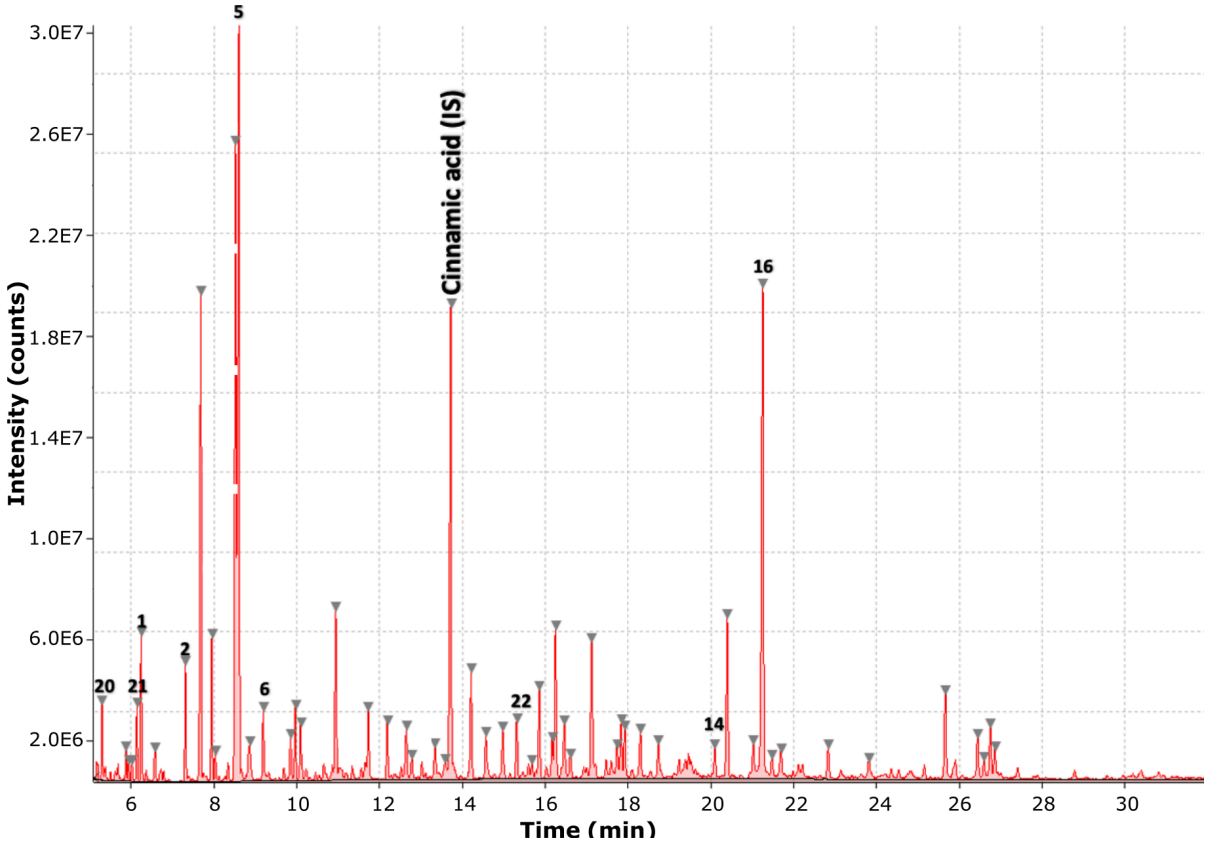


**Figure 87. Chromatogram showing relevant CuO oxidation products peaks from Portsmouth (Port Solent) macroalgae compared to the internal standard. Only peaks from compounds in common with sediment samples are labelled (More information about identity of relevant compounds in in Table 18).**

Portsmouth Grove Av macroalgae sample produced 32 CuO oxidation products in total and 8 relevant compounds. Abundance of compounds 5 and 16 were the two most abundant compounds for this sample although lower compared to other macroalgae samples (Figure 88).

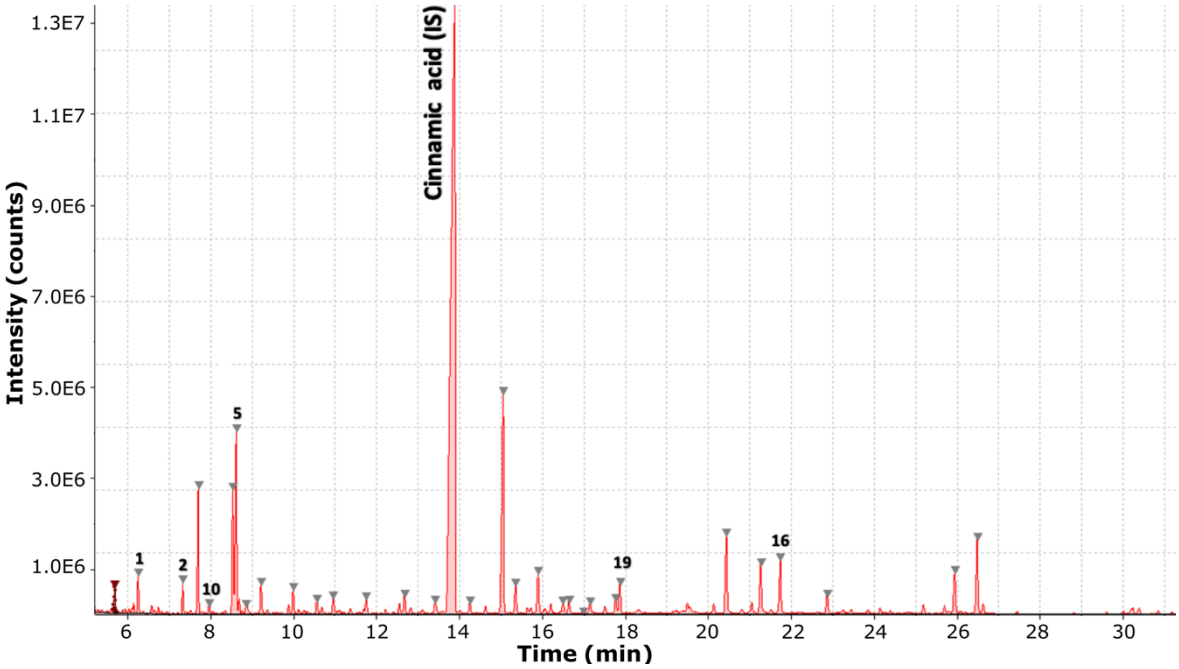


**Figure 88. Chromatogram showing relevant CuO oxidation products peaks from Portsmouth (Grove Avenue) macroalgae compared to the internal standard. Only peaks from compounds in common with sediment samples are labelled (More information about identity of relevant compounds in Table 18).**

### 5.4.1.2 Other green macroalgae

CuO products from macroalgae samples of *Enteromorpha* and *Cladophora* species were compared to determine if relevant compounds identified within green macroalgae samples from the southern estuaries where detectable in other green macroalgae species. The *Enteromorpha* sample produced 46 CuO oxidation products and 7 of them where in common with the other group of green macroalgae. Compound 8 was the highest in abundance compared to the rest of the compounds, nonetheless, compounds 5 and 16 followed and were also present in this macroalgae sample (Figure 89).

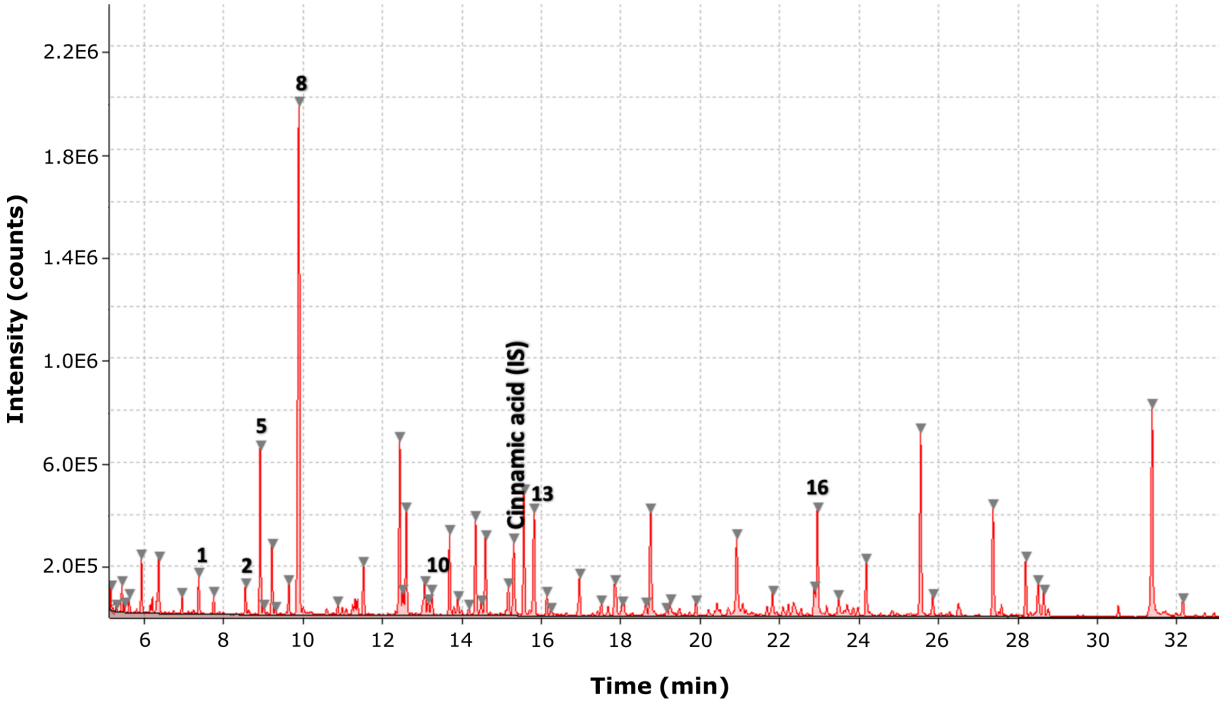


**Figure 89. Chromatogram showing relevant CuO oxidation products peaks from *Enteromorpha* macroalgae sample compared to the internal standard (Cinnamic acid). Only peaks from compounds in common with sediment samples are labelled (More information about identity of relevant compounds in Table 18).**

Green macroalgae *Cladophora* produced 57 CuO oxidation products in total of which 6 of them were identified as relevant, compounds 16 and 5 were the most abundant of the relevant compounds (Figure 90).

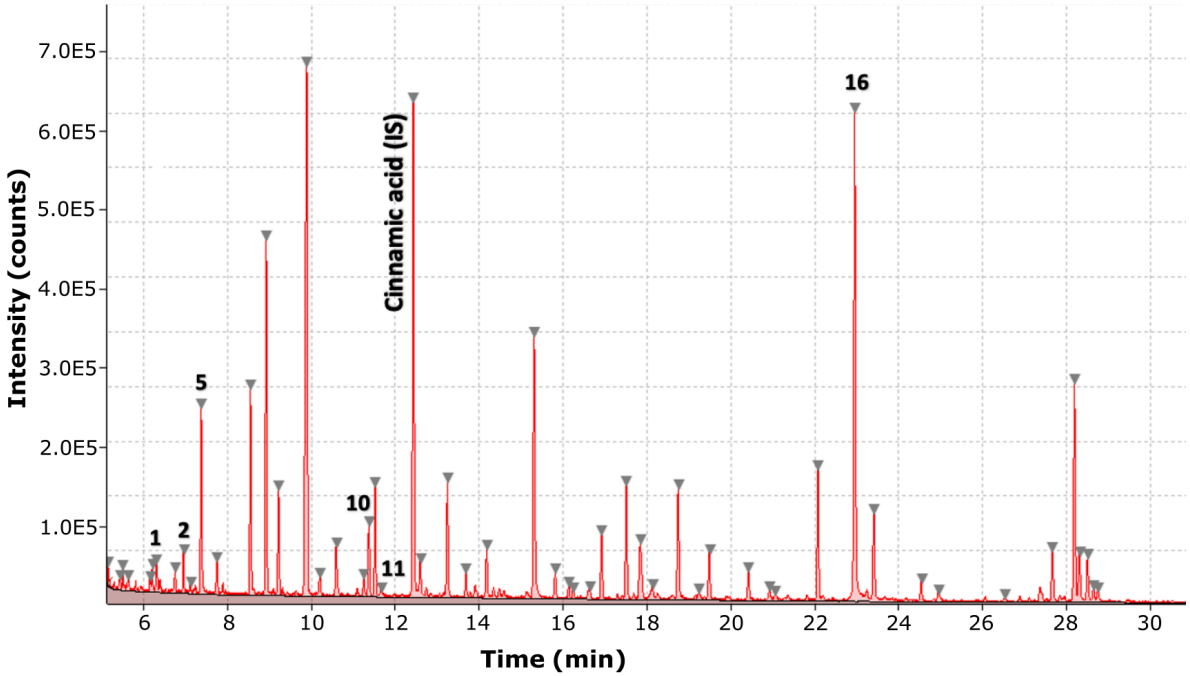


**Figure 90. Chromatogram showing relevant CuO oxidation products peaks from Cladophora macroalgae sample compared to the internal standard (Cinnamic acid). Only peaks from compounds in common with sediment samples are labelled (More information about identity of relevant compounds in Table 18).**

### 5.4.1.1 Brown macroalgae

Relevant CuO oxidation products from green macroalgae samples were compared to brown macroalgae samples to identify patterns and compounds in common between green and brown algae samples. There were four brown macroalgae samples analysed *Kelp*, *Fucus, Fucus vesiculosus* and *Dictyosiphon.* The oxidation of Kelp macroalgae produced 35 CuO oxidation products of which 6 CuO oxidation products were also relevant compounds. Most abundant compound for *Kelp* macroalgae where compound 5 and compound 14, compound 16 was also identified but its abundance was lower compared to the previously mentioned (Figure 91).

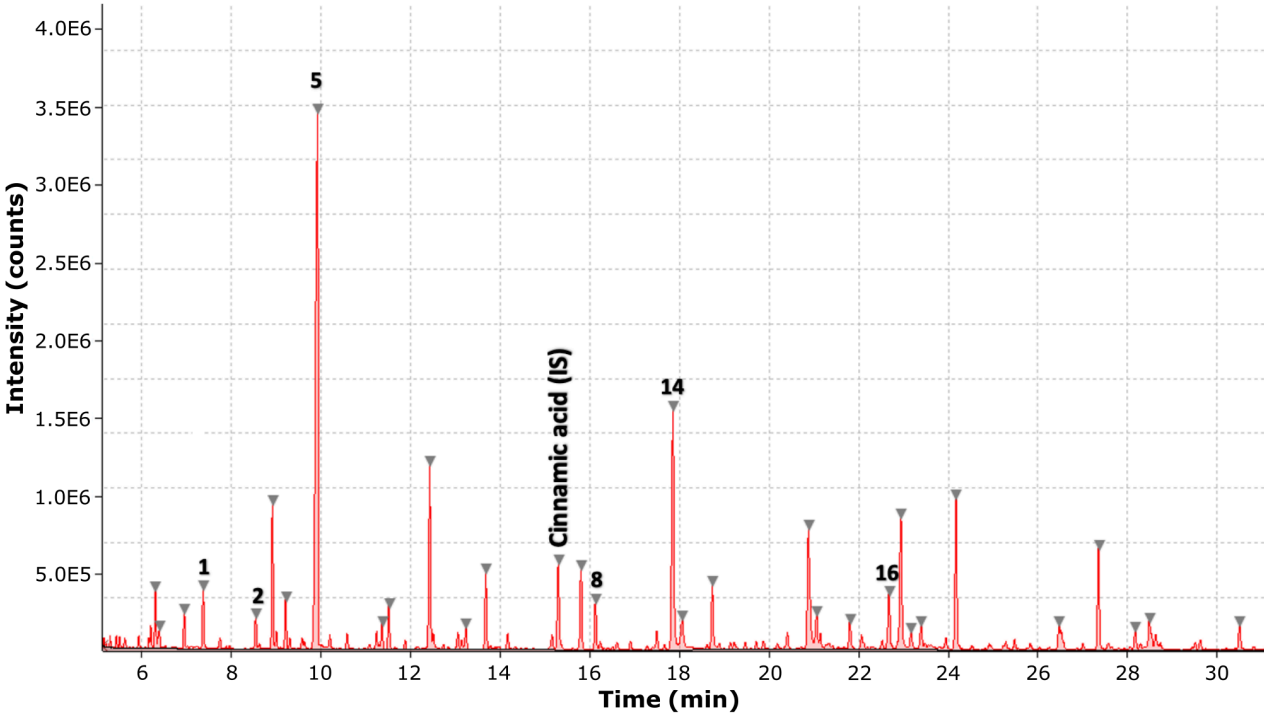


**Figure 91. Chromatogram showing relevant CuO oxidation products peaks from *Kelp* macroalgae sample compared to the internal standard (Cinnamic acid). Only peaks from compounds in common with sediment samples are labelled (More information about identity of relevant compounds in Table 18).**

*Fucus* macroalgae had 22 CuO oxidation products, 4 of them were also found to be relevant in green macroalgae samples. Compound 5 stood out as the most

abundant and compound 1 was the second most abundant, compound 16 was produced at lower abundances in this sample (Figure 92).

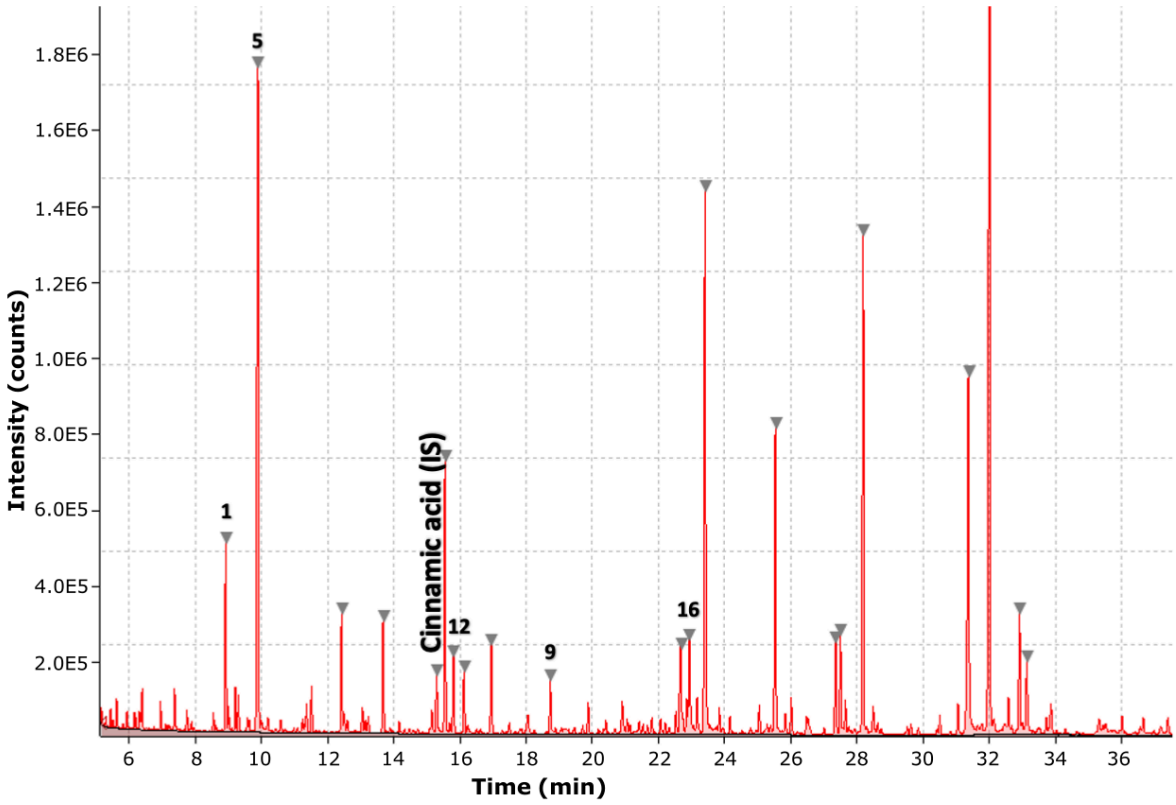


**Figure 92. Chromatogram showing relevant CuO oxidation products peaks from *Fucus* macroalgae sample compared to the internal standard (Cinnamic acid). Only peaks from compounds in common with sediment samples are labelled (More information about identity of relevant compounds in Table 18).**

*Fucus vesiculosus* macroalgae produced 28 CuO oxidation products of which 7 were in common with those relevant in green macroalgae. Most abundant compound was compound 5, while compounds 9, 14 and 16 had similar abundances (Figure 93).

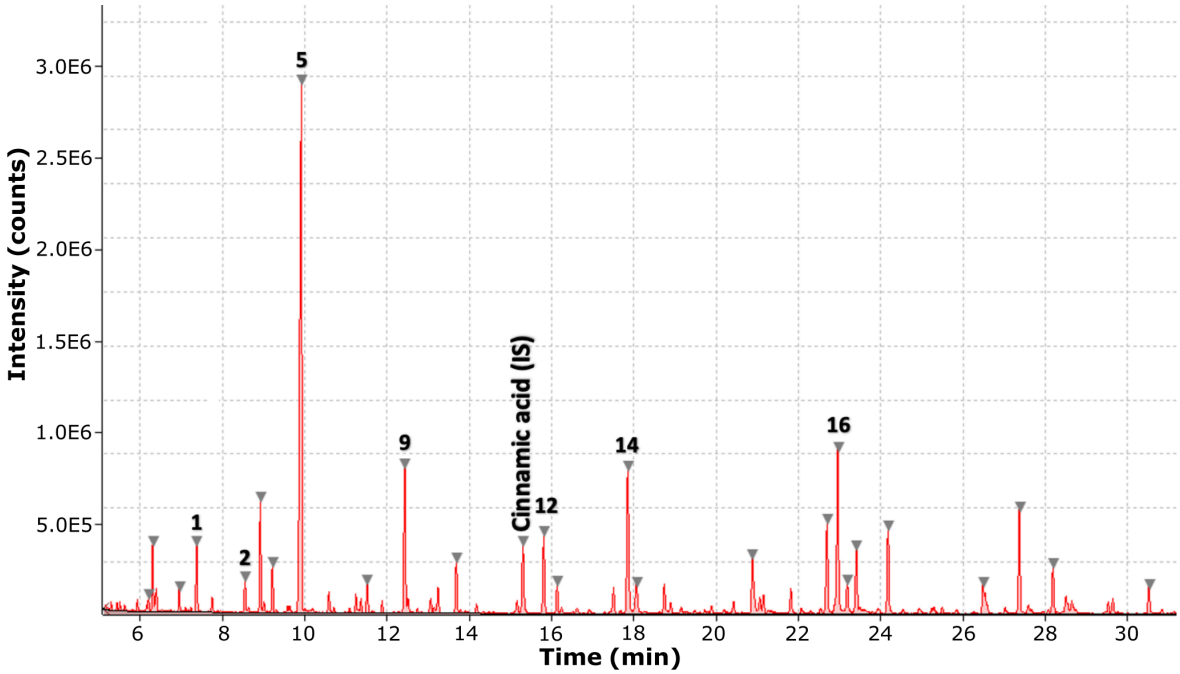


**Figure 93. Chromatogram showing relevant CuO oxidation products peaks from *Fucus vesiculosus* macroalgae sample compared to the internal standard (Cinnamic acid). Only peaks from compounds in common with sediment samples are labelled (More information about identity of relevant compounds in Table 18).**

The *Dictyosiphon* macroalgae sample had 8 relevant CuO oxidation products in common with green macroalgae samples and 32 compounds in total. Compounds 5, 9 and 13 were the most abundant compounds (Figure 94).

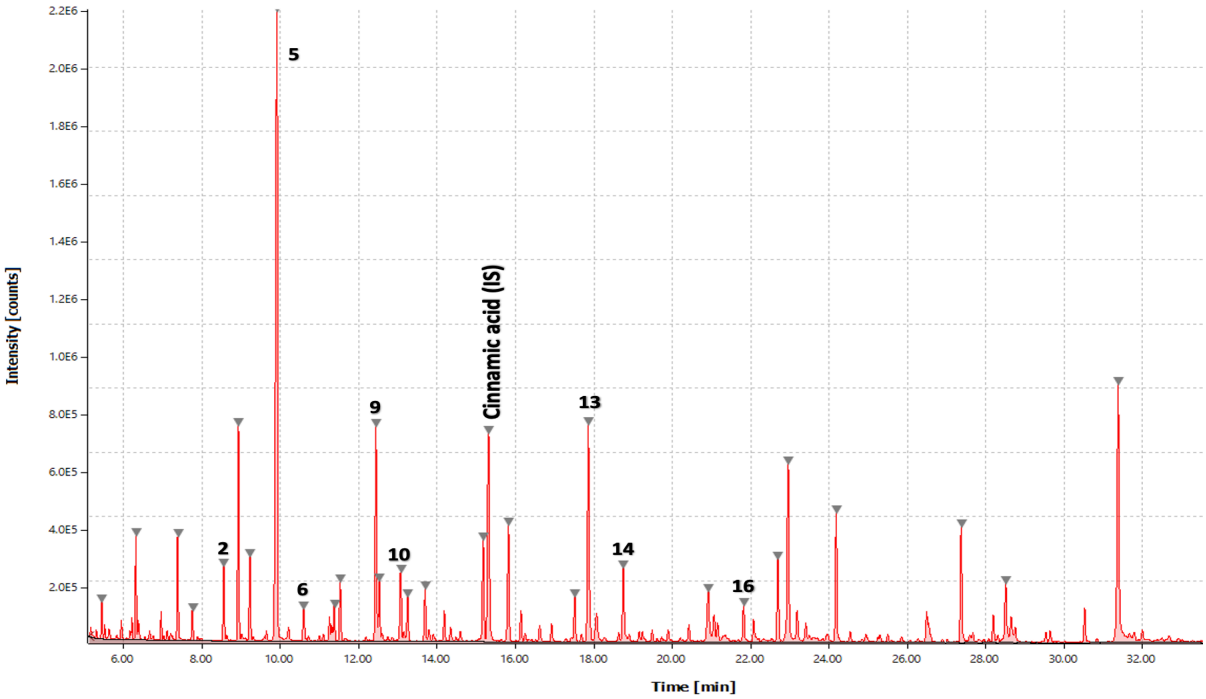


**Figure 94. Chromatogram showing relevant CuO oxidation products peaks from *Dictosyphon* macroalgae sample compared to the internal standard (Cinnamic acid). Only peaks from compounds in common with sediment samples are labelled (More information about identity of relevant compounds in Table 18).**

A total of 11 CuO oxidation products were fund in common between green and brown macroalgae samples (Table 17). Compounds 1, 5 and 16 where present in most of the samples analysed. Compound 5 was abundant in both green and brown macroalgae whereas compound 16 had higher abundance in green macroalgae samples. On the other hand, compound 9 was present in all brown macroalgae samples and only in 2 green macroalgae samples at lower levels.

**Table 17. Relevant compounds in common between green macroalgae species (Southern estuaries samples and *Enteromorpha* and *Cladophora*) and brown macroalgae species (*Kelp, Fucus, Fucus vesiculosus,* and *Dictyosiphon).* Compound identities are shown as their compound name (When available) and compound ID).**

| ID | Compound | Brown algae | Green algae | |
|---|---|---|---|---|
| | | | Southern estuaries | Green macroalgae |
| **1** | Benzoic acid trimethylsilyl ester | *Kelp*<br>*Fucus*<br>*Fucus Finland* | Langstone<br>Poole H<br>Grove Avenue<br>Port Solent | *Enteromorpha*<br>*Cladophora* |
| **2** | Benzeneacetic acid, trimethylsilyl ester | *Fucus Finland*<br>*Dictyosiphon* | Langstone<br>Poole H<br>Grove Avenue<br>Port Solent | *Enteromorpha*<br>*Cladophora* |
| **5** | 2-Butenedioic acid (E)-, bis(trimethylsilyl) ester | *Kelp*<br>*Fucus*<br>*Fucus Finland*<br>*Dictyosiphon* | Langstone<br>Poole H<br>Grove Avenue | *Enteromorpha*<br>*Cladophora* |
| **6** | Benzaldehyde, 4-[(trimethylsilyl)oxy]-trimethylsilyl ester | *Dictyosiphon* | Poole H | *Enteromorpha*<br>*Cladophora* |
| **8** | Unknown | *Kelp* | Poole H | - |
| **9** | Unknown | *Kelp*<br>*Fucus*<br>*Fucus Finland*<br>*Dictyosiphon* | Poole H | *Cladophora* |
| **10** | Acetophenone, 4'-(trimethylsiloxy) | *Dictyosiphon* | Poole H | *Enteromorpha*<br>*Cladophora* |
| **12** | Benzoic acid, 3-[(trimethylsilyl)oxy]-, trimethylsilyl ester | *Kelp*<br>*Fucus* | Langstone<br>Poole H | *Cladophora* |
| **13** | Benzoic acid, 4-[(trimethylsilyl)oxy]-, trimethylsilyl ester | *Dictyosiphon* | Langstone<br>Poole H<br>Grove Avenue<br>Port Solent | *Cladophora* |
| **14** | Unknown | *Fucus*<br>*Fucus Finland*<br>*Dictyosiphon* | Poole H<br>Port Solent | *Cladophora* |
| **16** | Unknown | *Kelp*<br>*Fucus Finland*<br>*Dictyosiphon* | Langstone<br>Poole H<br>Grove Avenue<br>Port Solent | *Enteromorpha*<br>*Cladophora* |

### 5.4.2 Relevant CuO oxidation products in southern estuaries samples

The number of compounds in common between macroalgae and sediment samples from respective sites were narrowed down to the compounds that were most frequent in sediment samples. These new group of compounds was named relevant compounds, in the case of Langstone relevant frequency was established as 66% (4/6 sediment samples) and for Poole 71% (7/7 sediment samples) of the sediment samples analysed for CuO oxidation products. Regarding Portsmouth, Port Solent and Grove Av with only 2 sediment samples each, a relevant compound was selected if present in all samples.

The oxidation of the macroalgae collected in Poole H produced a total of 79 compounds, being the site with the greater number of relevant CuO oxidation products at 18, was followed by the macroalgae from Portsmouth Port Solent that produced 55 CuO oxidation products, however relevant compounds for this site were half the amount at 9. Lastly, of the 40 CuO oxidation products produced by Langstone macroalgae only 8 were present in the sediment samples. Only the relevant compounds were considered for calculating the concentrations relative to the internal standard (Cinnamic acid).

Sediment core “A” from Poole Harbour, produced 95 CuO products in the surface sediment and 74 in deep sediment of which 6 and 7 were relevant respectively. Most abundant compound in both samples was compound 5 followed by compound 16 (Figure 95).

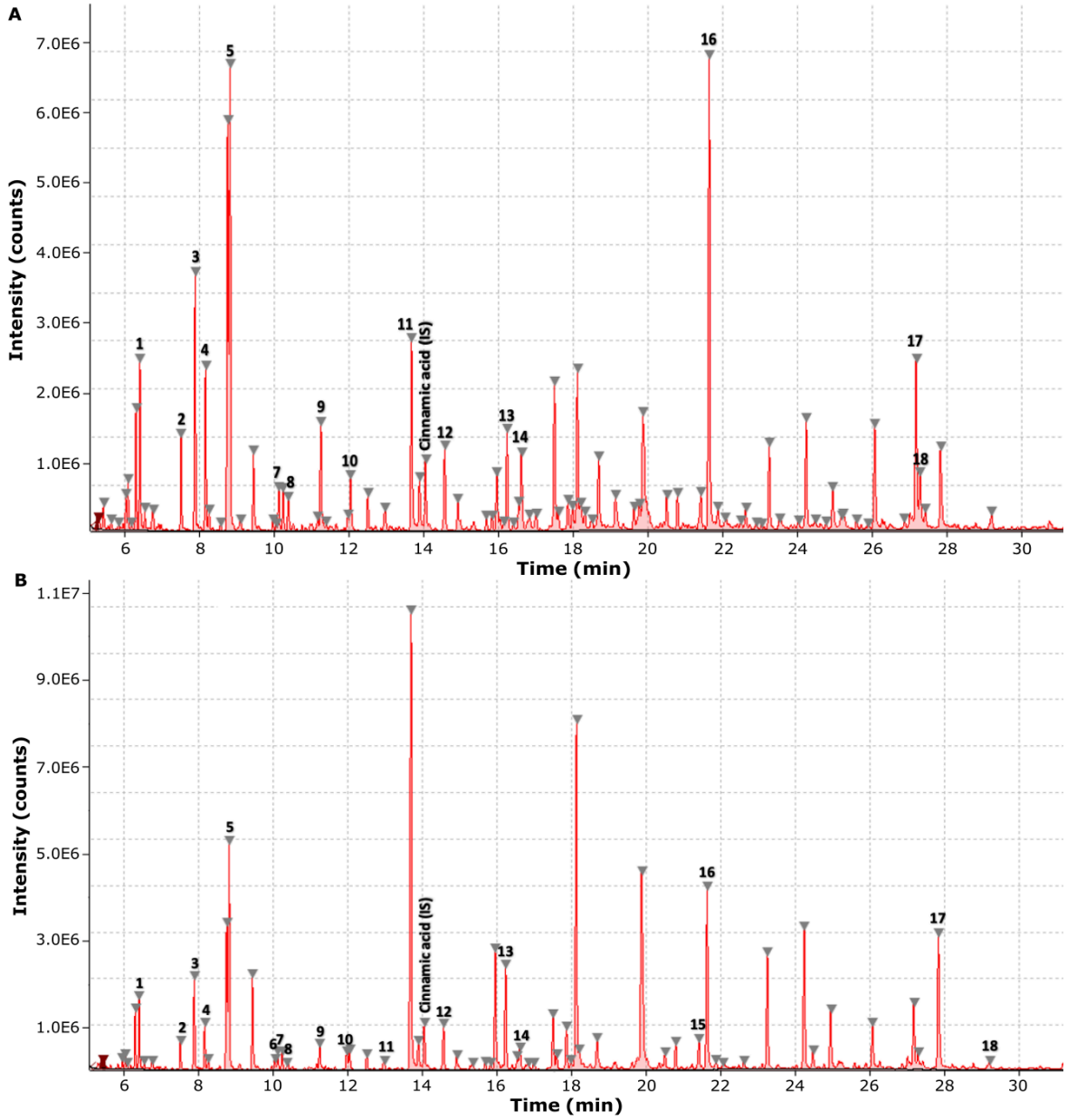


**Figure 95. Chromatograms showing relevant CuO oxidation products in sediment samples from Poole East (A. Surface (0-0.5 cm), B. Deep (9-10 cm); Core: A, macroalgae absent sediment). Only peaks from compounds in common with green macroalgae samples are labelled (More information about identity of relevant compounds in Table 18).**

Surface sediment from core “C” from Poole produced 122 CuO products whereas deep sediment produced 71 products in total. In both samples 16 compounds were relevant. In surface sediment 16 was the most abundant compound whereas in deep sediment compound 5 was more abundant than 16 (Figure 96).

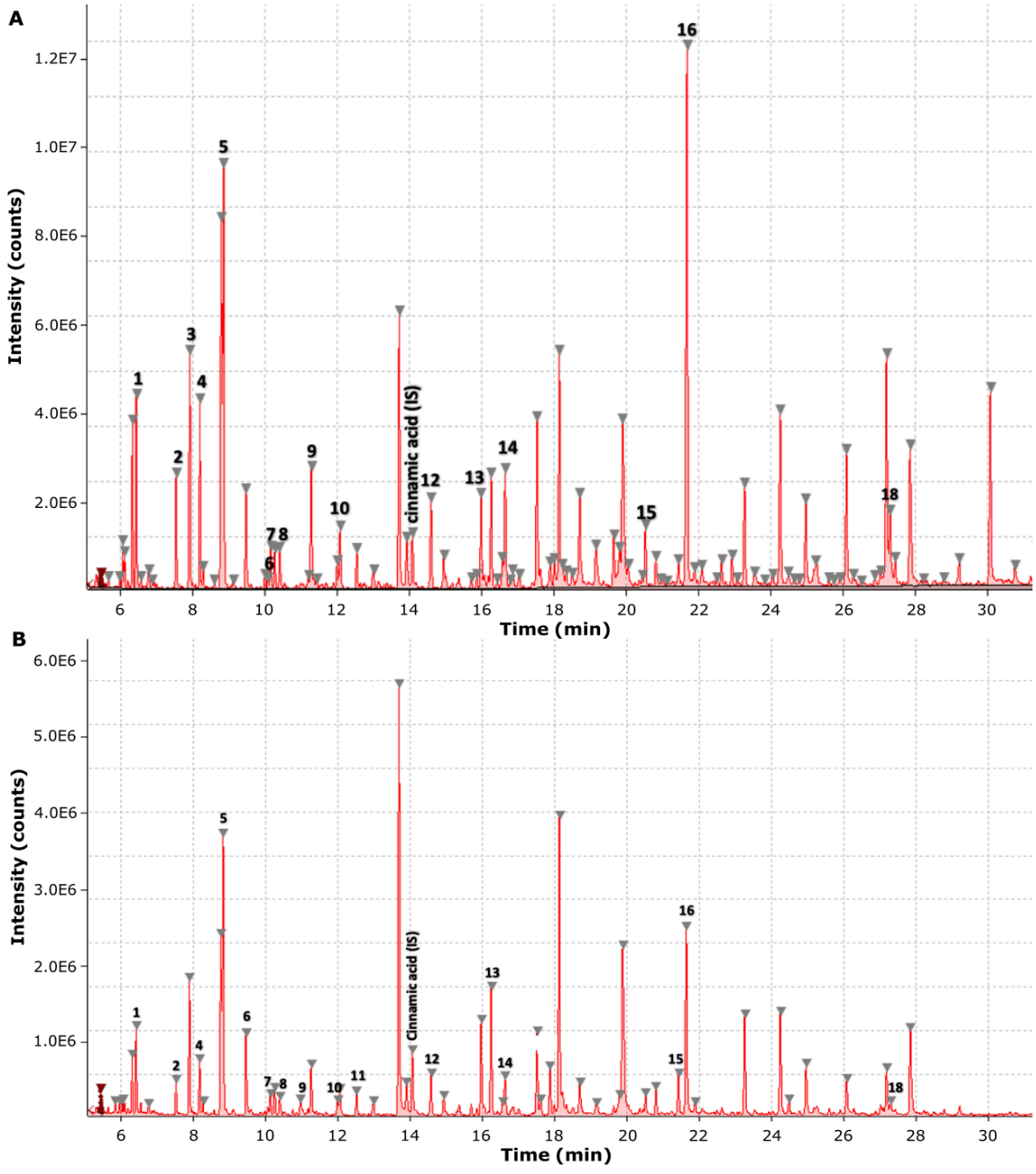


**Figure 96. Chromatograms showing relevant CuO oxidation products in sediment samples from Poole East (A. Surface (0-0.5 cm), B. Deep (9-10 cm); Core: C, macroalgae present sediment). Only peaks from compounds in common with green macroalgae samples are labelled (More information about identity of re levant compounds in Table 18).**

Poole Harbour sediment from core “D” surface produced a total of 110 CuO products, middle sediment 104 and deep 60. Relevant compounds for surface and deep samples were 16 while the middle sample had 15 On the surface sediment of this core, compound 16 was the most abundant followed by compound 5, on the middle and deep sample this pattern was the opposite (Figure 97).

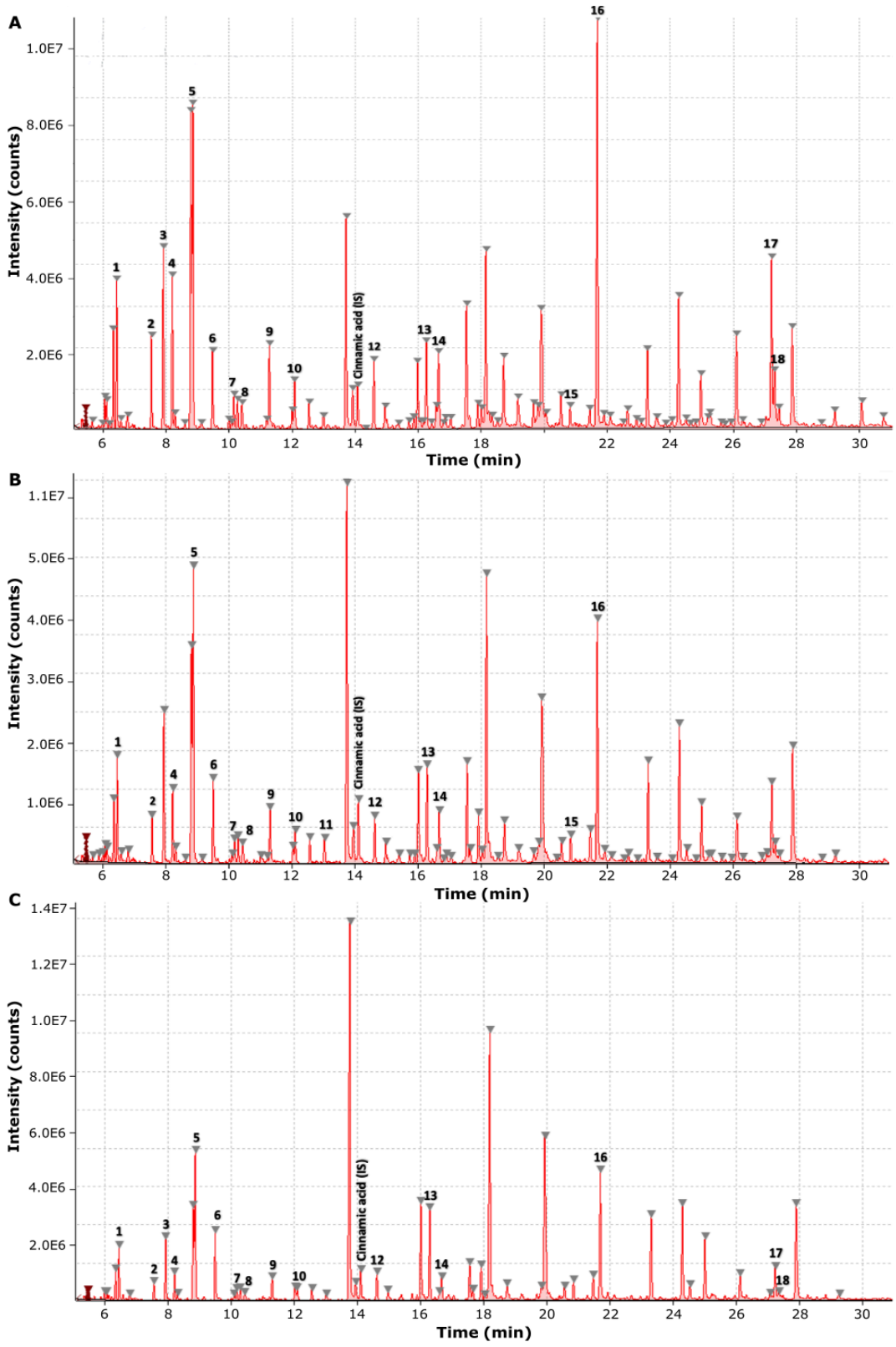


**Figure 97. Chromatograms showing relevant CuO oxidation products in sediment samples from Poole East (A. Surface (0-0.5 cm), B. Middle (4-5 cm) and C. Deep (9-10 cm); Core: D, macroalgae present sediment). Only peaks from compounds in common with green macroalgae samples are labelled (More information about identity of relevant compounds in Table 18).**

Langstone sediment core “B” produced 75 and 76 CuO products for surface and deep sediment samples respectively. Relevant compounds were 6 for surface and 7 for deep sediments and in both cases compound 5 was the most abundant followed by compound 16 (Figure 98).

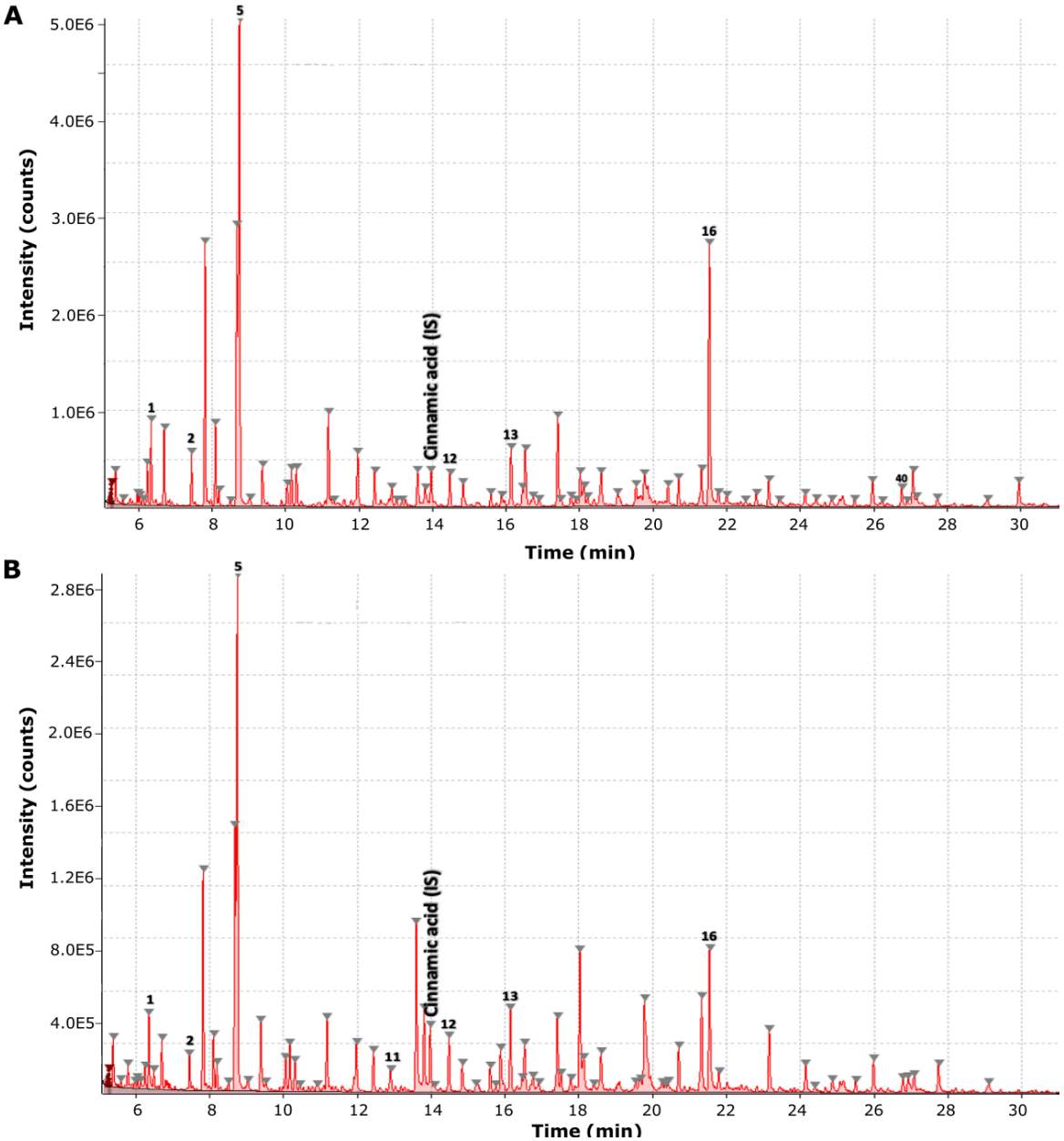


**Figure 98. Chromatograms showing relevant CuO oxidation products in sediment samples from Langstone (A. Surface (0-0.5 cm), B. Deep (9-10 cm); Core: B, Macroalgae absent). Only peaks from compounds in common with green macroalgae samples are labelled (More information about identity of relevant compounds in Table 18).**

Surface sediment from Langstone core “C” produced 76 CuO products from which 8 where relevant compounds, whereas deep sediment produced 78 CuO products and 6 relevant compounds. In both samples compound 5 and 16 where the most abundant ones (Figure 99).

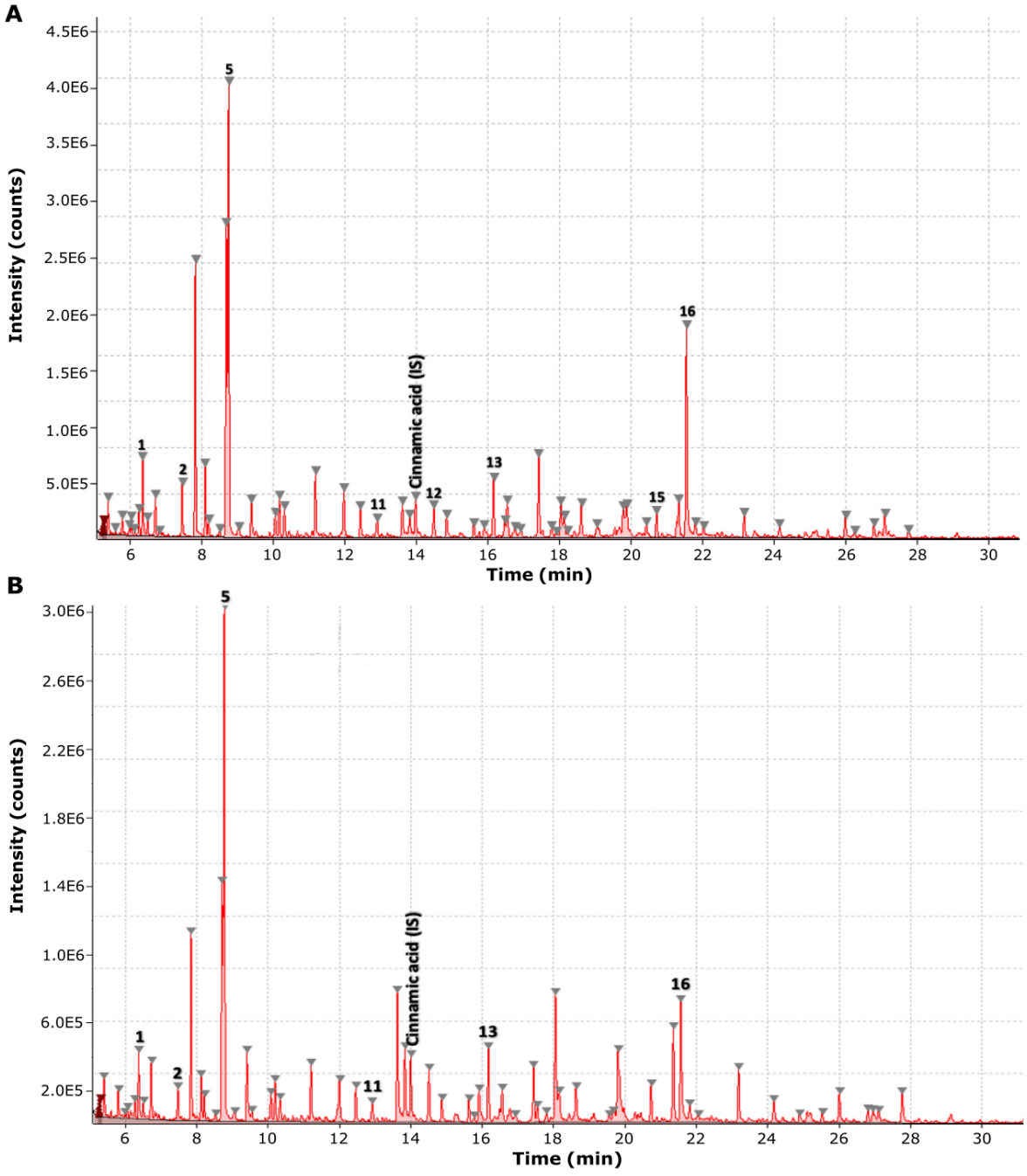


**Figure 99. Chromatograms showing relevant CuO oxidation products in sediment samples from Langstone (A. Surface (0-0.5 cm), B. Deep (9-10 cm); Core: C, macroalgae present sediment). Only peaks from compounds in common with green macroalgae samples are labelled (More information about identity of relevant compounds in Table 18).**

In core “D” from Langstone, 64 and 65 CuO products were produced in total for surface and deep sediment respectively. Of which 7 were relevant compounds in surface sample and 6 in deep sediment. Compound 6 was the most abundant in both samples followed by compound 16 (Figure 100).

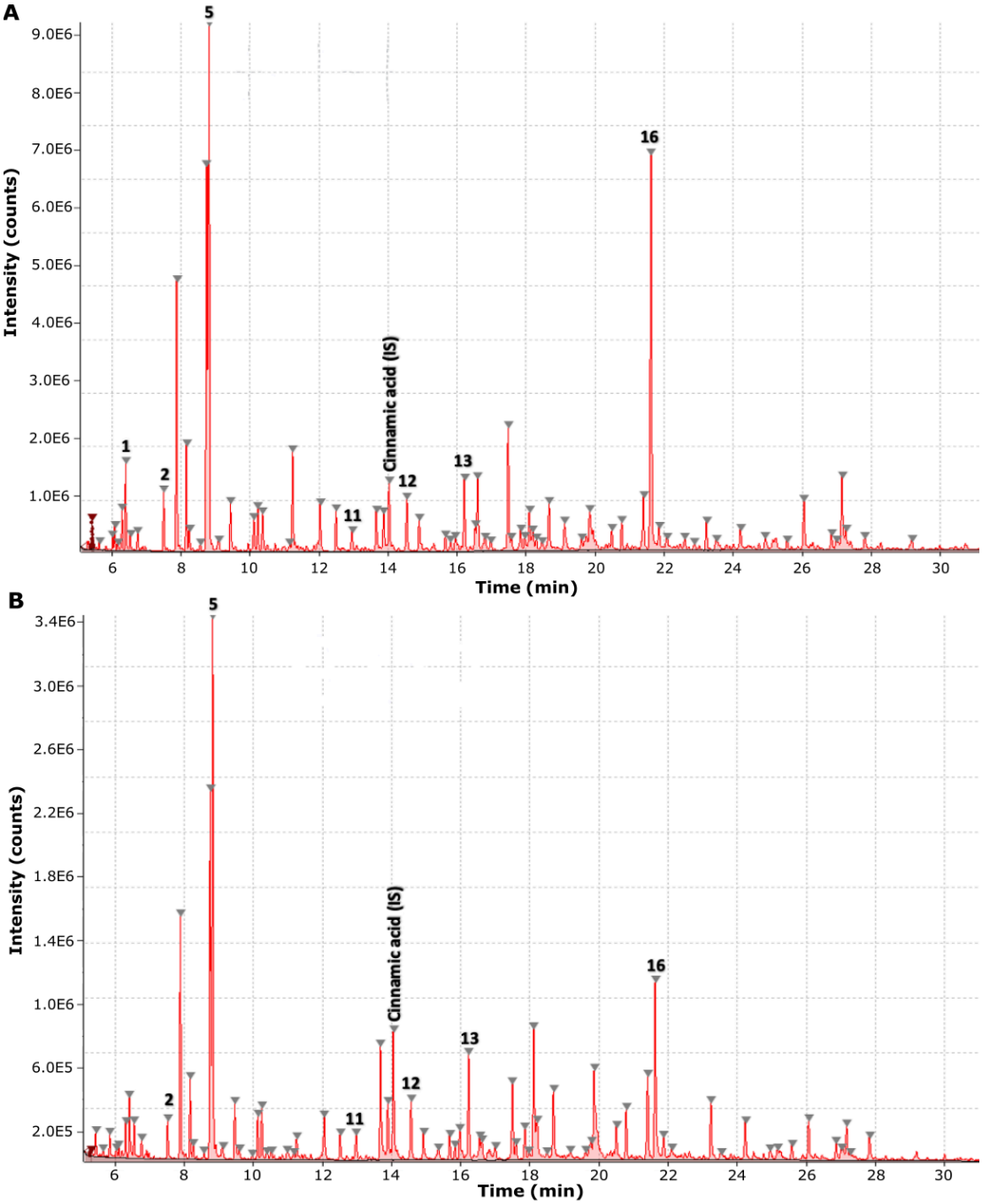


**Figure 100. Chromatograms showing relevant CuO oxidation products in sediment samples from Langstone (A. Surface (0-0.5 cm), B. Deep (9-10 cm); Core: D, macroalgae present sediment). Only peaks from compounds in common with green macroalgae samples are labelled (More information about identity of relevant compounds in Table 18).**

Port Solent sediment core “D” produced 57 CuO products in the surface and deep samples with 6 relevant compounds in both samples as well. Compounds 5 stood out as the most abundant compound at the surface and deeper section of the core (Figure 101).

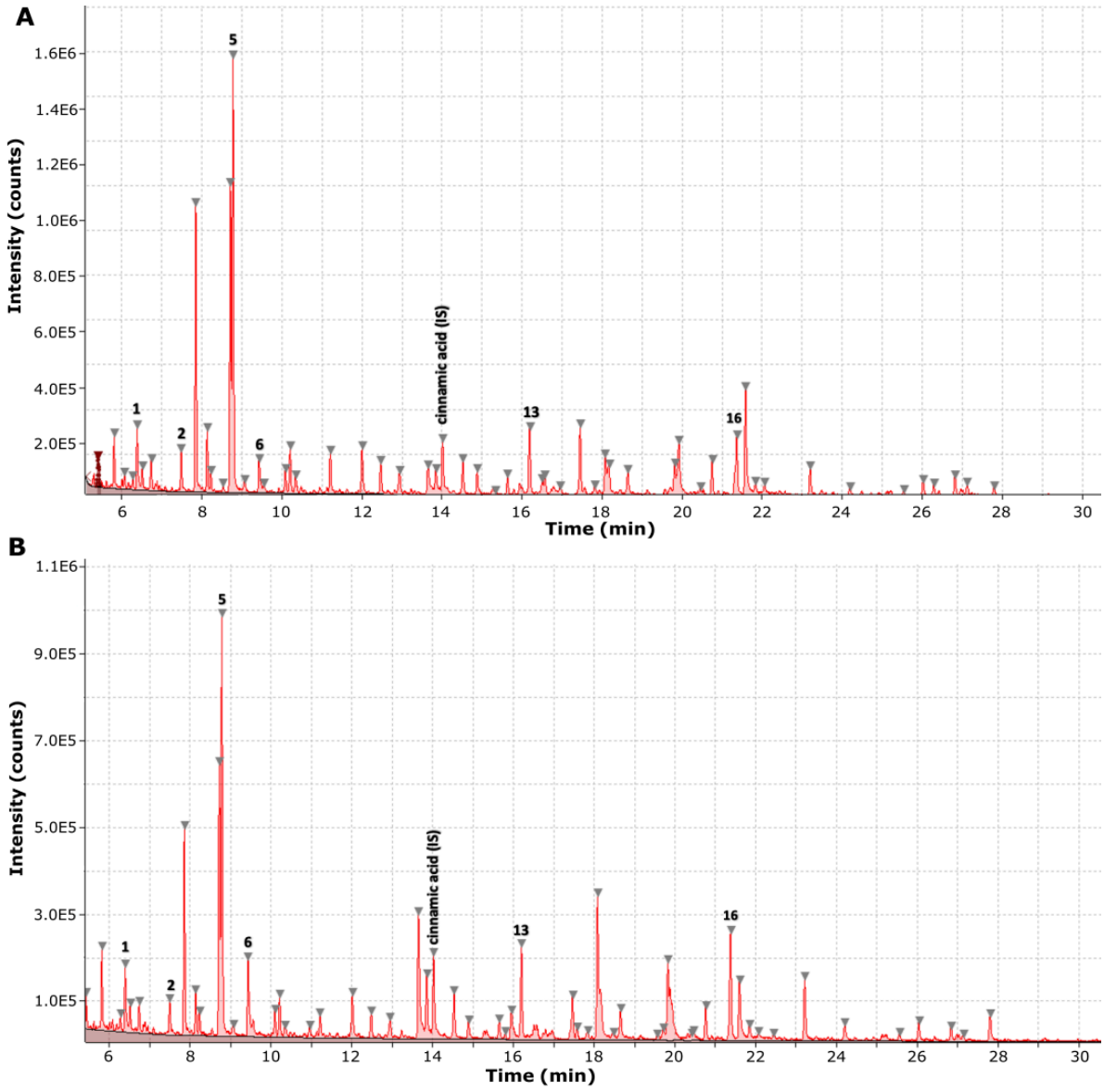


**Figure 101. Chromatograms showing relevant CuO oxidation products in sediment samples from Port Solent (A. Surface (0-0.5 cm), B. Deep (9-10 cm); Core: D, macroalgae present sediment). Only peaks from compounds in common with green macroalgae samples are labelled (More information about identity of relevant compounds in Table 18).**

Lastly, Portsmouth Grove Av sediment core “D” produced 46 CuO products on the surface sample and 69 on the deep sample. 8 were relevant compounds in the surface sample and 10 relevant compounds were identified in the deep sample. Compounds 21, 22 and 23 were unique to this site, and added to the list of relevant compounds (Figure 102).

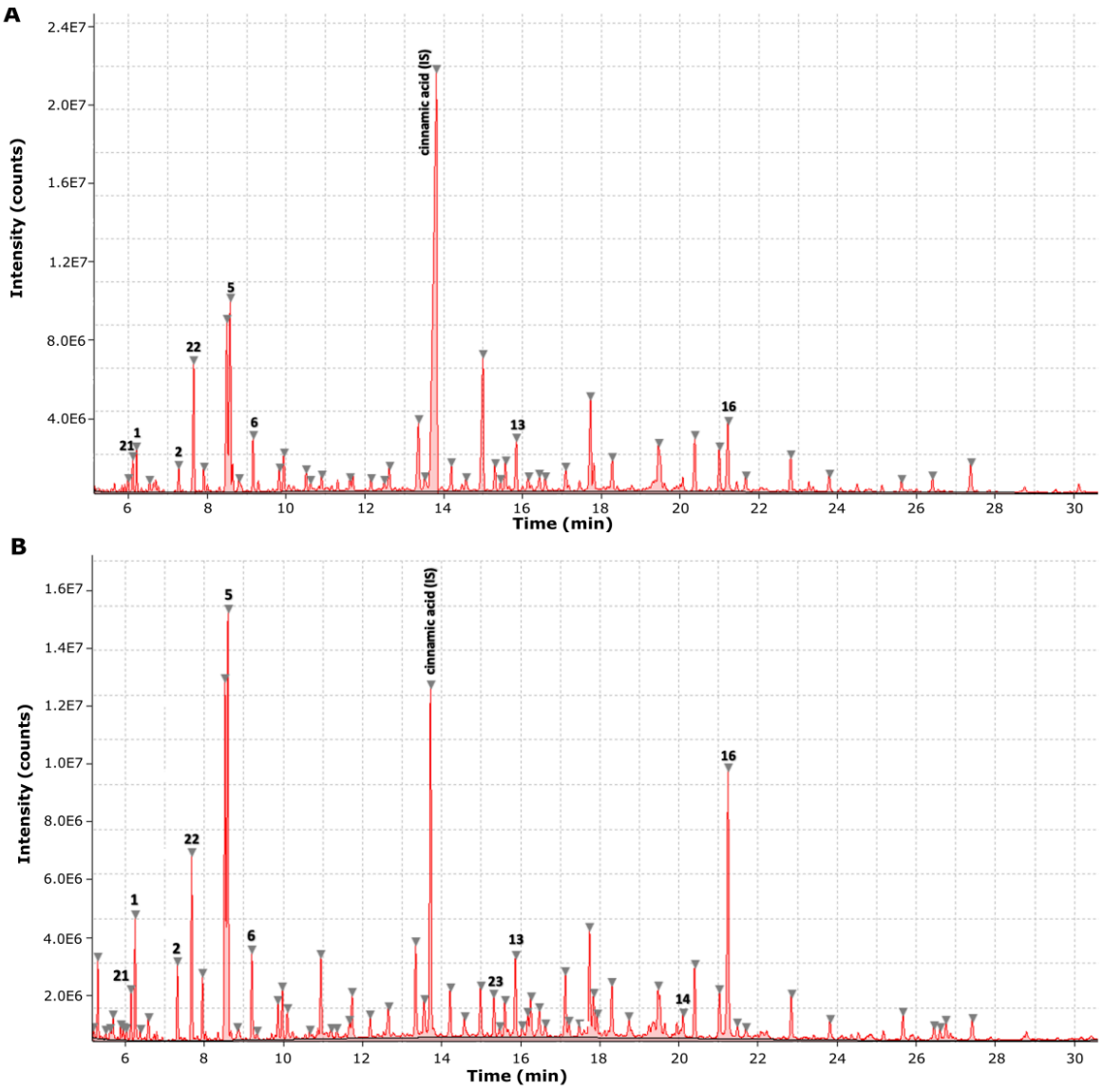


**Figure 102. Chromatograms showing relevant CuO oxidation products in sediment samples from Grove Avenue (A. Surface (0-0.5 cm), B. Deep (9-10 cm); Core: D, macroalgae present sediment). Only peaks from compounds in common with green macroalgae samples are labelled (More information about identity of relevant compounds in Table 18).**

**Table 18. Relevant CuO oxidation products in present in green algae and sediment samples from southern estuaries. *Compounds identities were included only when matched with the library search (NIST) otherwise they were named unknowns. Base ions (most abundant) are in bold and underlined. Algae and sediment samples are mentioned only when the compound was detected within that sample.**

| Code | Compound name | Major ions | | | | | Present in | |
|---|---|---|---|---|---|---|---|---|
| | | | | | | | Algae | Sediment samples |
| **1** | Benzoic acid trimethylsilyl ester | 77 | 105 | 135 | **179** | 180 | Langstone<br>Poole H<br>Grove Avenue<br>Port Solent | Langstone: 6/6<br>Poole H: 7/7<br>Grove Av: 2/2<br>Port Solent: 2/2 |
| **2** | Benzeneacetic acid, trimethylsilyl ester | **73** | 75 | 91 | 164 | 193 | Langstone<br>Poole H<br>Grove Avenue<br>Port Solent | Langstone: 6/6<br>Poole H: 7/7<br>Grove Av: 2/2<br>Port Solent: 2/2 |
| **3** | Butanedioic acid, bis(trimethylsilyl) ester | 9 | 75 | **147** | 148 | 247 | Poole H | Poole H: 5/7 |
| **4** | Butanedioic acid, methyl-, bis(trimethylsilyl) ester | 73 | 75 | **147** | 148 | 261 | Poole H | Poole H: 7/7 |
| **5** | 2-Butenedioic acid (E)-, bis(trimethylsilyl) ester | 73 | 75 | 147 | **245** | 246 | Langstone<br>Poole H<br>Grove Avenue<br>Port Solent | Langstone: 6/6<br>Poole H: 7/7<br>Grove Av: 2/2<br>Port Solent: 2/2 |
| **6** | Benzaldehyde, 4-[(trimethylsilyl)oxy]- | 73 | 151 | **179** | 180 | 194 | Poole H<br>Grove Avenue<br>Port Solent | Poole H: 6/7<br>Grove Av: 2/2<br>Port Solent: 2/2 |
| **7** | Methylmaleic acid, bis(trimethylsilyl) ester | **73** | 75 | 147 | 184 | 259 | Poole H | Poole H: 7/7 |

| | | | | | | | | |
|---|---|---|---|---|---|---|---|---|
| **8** | Unknown* | 57 | **73** | 147 | 247 | 320 | Poole H | Poole H: 6/7 |
| **9** | Unknown* | **73** | 129 | **147** | 261 | 363 | Poole H | Poole H: 7/7 |
| **10** | Acetophenone, 4'-(trimethylsiloxy)- | 73 | 147 | **179** | 180 | 253 | Poole H | Poole H: 7/7 |
| **11** | Hexanedioic acid, bis(trimethylsilyl) ester | **73** | 75 | **111** | 147 | 267 | Poole H | Poole H: 4/7 |
| **12** | Benzoic acid, 3-[(trimethylsilyl)oxy]-, trimethylsilyl ester | 73 | 193 | 223 | **267** | 282 | Langstone<br>Poole H | Langstone: 6/6<br>Poole H: 7/7 |
| **13** | Benzoic acid, 4-[(trimethylsilyl)oxy]-, trimethylsilyl ester | 73 | 193 | 223 | **267** | 282 | Langstone<br>Poole H<br>Grove Avenue<br>Port Solent | Langstone: 6/6<br>Poole H: 7/7<br>Grove Av: 2/2<br>Port Solent: 2/2 |
| **14** | Unknown* | 73 | 147 | 217 | **245** | 273 | Poole H<br>Port Solent | Poole H: 7/7<br>Port Solent: 1/2 |
| **15** | Azelaic acid, bis(trimethylsilyl) ester | **73** | 75 | 147 | 201 | 317 | Langstone<br>Poole H | Langstone: 4/6<br>Poole H: 5/7 |
| **16** | Unknown* | 73 | **193** | 194 | 265 | 295 | Langstone<br>Poole H<br>Grove Av Avenue<br>Port Solent | Langstone: 6/6<br>Poole H: 7/7<br>Grove Av: 2/2<br>Port Solent: 2/2 |
| **17** | Unknown* | **73** | 117 | 147 | **235** | 247 | Poole H | Poole H: 4/7 |
| **18** | Unknown* | 73 | 269 | 343 | **358** | 359 | Poole H | Poole H: 5/7 |
| **19** | Unknown* | **73** | 75 | 111 | 147 | 275 | Langstone<br>Poole H | Langstone: 5/6<br>Poole H: 4/7 |

| | | | | | | | | |
|---|---|---|---|---|---|---|---|---|
| **20** | Unknown* | 73 | 75 | **147** | 148 | 247 | Port Solent | Port Solent: 2/2 |
| **21** | Unknown* | 73 | 75 | **147** | 148 | 259 | Port Solent | Port Solent: 2/2 |
| **22** | Unknown* | 73 | **75** | 125 | 147 | 155 | Port Solent | Port Solent: 2/2 |

### 5.4.3 Relevant CuO oxidation products relative concentrations

#### 5.4.3.1 Relevant CuO oxidation products concentrations in macroalgae samples

A variety of non-lignin CuO oxidation products were identified for macroalgae and sediment samples from the different sediment samples. These products were mainly aromatic products, dicarboxylic acids and some compounds that could not be identified by the library searches (Table 18). Among the four macroalgae CuO oxidation products from the southern estuaries, compounds 1, 2, 5, 13 and 16 were persistent in every site (Table 18). Although relative concentrations vary between samples, concentrations bar plot showed a similar general pattern of distribution and abundance in every macroalgae sample (Figure 103).

Poole East macroalgae sample was the one with the highest number of relevant CuO oxidation products with 18. Langstone macroalgae had only 9 relevant compounds identified, however these were also present in Poole East macroalgae. Port Solent macroalgae sample had 9 relevant compounds however only 6 of them where in common with Langstone and Poole. Whereas Grove Av macroalgae sample only had 8 relevant CuO oxidation products all of them in common with the rest of the samples (Figure 103).

**Table 19. Relevant CuO oxidation products in common with those produced by (Goñi & Hedges, 1995) and this study, showing peak identification number and major ions in literature. Base ion (most abundant) in bold and underlined.**

| ID | (Compounds identified in Goñi and Hedges only for marine sources) | Major ions reported G&H (Base ion in bold) | | | | Given name in our library search | Major ions in estuaries samples | | | |
|---|---|---|---|---|---|---|---|---|---|---|
| **Aromatic products** | | | | | | | | | | |
| 1 | Benzoic acid | 194 | **179** | 135 | 105 | Benzoic acid trimethylsilyl ester | 77 | 105 | 135 | **179** |
| 6 | *p*-Hydroxybenzaldehyde | 194 | **179** | 151 | | Benzaldehyde, 4-[(trimethylsilyl)oxy]-trimethylsilyl ester | 73 | 75 | 151 | **179** |
| 12 | *m*-Hydroxybenzoic Acid | 282 | **267** | 223 | 193 | Benzoic acid, 3-[(trimethylsilyl)oxy]-, trimethylsilyl ester | 73 | 193 | 223 | **267** |
| 13 | p- Hydroxybenzoic Acid | 282 | **267** | 223 | 193 | Benzoic acid, 4-[(trimethylsilyl)oxy]-, trimethylsilyl ester | 73 | 193 | 223 | **267** |
| 2 | Phenylacetic Acid | 208 | 193 | 164 | **73** | Benzeneacetic acid, trimethylsilyl ester | **73** | 75 | 941 | **164** |
| **Unknowns** | | | | | | | | | | |
| 11 | 21 | 273 | **245** | 217 | | Unknown | 73 | 147 | 217 | **245** |

The macroalgae sample with the highest organic carbon content was Poole East with 19.3% followed by Port Solent macroalgae with 16.44%, while Langstone and Grove Av macroalgae had similar values, 11.36% and 10.72% in Langstone and Grove Av respectively. Concentrations of CuO oxidation products do not seem to increase uniformely with higher organic C content, but it does with number of CuO oxidation products. The macroalgae sample with highest concentrations of CuO oxidation products was Port Solent macroalgae, followed by Poole East and Langstone. Grove Avenue macroalgae on the other hand, had substantially lower concentrations

compared to the other macroalgae samples. All macroalgae samples although with differences in relative concentrations, presented a similar pattern of abundance from CuO oxidation products (Figure 103).

Compound 5 was identified as 2-Butenedioic acid (E)-, bis(trimethylsilyl) ester and had the highest concentration in all macroalgae samples. Relative concentration of this compound was 156.3 µg/gOC in Port Solent macroalgae, 101.9 µg/gOC in Poole East 73.3 µg/gOC in Langstone, while Grove Av macroalgae only 14.1 µg/gOC. Compound 16 (Unknown) was the second most abundant CuO product in all macroalgae, with relative concentrations being 115.8 µg/gOC in Port Solent, 96.6 µg/gOC in Poole, 68.3 µg/gOC in Langstone and 5.6 µg/gOC in Grove Avenue macroalgae samples. Poole East macroalgae had a third unknown compound with relatively high concentration. Compound 9 had a relative concentration of 48.4 µg/gOC. The rest of the compounds presented similar and lower concentrations compared with compounds 5 and 16 in all macroalgae samples.

Concentrations of compounds 5 and 16 were tested against organic C content, there was a significant positive relationship found between concentrations of these two compounds and organic C content of macroalgae samples (Spearmans rank, $p<0.05$, rho= 0.78).

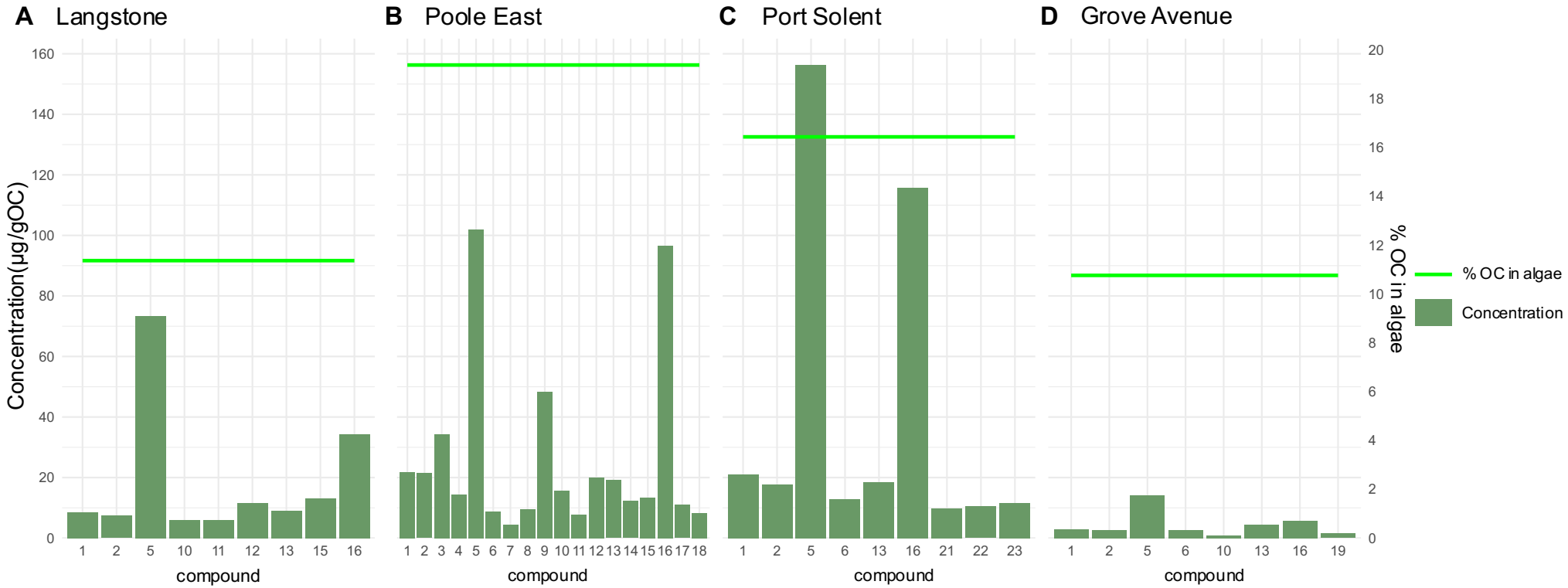


**Figure 103. Bar plot showing concentrations of CuO oxidation products from southern estuaries macroalgae samples. Green horizontal line represents organic carbon (%) for each sample. A. Langstone macroalgae, B. Poole East macroalgae, C. Port Solent macroalgae and D. Grove Av macroalgae.**

### 5.4.3.2 Relative CuO oxidation products concentrations in sediment samples

#### 5.4.3.2.1 Langstone Harbour

CuO oxidation products in Langstone sediment samples were analysed for macroalgae absent core B and macroalgae present cores C and D. Relevant products detected to in macroalgae and sediment samples from Langstone relevant products had a similar pattern of abundance.

Higher relative concentrations for compound 5 were measured in the macroalgae absent core B (Figure 104), reaching 163.1 µg/gOC in the surface sediment. At 10 cm depth compound 5 concentration (114 µg/gOC) decreased by 30% from its surface concentration. Compound 16 had a surface concentration in core B of 100.9 µg/gOC and 37.4 µg/gOC by the deep sample with a loss of 63% of its initial concentration. Compounds 1, and 2 also decreased concentration with depth, while compounds 12 13 and 15 remained less than 10% of their surface concentrations. Compound 11 on the other hand, present at low concentrations in the macroalgae sample, was not detected at the surface but in deeper sediment presented similar concentrations that the macroalgae sample (Figure 105).

Sediment core C from Langstone, had higher concentrations of compounds 5 and 16 in the surface with 114.2 and 107.8 µg/gOC respectively than in the deeper sediment sample where compound 5 decreased to 92.3 µg/gOC and compound 1.6 to 44.3 µg/gOC, decreasing 19% and 59% with depth. Compounds 1 and 2 decreased with depth and compounds 10 and 15 completely disappeared by 10 cm depth. On the

other hand, compounds 12 and 13 increased their initial surface concentration by 41 and 80% at deep sediment (Figure 105).

In the macroalgae present core D compound 5 was still abundant in the deep sediment sample at 96% from its surface concentration of 140.6 µg/gOC while compound 16 lost 49% from its surface concentration of 79.1 µg/gOC. Compounds 1, 2, 10 and 11 decreased slightly in the deep sediment sample while compound 15 was not detected. Compounds 12 and 13 slightly increased concentrations with depth by 25 and 6% respectively (Figure 106).

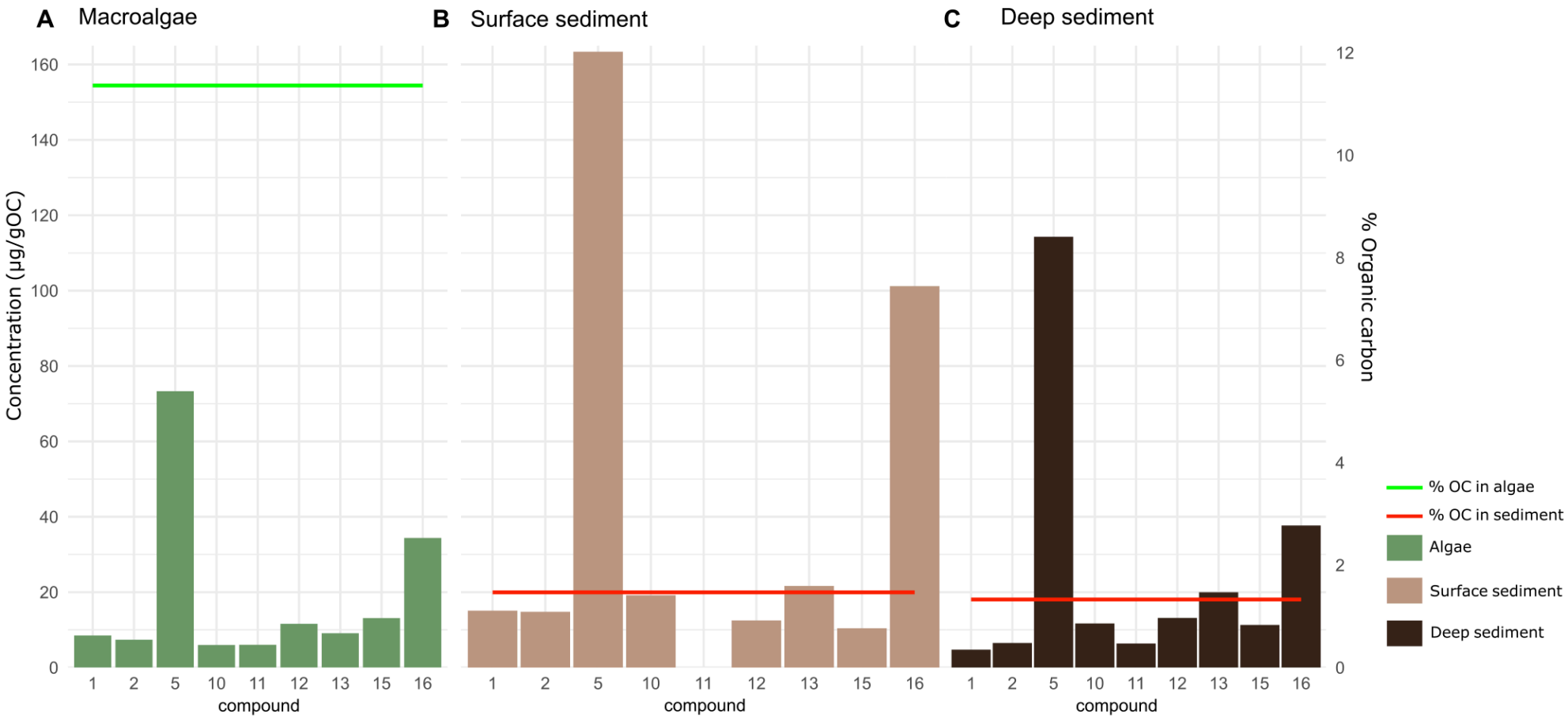


**Figure 104. Bar plot showing concentrations of CuO oxidation products in µg/gOC from A) Langstone macroalgae, B) Surface sediment and C) Deep sediment samples. Sediment samples from the macroalgae absent core B. Horizontal lines represent organic carbon (%) for each sample. Scale factor for the secondary y-axis = 10.8.**

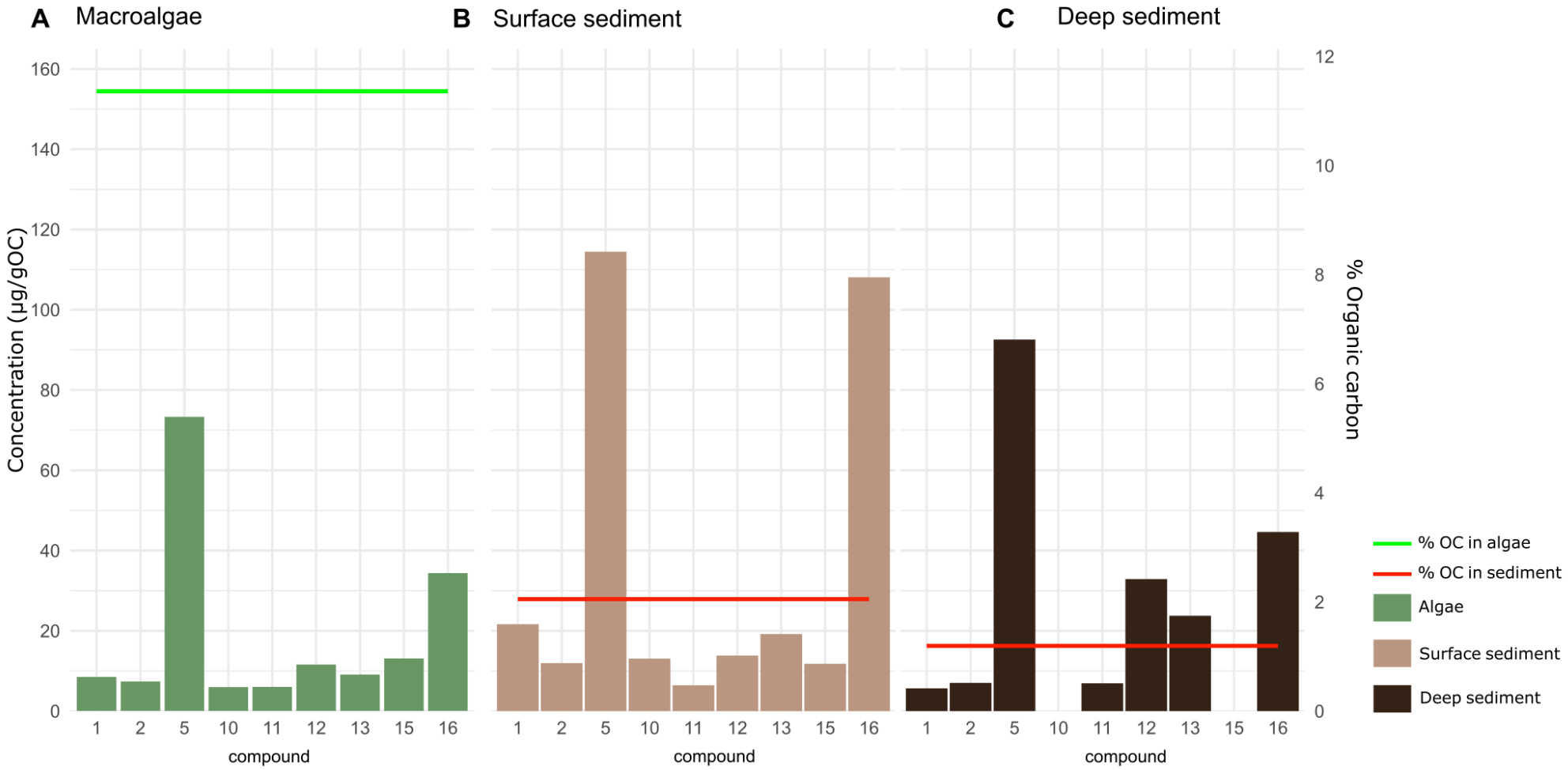


**Figure 105. Bar plot showing concentrations of CuO oxidation products in µg/gOC from A) Langstone macroalgae, B) Surface sediment and C) Deep sediment samples. Sediment samples from the macroalgae present core C. Horizontal lines represent organic carbon (%) for each sample. Scale factor for the secondary y-axis = 10.8.**

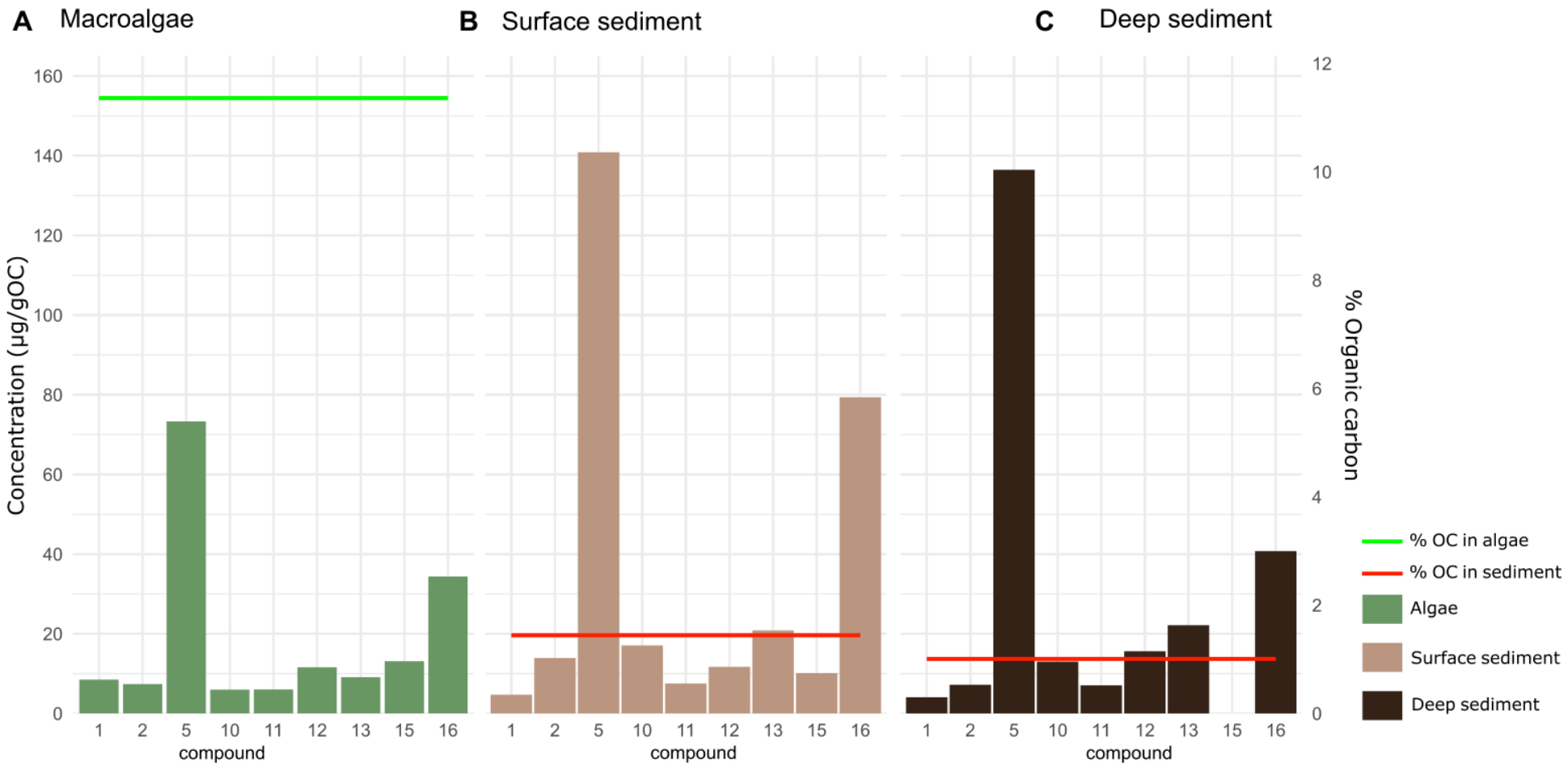


**Figure 106. Bar plot showing concentrations of CuO oxidation products in µg/gOC from A) Langstone macroalgae, B) Surface sediment and C) Deep sediment samples. Sediment samples from the macroalgae present core D. Horizontal lines represent organic carbon (%) for each sample. Scale factor for the secondary y-axis = 10.8.**

#### 5.4.3.2.2 Poole Harbour

Poole Harbour sediment samples had higher concentrations of compounds 5 and 16 compared to Langstone sediment samples. Concentrations in surface sediment samples analysed in this site where closer to the ones found in the macroalgae sample. Poole East sediment core A preserved most of compounds 5 and 16 concentrations with depth, preserving 76 and 61% of their surface concentrations respectively. Compounds 4, 6, 11, 13 and 14 increased concentrations with depth while compounds 1, 2, 3, 7, 8, 9, 10, 12, 15 and 18 decreased in concentration in the deep sample (Figure 107).

In sediment from Poole East core C, compound 16 had higher concentrations than compound 5 at the surface with 116.6 µg/gOC compared to 73.3 µg/gOC. In the deeper sample reduction for both compounds were less compared to core A (14.4 and 14.5%). Compounds 1, 2, 3, 7, 8 ,9, 12, 15 and 18 decreased their abundance with depth and compounds 4, 6, 11, 13 and 14 increased (Figure 108).

Sediment core D from Poole East was analysed at three different depths, surface, 4-5 cm and 9-10cm. Concentrations of compounds 5 and 16 were very similar at the 3 different depths (Figure 109).

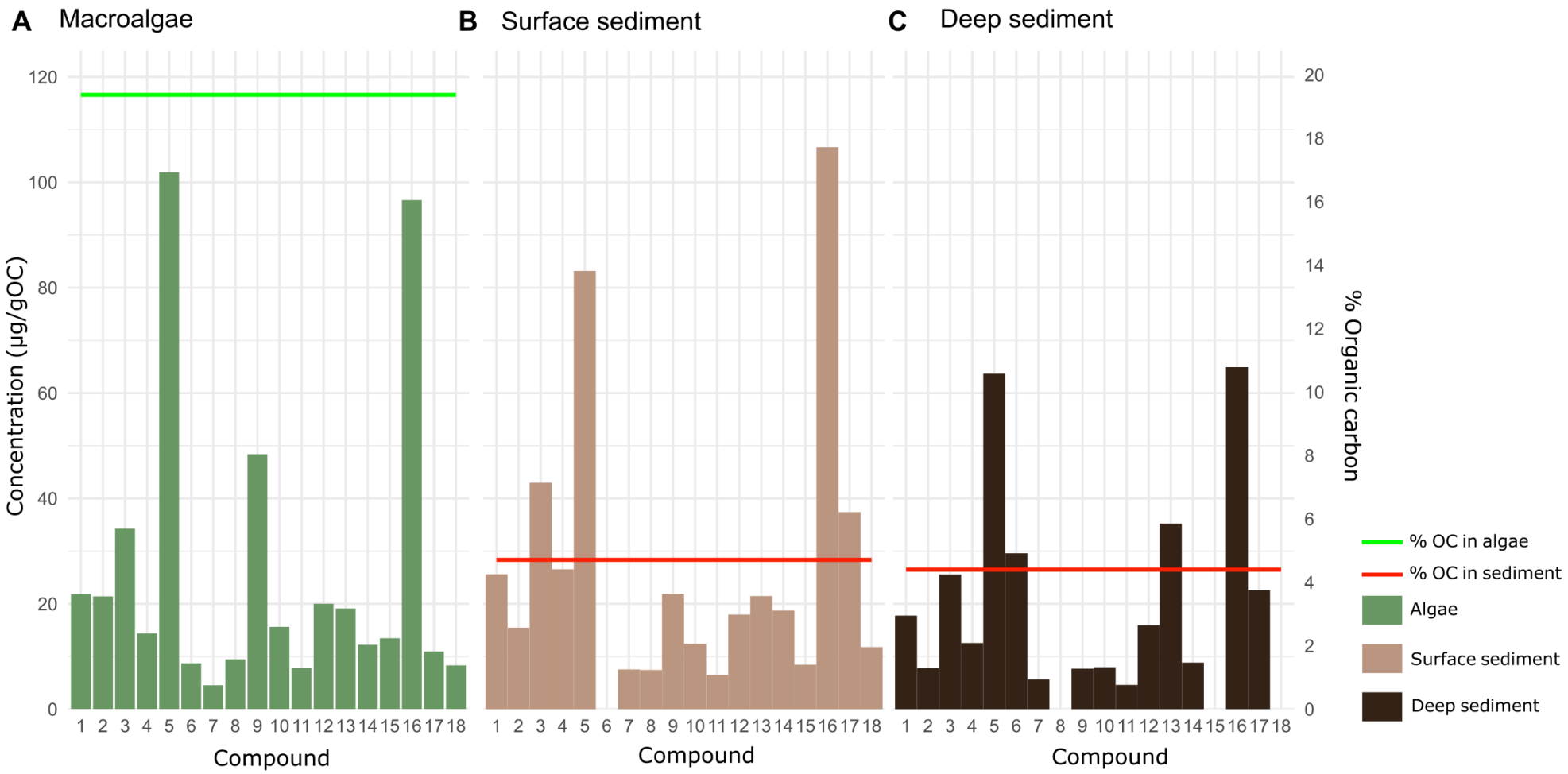


**Figure 107. Bar plot showing concentrations of CuO oxidation products in µg/gOC from A) Poole macroalgae, B) Surface sediment and C) Deep sediment samples. Sediment samples from the macroalgae absent core A. Horizontal lines represent organic carbon (%) for each sample. Scale factor for the secondary y-axis = 6.01.**

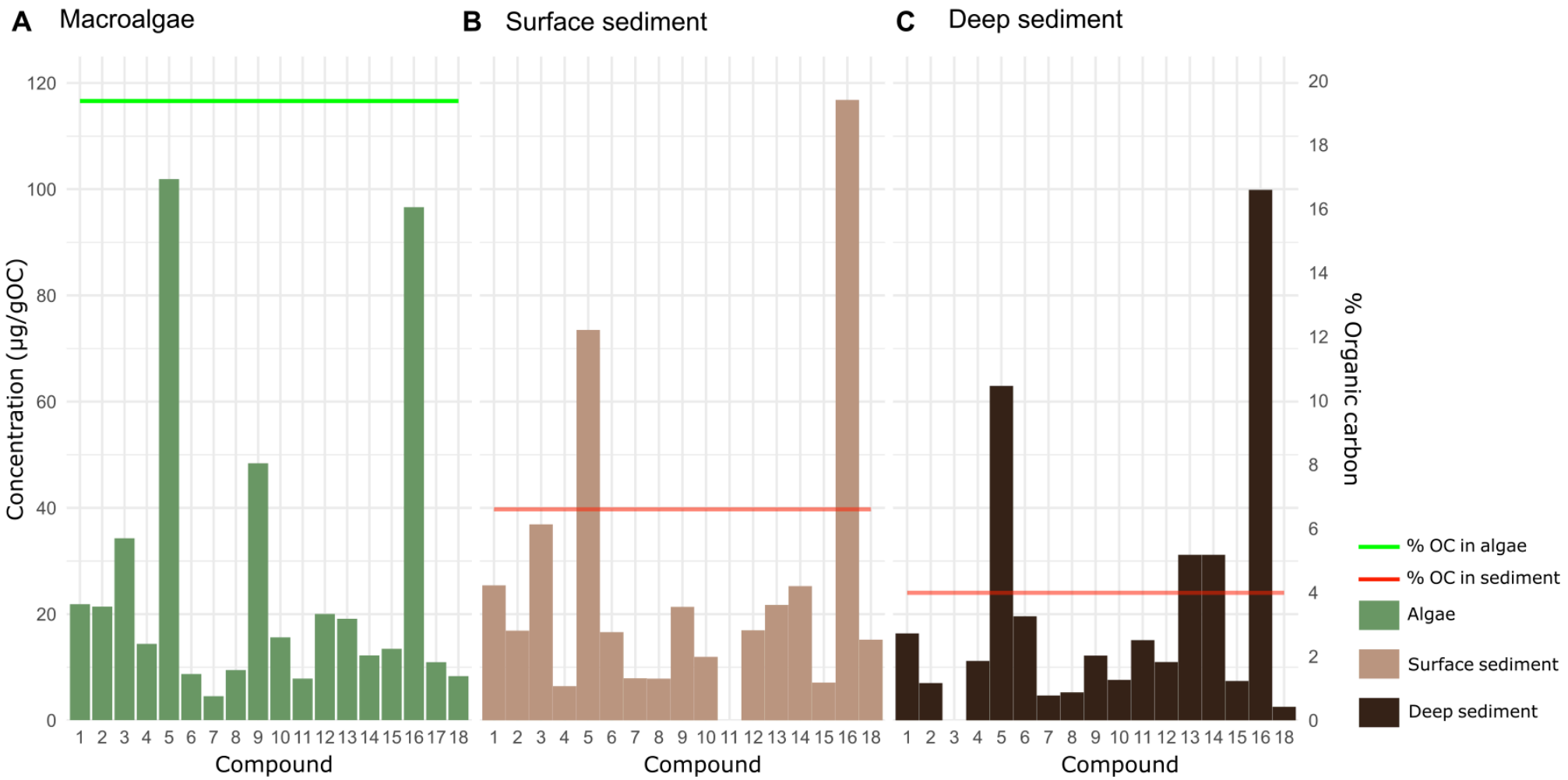


**Figure 108. Bar plot showing concentrations of CuO oxidation products in µg/gOC from A) Poole macroalgae, B) Surface sediment and C) Deep sediment samples. Sediment samples from the macroalgae present core C. Horizontal lines represent organic carbon (%) for each sample. Scale factor for the secondary y-axis = 6.01.**

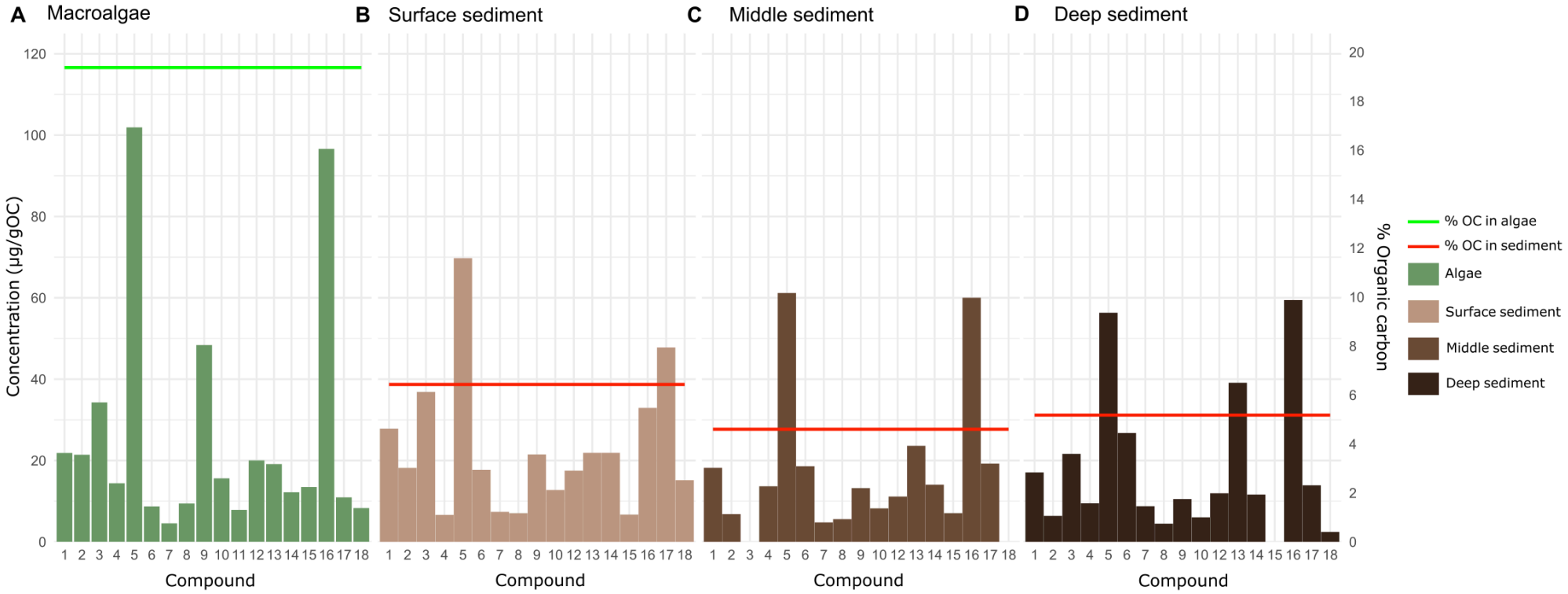


**Figure 109. Bar plot showing concentrations of CuO oxidation products in µg/gOC from A) Poole macroalgae, B) Surface sediment and C) Deep sediment samples. Sediment samples from the macroalgae present core D. Horizontal lines represent organic carbon (%) for each sample. Scale factor for the secondary y-axis = 6.01.**

### 5.4.3.2.3 Portsmouth Port Solent and Grove Avenue.

Compounds 5 and 16 were very low in concentrations in the algae from Grove Avenue, however surface sediment sample had comparable abundance with other sites (133.1 µg/gOC). Major differences in concentrations in compound 16 were also observed between macroalgae and sediment, with minimal surface relative abundance for this compound, 18.1 µg/gOC and remained similar in deeper sediment.

Macroalgae collected in Portsmouth Port Solent, had considerably higher relative concentrations of CuO oxidation products compared with Grove Av algae. However, this was not reflected in sediment samples despite having considerably higher organic carbon than Grove Av. In this case, compound 5 was not abundant in the surface sample, but increased concentration with depth (from 3.1 to 5.5 µg/gOC). Compound 16 on the other hand, showed a decline with depth from 6.4 to 2.8 µg/gOC. Compound 2 was the most abundant in the surface with a relative concentration of 7.8 µg/gOC and decreased in deeper sediment to 6.8 µg/gOC (Figure 110).

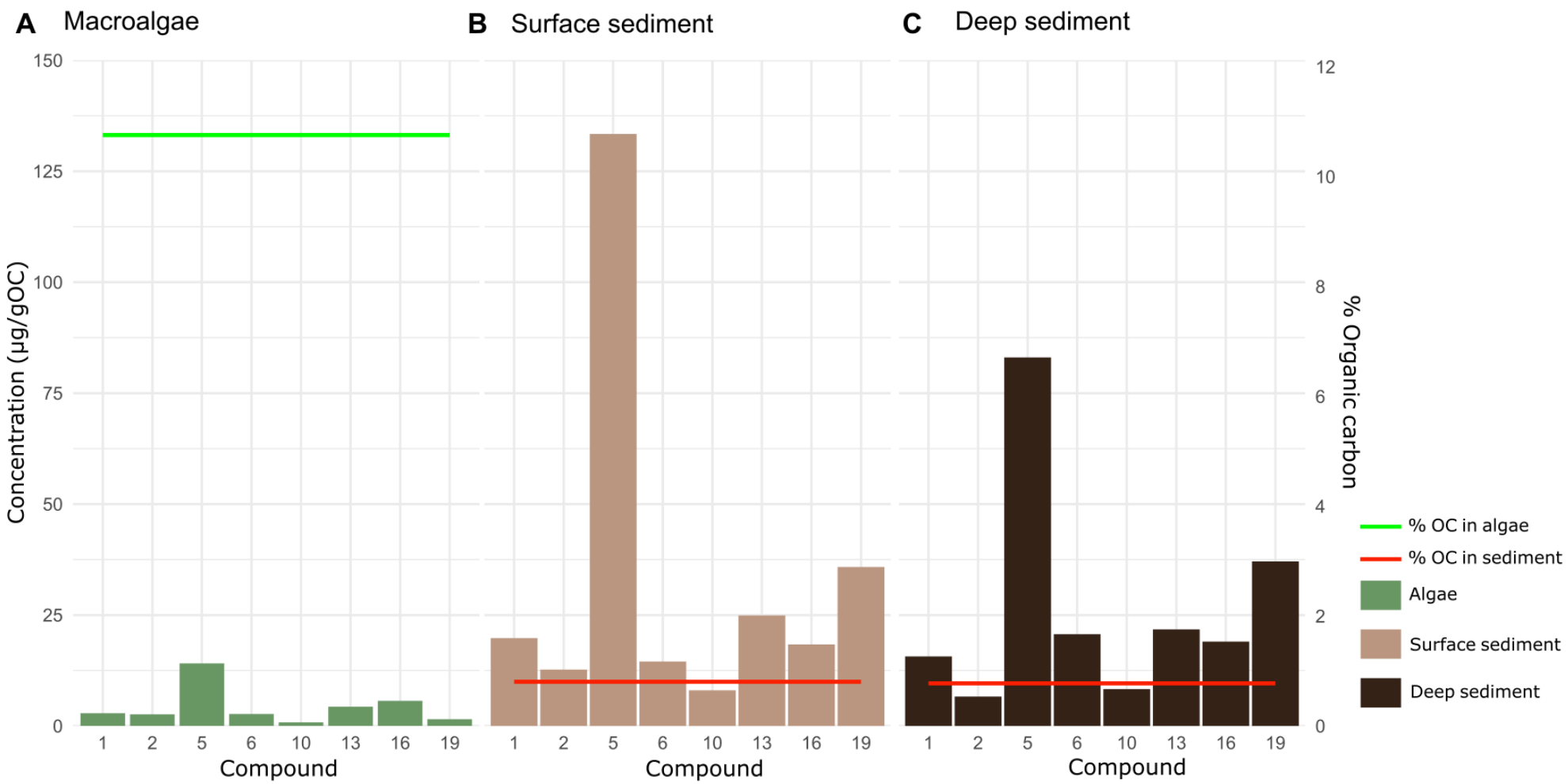


**Figure 110. Bar plot showing concentrations of CuO oxidation products in µg/gOC from A) Grove Av macroalgae, B) Surface sediment and C) Deep sediment samples. Sediment samples from the macroalgae present core D. Horizontal lines represent organic carbon (%) for each sample. Scale factor for the secondary y-axis = 12.37.**

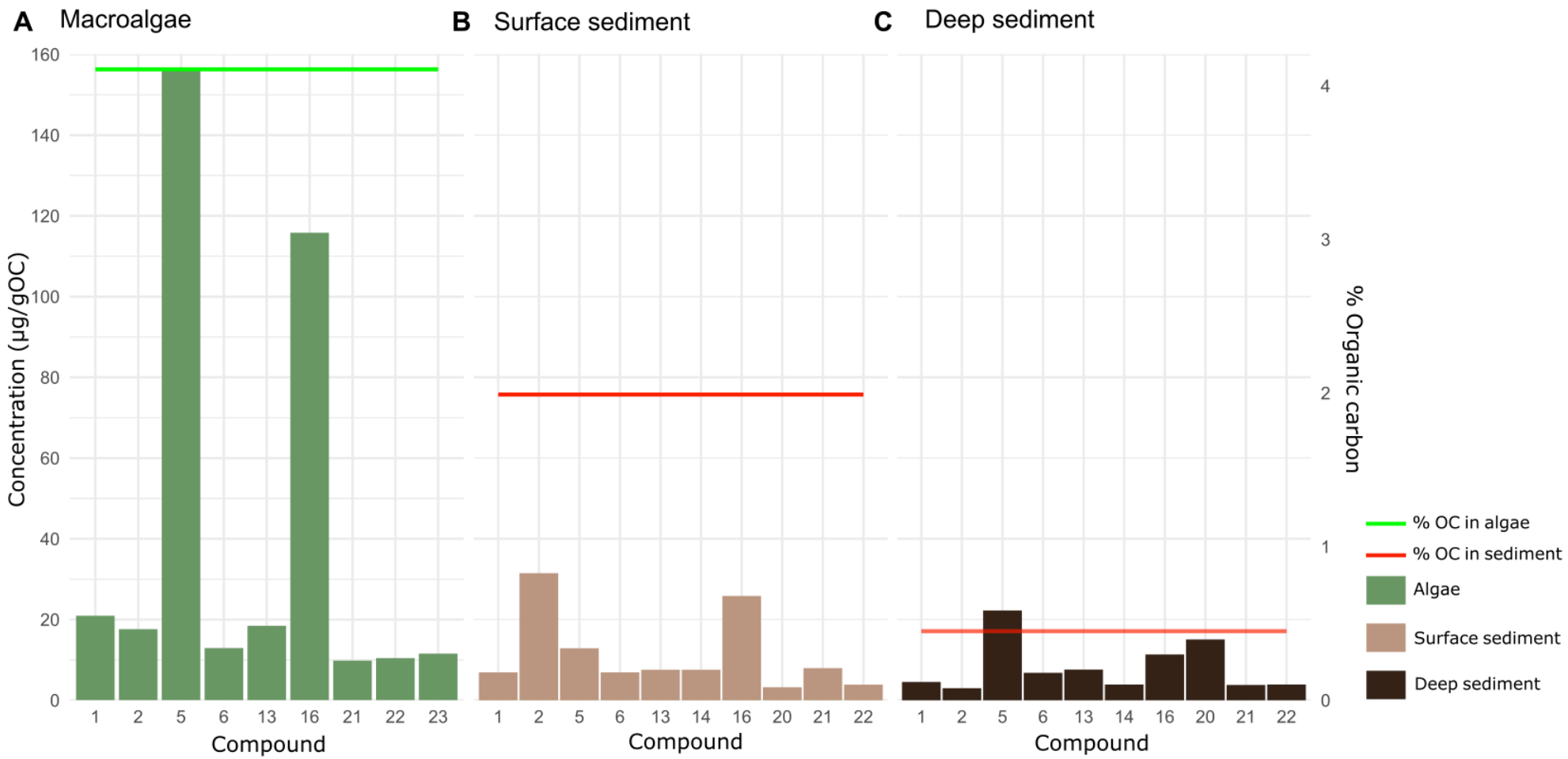


**Figure 111. Bar plot showing concentrations of CuO oxidation products in µg/gOC from A) Port Solent macroalgae, B) Surface sediment and C) Deep sediment samples. Sediment samples from the macroalgae present core D. Horizontal lines represent organic carbon (%) for each sample. Scale factor for the secondary y-axis = 9.51.**

Sediment samples from Langstone presented comparable pattern of CuO oxidation products concentrations with the macroalgae, with compounds 5 and 16 standing out from others with greater concentrations. What stands out is the difference in concentrations between the macroalgae and sediment samples in compound 1. Compound 1 identified as the aromatic product benzoic acid, was present in macroalgae CuO oxidation products as the smaller concentration (3.6 μg/gOC) increasing concentration in the sediment samples up to 110 μg/gOC in the macroalgae present core. Concentrations of compounds 2, 10, 11, 12, 13, and 15 did not varied from the macroalgae to sediment samples.

While the great majority of compounds concentrations decreased with depth (surface vs deep sediment), some interesting patterns could be observed between macroalgae presence and absence. For instance, although compound 5 reached its maximum concentration in the absence of macroalgae (163.1 μg/gOC), when reaching the deep sediment 30% of the concentration was lost (114 μg/gOC). On the other hand, the presence of algae seemed to mitigate this loss effect, preserving 80% and 96% of the surface concentration with depth. In the case of compound 16, all sediment samples displayed close concentrations in both surface and deep parts of the cores, with a tendency of decreasing between 37-50% of the initial concentration at the surface.

Compound 1 and 15 concentrations did not show a clear pattern between presence and absence of algae in the sediment. Sediment with and without algae had comparable concentrations of compound 1 both decreasing with depth, whereas the

replicate core with macroalgae present had not only much less but this compound increase slightly in the deeper sediment. And compound 15 presented a slight increase with depth in the absence of algae but was not detected at surface and deep sediment for both algae present cores. The remaining compounds did not show a difference between macroalgae presence and absence in terms of concentrations. Compounds 2, 10 and 15 tended to decrease slightly with depth, while compounds 12 and 13 concentrations increased with depth in all sediment cores.

Eighteen relevant CuO oxidation products were identified between sediment and algae from Poole H. Compounds 5 and 16 were the two most abundant in all sediment samples however, in this case concentrations were highly comparable with those in the macroalgae. Compound 5 in algae reached a 101.9 μg/gOC and the average concentration within the sediment samples was of 670 μg/gOC. Similarly, compound 16 concentration in the algae was of 96.6 μg/gOC while the average of the sediment 77 μg/gOC.

Compound 9 displayed the third most abundant concentration among the CuO oxidation products produced by the macroalgae (48.4 μg/gOC). Nonetheless, compound 9 did not stand out as abundant in the sediment CuO oxidation products with an average concentration of 15.2 μg/gOC. The remaining compounds concentrations ranged from 8 – 21.8 μg/gOC in both macroalgae and sediment samples.

Concentrations of compound 5 showed no differences between presence or absence of algae, the decrease with depth was very similar ranging from 14-23%. However, compound 16 in the absence of algae lost 40% of the surface concentration at 9-10 cm, while the present core just decreased a 14%, interestingly the replicate core for the macroalgae present sediment even increased with depth, reaching the highest in the middle of the core at 4 cm depth with 59.8 μg/gOC.

### 5.4.3.3 Principal component analysis

Principal Component Analysis was performed to evaluate the influence of different CuO products in different primary producers and sediment samples. Compounds identities used for this analysis are included in Table 20.

**Table 20. ID codes for principal component analysis, compounds, and loadings for each principal component.**

| Principal Component Loadings | | | | | | | | |
|---|---|---|---|---|---|---|---|---|
| ID | Compound | PC1 | PC2 | PC3 | PC4 | PC5 | PC6 | PC7 |
| **Bd** | Benzoic Acid | -0.41 | 0.31 | 0.39 | 0.06 | -.39 | -0.62 | -0.17 |
| **Pl** | *p*-Hydroxybenzaldehyde | 0.31 | -0.43 | 0.03 | 0.80 | -0.05 | -0.26 | -0.09 |
| **Bed** | Phenylacetic Acid | -0.50 | -0.23 | 0.11 | 0.19 | -0.29 | 0.61 | -0.44 |
| **mBd** | *m*-Hydroxybenzoic Acid | 0.09 | 0.43 | -0.77 | 0.15 | -0.28 | -0.04 | -0.34 |
| **Pd** | *p*-Hydroxybenzoic Acid | -0.38 | -0.42 | -0.31 | -0.21 | 0.50 | -0.38 | -0.38 |
| **Unknown** | Comp 11 | 0.29 | -0.51 | -0.08 | -0.48 | -0.62 | -0.13 | -0.07 |
| **Comp16** | Comp 16 | 0.50 | 0.19 | 0.37 | -0.15 | 0.21 | 0.05 | -0.71 |

Results from the Principal Component Analysis indicated that 69.9% of the variation can be explained by PC1 and PC2 with 42.4% and 27.5% respectively. Although green macroalgae samples were not clustered together, indicating different composition; sediment samples and macroalgae from the same site had similar compositions. For example, all sediment samples and macroalgae from Poole Harbour are in between vectors unknown and comp16. Langstone sediment and algae samples are between vectors Bd and comp16 (Figure 112).

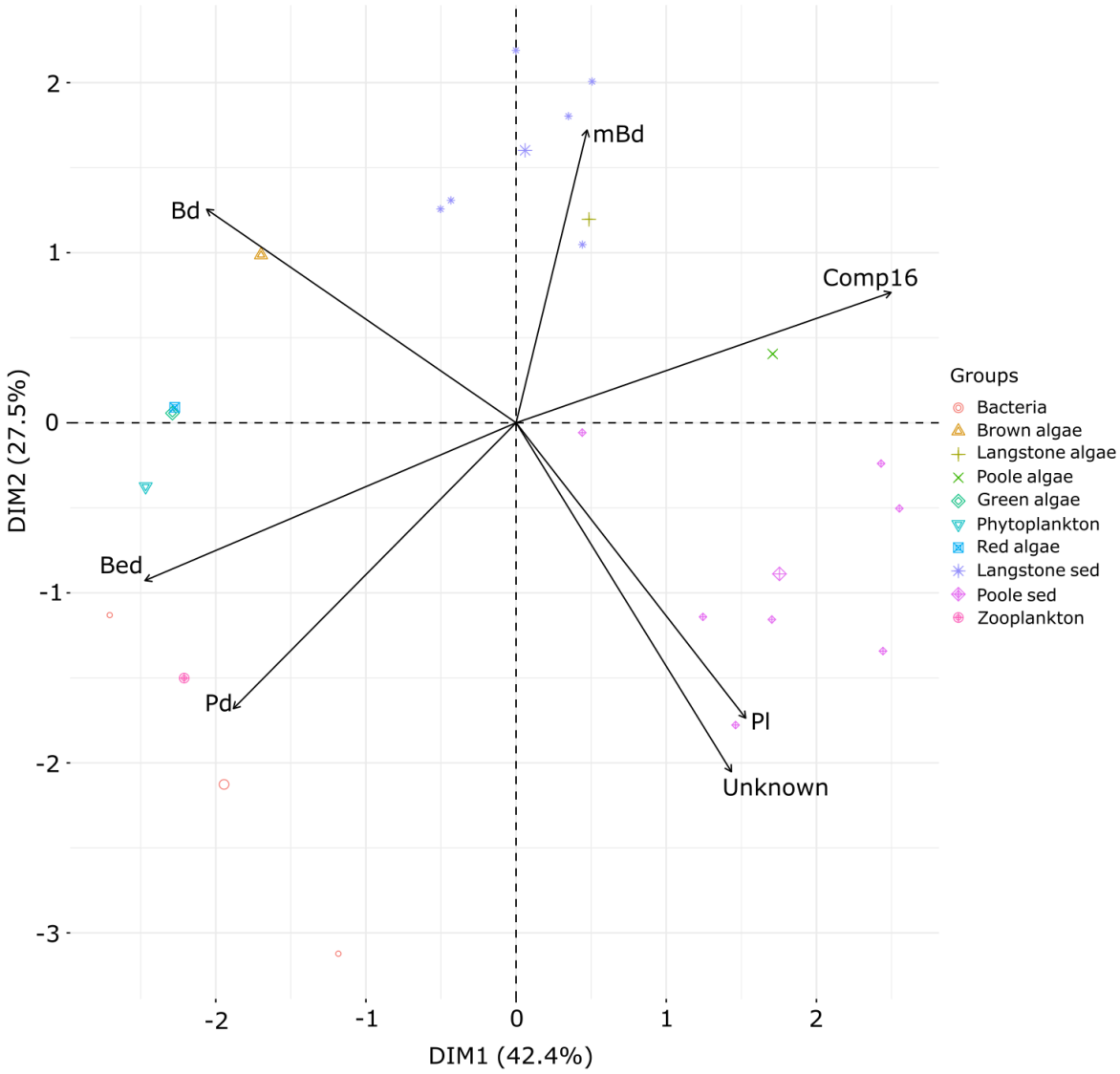


**Figure 112. PCA biplot showing southern estuaries sediment and green algae composition with respect to relevant CuO oxidation products concentrations. Other primary producers CuO oxidation products were taken from (Goni and Hedges, 1995) for comparison. ID for compounds and PCA loadings are defined in (Table 20).**

### 5.4.4 Bulk stable isotopes ($\delta^{13}C$, $\delta^{15}N$ and $\delta^{2}H$)

From primary producers, Brown algae had a lighter $\delta^{13}C$ (-11.9‰) than green algae $\delta^{13}C$ (-14.6 ± 3.15 ‰), while phytoplankton had a lighter $\delta^{13}C$ (-21.6 ± 1.52‰) than both algae groups (Table 21). There were not significant differences in $\delta^{13}C$ between primary producers (*Kruskal-Wallis*= $P > 0.05$). $\delta^{15}N$ values green algae (10.4 ± 6.8‰) where slightly higher than those found in the brown algae (Finland) (5.04‰) and phytoplankton fall in between (6.78 ± 0.3‰). There were not significant differences between these groups for $\delta^{15}N$ (*Kruskal-Wallis*= $P < 0.01$; *Wilcoxon*= $p$= >0.05). Nonetheless, $\delta^{2}H$ values where significantly different for phytoplankton ($\delta^{2}H$= -91.9 ± 9.92‰) and both green (-143 ± 6.02‰) and brown algae ($\delta^{2}H$ = -121‰) (ANOVA= $p$ <0.001; *Tukey*= $p$ <0.001).

**Table 21. Stable isotope values ($\delta^{13}C$, $\delta^{15}N$, $\delta^{2}H$), from sediment, phytoplankton and macroalgae samples from the different sampling locations. *Sedimenting matter was only collected from Finland sites.**

| Primary producers | | | |
|---|---|---|---|
| | $\delta^{13}C$ (‰) | $\delta^{15}N$ (‰) | $\delta^{2}H$ (‰) |
| Green macroalgae Langstone | –17.6 | 6.1 | –147.8 |
| Green macroalgae Poole East | –11.3 | 18.2 | –143.8 |
| Green macroalgae Port Solent | –14.8 | 6.9 | –136 |
| *Fucus vesiculosus* (Finland) | –11.9 | 5 | –120.7 |
| Finland Phytoplankton | –27.6 ± 0.2[1] | 1.6 ± 0.7[1] | –138.6 |
| Phytoplankton Langstone | –21.6 ± 1.5 | 6.8 ± 0.3 | –91.9 ± 9.9 |
| **Sedimenting material and particulate matter** | | | |
| | $\delta^{13}C$ (‰) | $\delta^{15}N$ (‰) | $\delta^{2}H$ (‰) |
| Finland particulate matter site 1 | –23.9 | 4.3 | –117.5 |
| Finland particulate matter site 2 | –24 | 3.6 | –125.7 |

| | | | |
|---|---|---|---|
| Finland particulate matter site 3 | –23.8 | 2.2 | –123.9 |
| Sedimenting material site 1 | –23.8 | 4.4 | –126.4 |
| Sedimenting material site 2 | –24 | 3.6 | –131.7 |
| Sedimenting material site 3 | –24.4 | 2.8 | –118.07 |

| Sediment samples | | | | | | |
|---|---|---|---|---|---|---|
| | Surface | | | Deep | | |
| Site | $\delta^{13}C$ (‰) | $\delta^{15}N$ (‰) | $\delta^{2}H$ (‰) | $\delta^{13}C$ (‰) | $\delta^{15}N$ (‰) | $\delta^{2}H$ (‰) |
| Langstone | –15.5 | 5.9 | –96 | –16.7 | 5.1 | –101.4 |
| Poole | –17.2 | 13.7 | –99.1 | –18.7 | 8.7 | –100.2 |
| Port Solent | –15.5 | 5.7 | –95.2 | –8.1 | 3 | –90.4 |
| Finland site 1 | –22.7 | 4.2 | –106.9 | –22.5 | 3.9 | –113.1 |
| Finland site 2 | –22.7 | 4.3 | –116.8 | –21.5 | 2.3 | –116.9 |
| Finland site 3 | –23.3 | 4.8 | –122.8 | –23.1 | 4.1 | –116.9 |

[1] The mean (± SD) $\delta^{13}C$ and $\delta^{15}N$ values from Finland phytoplankton were extracted from the literature (Kahma et al., 2020).

Sediment samples from southern estuaries had a heavier $\delta^{13}C$ (-15.3 ± 3.7‰) than Finland sediment $\delta^{13}C$ (-22.6 ± 0.7‰), the same pattern was observed for $\delta^{2}H$ values with -116 ± 5.3‰ and -97 ± 4‰ for Finland and Southern estuaries samples respectively. On the contrary, $\delta^{15}N$ values were more enriched in sediment from the southern estuaries, $\delta^{15}N$ (7.02 ± 3.8‰) than in Finland $\delta^{15}N$ (3.92 ± 0.9‰) (Figure 113 & Figure 114). Significant differences were observed between both sediment groups for $\delta^{13}C$ (Wilcox, $p$= 0.032) and $\delta^{2}H$ (*Tukey*, $p$= <0.05), but not for $\delta^{15}N$ (Wilcox, $p$= >0.05).

For southern estuaries samples, macroalgae had closer $\delta^{13}C$ values than the ones found in sediment samples while phytoplankton, macroalgae and sediment overlapped in $\delta^{15}N$ (Figure 105). $\delta^{2}H$ had a clear differentiation between phytoplankton and macroalgae and sediment samples where within the same range than phytoplankton for $\delta^{2}H$, having lighter values than the ones observed for green macroalgae (Figure 113).

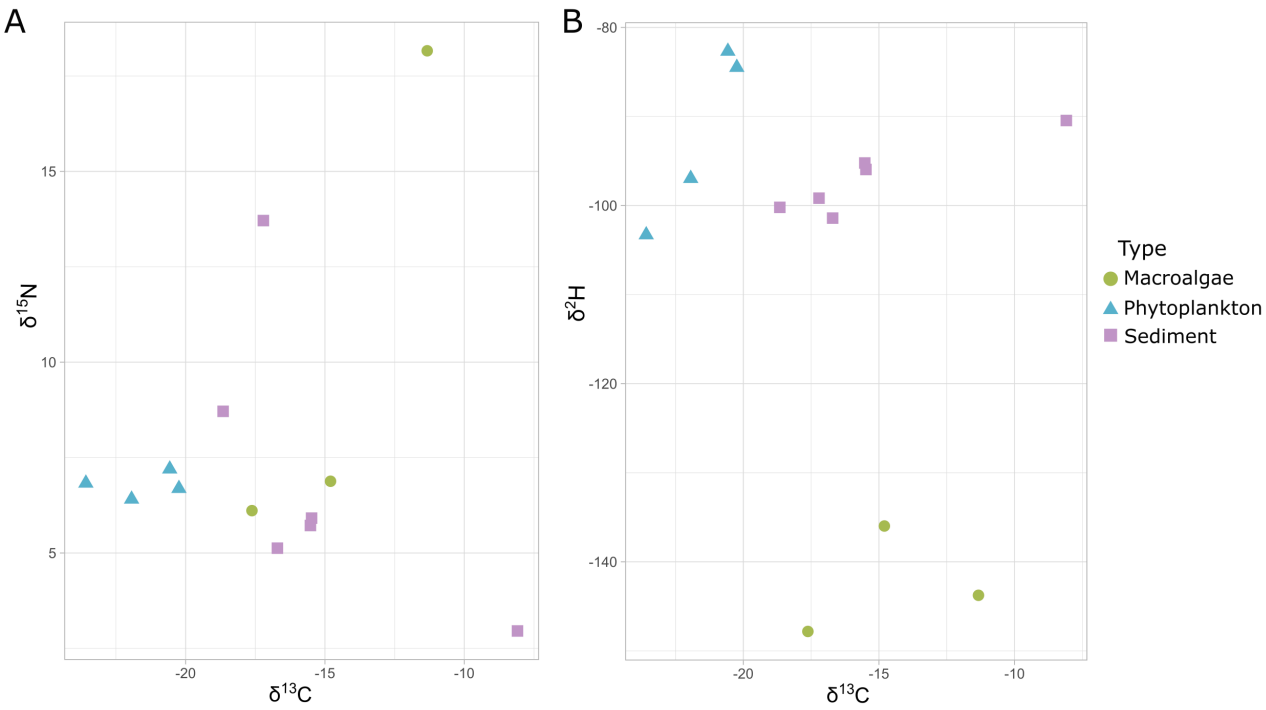


**Figure 113. Dual isotope plots showing A. $\delta^{15}N$ vs $\delta^{13}C$ and $\delta^{2}H$ vs $\delta^{13}C$ (right panel) for green macroalgae (green circles), phytoplankton (blue triangles), and sediment (purple squares), samples from southern estuaries.**

On the other hand, Finland samples only differed in $\delta^{13}C$ but not in $\delta^{15}N$ and $\delta^{2}H$ values. *Fucus* macroalgae was more enriched in $\delta^{13}C$ than phytoplankton and sediment samples. While no clear separation was observed in $\delta^{15}N$ and $\delta^{2}H$ values (Figure 114).

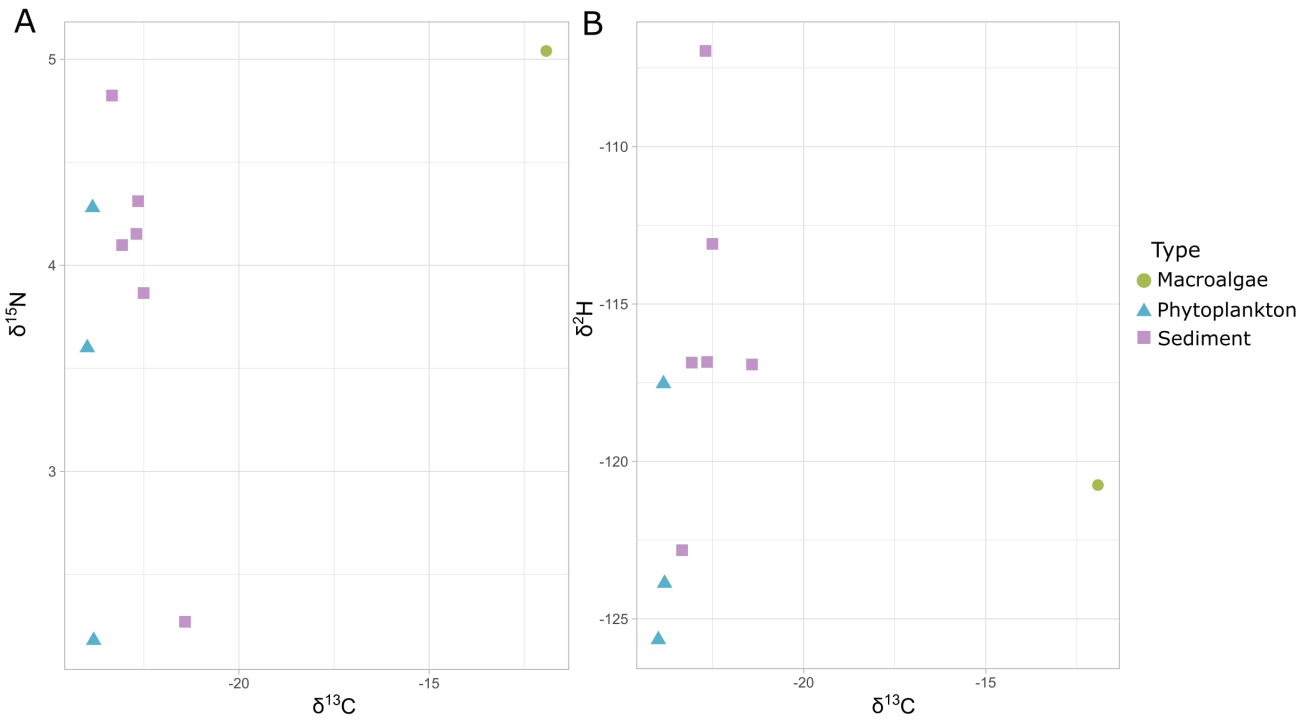


**Figure 114. Dual isotope plots showing A. δ¹⁵N vs δ¹³C and δ²H vs δ¹³C (right panel) for green macroalgae (green circles), phytoplankton (blue triangles), and sediment (purple squares), samples from Finland.**

Finland particulate matter had lower $\delta^{13}C$ values compared to *Fucus* macroalgae but closer to Finland sediment. $\delta^{15}N$ and $\delta^{2}H$ values where similar for the three groups (Figure 115).

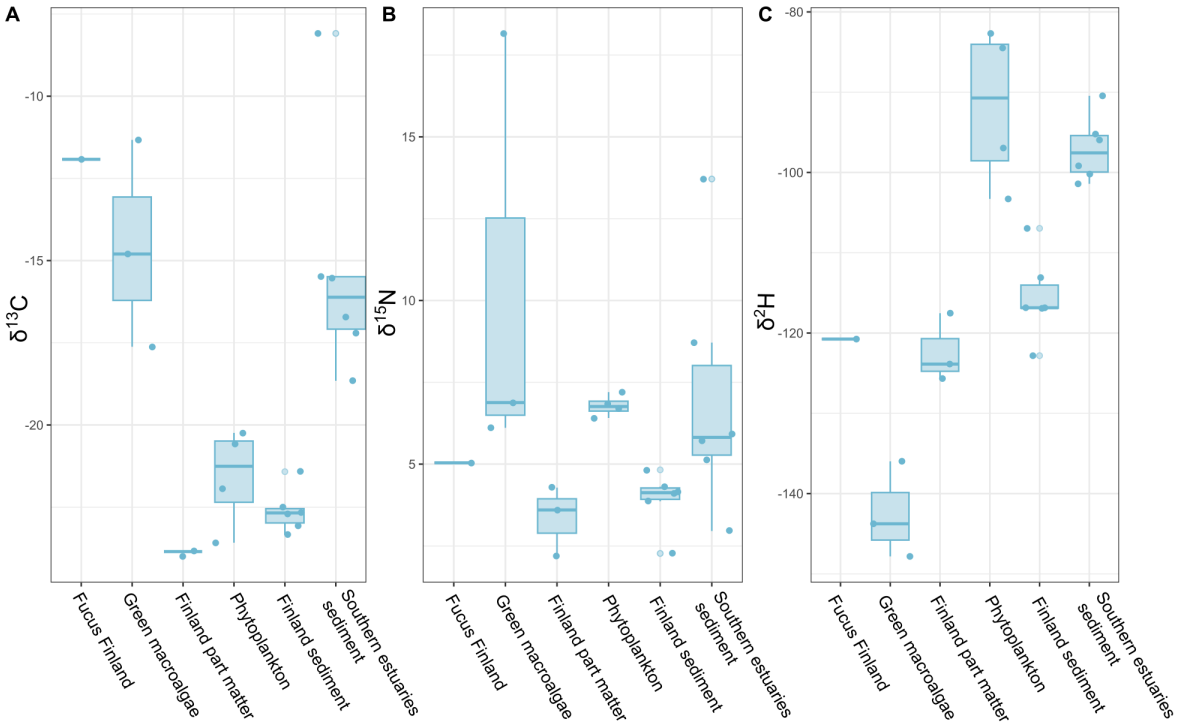


**Figure 115. Boxplots displaying the ranges of δ¹³C (A), δ¹⁵N (B), and δ²H (C) isotopic values across various sample types, including *Fucus* from Finland, green macroalgae, particulate organic matter (POM), phytoplankton, and sediments from Finland and southern estuaries.**

The isotopic composition of sedimenting material and particulate matter at three sites in Finland shows variability in δ¹³C, δ¹⁵N, and δ²H values. Particulate matter across the sites displays relatively consistent carbon isotope values, with δ¹³C ranging from -23.8‰ to -24.0‰, while δ¹⁵N vary more widely, from 2.2‰ at Site 3 to 4.3‰ at Site 1. δ²H also exhibit variability, ranging from -117.5‰ at Site 1 to -125.7‰ at Site 2. The sedimenting material had similar values than those found in particulate matter, with δ¹³C values between -23.8‰ and -24.4‰ across the three sites. δ¹⁵N values range from 2.8‰ at Site 3 to 4.4‰ at Site 1, while δ²H values range from -118.1‰ to -131.7‰.

## 5.4.5 C:N ratios and sediment organic C content

Total organic carbon of green macroalgae from the southern estuaries ranged from 10.8-19.4%, phytoplankton from Langstone harbour had a lower %C content of 0.7 ± 0.3%. %N showed a similar pattern where higher values were observed in macroalgae compared to phytoplankton samples, range= 0.72-2.4% and 0.1 ± 0.05% respectively. C:N ratios for green macroalgae were similar in Langstone and Grove Av (15.58 and 15) and Poole East and Port Solent macroalgae (8.08 and 8.1) (Table 22).

Sedimenting material from Finland samples %C ranged from 4-7.5% and 2.7-4.3% for %N. C:N ratios ranged from 0.9 to 2.7 and increased from site 1 to site 3 (Table 22). Particulate matter showed a higher %C content ranging from 7.7-9.3% while %N values ranged from 1.1-4 (Table 22).

Surface sediment %C from Langstone had the lowest value among the southern estuaries with 1.9%, followed by Port Solent with 2.4% and Poole Harbour with considerably higher %C of 6.6%. %N fall in the range of 0.3-0.9% being Langstone the site with lowest value and Poole Harbour the highest, while Port Solent had 0.4%. C:N ratios for surface sediment from southern estuaries were relatively low for all sites being 7.3, 6.7, and 5.7% for Poole Langstone and Port Solent respectively.

Deeper sediment from southern estuaries, presented a decrease in %C, values where lower in Langstone with 1.2%, then Port Solent followed with 1.5 and Poole harbour had 4%. %N presented lower values than surface sediment with values starting at 0.2% in Langstone, 0.3% in Port Solent and 0.3% in Poole. C:N ratios in

Langstone and Port Solent remained similar to the ones found in surface sediment, with 7.24 and 5.58 respectively, whereas Poole Harbour had a substantial increase to 12.7.

Sediment surface samples from Finland, had similar values of %C in site 1 and site 3 (5.1 and 5.7%), while site 2 had a lower %C of 3.2%. Similarly, %N for site 1 and 3 where 0.7 and 0.8% respectively and site 2 had slightly lower %N of 0.4%. C:N ratios for surface sediment where comparable for the three sites, decreasing with distance, from 7.8 to 7.3. In the deepest sediment, %C decreased in site 1 and 2 (4.5 and 4.3%) while for site 2 increased to 4.3%. %N was comparable at all sites ranging from 0.56-0.58 and C:N ratios remained similar to surface sediments (7.5-7.9) (Table 22).

**Table 22. Elemental %C, %N and C:N ratios for the different sample groups: Primary producers, sediment, and particulate matter samples. NM= Not measures, standard deviation was provided when multiple samples were available.**

| Macroalgae | | | |
|---|---|---|---|
| **Site** | **%C** | **%N** | **C:N** |
| Green macroalgae Langstone | 11.36 | 0.73 | 15.58 |
| Green macroalgae Poole East | 19.37 | 2.39 | 8.11 |
| Green macroalgae Port Solent | 16.44 | 2.03 | 8.08 |
| Green macroalgae Grove Av | 10.76 | 0.72 | 15 |
| *Fucus vesiculosus* (Finland) | NM | NM | NM |
| Phytoplankton Langstone | 0.7±0.32 | 0.09±0.04 | 0.1±0.05 |
| **Sedimenting material and particulate matter** | | | |
| **Site** | **%C** | **%N** | **C:N** |
| Finland particulate matter site 1 | 7.93 | 1.11 | 7.14 |

| | | | |
|---|---|---|---|
| Finland particulate matter site 2 | 7.67 | 1.59 | 4.82 |
| Finland particulate matter site 3 | 9.34 | 3.96 | 2.35 |
| Sedimenting material site 1 | 4 | 4.35 | 0.92 |
| Sedimenting material site 2 | 6.82 | 3.63 | 1.88 |
| Sedimenting material site 3 | 7.51 | 2.75 | 2.73 |

| Sediment samples | | | | | | |
|---|---|---|---|---|---|---|
| | Surface | | | Deep | | |
| Site | %C | %N | C:N | %C | %N | C:N |
| Langstone | 1.94 | 0.28 | 6.74 | 1.19 | 0.16 | 7.24 |
| Poole | 6.6 | 0.9 | 7.3 | 3.99 | 0.31 | 12.7 |
| Port Solent | 2.41 | 0.42 | 5.67 | 1.55 | 0.28 | 5.58 |
| Finland site 1 | 5.10 | 0.66 | 7.78 | 4.46 | 0.56 | 7.95 |
| Finland site 2 | 3.12 | 0.41 | 7.69 | 4.33 | 0.58 | 7.48 |
| Finland site 3 | 5.67 | 0.78 | 7.26 | 4.28 | 0.57 | 7.5 |

# 5.5 Discussion

## 5.5.1 C:N ratios

Low C:N ratios of 4-10 are indicative of unaltered algal derived organic carbon while vascular plants display C:N ratios >20 (Meyers, 1994), Poole East and Port Solent macroalgae had relatively low C:N ratios of 8.1 and 8.08 respectively, however Grove Avenue and Langstone macroalgae C:N ratios were considerably higher 15 and 15.6. Higher C:N ratios have been reported for macroalgae samples with a wide range depending on genre (Goni & Hedges, 1995).

Surface sediment samples for the three sites where on the lower end, Langstone 6.7, Poole 7.3 and Port Solent 5.7, closer values for autochthonous origin. In deeper sediment from Langstone and Port Solent C:N ratios remained relatively low close to surface values, 6.7 and 5.8 respectively whereas deeper sediment from Poole had a substantial C:N increase to 12.7.

Organic matter loss as degradation progress with depth can complicate the source identification using C:N ratios (Lamb et al., 2006), especially in sites with low organic carbon due to the to absorb ammonium ions produced by the decomposition of organic material (Goni & Hedges, 1995). This diagenetic transformation has been linked to lower ratios with depth (Cowie et al., 2009; Müller, 1977). However, sediment incubation experiments with marine macroalgae have shown an increase in C:N to be greater in anaerobic settings (Kristensen, 1994). The increase of C:N ratios observed in Poole Harbour with depth, also supported in downcore profiles (Table 22), could be attributed to preferential loss of N, nonetheless organic C

remained considerably higher than in other sites which might have outweigh the lowering of C:N ratio.

The transformations of C:N ratios as organic material decay are not clearly understood, which difficult the use of ratios especially in deeper sediment, however C:N ratios observed in surface sediments from southern estuaries suggest the relevance of marine derived primary organic carbon within these sites. Furthermore, seasonal patterns observed in Langstone for C:N ratios, where lower ratios were observed during winter also support the hypothesis of autochthonous contribution to the sediment organic C pool.

### 5.5.2 CuO oxidation products and principal component analysis

A total of 11 CuO oxidation products from green macroalgae samples were produced from brown macroalgae species. 2-Butenedioic acid (Compound 5) was an abundant compound in both macroalgae groups. This compound is a dicarboxylic acid and was also the most abundant CuO product from brown and green algae collected from Skay Bay (Goni & Hedges, 1995) and in other brown macroalgae species from the Portuguese coast, *Undaria pinnatifida, Laminaria ochroleuca, Cystoseira tamariscifolia, Himanthalia elongate and Sargassum muticum* (Santos et al., 2016).

2-Butenedioic acid was generally present and abundant in both sediment and macroalgae samples, this compound was persistent with depth suggesting resistant

to degradation. However, giving that it is also produced as a CuO product of other primary producers such as brown algae, bacteria, and phytoplankton (Goni & Hedges, 1995), this could not be used as a green macroalgae biomarker.

Nonetheless, the abundant compound 16 (unknown) was present in all green macroalgae in greater amounts than in brown macroalgae. The abundance of this compound was also linked to the amount of organic C of the sediment samples. For example, the sub surface peak of organic C in the core D from Poole East was correspondent to the increase in concentration of compound 16. Suggesting the potential link with the source macroalgae. Further identification of the identity of compound 16 is beyond the scope of this project, however a first step of discrimination is the fact that is a non-lignin phenol as a result of the method application (Goni and Hedges, 1995). Further investigation on the identity of this compound and more accurate measurement of its concentration within macroalgae and sediment C stocks can strengthen the confidence of its potential use of compound 16 as a biomarker for green macroalgae.

When CuO oxidation products from the green macroalgae and sediment from the same sites were analysed, there was a clear agreement on the number of compounds produced by the oxidation with CuO. Therefore, success in the use of CuO oxidation products for identifying macroalgal C inputs to sediment will be greatly enhanced if local macroalgal samples are collected and analysed.

4-Hydroxybenzoic acid, labelled as compound 13 was present at low concentrations in macroalgae samples. Nonetheless, this compound is also one of the most common lignin phenols *p*-Hyroxybenzoic acid (PHACID) which is traditionally linked to terrestrial origin (Hedges & Mann, n.d.; Sun et al., 2017). However, lignin phenols have been reported in marine vascular plants such as seagrasses (Cragg et al, 2020) and particularly PHACID was found in the brown algae *Undaria* pinnatifida (Mekinić et al., 2019). This is of major importance to be recognised as the application of this approach in marine sediments could be overestimating terrestrial contribution in marine sediments. Although in a smaller proportion, PHACID (Compound 13) was identified within the brown algae *Dictyosiphon*, green algae *Cladophora* and all green macroalgae from southern estuaries (Langstone, Poole E, Grove Av and Port Solent).

The sites with higher organic C content within the sediment were also the sites where the macroalgae samples had higher organic C. For example, Poole Harbour macroalgae had the highest organic C (19.4%) from all the green algae analysed and this site was also the site with more organic C sediment content (range organic C) and the greatest number of relevant CuO oxidation products. Similarly, in Grove Avenue where macroalgae organic C was lowest (10.8%) reflected with lower organic C in the sediment and a lower number of CuO oxidation products. Same from macroalgae cover/biomass add.

Despite being seagrass observed during fieldwork in Grove Avenue (Portsmouth site) this was not reflected in more organic carbon within sediment. This further suggests a link between macroalgae and sediment C stocks, and indicates that total CuO oxidation product concentration, or the CuO oxidation product suite (e.g. as

indicated by PCA) may be helpful indicators of macroalgal C. This work has produced some early indicators of how CuO oxidation products could be used to identify macroalgal C in sediments, and further follow up work is now required to test the ideas in a wider range of sites.

### 5.5.3 Stable Isotopes

Green macroalgae samples from southern estuaries had similar $\delta^{13}C$ values ranging from –17.6 to –11.3‰, and $\delta^{15}N$ values where 6.1‰ and 6.9‰ for Langstone and Port Solent algae respectively (Table 21). Marine macroalgae show $\delta^{13}C$ values ranging from -10‰ to -15‰, whereas phytoplankton tend to have lighter $\delta^{13}C$ values, around -27 to -22‰ (Duarte et al., 2018; Golubkov et al.,2020). The ability of green macroalgae to utilize bicarbonate ($HCO_3^-$) as a carbon source makes $\delta^{13}C$ values for macroalgae heavier than those for phytoplankton (Golubkov et al.,2020). The $\delta^{13}C$ values for green macroalgae from Langstone (-17.6‰) and Poole East (-11.3‰) reflected this typical pattern.

Enriched $\delta^{15}N$ in macroalgae has been linked to the influence of anthropogenic N in coastal environments (McClelland & Valiela, 1998) and primary producers (Jones et al., 2018). Due to the lack of fractionation within macroalgal tissue, macroalgae has been proposed as a bio indicator for N sources reflecting the environmental $\delta^{15}N$ conditions of the site (Cohen & Fong, 2005). Poole East macroalgae presented a considerably higher $\delta^{15}N$ value of 18.2‰ that reflects the degree of anthropogenic impact within this site compared to lower values of Langstone (6.1‰) and Port Solent (6.8‰) macroalgae samples. This enrichment in $\delta^{15}N$ was also observed in

Poole Harbour surface sediment (13.7‰) yet decreased to 8.71‰ in the deeper sediment. On the other hand, Langstone and Port Solent had lower values of (5.7-5.9‰) at the surface and decreased in deeper sediment in Port Solent to 2.9‰ while Langstone remained similar 5.1‰.

Values of $\delta^2H$ for marine macroalgae in the literature are currently limited compared to those of $\delta^{13}C$ and $\delta^{15}N$, although some studies have reported seagrass and macroalgal $\delta^2H$. For instance, macroalgae and seagrasses from the Red Sea were distinct in $\delta^2H$ values as well, while seagrasses had heavier $\delta^2H$ (-56.6 ± 2.7‰) compared to macroalgae (-95.7 ± 3.6‰) (Duarte et al., 2018). In contrast, the $\delta^2H$ values for phytoplankton from Langstone (-91.9‰) and Finland (-138.6‰) show a broader range, with phytoplankton from Langstone exhibiting less negative values, which may reflect local environmental differences, such as freshwater input or varying salinity levels (Sauer et al. 2001).

Sediment samples showed to be closer to the $\delta^2H$ values observed for phytoplankton, especially in Langstone where phytoplankton $\delta^2H$ values are less negative, around -91.9‰. However, in other regions where macroalgae show highly negative $\delta^2H$ values (as seen in Poole East and Port Solent), the deeper sediment $\delta^2H$ values are closer to macroalgae, suggesting a potential contribution from macroalgae-derived organic matter at greater depths. This variability highlights the complexity of isotopic signals in coastal sediments, which are likely influenced by a combination of both macroalgae and phytoplankton inputs, as well as other

environmental factors like salinity and freshwater mixing (Sachse et al., 2012; Sauer et al., 2001).

*Fucus vesiculosus* did not differ from green macroalgae $\delta^{13}C$ values, however it was different from phytoplankton values reported in the literature, with more depleted values (-27.6 ± 0.2‰) than the macroalgae (–11.9‰). $\delta^{13}C$ values for sedimenting material ranged (–24.4 to –23.8‰) and particulate matter (–24 to –23.8‰). Surface sediment samples displayed similar values $\delta^{13}C$ (–23.3 to –22.6‰) and these remained constant for deeper sediment presenting a slight increase in all sites (–23.1 to –21.4‰). $\delta^{15}N$ values for particulate matter and sedimenting material ranged between 2.2‰ and 4.3‰, showing in both cases a depletion with distance (Site 1 to site 3) (Table 14). Phytoplankton had a lower $\delta^{15}N$ (1.6 ± 0.7‰) whereas *Fucus* macroalgae had a higher $\delta^{15}N$ value compared to other material (5.04‰). On the other hand, surface sediment samples $\delta^{15}N$ were similar for all sites (4.1 – 4.8‰) nonetheless, deeper sediment $\delta^{15}N$ values decreased in all sites (2.3 – 4.1‰). There were not significant differences between $\delta^{2}H$ primary producers, however all sediment samples had lighter $\delta^{2}H$ values (–122.8 to –107‰).

When grouped separately brown and green algae are significantly different from each other as demonstrated by Carvalho et al. (2017), that reported bulk $\delta^{2}H$ values for different macroalgae collected from the coasts of Argentina, Brazil, and Australia. There was a significant difference between the two groups of macroalgae, where *Ulvophyceae* presented depleted $\delta^{2}H$ values regarding of their location, (-135‰, -

112.5 ± 13.5‰ and -115.5 ± 9.9‰) and were significantly lower in $\delta^2H$ compared to brown macroalgae (Carvalho et al. 2017).

Green macroalgae from southern estuaries (Table 21) depleted values of $\delta^2H$ (-147.8 to -136‰) are comparable to the ones reported previously in the literature. Results presented for Langstone phytoplankton showed a clear differentiation between from green macroalgae in $\delta^2H$. Providing promising use for $\delta^2H$ in distinguishing microalgae from macroalgae contributions to sediment organic C, especially when $\delta^{13}C$ and $\delta^{15}N$ values overlap. It is of great importance to have a good representation of isotopic signatures from the possible C contributors and have previous evidence of distinctive values in order to accurately predict sedimentary contributions of organic carbon.

## 5.6 Conclusion

It is crucial to identify the sources, or endmembers, of sediment organic carbon in coastal environments to improve our understanding of the carbon cycle and to highlight the significant role that macroalgae-derived carbon plays in these ecosystems. This chapter gathered data from different analyses including CuO oxidation products, triple isotopic $\delta^{13}C$, $\delta^{15}N$ and $\delta^{2}H$ and C:N to evaluate the possible contribution from macroalgae to sediment organic carbon. Furthermore, comparisons were made with different macroalgae groups specifically on CuO products method to identify patterns among the different species.

Given the previous results from the different analyses performed in different groups of macroalgae and sediment samples, there are indicative evidence of marine derived organic carbon within the southern estuaries sites specifically from green macroalgae. For instance, the pattern in CuO oxidation products from the green macroalgae was found in both surface and deeper sediment samples. There is the potential to utilise the CuO oxidation pattern from primary producers and elucidate contribution for macroalgae derived carbon. This was also further confirmed with the PCA were sediment samples from Langstone and Poole Harbour clustered close to the corresponding green macroalgae, reflecting the similar composition of macroalgae and sediment samples (RQ9 & RQ10).

The C:N and use of bulk isotopes $\delta^{13}C$, $\delta^{15}N$ and $\delta^{2}H$ pointed out the possible contribution of these green macroalgae to the sediment, showing that the combination of these three isotopic signatures can be used to discern between

phytoplankton and macroalgae producers contributing to the sedimentary organic C. While $\delta^2H$ was effective in distinguishing between phytoplankton and green macroalgae, it did not differentiate brown macroalgae, which could be attributed to site-specific factors or variations in isotopic assimilation. With a sufficient number of samples and a low number of endmembers the use of bulk $\delta^{13}C$, $\delta^{15}N$ and $\delta^2H$ in mixing models could be used to quantify contributions of marine derived organic carbon in sediment samples (RQ11).

This chapter presented evidence of promising analytical tools for the identification of macroalgae derived carbon within estuarine sediments. Providing a basis for more detailed investigation of macroalgae derived organic C in these sites. Furthermore, this is one of the first investigations on the use of $\delta^2H$ as a tool for discriminating marine organic carbon in estuarine sediments.

Chapter 6.

# Synthesis

The present thesis explored the historical trends on eutrophication within the UK estuaries, evaluated the impact of macroalgae blooms on sediment biogeochemistry between different systems and seasons and explored the possibility for identifying macroalgae derived carbon in coastal sediments.

## 6.1 Role of macroalgae on the organic carbon cycle and estuarine dynamics

The different chapters within this thesis are interconnected through the holistic understanding the role of benthic macroalgae in shaping estuarine ecosystems functioning. The present work starts by examining the factors controlling macroalgae blooms (Chapter 1), identifying the key environmental drivers that contribute to the formation and persistence of these blooms. This foundational understanding is crucial, as macroalgae blooms play a significant role in altering sediment dynamics and influencing ecosystem health.

Building on this, Chapter 3 presented the comparison of sediment biogeochemistry of three estuaries in the UK, offering insight into the impact of macroalgae blooms on sediment biogeochemistry particularly on larger spatial areas than patches with or without macroalgae. Extensive and persistent macroalgae blooms create a long-term barrier over the sediment-water interface, physically preventing oxygen from penetrating the sediment underneath. This heavily impacts nutrient dynamics, redox

conditions, and organic carbon cycling and as a whole these conditions can favour organic carbon preservation in these systems. In Chapter 4, the factor of seasonality specifically with macroalgae blooms is evaluated. The results supported the findings from the previous chapter, demonstrating that the biogeochemical modifications driven by excessive macroalgal growth persist throughout the summer and autumn seasons. Additionally, the data on organic carbon content, combined with C:N ratios

ratios, suggest contribution of marine autochthonous material to sediment carbon stocks.

The final Chapter 5 brings together the previous findings by investigating the extent to which carbon derived from macroalgae contributes to sediment carbon stocks. This was evaluated by the use of two methods that included CuO oxidation products and a triple isotope approach using $\delta^{13}C$, $\delta^{15}N$ and $\delta^{2}H$. With CuO products results it was possible to identify patterns and compounds produce by the oxidation of macroalgae and sediment samples, which directly linked the sediment composition to the one observed in the macroalgae. Further exploration with a PCA analysis confirmed the similarities between macroalgae as a source to the sediment samples. On the other hand, the incorporation of $\delta^{2}H$ was capable of distinguish between green macroalgae and phytoplankton, and results are also supportive of autochthonous material in the sediment.

This work provides a deeper understanding of the role macroalgae play in carbon cycling and potential carbon sequestration within these estuarine systems. Providing a cohesive exploration of how macroalgae influence sedimentary

processes, ultimately contributing to broader discussions on ecosystem function and carbon dynamics in coastal environments.

## 6.2 Monitoring eutrophication

There is a robust data set for water column nutrients within the UK monitoring programs compared to macroalgal biomass and cover which complicates comparisons between temporal and spatial scales as showed in Chapter 2. Data collection for monitoring programs is a challenging, time and resource consuming. However, there has been successful programs that involve citizen science to improve data collection capacity specifically for the purpose of monitoring eutrophication within UK estuaries. For example, Marine Forests program is an initiative where volunteers provide photos with date and location to improve understanding of distribution and monitoring of marine organisms including macroalgae, seagrass and fauna (www.marineforests.com).

Another successful case of monitoring algae blooms using citizen science is run by the UK Centre of Ecology and Hydrology who developed a smartphone app called Bloomin' Algae, which is currently focused on cyanobacteria blue-green blooms (Centre for Ecology & Hydrology, n.d.). Nonetheless, there is an opportunity to expand the use of these technologies alongside citizen science in order to inform government agencies, monitoring programs and public awareness of these issues. The use of citizen science thus, is a great tool that cover great spatial extents by

encouraging society participation benefiting data collection and reducing its associated costs (Duffi et al., 2019).

## 6.3 Macroalgae blooms, controlling factors and sediment biogeochemistry.

Macroalgae blooms are a persistent sign of eutrophication in several estuaries in the UK. Secondary data for nutrient concentration, macroalgae cover and biomass, along with some physical characteristics which could potentially control macroalgae growth were analysed. Solely water column nutrient enrichment did not appear to control macroalgae blooms in the UK estuaries. Instead, several factors must combine to promote eutrophication symptoms to develop, including sufficient nutrients for algae growth, enough time for the nutrients to be assimilated by the algae and a suitable intertidal area where light is available for photosynthesis to occur (Chapter 2).

Secondary historical data for macroalgae biomass indicated an increase in Langstone and Poole Harbours biomass production in the affected intertidal area. Whereas Portsmouth Harbour saw a considerable decrease in macroalgae cover, however the last biomass data indicated comparable values than the ones with more macroalgae cover. This suggests that although a reduction in the extension of macroalgae blooms has been achieved in Portsmouth site, the biomass production remains high for the particularly affected sites within the same estuary. This is also reflected in sediment biogeochemistry in Portsmouth Harbour, where the two sampled sites showed a considerable difference in the observed macroalgae cover

during fieldwork, this was reflected in benthic nutrient concentrations and organic carbon storage.

Langstone Harbour records showed a persistent problem in macroalgae biomass production. This site showed the highest DIN within porewaters, and a clear differentiation was observed in porewater profiles, where the presence of macroalgae fuelled the production of ammonium within the sediment particularly on the top. This same patter was observed in Poole Harbour where ammonium concentrations at the top where considerably higher, besides concentrations on the presence of macroalgae was higher at Poole East.

Higher ammonium concentrations within porewaters have been associated with decomposition of macroalgae detritus in the sediment (Garcia-Robledo et al., 2013) and during growing phase benthic ammonium can be utilised for macroalgae to produce more biomass (Trimmer et al., 2000). This process will make macroalgae mats self-sustained and therefore not dependant of water column nutrient enrichment. It is highly possible that this mechanism was occurring in the most impacted sites Poole and Langstone Harbours.

The general trend observed for Fe concentrations in porewaters was of depletion and absence of Fe under macroalgae mats, suggesting that redox biogeochemistry for these sites could be sub-oxic and anoxic especially in Langstone and Poole Harbours. Mn profiles under macroalgae mats where accumulation was happening downcore, can be the result of organic carbon decomposition in which, with the

resulting dissolved Mn remaining in porewaters rather than precipitating as a sulphide (Luther et al., 1998).

Previously mentioned ammonium, Fe and Mn trends coupled with the reduction in S/Na ratios downcore provides evidence of the limited oxygen penetration within these sediments especially when macroalgae was on top of the sediment, more remineralisation of organic carbon could be occurring at the same time.

The analysis in eutrophication status compared to biomass data and sediment biogeochemistry also emphasises the importance of the evaluation of eutrophication in the UK estuaries through field campaigns, since eutrophication impacts cannot be predicted solely by remote sensing or aerial imagery. Besides, impacts on benthic biogeochemistry are persistent on the sites where macroalgae blooms are still an occurring problem.

## 6.4 Macroalgae blooms and carbon storage

Results from macroalgae and sediment CuO oxidation products and triple isotope discrimination suggest that macroalgal derived organic C is present in the sediment. Furthermore, some of these compounds are also present at 10-12 cm depth, potentially being resistant to degradation.

Previous biomass data and field observations support that more macroalgae tends to result in more sediment organic carbon being stored. The organic carbon present in the top 12 cm of these sediments is considerable, ranging between 0.25-6.6%. Grove Av being the site with the lowest (0.7 ± 0.16%) followed by Langstone (1.36

± 0.2%) and Port Solent (1.7 ± 0.6%). While Poole Harbour sites had the highest mean OC values with 3.7 ± 0.2 and 4.64 ± 0.85 in Poole West and East respectively. Given that the more impacted sites also showed more and relatively constant organic carbon downcore, sub-oxic and anoxic conditions taking place in the sediments are indicative of an additional mechanism contributing to the increase of organic C when the macroalgae biomass is considerable. This has been observed previously at smaller scales in incubation experiments (Corzo et al., 2009).

Results also suggest that non-vegetated intertidal areas are more relevant to organic carbon storage than initially thought. Although, there are requirements for blue carbon that opportunistic macroalgae do not meet such as the opportunity to apply policies to protect these ecosystems, we cannot neglect the fact that substantial amounts of autochthonous biomass whether is phytoplankton or macroalgal origin is being produced within these systems. Understanding the fate of this production is crucial for comprehending the organic carbon cycle and relevance of these ecosystems on capturing carbon. Work presented within this thesis is valuable evidence for the understanding on possible contribution of benthic macroalgal derived C to sediment C stocks.

Although eutrophication is a recognised threat to the natural functioning of ecosystems, the excess of biomass produced by macroalgae blooms particularly benthic macroalgae that grow on top of the sediment, is relevant for organic carbon storage on these sites. The physical capping mechanism creates the biogeochemical conditions that could favour preservation of more organic C within

these ecosystems. Furthermore, was a seasonal increase in sediment organic C during winter which represent an opportunity for further investigation. While there is indication of autochthonous biomass being responsible for this increase, further evidence would be needed to elucidate the source and fate of the accumulated organic C.

This work presented evidence of promising analytical tools for the identification of macroalgae derived carbon within estuarine sediments including CuO oxidation products and triple in $\delta^{13}C$, $\delta^{15}N$ and $\delta^{2}H$ isotopes. Providing a basis for more detailed investigation of macroalgae derived organic C in these sites. this is one of the first investigations on the use of $\delta^{2}H$ as a tool for discriminating marine organic carbon in estuarine sediments.

## 6.5 Limitations and future work

Comparing historical data on macroalgal biomass and coverage proved challenging due to a lack of consistent data, making it difficult to analyse historical trends across different temporal and spatial scales. There is significant potential for incorporating citizen science to collect data, which could greatly enhance our understanding of macroalgal blooms in these ecosystems.

Long-term seasonal studies in estuarine environments with high benthic macroalgal production offer a valuable opportunity to assess the accumulation of marine-derived organic carbon within these systems. The evidence presented in this work highlights the critical role of intertidal ecosystems (Often overlooked in the context

of blue carbon) in the organic carbon cycle. Although traditionally not considered significant in blue carbon research, these ecosystems are gaining increasing recognition for their potential contribution to organic carbon storage and sequestration and more evidence is needed to inform policy makers on this regard.

As the nature of this work was to explore the possibility of being able to identify macroalgal carbon, this translated in a limited number of samples analysed. Therefore, there is opportunity for further investigation of isotopic signatures using bulk stable isotopes ($\delta^{13}C$, $\delta^{15}N$ and $\delta^{2}H$) and with a robust data set there is the option to use mixing models to elucidate more information regarding sedimentary organic carbon sources. Future work should focus on increasing the confidence in the use of $\delta^{2}H$ alongside $\delta^{13}C$ and $\delta^{15}N$ within different systems in order to be confident of their wider application for organic C fate studies specially within dynamic environments such as estuaries.

Additionally, some of the CuO oxidation products presented in this study show potential for further investigation as biomarkers for green macroalgae. However, uncertainties remain, such as the identification of these compounds and their transformations during the remineralization of organic matter. Isolating these compounds and understanding their transformations as they are deposited in sediments would be a significant step toward identifying a reliable biomarker for macroalgal carbon in these environments.

# References


Aldridge, J. N., & Trimmer, M. (2009). Modelling the distribution and growth of “problem” green seaweed in the Medway estuary, UK. *Hydrobiologia*, *629*(1), 107–122. https://doi.org/10.1007/s10750-009-9760-6

Aller, R. C. (1994). Bioturbation and remineralization of sedimentary organic matter: Effects of redox oscillation. *Chemical Geology*, *114*, 331–345. https://doi.org/10.1016/0009-2541(93)E0257-T

Anderson, G. F. (1986). Silica, diatoms, and a freshwater productivity maximum in Atlantic Coastal Plain estuaries, Chesapeake Bay. *Estuarine, Coastal and Shelf Science*, *22*(2), 183-197. https://doi.org/10.1016/0272-7714(86)90112-5

Atkinson, M. J., & Smith, S. V. (1983). C:N:P ratios of benthic marine plants. In *Limnology and Oceanography* (Vol. 28, Issue 3, pp. 568–574). https://doi.org/10.4319/lo.1983.28.3.0568

Bally, G., Mesnage, V., Deloffre, J., Clarisse, O., Lafite, R., & Dupont, J. P. (2004). Chemical characterization of porewaters in an intertidal mudflat of the Seine estuary: Relationship to erosion-deposition cycles. *Marine Pollution Bulletin*, *49*(3), 163–173. https://doi.org/10.1016/j.marpolbul.2004.02.005

Bergstrom, U., Sundblad, G., Downie, A. L., Snickars, M., Bostrom, C., & Lindegarth, M. (2013). Evaluating eutrophication management scenarios in the Baltic Sea using species distribution modelling. *Journal of Applied Ecology*, *50*(3), 680–690. https://doi.org/10.1111/1365-2664.12083

Bermejo, R., Golden, N., Schrofner, E., Knöller, K., Fenton, O., Serrão, E., & Morrison, L. (2022). Biomass and nutrient dynamics of major green tides in Ireland: Implications for biomonitoring. *Marine Pollution Bulletin*, *175*. https://doi.org/10.1016/j.marpolbul.2021.113318

Bermejo, R., Heesch, S., Mac Monagail, M., O’Donnell, M., Daly, E., Wilkes, R. J., & Morrison, L. (2019). Spatial and temporal variability of biomass and composition of green tides in Ireland. *Harmful Algae*, *81*, 94–105. https://doi.org/10.1016/j.hal.2018.11.015

Berner Robert A. (1982). Burial of organic carbon and pyrite sulfur in the modern ocean; its geochemical and environmental significance. *American Journal of Science*, *282*(4), 451–473.

Björnsäter, B. R., & Wheeler, P. A. (1990). EFFECT OF NITROGEN AND PHOSPHORUS SUPPLY ON GROWTH AND TISSUE COMPOSITION OF ULVA FENESTRATA AND ENTEROMORPHA INTESTINALIS (ULVALES, CHLOROPHYTA). *Journal of Phycology*, *26*(4), 603–611. https://doi.org/10.1111/j.0022-3646.1990.00603.x

Bonsdorff, E., Blomqvist, E. M., Mattila, J., & Norkko, A. (1997). Coastal eutrophication: Causes, consequences and perspectives in the Archipelago areas of the northern Baltic Sea. *Estuarine Coastal and Shelf Science*, *44*, 63–72. https://doi.org/10.1016/s0272-7714(97)80008-x

Bonsdorff, E., Ronnberg, C., & Aarnio, K. (2002). Some ecological properties in relation to eutrophication in the Baltic Sea. *Hydrobiologia*, *475*(1), 371–377. https://doi.org/10.1023/a:1020395526898

Boudreau, B. P. (1998). Mean mixed depth of sediments: The wherefore and the why. *Limnology and Oceanography*, *43*(3), 524–526. https://doi.org/10.4319/lo.1998.43.3.0524

Boynton, W. R., Kemp, W. M., & Keefe, C. W. (1982). A COMPARATIVE ANALYSIS OF NUTRIENTS AND OTHER FACTORS INFLUENCING ESTUARINE PHYTOPLANKTON PRODUCTION. *Estuarine Comparisons*, 69–90. https://doi.org/10.1016/B978-0-12-404070-0.50011-9

Breithaupt, J. L., Smoak, J. M., Smith, T. J., Sanders, C. J., & Hoare, A. (2012). Organic carbon burial rates in mangrove sediments: Strengthening the global budget. *Global Biogeochemical Cycles*, *26*(3). https://doi.org/10.1029/2012GB004375

Bricker, S. B., Longstaff, B., Dennison, W., Jones, A., Boicourt, K., Wicks, C., & Woerner, J. (2008). Effects of nutrient enrichment in the nation's estuaries: A decade of change. *Harmful Algae*, *8*(1), 21–32. https://doi.org/10.1016/j.hal.2008.08.028

Broch, O. J., & Slagstad, D. (2012). Modelling seasonal growth and composition of the kelp Saccharina latissima. *Journal of Applied Phycology*, *24*(4), 759–776. https://doi.org/10.1007/s10811-011-9695-y

Brown, J. R., Gowen, R. J., & McLusky, D. S. (1987). THE EFFECT OF SALMON FARMING ON THE BENTHOS OF A SCOTTISH SEA LOCH. *Journal of Experimental Marine Biology and Ecology*, *109*(1), 39–51. https://doi.org/10.1016/0022-0981(87)90184-5

Burdige, D. J. (2007). Preservation of organic matter in marine sediments: Controls, mechanisms, and an imbalance in sediment organic carbon budgets? *Chemical Reviews*, *107*(2), 467–485. https://doi.org/10.1021/cr050347q

Burdige, D. J. (2012). Estuarine and Coastal Sediments - Coupled Biogeochemical Cycling. In *Treatise on Estuarine and Coastal Science* (Vol. 5, pp. 279–316). Elsevier Inc. https://doi.org/10.1016/B978-0-12-374711-2.00511-8

Burson, A., Stomp, M., Greenwell, E., Grosse, J., & Huisman, J. (2018). Competition for nutrients and light: testing advances in resource competition with a natural phytoplankton community. *Ecology*, *99*(5), 1108–1118. https://doi.org/10.1002/ecy.2187

Caffrey J. M. (2002). Biogeochemical processes in a small California estuary. 1. Benthic fluxes and pore water constituents reflect high nutrient freshwater inputs. *MARINE ECOLOGY PROGRESS SERIES*, *233*, 39–53.

Carstensen, J., Andersen, J. H., Gustafsson, B. G., & Conley, D. J. (2014). Deoxygenation of the Baltic Sea during the last century. *Proceedings of the National Academy of Sciences of the United States of America*, *111*(15), 5628–5633. https://doi.org/10.1073/pnas.1323156111

Carstensen, J., Sánchez-Camacho, M., Duarte, C. M., Krause-Jensen, D., & Marbà, N. (2011). Connecting the dots: Responses of coastal ecosystems to changing nutrient concentrations. *Environmental Science and Technology*, *45*(21), 9122–9132. https://doi.org/10.1021/es202351y

Carvalho, M. C., Carneiro, P. B. de M., Dellatorre, F. G., Gibilisco, P. E., Sachs, J., & Eyre, B. D. (2017). Bulk hydrogen stable isotope composition of seaweeds: Clear separation between Ulvophyceae and other classes. *Journal of Phycology*, *53*(5), 961–969. https://doi.org/10.1111/jpy.12558

CEFAS. (2003). *Investigation of factors controlling the presence of macroalgae in some estuaries of the Southern Water Region.*

Chen, Z. L., & Lee, S. Y. (2022). Tidal Flats as a Significant Carbon Reservoir in Global Coastal Ecosystems. In *Frontiers in Marine Science* (Vol. 9). Frontiers Media S.A. https://doi.org/10.3389/fmars.2022.900896

Choi, T.-S., Kang, E.-J., Kim, J.-H., & Kim, K.-Y. (2010). Effect of salinity on growth and nutrient uptake of Ulva pertusa (Chlorophyta) from an eelgrass bed. *ALGAE*, *25*(1), 17–26. https://doi.org/10.4490/algae.2010.25.1.017

Cloern, J. E. (2001). Our evolving conceptual model of the coastal eutrophication problem. *Marine Ecology Progress Series*, *210*, 223–253. https://doi.org/10.3354/meps210223

Cloern, J. E., Canuel, E. A., & Harris, D. (2002). Stable carbon and nitrogen isotope composition of aquatic and terrestrial plants of the San Francisco Bay estuarine system. *Limnology and Oceanography*, *47*(3), 713–729. https://doi.org/10.4319/lo.2002.47.3.0713

Cohen, R. A., & Fong, P. (2005). Experimental evidence supports the use of δ15N content of the opportunistic green macroalga Enteromorpha intestinalis (Chlorophyta) to determine nitrogen sources to estuaries. *Journal of Phycology*, *41*(2), 287–293. https://doi.org/10.1111/j.1529-8817.2005.04022.x

Cole, J. J., Carpenter, S. R., Kitchell, J., Pace, M. L., Solomon, C. T., & Weidel, B. (2011). Strong evidence for terrestrial support of zooplankton in small lakes based on stable isotopes of carbon, nitrogen, and hydrogen. *Proceedings of the National Academy of Sciences of the United States of America*, *108*(5), 1975–1980. https://doi.org/10.1073/pnas.1012807108

Conley, D. J., & Malone, T. C. (1992). Annual cycle of dissolved silicate in Chesapeake Bay: Implications for the production and fate of phytoplankton biomass. *Marine Ecology Progress Series*, *81*, 121-128. https://doi.org/10.3354/meps081121

Corzo, A., van Bergeijk, S. A., & Garcia-Robledo, E. (2009). Effects of green macroalgal blooms on intertidal sediments: net metabolism and carbon and nitrogen contents. *Marine Ecology Progress Series*, *380*, 81–93. https://doi.org/10.3354/meps07923

Cowie, G. L., Mowbray, S., Lewis, M., Matheson, H., & McKenzie, R. (2009). Carbon and nitrogen elemental and stable isotopic compositions of surficial sediments from the Pakistan margin of the Arabian Sea. *Deep-Sea Research Part II: Topical Studies in Oceanography*, *56*(6–7), 271–282. https://doi.org/10.1016/j.dsr2.2008.05.031

Den Hartog, C. (1994). Suffocation of a littoral *Zostera* bed by *Enteromorpha radiata*. *Aquatic Botany*, *47*, 21-28. https://doi.org/10.1016/0304-3770(94)90018-3

De, T. K., De, M., Das, S., Chowdhury, C., Ray, R., & Jana, T. K. (2011). Phytoplankton abundance in relation to cultural eutrophication at the land-ocean boundary of Sunderbans, NE Coast of Bay of Bengal, India. *Journal of Environmental Studies and Sciences*, *1*, 169-180. https://doi.org/10.1007/s13412-011-0022-3

Deines, P. (1980). The carbon isotopic composition of diamonds: relationship to diamond shape, color, occurrence and vapor composition. In *Geochmru et Cosmochmica Acra* (Vol. 44).

Devlin, M., Bricker, S., & Painting, S. (2011). Comparison of five methods for assessing impacts of nutrient enrichment using estuarine case studies. *Biogeochemistry*, *106*(2), 177–205. https://doi.org/10.1007/s10533-011-9588-9

Diaz, R. J., & Rosenberg, R. (1995). Marine benthic hypoxia: A review of its ecological effects and the behavioural responses of benthic macrofauna. In A. D. Ansell, R. N. Gibson, & M. Barnes (Eds.), *Oceanography and Marine Biology - an Annual Review, Vol 33* (Vol. 33, pp. 245–303). <Go to ISI>://WOS:A1995BE76V00004

Diaz, R. J., & Rosenberg, R. (2008). Spreading dead zones and consequences for marine ecosystems. *Science*, *321*(5891), 926–929. https://doi.org/10.1126/science.1156401

Diesing, M., Kroger, S., Parker, R., Jenkins, C., Mason, C., & Weston, K. (2017). Predicting the standing stock of organic carbon in surface sediments of the North-West European continental shelf. *Biogeochemistry*, *135*(1–2), 183–200. https://doi.org/10.1007/s10533-017-0310-4

Dimitriou, P. D., Papageorgiou, N., & Karakassis, I. (2017). Response of Benthic Macrofauna to Eutrophication in a Mesocosm Experiment: Ecosystem Resilience Prevents Hypoxic Conditions. *Frontiers in Marine Science*, *4*, 10. https://doi.org/10.3389/fmars.2017.00391

Downie, A. L., von Numers, M., & Bostrom, C. (2013). Influence of model selection on the predicted distribution of the seagrass Zostera marina. *Estuarine Coastal and Shelf Science*, *121*, 8–19. https://doi.org/10.1016/j.ecss.2012.12.020

Downing, J. A. (1997). Marine nitrogen: Phosphorus stoichiometry and the global N:P cycle. *Biogeochemistry*, *37*(3), 237–252. https://doi.org/10.1023/a:1005712322036

Duarte, C. M., Delgado-Huertas, A., Anton, A., Carrillo-de-Albornoz, P., López-Sandoval, D. C., Agustí, S., Almahasheer, H., Marbá, N., Hendriks, I. E., Krause-Jensen, D., & Garcias-Bonet, N. (2018). Stable Isotope (δ13C, δ15N, δ18O, δD) composition and nutrient concentration of Red Sea primary producers. *Frontiers in Marine Science*, *5*(AUG). https://doi.org/10.3389/fmars.2018.00298

Duarte, C. M., Losada, I. J., Hendriks, I. E., Mazarrasa, I., & Marba, N. (2013). The role of coastal plant communities for climate change mitigation and adaptation. *Nature Climate Change*, *3*(11), 961–968. https://doi.org/10.1038/nclimate1970

Emerson, S. (1985). Organic carbon preservation in marine sediments. *The Carbon Cycle and Atmospheric CO*, 78–87. https://doi.org/10.1029/gm032p0078

Emerson, S., & Hedges, J. I. (1988). Processes controlling the organic carbon content of open ocean sediments. *Paleoceanography*, *3*(5), 621–634. https://doi.org/10.1029/PA003i005p00621

FitzGerald, W. J. (1978). *Environmental Parameters Influencing the Growth of Enteromorpha clathrata (Roth) J. Ag. in the Intertidal Zone on Guam*. *21*(4), 207–220. https://doi.org/doi:10.1515/botm.1978.21.4.207

Fleming-Lehtinen, V., Andersen, J. H., Carstensen, J., Łysiak-Pastuszak, E., Murray, C., Pyhälä, M., & Laamanen, M. (2015). Recent developments in assessment

methodology reveal that the Baltic Sea eutrophication problem is expanding. *Ecological Indicators, 48*, 380-388. https://doi.org/10.1016/j.ecolind.2014.08.022

Frankel, L. T., Friedrichs, M. A. M., St-Laurent, P., Bever, A. J., Lipcius, R. N., Bhatt, G., & Shenk, G. W. (2022). Nitrogen reductions have decreased hypoxia in the Chesapeake Bay: Evidence from empirical and numerical modeling. *Science of The Total Environment, 814*, 152722. https://doi.org/10.1016/j.scitotenv.2021.152722

Fong, P., Boyer, K. E., Desmond, J. S., & Zedler, J. B. (1996). Salinity stress, nitrogen competition, and facilitation: what controls seasonal succession of two opportunistic green macroalgae? *Journal of Experimental Marine Biology and Ecology*, *206*(1–2), 203–221. https://doi.org/10.1016/S0022-0981(96)02630-5

Fourqurean, J. W., Duarte, C. M., Kennedy, H., Marbà, N., Holmer, M., Mateo, M. A., Apostolaki, E. T., Kendrick, G. A., Krause-Jensen, D., McGlathery, K. J., & Serrano, O. (2012). Seagrass ecosystems as a globally significant carbon stock. *Nature Geoscience*, *5*(7), 505–509. https://doi.org/10.1038/ngeo1477

Galparsoro, I., Borja, A., & Uyarra, M. C. (2014). Mapping ecosystem services provided by benthic habitats in the European North Atlantic Ocean. *Frontiers in Marine Science*, *1*, 14. https://doi.org/10.3389/fmars.2014.00023

García-Robledo, E., & Corzo, A. (2011). Effects of macroalgal blooms on carbon and nitrogen biogeochemical cycling in photoautotrophic sediments: An experimental mesocosm. *Marine Pollution Bulletin*, *62*(7), 1550–1556. https://doi.org/10.1016/j.marpolbul.2011.03.044

García-Robledo, E., Corzo, A., García De Lomas, J., & Van Bergeijk, S. A. (2008). Biogeochemical effects of macroalgal decomposition on intertidal microbenthos: A microcosm experiment. *Marine Ecology Progress Series*, *356*, 139–151. https://doi.org/10.3354/meps07287

Garcia-Robledo, E., Revsbech, N. P., Risgaard-Petersen, N., & Corzo, A. (2013). Changes in N cycling induced by Ulva detritus enrichment of sediments. *Aquatic Microbial Ecology*, *69*(2), 113–122. https://doi.org/10.3354/ame01626

Garcias-Bonet, N., Delgado-Huertas, A., Carrillo-de-Albornoz, P., Anton, A., Almahasheer, H., Marba, N., Hendriks, I. E., Krause-Jensen, D., & Duarte, C. M. (2019). Carbon and Nitrogen Concentrations, Stocks, and Isotopic Compositions in Red Sea Seagrass and Mangrove Sediments. *Frontiers in Marine Science*, *6*, 12. https://doi.org/10.3389/fmars.2019.00267

Geoghegan, E. K., Caplan, J. S., Leech, F. N., Weber, P. E., Bauer, C. E., & Mozdzer, T. J. (2018). Nitrogen enrichment alters carbon fluxes in a New England salt marsh. *Ecosystem Health and Sustainability*, *4*(11), 277–287. https://doi.org/10.1080/20964129.2018.1532772

Geraldi, N. R., Ortega, A., Serrano, O., Macreadie, P. I., Lovelock, C. E., Krause-Jensen, D., Kennedy, H., Lavery, P. S., Pace, M. L., Kaal, J., & Duarte, C. M. (2019). Fingerprinting Blue Carbon: Rationale and Tools to Determine the Source of Organic Carbon in Marine Depositional Environments. *Frontiers in Marine Science*, *6*, 9. https://doi.org/10.3389/fmars.2019.00263

Golubkov, S. M., Nikulina, V. N., & Tiunov, A. V. (2020). Stable C and N isotope composition of suspended particulate organic matter in the Neva Estuary: The role of abiotic factors, productivity, and phytoplankton taxonomic composition. *Journal*

*of Marine Science and Engineering, 8*(12), 959. https://doi.org/10.3390/jmse8120959

Goni, M. A., & Hedges, J. I. (1995). SOURCES AND REACTIVITIES OF MARINE-DERIVED ORGANIC-MATTER IN COASTAL SEDIMENTS AS DETERMINED BY ALKALINE CUO OXIDATION. *Geochimica Et Cosmochimica Acta*, *59*(14), 2965–2981. https://doi.org/10.1016/0016-7037(95)00188-3

Gooday, A. J., Jorissen, F., Levin, L. A., Middelburg, J. J., Naqvi, S. W. A., Rabalais, N. N., Scranton, M., & Zhang, J. (2009). Historical records of coastal eutrophication-induced hypoxia. *Biogeosciences*, *6*(8), 1707–1745. https://doi.org/10.5194/bg-6-1707-2009

Graiff, A., Karsten, U., Radtke, H., Wahl, M., & Eggert, A. (2020). Model simulation of seasonal growth of Fucus vesiculosus in its benthic community. *Limnology and Oceanography-Methods*, *18*(3), 89–115. https://doi.org/10.1002/lom3.10351

Grall, J., & Chauvaud, L. (2002). Marine eutrophication and benthos: the need for new approaches and concepts. *Global Change Biology*, *8*(9), 813–830. https://doi.org/10.1046/j.1365-2486.2002.00519.x

Gray, J. S., Wu, R. S. S., & Or, Y. Y. (2002). Effects of hypoxia and organic enrichment on the coastal marine environment. *Marine Ecology Progress Series*, *238*, 249–279. https://doi.org/10.3354/meps238249

Gren, I. M., Soderqvist, T., & Wulff, F. (1997). Nutrient reductions to the Baltic Sea: Ecology, costs and benefits. *Journal of Environmental Management*, *51*(2), 123–143. https://doi.org/10.1006/jema.1997.0137

Gudasz, C., Ruppenthal, M., Kalbitz, K., Cerli, C., Fiedler, S., Oelmann, Y., Andersson, A., & Karlsson, J. (2017). Contributions of terrestrial organic carbon to northern lake sediments. *Limnology and Oceanography Letters*, *2*(6), 218–227. https://doi.org/10.1002/lol2.10051

Hale, S. S., Buffum, H. W., & Hughes, M. M. (2018). Six decades of change in pollution and benthic invertebrate biodiversity in a southern New England estuary. *Marine Pollution Bulletin*, *133*, 77–87. https://doi.org/10.1016/j.marpolbul.2018.05.019

Hamilton, S. E., & Hedges, J. I. (1988). THE COMPARATIVE GEOCHEMISTRIES OF LIGNINS AND CARBOHYDRATES IN AN ANOXIC FJORD. *Geochimica Et Cosmochimica Acta*, *52*(1), 129–142. https://doi.org/10.1016/0016-7037(88)90062-2

Harding, L. W. Jr., Mallonee, M. E., Perry, E. S., Miller, W. D., Adolf, J. E., Gallegos, C. L., & Paerl, H. W. (2020). Seasonal to inter-annual variability of primary production in Chesapeake Bay: Prospects to reverse eutrophication and change trophic classification. *Scientific Reports, 10*(2019). https://doi.org/10.1038/s41598-020-58702-3

Hardison, A. K., Canuel, E. A., Anderson, I. C., & Veuger, B. (2010). Fate of macroalgae in benthic systems: Carbon and nitrogen cycling within the microbial community. *Marine Ecology Progress Series*, *414*, 41-55. https://doi.org/10.3354/meps08720

Hardison, A. K., Anderson, I. C., Canuel, E. A., Tobias, C. R., & Veuger, B. (2011). Carbon and nitrogen dynamics in shallow photic systems: Interactions between macroalgae, microalgae, and bacteria. *Limnology and Oceanography*, *56*(4), 1489-1503. https://doi.org/10.4319/lo.2011.56.4.1489

Hartnett, H. E., Keil, R. G., Hedges, J. I., & Devol, A. H. (1988). Influence of oxygen exposure time on organic carbon preservation in continental marginsediments. *Nature*, *39*, 572–574.

Hedges, J. I., Clark, W. A., Quay, P. D., Richey, J. E., Devol, A. H., & Santos, M. (1986). Compositions and fluxes of particulate organic material in the Amazon River. *Limnology and Oceanography*, *31*(4), 717–738. https://doi.org/10.4319/lo.1986.31.4.0717

Hedges, J. I., & Ertel, J. R. (1982). CHARACTERIZATION OF LIGNIN BY GAS CAPILLARY CHROMATOGRAPHY OF CUPRIC OXIDE OXIDATION-PRODUCTS. *Analytical Chemistry*, *54*(2), 174–178. https://doi.org/10.1021/ac00239a007

Hedges, J. I., & Keil, R. G. (1995). Sedimentary organic matter preservation: an assessment and speculative synthesis. In *J.I. Hedges, R.G. Keil/Marine Chemistry* (Vol. 49).

Hedges, J. I., & Mann, D. C. (n.d.). *The characterization of plant tissues by their lignin oxidation products*.

Hedges, J. I., & Parker, P. L. (1976). *Land-delved organic matter in surface sediments from the Gulf of Mexico* (Vol. 40). Pergamon Pres.

Hill, R., Bellgrove, A., Macreadie, P. I., Petrou, K., Beardall, J., Steven, A., & Ralph, P. J. (2015). Can macroalgae contribute to blue carbon? An Australian perspective. *Limnology and Oceanography*, *60*(5), 1689–1706.https://doi.org/10.1002/lno.10128

Hoefs, J. (1980). *Stable isotope geochemistry* (2nd ed., pp. 60-165). Springer-Verlag Berlin Heidelberg. https://doi.org/10.1007/978-3-662-02290-0

Hondula, K. L., Pace, M. L., Cole, J. J., & Batt, R. D. (2014). Hydrogen isotope discrimination in aquatic primary producers: implications for aquatic food web studies. *Aquatic Sciences*, *76*(2), 217–229. https://doi.org/10.1007/s00027-013-0331-6

Howarth, R., Chan, F., Conley, D. J., Garnier, J., Doney, S. C., Marino, R., & Billen, G. (2011). Coupled biogeochemical cycles: Eutrophication and hypoxia in temperate estuaries and coastal marine ecosystems. *Frontiers in Ecology and the Environment*, *9*(1), 18–26. https://doi.org/10.1890/100008

Humphreys, J. (2005). 3. Salinity and tides in Poole Harbour: Estuary or lagoon? *Proceedings in Marine Science*, *7*(C), 35–47. https://doi.org/10.1016/S1568-2692(05)80008-7

Humphreys, J. (2008). Nutrient issues on Irish farms and solutions to lower losses. In *International Journal of Dairy Technology* (Vol. 61, Issue 1, pp. 36–42). https://doi.org/10.1111/j.1471-0307.2008.00372.x

Idestam-Almquist, J., & Kautsky, L. (1995). Plastic responses in morphology of Potamogeton pectinatus L. to sediment and above-sediment conditions at two sites in the northern Baltic proper. *Aquatic Botany*, *52*(3), 205–216. https://doi.org/10.1016/0304-3770(95)00499-8

Jorgensen, B., & Richardson, K. (1997). Coastal and Estuarine Studies. In *Coastal and Estuarine Studies*.

Kahma, T. I., Karlson, A. M. L., Sun, X., Mörth, C.-M., Humborg, C., Norkko, A., & Rodil, I. F. (2020). Macroalgae fuels coastal soft-sediment macrofauna: A triple-isotope approach across spatial scales. *Marine Environmental Research*, *162*, 105163. https://doi.org/10.1016/j.marenvres.2020.105163

Kaiser, K., & Benner, R. (2012). Characterization of Lignin by Gas Chromatography and Mass Spectrometry Using a Simplified CuO Oxidation Method. *Analytical Chemistry*, *84*(1), 459–464. https://doi.org/10.1021/ac202004r

Kalantzi, I., & Karakassis, I. (2006). Benthic impacts of fish farming: Meta-analysis of community and geochemical data. *Marine Pollution Bulletin*, *52*(5), 484–493. https://doi.org/10.1016/j.marpolbul.2005.09.034

Kamer, K., Boyle, K. A., & Fong, P. (2001). *Macroalgal Bloom Dynamics in a Highly California Estuary Eutrophic Southern* (Vol. 24, Issue 4).

Kamer, K., & Fong, P. (2000). A fluctuating salinity regime mitigates the negative effects of reduced salinity on the estuarine macroalga, Enteromorpha intestinalis (L.) link. *Journal of Experimental Marine Biology and Ecology*, *254*(1), 53–69. https://doi.org/10.1016/S0022-0981(00)00262-8

Kamer, K., Fong, P., Kennison, R. L., & Schiff, K. (2004). The relative importance of sediment and water column supplies of nutrients to the growth and tissue nutrient content of the green macroalga Enteromorpha intestinalis along an estuarine resource gradient. *Aquatic Ecology*, *38*(1), 45–56. https://doi.org/10.1023/b:aeco.0000021041.31385.19

Kennedy, H., Beggins, J., Duarte, C. M., Fourqurean, J. W., Holmer, M., Marba, N., & Middelburg, J. J. (2010). Seagrass sediments as a global carbon sink: Isotopic constraints. *Global Biogeochemical Cycles*, *24*. https://doi.org/10.1029/2010gb003848

Kindeberg, T., Orberg, S. B., Rohr, M. E., Holmer, M., & Krause-Jensen, D. (2018). Sediment Stocks of Carbon, Nitrogen, and Phosphorus in Danish Eelgrass Meadows. *Frontiers in Marine Science*, *5*, 14. https://doi.org/10.3389/fmars.2018.00474

Krause-Jensen, D., & Duarte, C. M. (2016). Substantial role of macroalgae in marine carbon sequestration. *Nature Geoscience*, *9*(10), 737-+. https://doi.org/10.1038/ngeo2790

Krause-Jensen, D., Lavery, P., Serrano, O., Marba, N., Masque, P., & Duarte, C. M. (2018a). Sequestration of macroalgal carbon: the elephant in the Blue Carbon room. *Biology Letters*, *14*(6), 6. https://doi.org/10.1098/rsbl.2018.0236

Krause-Jensen, D., Lavery, P., Serrano, O., Marba, N., Masque, P., & Duarte, C. M. (2018b). Sequestration of macroalgal carbon: the elephant in the Blue Carbon room. *Biology Letters*, *14*(6), 6. https://doi.org/10.1098/rsbl.2018.0236

Krause-Jensen, D., Middelboe, A. L., Sand-Jensen, K., & Christensen, P. B. (2000). Eelgrass, Zostera marina, growth along depth gradients: upper boundaries of the variation as a powerful predictive tool. *Oikos*, *91*(2), 233–244. https://doi.org/10.1034/j.1600-0706.2001.910204.x

Kregting, L. T., Hepburn, C. D., Hurd, C. L., & Pilditch, C. A. (2008). Seasonal patterns of growth and nutrient status of the macroalga Adamsiella chauvinii (Rhodophyta)

in soft sediment environments. *Journal of Experimental Marine Biology and Ecology*, *360*(2), 94–102. https://doi.org/10.1016/j.jembe.2008.04.001

Kristensen, E. (1994). Decomposition of macroalgae, vascular plants and sediment detritus in seawater: Use of stepwise thermogravimetry. In *Biogeochemistry* (Vol. 26).

Kristensen, E., Penha-Lopes, G., Delefosse, M., Valdemarsen, T., Quintana, C. O., & Banta, G. T. (2012). What is bioturbation? The need for a precise definition for fauna in aquatic sciences. *Marine Ecology Progress Series*, *446*, 285–302. https://doi.org/10.3354/meps09506

Lamb, A. L., Wilson, G. P., & Leng, M. J. (2006). A review of coastal palaeoclimate and relative sea-level reconstructions using δ13C and C:N ratios in organic material. *Earth-Science Reviews*, *75*(1–4), 29–57. https://doi.org/10.1016/j.earscirev.2005.10.003

Lane, R. R., Day, J. W., Justic, D., Reyes, E., Marx, B., Day, J. N., & Hyfield, E. (2004). Changes in stoichiometric Si, N and P ratios of Mississippi River water diverted through coastal wetlands to the Gulf of Mexico. *Estuarine, Coastal and Shelf Science*, *60*(1), 1–10. https://doi.org/10.1016/j.ecss.2003.11.015

Lapointe, B. E. (1989). MACROALGAL PRODUCTION AND NUTRIENT RELATIONS IN OLIGOTROPHIC AREAS OF FLORIDA BAY. In *BULLETIN OF MARINE SCIENCE* (Vol. 44, Issue I).

Lapointe, B. E., & Bedford, B. J. (2011). Stormwater nutrient inputs favor growth of non-native macroalgae (Rhodophyta) on O'ahu, Hawaiian Islands. *Harmful Algae*, *10*(3), 310–318. https://doi.org/10.1016/j.hal.2010.11.004

Lapointe, B. E., Littler, M. M., & Littler, D. S. (1992). NUTRIENT AVAILABILITY TO MARINE MACROALGAE IN SILICICLASTIC VERSUS CARBONATE-RICH COASTAL WATERS. *Estuaries*, *15*(1), 75–82. https://doi.org/10.2307/1352712

LaRowe, D. E., Arndt, S., Bradley, J. A., Estes, E. R., Hoarfrost, A., Lang, S. Q., Lloyd, K. G., Mahmoudi, N., Orsi, W. D., Shah Walter, S. R., Steen, A. D., & Zhao, R. (2020). The fate of organic carbon in marine sediments - New insights from recent data and analysis. *Earth-Science Reviews*, *204*, 103146. https://doi.org/https://doi.org/10.1016/j.earscirev.2020.103146

Levin, L. A., Ekau, W., Gooday, A. J., Jorissen, F., Middelburg, J. J., Naqvi, S. W. A., Neira, C., Rabalais, N. N., & Zhang, J. (2009). Effects of natural and human-induced hypoxia on coastal benthos. *Biogeosciences*, *6*(10), 2063–2098. https://doi.org/10.5194/bg-6-2063-2009

Lima, M. D. A. C., Ward, R. D., & Joyce, C. B. (2020). Environmental drivers of sediment carbon storage in temperate seagrass meadows. *Hydrobiologia*, *847*, 1773-1792. https://doi.org/10.1007/s10750-019-04153-5

Liu, D., Keesing, J. K., He, P., Wang, Z., Shi, Y., & Wang, Y. (2013). The world's largest macroalgal bloom in the Yellow Sea, China: Formation and implications. *Estuarine, Coastal and Shelf Science*, *129*, 2-10. https://doi.org/10.1016/j.ecss.2013.05.021

Liu, S., Jiang, Z., Wu, Y., Deng, Y., Chen, Q., Zhao, C., Cui, L., & Huang, X. (2019). Macroalgae bloom decay decreases the sediment organic carbon sequestration potential in tropical seagrass meadows of the South China Sea. *Marine Pollution Bulletin*, *138*, 598–603. https://doi.org/10.1016/j.marpolbul.2018.12.009

Lønborg, C., & Søndergaard, M. (2009). Microbial availability and degradation of dissolved organic carbon and nitrogen in two coastal areas. *Estuarine, Coastal and Shelf Science*, *81*(4), 513–520. https://doi.org/10.1016/j.ecss.2008.12.009

Luisetti, T., Jackson, E. L., & Turner, R. K. (2013). Valuing the European "coastal blue carbon" storage benefit. *Marine Pollution Bulletin*, *71*(1–2), 101–106. https://doi.org/10.1016/j.marpolbul.2013.03.029

Luther, G. W., Brendel, P. J., Lewis, B. L., Sundby, B., Lefrançois, L., Silverberg, N., & Nuzzio, D. B. (1998). Simultaneous measurement of O2, MN, Fe, I-, and S(-II) in marine pore waters with a solid-state voltammetric microelectrode. *Limnology and Oceanography*, *43*(2), 325–333. https://doi.org/10.4319/lo.1998.43.2.0325

Magni, P., Tagliapietra, D., Lardicci, C., Balthis, L., Castelli, A., Como, S., Frangipane, G., Giordani, G., Hyland, J., Maltagliati, F., Pessa, G., Rismondo, A., Tataranni, M., Tomassetti, P., & Viaroli, P. (2009). Animal-sediment relationships: Evaluating the "Pearson-Rosenberg paradigm" in Mediterranean coastal lagoons. *Marine Pollution Bulletin*, *58*(4), 478–486. https://doi.org/10.1016/j.marpolbul.2008.12.009

Manning, A. J. (2012). *TR167 – Enhanced UK Estuaries database: explanatory notes and metadata. HR Wallingford Report DDY0427-RT002-R02-00*.

Maurer, A. S., Gross, K., & Stapleton, S. P. (2022). Beached Sargassum alters sand thermal environments: Implications for incubating sea turtle eggs. *Journal of Experimental Marine Biology and Ecology*, *546*, 151650. https://doi.org/10.1016/j.jembe.2021.151650

Mayor, D. J., Zuur, A. F., Solan, M., Paton, G. I., & Killham, K. (2010). Factors Affecting Benthic Impacts at Scottish Fish Farms. *Environmental Science & Technology*, *44*(6), 2079–2084. https://doi.org/10.1021/es903073h

McClelland, J. W., & Valiela, I. (1998). Linking nitrogen in estuarine producers to land-derived sources. *Limnology and Oceanography*, *43*(4), 577–585. https://doi.org/10.4319/lo.1998.43.4.0577

McGlathery, K. J. (2001). Macroalgal blooms contribute to the decline of seagrass in nutrient-enriched coastal waters. *Journal of Phycology*, *37*(4), 453–456. https://doi.org/10.1046/j.1529-8817.2001.037004453.x

McKinney, C. R., McCrea, J. M., Epstein, S., Allen, H. A., & Urey, H. C. (1950). Improvements in mass spectrometers for the measurement of small differences in isotope abundance ratios. *Review of Scientific Instruments*, *21*(8), 724–730. https://doi.org/10.1063/1.1745698

Mermillod-Blondin, F., Rosenberg, R., Francois-Carcaillet, F., Norling, K., & Mauclaire, L. (2004). Influence of bioturbation by three benthic infaunal species on microbial communities and biogeochemical processes in marine sediment. *Aquatic Microbial Ecology*, *36*(3), 271–284. https://doi.org/10.3354/ame036271

Meyers, P. A. (1994). Preservation of elemental and isotopic source identification of sedimentary organic matter. *Chemical Geology*, *114*(3–4), 289–302. https://doi.org/10.1016/0009-2541(94)90059-0

Middelburg, J. J. (2018). Reviews and syntheses: to the bottom of carbon processing at the seafloor. *Biogeosciences*, *15*(2), 413–427. https://doi.org/10.5194/bg-15-413-2018

Middelburg, J. J., & Herman, P. M. J. (2007). Organic matter processing in tidal estuaries. *Marine Chemistry*, *106*(1-2 SPEC. ISS.), 127–147. https://doi.org/10.1016/j.marchem.2006.02.007

Müller, P. J. (1977). *C:N ratios in Pacific deep-sea sediments: Effect of inorganic ammonium and organic nitrogen compounds sorbed by clays* (Vol. 41). Pergamon Press.

Murray, F., Solan, M., & Douglas, A. (2017). Effects of algal enrichment and salinity on sediment particle reworking activity and associated nutrient generation mediated by the intertidal polychaete Hediste diversicolor. *Journal of Experimental Marine Biology and Ecology*, *495*, 75–82. https://doi.org/10.1016/j.jembe.2017.06.002

Murray, C. J., Müller-Karulis, B., Carstensen, J., Gustafsson, B. G., & Andersen, J. H. (2019). Past, present and future eutrophication status of the Baltic Sea. *Biogeochemistry*, 141(3), 267-293. https://doi.org/10.1007/s10533-018-0500-9

Nellemann, C., Corcoran, E., Duarte, C. M., De Young, C., Fonseca, L. E., & Grimsdith, G. (2010). *Blue carbon: The role of healthy oceans in binding carbon*. UNEP/GRID-Arendal. https://scholars.unh.edu/ccom/132

Ni Longphuirt, S., O'Boyle, S., Wilkes, R., Dabrowski, T., & Stengel, D. B. (2016a). Influence of Hydrological Regime in Determining the Response of Macroalgal Blooms to Nutrient Loading in Two Irish Estuaries. *Estuaries and Coasts*, *39*(2), 478–494. https://doi.org/10.1007/s12237-015-0009-5

Ni Longphuirt, S., O'Boyle, S., Wilkes, R., Dabrowski, T., & Stengel, D. B. (2016b). Influence of Hydrological Regime in Determining the Response of Macroalgal Blooms to Nutrient Loading in Two Irish Estuaries. *Estuaries and Coasts*, *39*(2), 478–494. https://doi.org/10.1007/s12237-015-0009-5

Nicholls, D. J., Tubbs, C. R., & Haynes, F. N. (1981). The effect of green algal mats on intertidal macrobenthic communities and their predators. *Kieler Meeresforschungen, Sonderheft*, *5*, 511-520.

Nilsson, H. C., & Rosenberg, R. (1997). Benthic habitat quality assessment of an oxygen stressed fjord by surface and sediment profile images. *Journal of Marine Systems*, *11*(3–4), 249–264. https://doi.org/10.1016/s0924-7963(96)00111-x

Nilsson, H. C., & Rosenberg, R. (2000). Succession in marine benthic habitats and fauna in response to oxygen deficiency: analysed by sediment profile-imaging and by grab samples. *Marine Ecology Progress Series*, *197*, 139–149. https://doi.org/10.3354/meps197139

Nixon, S. W. (1995). COASTAL MARINE EUTROPHICATION - A DEFINITION, SOCIAL CAUSES, AND FUTURE CONCERNS. *Ophelia*, *41*, 199–219. https://doi.org/10.1080/00785236.1995.10422044

Ochoa-Izaguirre, M. J., Carballo, J. L., & Paez-Osuna, E. (2002). Qualitative changes in macroalgal assemblages under two contrasting climatic conditions in a subtropical estuary. *Botanica Marina*, *45*(2), 130–138. https://doi.org/10.1515/bot.2002.014

Ortega, A., Geraldi, N. R., Alam, I., Kamau, A. A., Acinas, S. G., Logares, R., Gasol, J. M., Massana, R., Krause-Jensen, D., & Duarte, C. M. (2019). Important contribution of macroalgae to oceanic carbon sequestration. *Nature Geoscience*, *12*(9), 748-+. https://doi.org/10.1038/s41561-019-0421-8

Ortega, A., Geraldi, N. R., & Duarte, C. M. (2020). Environmental DNA identifies marine macrophyte contributions to Blue Carbon sediments. *Limnology and Oceanography*, *65*(12), 3139–3149. https://doi.org/https://doi.org/10.1002/lno.11579

OSPAR. (2003). *OSPAR Integrated Report 2003 on the Eutrophication Status of the OSPAR Maritime Area Based Upon the First Application of the Comprehensive Procedure*.

OSPAR. (2017). *Third Integrated Report on the Eutrophication Status of the OSPAR Maritime Area*.

Paerl, H. W. (1995). COASTAL EUTROPHICATION IN RELATION TO ATMOSPHERIC NITROGEN DEPOSITION - CURRENT PERSPECTIVES. *Ophelia*, *41*, 237–259. https://doi.org/10.1080/00785236.1995.10422046

Paerl, H. W., Hall, N. S., Peierls, B. L., & Rossignol, K. L. (2014). Evolving Paradigms and Challenges in Estuarine and Coastal Eutrophication Dynamics in a Culturally and Climatically Stressed World. *Estuaries and Coasts*, *37*(2), 243–258. https://doi.org/10.1007/s12237-014-9773-x

Pawlowski, J., Apothéloz-Perret-Gentil, L., & Altermatt, F. (2020). Environmental DNA: What's behind the term? Clarifying the terminology and recommendations for its future use in biomonitoring. *Molecular Ecology*, *29*(22), 4258–4264. https://doi.org/10.1111/mec.15643

Pearl, I. A., & Dickey, E. E. (1952). *Studies on Lignin and Related Products VII The Isolation of Certain Compounds from Lignin Oxidation Mixtures by Chromatographic Techniques*. *74*, 614–617.

Pearson, T., Rosenberg, R., 1977/11/30, P. Y.-, -, S. P., & T1 - Pearson TH, R. R. . M. succession in relation to organic enrichment and pollution of the marine environment. O. M. B. A. R. 16: 229-311. (1978). Macrobenthic succession in relation to organic enrichment and pollution of the marine environment. *Oceanography and Marine Biology*, *16*.

Pedersen, M. F., & Borum, J. (1997). Nutrient control of estuarine macroalgae: growth strategy and the balance between nitrogen requirements and uptake. *Marine Ecology Progress Series*, *161*, 155–163. https://doi.org/10.3354/meps161155

Pihl, L., Svenson, A., Moksnes, P. O., & Wennhage, H. (1999). Distribution of green algal mats throughout shallow soft bottoms of the Swedish Skagerrak archipelago in relation to nutrient sources and wave exposure. *Journal of Sea Research*, *41*(4), 281–294. https://doi.org/10.1016/s1385-1101(99)00004-0

Pinckney, J. L., Paerl, H. W., Tester, P., & Richardson, T. L. (2001). The role of nutrient loading and eutrophication in estuarine ecology. *Environmental Health Perspectives*, *109*, 699–706. https://doi.org/10.2307/3454916

Poursanidis, D., Topouzelis, K., & Chrysoulakis, N. (2018). Mapping coastal marine habitats and delineating the deep limits of the Neptune's seagrass meadows using very high resolution Earth observation data. *International Journal of Remote Sensing*, *39*(23), 8670–8687. https://doi.org/10.1080/01431161.2018.1490974

Prahl, F. G., Ertel, J. R., Goni, M. A., Sparrow, M. A., & Eversmeyer, B. (1994). TERRESTRIAL ORGANIC-CARBON CONTRIBUTIONS TO SEDIMENTS ON THE WASHINGTON MARGIN. *Geochimica Et Cosmochimica Acta*, *58*(14), 3035–3048. https://doi.org/10.1016/0016-7037(94)90177-5

Quan, T. M., & Falkowski, P. G. (2009). Redox control of N:P ratios in aquatic ecosystems. *Geobiology*, *7*(2), 124–139. https://doi.org/10.1111/j.1472-4669.2008.00182.x

Rabalais, N. N., Cai, W. J., Carstensen, J., Conley, D. J., Fry, B., Hu, X. P., Quinones-Rivera, Z., Rosenberg, R., Slomp, C. P., Turner, R. E., Voss, M., Wissel, B., & Zhang, J. (2014). Eutrophication-Driven Deoxygenation in the Coastal Ocean. *Oceanography*, *27*(1), 172–183. https://doi.org/10.5670/oceanog.2014.21

Rabalais, N. N., Turner, R. E., Diaz, R. J., & Justic, D. (2009). Global change and eutrophication of coastal waters. *Ices Journal of Marine Science*, *66*(7), 1528–1537. https://doi.org/10.1093/icesjms/fsp047

Raffaelli, D. (2000). Interactions between macro-algal mats and invertebrates in the Ythan estuary, Aberdeenshire, Scotland. *Helgoland Marine Research*, *54*(2–3), 71–79. https://doi.org/10.1007/s101520050004

Raffaelli, D. G., Raven, J. A., & Poole, L. J. (1998). ECOLOGICAL IMPACT OF GREEN MACROALGAL BLOOMS. *Oceanography and Marine Biology <D>*, *36*, 97–125. <Go to ISI>://WOS:000321543000004

Ratmaya, W., Laverman, A. M., Rabouille, C., Akbarzadeh, Z., Andrieux-Loyer, F., Barillé, L., Barillé, A. L., Le Merrer, Y., & Souchu, P. (2022). Temporal and spatial variations in benthic nitrogen cycling in a temperate macro-tidal coastal ecosystem: Observation and modeling. *Continental Shelf Research*, *235*, 104649. https://doi.org/10.1016/J.CSR.2022.104649

Raven, J. (2018). Blue carbon: Past, present and future, with emphasis on macroalgae. *Philosophical Transactions of the Royal Society B: Biological Sciences*, *373*(1760), 20170362. https://doi.org/10.1098/rstb.2017.0362

Redfield, A. C. (1934). On the proportions of organic derivatives in sea water and their relation to the composition of plankton. *James Johnstone Memorial*, 176–192. https://www.researchgate.net/publication/344709447

Renz, J. R., & Forster, S. (2014). Effects of bioirrigation by the three sibling species of Marenzelleria spp. on solute fluxes and porewater nutrient profiles. *Marine Ecology Progress Series*, *505*, 145–159. https://doi.org/10.3354/meps10756

Riekenberg, P. M., Oakes, J. M., & Eyre, B. D. (2018). Short-term fate of intertidal microphytobenthos carbon under enhanced nutrient availability: a 13C pulse-chase experiment. *Biogeosciences*, *15*(9), 2873–2889. https://doi.org/10.5194/bg-15-2873-2018

Robertson, B. P., & Savage, C. (2018). Mud-entrained macroalgae utilise porewater and overlying water column nutrients to grow in a eutrophic intertidal estuary. *Biogeochemistry*, *139*(1), 53–68. https://doi.org/10.1007/s10533-018-0454-x

Robledo, D., Vázquez-Delfín, E., Freile-Pelegrín, Y., Vásquez-Elizondo, R. M., Qui-Minet, Z. N., & Salazar-Garibay, A. (2021). Challenges and opportunities in relation to Sargassum events along the Caribbean Sea. *Frontiers in Marine Science*, *8,* 699664. https://doi.org/10.3389/fmars.2021.699664

Rosenberg, R. (2001a). Marine benthic faunal successional stages and related sedimentary activity. *Scientia Marina*, *65*, 107–119. https://doi.org/10.3989/scimar.2001.65s2107

Rosenberg, R. (2001b). Marine benthic faunal successional stages and related sedimentary activity. *Scientia Marina*, *65*, 107–119. https://doi.org/10.3989/scimar.2001.65s2107

Rosenberg, R., Elmgren, R., Fleischer, S., Jonsson, P., Persson, G., & Dahlin, H. (1990). MARINE EUTROPHICATION CASE-STUDIES IN SWEDEN. *Ambio*, *19*(3), 102–108.

Rosenberg, R., Nilsson, H. C., & Diaz, R. J. (2001). Response of benthic fauna and changing sediment redox profiles over a hypoxic gradient. *Estuarine Coastal and Shelf Science*, *53*(3), 343–350. https://doi.org/10.1006/ecss.2001.0810

Rozan, T. F., Taillefert, M., Trouwborst, R. E., Glazer, B. T., Ma, S., Herszage, J., Valdes, L. M., Price, K. S., & Luther, G. W. (2002). Iron-sulfur-phosphorus cycling in the sediments of a shallow coastal bay: Implications for sediment nutrient release and benthic macroalgal blooms. *Limnology and Oceanography*, *47*(5), 1346–1354. https://doi.org/10.4319/lo.2002.47.5.1346

Ruppenthal, M., Oelmann, Y., & Wilcke, W. (2013). Optimized Demineralization Technique for the Measurement of Stable Isotope Ratios of Nonexchangeable H in Soil Organic Matter. Environmental Science & Technology, 47(2), 949–957. https://doi.org/10.1021/es303448g

Sachse, D., Billault, I., Bowen, G. J., Chikaraishi, Y., Dawson, T. E., Feakins, S. J., ... & Polissar, P. (2012). Molecular paleohydrology: Interpreting the hydrogen-isotopic composition of lipid biomarkers from photosynthesizing organisms. *Annual Review of Earth and Planetary Sciences, 40*(1), 221-249. https://doi.org/10.1146/annurev-earth-042711-105535

Sanders, C. J., Eyre, B. D., Santos, I. R., Machado, W., Luiz-Silva, W., Smoak, J. M., Breithaupt, J. L., Ketterer, M. E., Sanders, L., Marotta, H., & Silva-Filho, E. (2014). Elevated rates of organic carbon, nitrogen, and phosphorus accumulation in a highly impacted mangrove wetland. Geophysical Research Letters, 41(7), 2475–2480. https://doi.org/10.1002/2014GL059789

Santos, S. A. O., Oliveira, C. S. D., Trindade, S. S., Abreu, M. H., Rocha, S. S. M., & Silvestre, A. J. D. (2016). Bioprospecting for lipophilic-like components of five Phaeophyta macroalgae from the Portuguese coast. Journal of Applied Phycology, 28(5), 3151–3158. https://doi.org/10.1007/s10811-016-0855-y

Sauer, P. E., Eglinton, T. I., Hayes, J. M., Schimmelmann, A., & Sessions, A. L. (2001). Compound-specific D/H ratios of lipid biomarkers from sediments as a proxy for environmental and climatic conditions. *Geochimica et Cosmochimica Acta, 65*(2), 213-222. https://doi.org/10.1016/S0016-7037(00)00520-2

Sinha, S. N., Biswas, S., & Bhattacharyya, M. (2011). Phytoplankton abundance in relation to cultural eutrophication at the land-ocean boundary of Sunderbans, NE Coast of Bay of Bengal, India. *Environmental Processes*, *1*(3), 169–180. https://doi.org/10.1007/s13412-011-0022-3

Smetacek, V., & Zingone, A. (2013). Green and golden seaweed tides on the rise. In *Nature* (Vol. 504, Issue 7478, pp. 84–88). https://doi.org/10.1038/nature12860

Smith, R. W., Bianchi, T. S., Allison, M., Savage, C., & Galy, V. (2015). High rates of organic carbon burial in fjord sediments globally. *Nature Geoscience*, *8*(6), 450–453. https://doi.org/10.1038/NGEO2421

Snickars, M., Weigel, B., & Bonsdorff, E. (2015). Impact of eutrophication and climate change on fish and zoobenthos in coastal waters of the Baltic Sea. *Marine Biology*, *162*(1), 141–151. https://doi.org/10.1007/s00227-014-2579-3

Solan, M., Cardinale, B. J., Downing, A. L., Engelhardt, K. A. M., Ruesink, J. L., & Srivastava, D. S. (2004). Extinction and ecosystem function in the marine benthos. *Science*, *306*(5699), 1177–1180. https://doi.org/10.1126/science.1103960

Somsueb, S., Ohno, M., & Kimura, H. (2001). Development of seaweed communities on suspended substrata with three slope angles. In *Journal of Applied Phycology* (Vol. 13).

Sondak, C. F. A., & Chung, I. K. (2015). Potential blue carbon from coastal ecosystems in the Republic of Korea. *Ocean Science Journal*, *50*(1), 1–8. https://doi.org/10.1007/s12601-015-0001-9

Smetacek, V., & Zingone, A. (2013). Green and golden seaweed tides on the rise. *Nature*, *504*, 84–88. https://doi.org/10.1038/nature12860

Spivak, A. C. (2015). Benthic biogeochemical responses to changing estuary trophic state and nutrient availability: A paired field and mesocosm experiment approach. *Limnology and Oceanography*, *60*(1), 3–21. https://doi.org/10.1002/lno.10001

Sun, S. W., Schefuss, E., Mulitza, S., Chiessi, C. M., Sawakuchi, A. O., Zabel, M., Baker, P. A., Hefter, J., & Mollenhauer, G. (2017). Origin and processing of terrestrial organic carbon in the Amazon system: lignin phenols in river, shelf, and fan sediments. *Biogeosciences*, *14*(9), 2495–2512. https://doi.org/10.5194/bg-14-2495-2017

Sundback, K., Miles, A., Hulth, S., Pihl, L., Engstrom, P., Selander, E., & Svenson, A. (2003). Importance of benthic nutrient regeneration during initiation of macroalgal blooms in shallow bays. *Marine Ecology Progress Series*, *246*, 115–126. https://doi.org/10.3354/meps246115

Taberlet, P., Coissac, E., Pompanon, F., Brochmann, C., & Willerslev, E. (2012). Towards next-generation biodiversity assessment using DNA metabarcoding. *Molecular Ecology*, *21*(8), 2045–2050. https://doi.org/10.1111/j.1365-294X.2012.05470.x

Tan, F. C., & Strain, P. M. (1979). ORGANIC-CARBON ISOTOPE RATIOS IN RECENT SEDIMENTS IN THE ST-LAWRENCE ESTUARY AND THE GULF OF ST-LAWRENCE. *Estuarine and Coastal Marine Science*, *8*(3), 213–225. https://doi.org/10.1016/0302-3524(79)90092-6

Taylor, D., Nixon, S., Granger, S., & Buckley, B. (1995). NUTRIENT LIMITATION AND THE EUTROPHICATION OF COASTAL LAGOONS. *Marine Ecology Progress Series*, *127*(1–3), 235–244. https://doi.org/10.3354/meps127235

Teichberg, M., Fox, S. E., Olsen, Y. S., Valiela, I., Martinetto, P., Iribarne, O., Muto, E. Y., Petti, M. A. V, Corbisier, T. N., Soto-Jimenez, M., Paez-Osuna, F., Castro, P., Freitas, H., Zitelli, A., Cardinaletti, M., & Tagliapietra, D. (2010). Eutrophication and macroalgal blooms in temperate and tropical coastal waters: nutrient enrichment experiments with Ulva spp. *Global Change Biology*, *16*(9), 2624–2637. https://doi.org/10.1111/j.1365-2486.2009.02108.x

Thamdrup, B., Hansen, J. W., & JÃ¸rgensen, B. B. (2009). Temperature dependence of aerobic respiration in a coastal sediment. *FEMS Microbiology Ecology*, *25*(2), 189–200. https://doi.org/10.1111/j.1574-6941.1998.tb00472.x

Toru Endo, & Sosuke Otani. (2019). Blue Carbon in Shallow Coastal Ecosystems. In *Blue Carbon in Shallow Coastal Ecosystems*. Springer Singapore. https://doi.org/10.1007/978-981-13-1295-3

Townsend, M., Thrush, S. F., & Carbines, M. J. (2011). Simplifying the complex: an "Ecosystem Principles Approach" to goods and services management in marine coastal ecosystems. *Marine Ecology Progress Series*, *434*, 291–301. https://doi.org/10.3354/meps09118

Trannum, H. C., Gundersen, H., Oug, E., Rygg, B., & Norderhaug, K. M. (2018). Soft bottom benthos and responses to climate variation and eutrophication in Skagerrak. *Journal of Sea Research*, *141*, 83–98. https://doi.org/10.1016/j.seares.2018.08.007

Trimmer, M., Nedwell, D. B., Sivyer, D. B., & Malcolm, S. J. (2000). Seasonal organic mineralisation and denitrification in intertidal sediments and their relationship to the abundance of Enteromorpha sp and Ulva sp. *Marine Ecology Progress Series*, *203*, 67–80. https://doi.org/10.3354/meps203067

Tubbs, C. R., & Tubbs, J. M. (1980). Wader and Shelduck feeding distribution in Langstone Harbour, Hampshire. *Bird Study*, *27*(4), 239-248. https://doi.org/10.1080/00063658009476684

Turner, R. E., Nancy, N. N., Justic, D., & Dortch, Q. (2003). Future aquatic nutrient limitations. *Marine Pollution Bulletin*, *46*(8), 1032–1034. https://doi.org/10.1016/s0025-326x(03)00049-3

Valdemarsen, T., Kristensen, E., & Holmer, M. (2010). Sulfur, carbon, and nitrogen cycling in faunated marine sediments impacted by repeated organic enrichment. *Marine Ecology Progress Series*, *400*, 37–53. https://doi.org/10.3354/meps08400

Valiela, I., McClelland, J., Hauxwell, J., Behr, P. J., Hersh, D., & Foreman, K. (1997). Macroalgal blooms in shallow estuaries: Controls and ecophysiological and ecosystem consequences. *Limnology and Oceanography*, *42*(5 II), 1105–1118. https://doi.org/10.4319/lo.1997.42.5_part_2.1105

Villares, R., & Carballeira, A. (2003). Seasonal variation in the concentrations of nutrients in two green macroalgae and nutrient levels in sediments in the Rías Baixas (NW Spain). *Estuarine, Coastal and Shelf Science*, *58*(4), 887–900. https://doi.org/10.1016/j.ecss.2003.07.004

Volkenborn, N., Hedtkamp, S. I. C., van Beusekom, J. E. E., & Reise, K. (2007). Effects of bioturbation and bioirrigation by lugworms (Arenicola marina) on physical and chemical sediment properties and implications for intertidal habitat succession. *Estuarine, Coastal and Shelf Science*, *74*(1–2), 331–343. https://doi.org/10.1016/j.ecss.2007.05.001

Vollenweider, R. A., Giovanardi, F., Montanari, G., & Rinaldi, A. (1998). Characterization of the trophic conditions of marine coastal waters with special reference to the NW Adriatic Sea: Proposal for a trophic scale, turbidity and generalized water quality index. *Environmetrics*, *9*(3), 329–357. https://doi.org/10.1002/(SICI)1099-095X(199805/06)9:3<329::AID-ENV308>3.0.CO;2-9

Vrede, T., Ballantyne, A., Mille-Lindblom, C., Algesten, G., Gudasz, C., Lindahl, S., & Brunberg, A. K. (2009). Effects of N : P loading ratios on phytoplankton community composition, primary production and N fixation in a eutrophic lake. *Freshwater Biology*, *54*(2), 331–344. https://doi.org/10.1111/j.1365-2427.2008.02118.x

Wallace, R. B., & Gobler, C. J. (2015). Factors Controlling Blooms of Microalgae and Macroalgae (Ulva rigida) in a Eutrophic, Urban Estuary: Jamaica Bay, NY, USA. *Estuaries and Coasts*, *38*(2), 519–533. https://doi.org/10.1007/s12237-014-9818-1

Watts, J., & Conklin, D. E. (1998). A review of the literature on the environmental impacts of marine fish cage culture. *Uniciencia*, *15*(1), 143–155.

Wang, B., Xin, M., Wei, Q., & Xie, L. (2018). A historical overview of coastal eutrophication in the China Seas. *Marine Pollution Bulletin*, *136*, 394–400. https://doi.org/10.1016/j.marpolbul.2018.09.044

Wells, E., Best, M., Scanlan, C., & Foden, J. (2010). *Water Framework Directive: Development of classification tools for ecological assessment – Opportunistic macroalgae blooming.* Water Framework Directive – United Kingdom Technical Advisory Group (WFD-UKTAG).

Wenig, P., & Odermatt, J. (2010). OpenChrom: a cross-platform open source software for the mass spectrometric analysis of chromatographic data. *Bmc Bioinformatics*, *11*. https://doi.org/10.1186/1471-2105-11-405

Weston, K., Greenwood, N., Fernand, L., Pearce, D. J., & Sivyer, D. B. (2008). Environmental controls on phytoplankton community composition in the Thames plume, UK. *Journal of Sea Research*, *60*(4), 262–270. https://doi.org/10.1016/j.seares.2008.09.003

Wheeler, P. A., & Bjornsater, B. R. (1992). SEASONAL FLUCTUATIONS IN TISSUE NITROGEN, PHOSPHORUS, AND N-P FOR 5 MACROALGAL SPECIES COMMON TO THE PACIFIC-NORTHWEST COAST. *Journal of Phycology*, *28*(1), 1–6. https://doi.org/10.1111/j.0022-3646.1992.00001.x

Woulds, C., & Cowie, G. L. (2009). Sedimentary pigments on the Pakistan margin: Controlling factors and organic matter dynamics. *Deep-Sea Research Part Ii-Topical Studies in Oceanography*, *56*(6–7), 347–357. https://doi.org/10.1016/j.dsr2.2008.05.033

Xia, S., Song, Z., Li, Q., Guo, L., Yu, C., Singh, B. P., Fu, X., Chen, C., Wang, Y., & Wang, H. (2020). Distribution, sources, and decomposition of soil organic matter along a salinity gradient in estuarine wetlands characterized by C:N ratio, δ13C-δ15N, and lignin biomarker. *Global Change Biology*, *26*(12), 724-738. https://doi.org/10.1111/gcb.15403

Yasui, S., Kanda, J., Usui, T., & Ogawa, H. (2016). Seasonal variations of dissolved organic matter and nutrients in sediment pore water in the inner part of Tokyo Bay. *Journal of Oceanography*, *72*(6), 851–866. https://doi.org/10.1007/s10872-016-0382-0

Zetsche, E., Thornton, B., Midwood, A. J., & Witte, U. (2011a). Utilisation of different carbon sources in a shallow estuary identified through stable isotope techniques. *Continental Shelf Research*, *31*(7–8), 832–840. https://doi.org/10.1016/j.csr.2011.02.006

Zimmermann, F., & Montgomery, J. R. (1984). *Effects of a decomposing drift algal mat on sediment pore water nutrient concentrations in a Florida seagrass bed*.

Zirino, A., Elwany, H., Facca, C., Maicu, F., Neira, C., & Mendoza, G. (2016). Nitrogen to phosphorus ratio in the Venice (Italy) Lagoon (2001-2010) and its relation to macroalgae. *Marine Chemistry*, *180*, 33–41. https://doi.org/10.1016/j.marchem.2016.01.002

# Appendix A: Data availability

The primary data generated and used for the analysis in this thesis is available in a publicly accessible repository. All datasets can be accessed and downloaded using the following DOI:

**DOI: 10.5518/1576**

The repository contains the following files:

- **Dataset 1:** Sediment biogeochemistry from UK southern estuaries
- **Dataset 2:** Sediment biogeochemistry from Gulf of Finland
- **Dataset 3:** Isotopes
- **Dataset 4:** CuO oxidation products relative concentrations

The data is licensed under license type CC and can be used for further research or replication studies. Please refer to the repository for any additional information or usage guidelines.